Construction and Analysis of Efficient Numerical Methods to Solve Mathematical Models of TB and HIV Co-infection

Hasim Abdalla Obaid Ahmed

A Thesis submitted in partial fulfillment of the requirements for the degree of Doctor of Philosophy in the Department of Mathematics and Applied Mathematics at the Faculty of Natural Sciences, University of the Western Cape

Supervisor: Prof. Kailash C. Patidar

Co-Supervisor: Dr. Rachid Ouifki

May 2011

KEYWORDS

Human Immunodeficiency Virus (HIV)

Tuberculosis (TB)

HIV-TB Co-infection

Dynamical System Theory

Distributed Delay

Bifurcation Analysis

Local Asymptotic Stability

Global Asymptotic Stability

Numerical Methods

Convergence Analysis.

ABSTRACT

Construction and Analysis of Efficient Numerical Methods to Solve Mathematical Models of TB and HIV Co-infection

H. A. Obaid

PhD thesis, Department of Mathematics and Applied Mathematics, Faculty of Natural Sciences, University of the Western Cape.

The global impact of the converging dual epidemics of tuberculosis (TB) and human immunodeficiency virus (HIV) is one of the major public health challenges of our time, because in many countries, human immunodeficiency virus (HIV) and mycobacterium tuberculosis (TB) are among the leading causes of morbidity and mortality. It is found that infection with HIV increases the risk of reactivating latent TB infection, and HIV-infected individuals who acquire new TB infections have high rates of disease progression. Research has shown that these two diseases are enormous public health burden, and unfortunately, not much has been done in terms of modeling the dynamics of HIV-TB co-infection at a population level. In this thesis, we study these models and design and analyze robust numerical methods to solve them. To proceed in this direction, first we study the sub-models and then the full model. The first sub-model describes the transmission dynamics of HIV that accounts for behavior change. The impact of HIV educational campaigns is also studied. Further, we explore the effects of behavior change and different responses of individuals to educational campaigns in a situation where individuals may not react immediately to these campaigns. This is done by considering a distributed time delay in the HIV sub-model. This leads to

Hopf bifurcations around the endemic equilibria of the model. These bifurcations correspond to the existence of periodic solutions that oscillate around the equilibria at given thresholds. Further, we show how the delay can result in more HIV infections causing more increase in the HIV prevalence. Part of this study is then extended to study a co-infection model of HIV-TB. A thorough bifurcation analysis is carried out for this model. Robust numerical methods are then designed and analyzed for these models. Comparative numerical results are also provided for each model.

May 2011.

DECLARATION

I declare that *Construction and Analysis of Efficient Numerical Methods to Solve Mathematical Models of TB and HIV Co-infection* is my own work, that it has not been submitted before for any degree or examination at any other university, and that all sources I have used or quoted have been indicated and acknowledged by complete references.

Hasim Abdalla Obaid Ahmed May 2011

Signed .....

ACKNOWLEDGEMENT

I want to express my deeply-felt gratitude to my primary supervisor, Professor Kailash C. Patidar. I appreciate all his continued encouragement, helpful discussions and thoughtful guidance. Without his support, this thesis would not have been possible. Special thanks go to his family for their lots of patience.

I am happy to acknowledge my debt to my co-supervisor, Dr Rachid Ouifki. I am very appreciative of his generosity with his time, thoughts and collaboration.

I thank the University of Khartoum who funded me for the PhD programme. Particularly, I would like to thank Dr. Mohsin H.A. Hashim (the principal, University of Khartoum) for his advice and support.

I am appreciative of my colleagues Abdelmgeed Sidahmed, Mohammed Hasan Khabeir, Ammar Fadul, Justin Munyakazi, Jules MBA, Edson Pindza, Edgard Ngounda, and especially Eihab Bashier, for making my time at the University of the Western Cape a more enjoyable experience.

I gratefully thank my wife Sara and our always joyful children Ayah and Aula. The encouragement and support from them have been powerful sources of inspiration and energy.

Finally, I would like to extend my deepest gratitude to my parents Abdalla and Aida, my brothers Obaid, Khalid, Khaleil, Osama, Tarig and my lovely sister Mona. They always have provided unwavering love and encouragement.

DEDICATION

Dedicated to my parents Abdalla and Aida for never-ending support and love.

Contents

List of Tables

List of Figures

List of Publications

Part of this thesis has been submitted in the form of the research papers listed below. We also have some technical reports whose revised form is being submitted to prestigious international journals for publications.

1. H.A. Obaid, R. Ouifki and K.C. Patidar, Analysis of an HIV model with distributed delay and behavior change, submitted for publication.

2. H.A. Obaid, R. Ouifki and K.C. Patidar, An unconditionally stable nonstandard finite difference methods applied to a mathematical model of HIV infection, submitted for publication.

3. H.A. Obaid, R. Ouifki and K.C. Patidar, A nonstandard finite difference method for a mathematical model of tuberculosis infection, submitted for publication.

4. H.A. Obaid, R. Ouifki and K.C. Patidar, Analysis of an HIV-TB co-infection model with behavior change, submitted for publication.

5. H.A. Obaid, R. Ouifki and K.C. Patidar, A nonstandard finite difference method for a mathematical model of HIV-TB co-infection, submitted for publication.

6. H.A. Obaid, R. Ouifki and K.C. Patidar, Analysis of an HIV mathematical model with behavior change, Report Nr. UWC-MRR 2011/12, University of the Western Cape, 2011.

7. H.A.O. Ahmed and K.C. Patidar, A robust computational method for a mathematical model of TB and HIV co-infection, Report Nr. UWC-MRR 2009/09, University of the Western Cape, 2009.

Chapter 1

General introduction

The global impact of the converging dual epidemics of human immunodeficiency virus (HIV) and tuberculosis (TB) is one of the major public health challenges of this time. The HIV pandemic presents a massive challenge to the control of tuberculosis (TB). On the other hand, tuberculosis is considered as one of the most common causes of morbidity and one of the leading causes of mortality in people living with HIV/AIDS. TB is found re-emerging with renewed vigor in the wake of HIV/AIDS epidemic [23]. People with HIV infection are both more likely to contract primary tuberculosis and at greater risk for reactivation of latent tuberculosis. Tuberculous may present with a typical signs and symptoms in HIV-infected hosts because of alterations in the immune system. Superimposed on the virulent interaction of HIV and tuberculosis is the emerging problem of multi-drug resistant strains that often resist currently available therapies. HIV positive health professionals working in high-risk environments pose a special problem, while populations unable to comply with currently available pharmacological therapies pose another.

Tuberculosis is a curable disease. By using directly observed treatment short-course (DOTS), cure rates of 80 to 90% have been achieved for passively diagnosed cases of smear-positive pulmonary tuberculosis [98]. On the other hand, anti-retroviral drugs (ARVs) increase survival time of HIV-infected individuals, but do not lead to viral eradication within individuals and hence do not completely block HIV transmission

[96]. Alternatively, efforts are focused on scaling up public awareness and knowledge about HIV through educational campaigns to possibly prevent the various routes of HIV transmissions. The sexual transmission is believed globally responsible for the majority of new HIV infections [87, 120], and hence many of these campaigns seek to encourage people to adopt safer sexual behaviors as delaying initiation of sexual activities, decreasing the number of sexual partners, encouraging people to use condoms and screening, etc. It is believed that behavioral interventions can be highly effective in reducing sexual risk behaviors and associated HIV infections [84, 145].

In this thesis, we focus on studying the effects of behavior change as a mean to tackle the HIV infections from mathematical point of view. We believe that there are certain issues related to this. Firstly, we want to investigate the impact of different responses of individuals in a community to higher HIV prevalence (a message delivered by an educational campaign) on the prevalence of HIV. Another concern is that individuals responses do not necessarily take place immediately. We study the effect of the time needed for individuals to reduce their risky behaviors on the HIV prevalence. For this we develop and analyze a mathematical model of the transmission dynamics of HIV that accounts for behavior change and time delay. Moreover, we study the impact of the behavior change and its implications on the dynamics of HIV and TB co-infections. For this a mathematical model of HIV-TB co-infection is considered and analyzed.

The mathematical models developed or considered in this thesis are described by autonomous systems of nonlinear ordinary differential equations. Very often, such systems are so complex that their exact solutions are not obtainable and hence the need for robust numerical methods arises. However, as is mentioned in [139], numerical methods like Euler, Runge-Kutta and others fail to solve nonlinear systems generating oscillations, chaos, and false steady states. Therefore, we design a special class of methods, known as nonstandard finite difference methods (NSFDMs) to avoid such numerical instabilities when solving these systems. The methods preserve a number of qualitative properties of the solutions as shown in individual chapters.

As far as possible, some of the terminologies we used in the thesis are adopted from

a recently released document from UNAIDS [136].

A brief background for HIV and TB co-infections is presented in the next section.

1.1 HIV-TB co-infections

The human immunodeficiency virus (HIV) causes AIDS (acquired immunodeficiency syndrome), the late clinical stage of infection with HIV. By infecting and depleting the T-helper cells ($CD4^+$), HIV attacks the immune system. The absolute T-helper cell ($CD4^+$) count or percentage is used most often to evaluate the progression of HIV infection and to help clinicians make treatment decisions. The presence of a $CD4^+$ cell count of under $200/mm^3$ or $CD4^+$ T-lymphocyte percentage of total lymphocytes under 14%, regardless of the clinical status, are regarded as AIDS cases if laboratory tests showed evidence of HIV infection [59].

HIV has various modes of transmission: through unprotected penile-vaginal or penile-anal intercourse; the use of HIV contaminated needles and syringes, including sharing by people who inject drugs; vertical transmission (mother to infant during pregnancy, delivery, or breastfeeding); transfusion of infected blood or its components. Some research works dealing with the HIV infections can be found in [53, 67, 140], where various HIV preventions and controls are considered.

TB in humans, is caused by the infectious agent called mycobacterium tuberculosis (an aerobic organism). Features of TB include individuals usually becoming initially infected by exposure to tubercule bacilli produced by an infective individual, and most initially infected individuals entering a long-term latent (exposed) phase. These individuals are not capable of transmitting the disease, but they may develop active TB at a later date, thereby becoming infective. In some individuals, initial TB infection may progress rapidly to active tuberculosis called primary TB disease. The risk of infection with the tubercule bacilli is directly related to the degree of exposure and less to genetic or other host factors. However, HIV infected persons may have a higher risk of infection following exposure. TB is a major global cause of disability and death,

especially in developing countries. Worldwide, 9.15 million new infections occurred in the year 2006. Over 95% of infections are in developing countries, where TB remains a dominant cause of morbidity and mortality [59].

While HIV infections increase the risk of many opportunistic infections, the interactions between HIV and several infectious disease agents have caused particular medical and public health concern. An interaction of major public health importance is with mycobacterium tuberculosis infections. Persons with latent tuberculosis infection who are also infected with HIV develop clinical tuberculosis at an increased rate, with a lifetime risk of developing tuberculosis that is multiplied by a factor of 6-8. For adults co-infected with HIV and latent TB, the lifetime risk of developing active TB disease rises from an estimated 10% to up to 50%. This resulted in a parallel pandemic of HIV/AIDS and TB disease where HIV prevalence is high [59]. Persons co-infected with TB and HIV may spread the disease not only to other HIV-infected persons, but also to members of the general population who do not participate in any of the high-risk behaviors associated with HIV. The largest increase in the number of TB cases has been in men aged 25-44, which is also the same category reporting the highest incidence of AIDS [141].

According to Narain *et al.* [105], the association between tuberculosis and HIV presents an immediate and grave public health and socioeconomic threat, particularly in the developing world. As per the information obtained from the website of WHO, millions of people had been infected with both mycobacterium tuberculosis and HIV since the beginning of the pandemic; 95% of them were in developing countries. The association between tuberculosis and HIV is evident from the high incidence of tuberculosis, estimated at 5–8% per year, among HIV-infected persons, the high occurrence of tuberculosis among AIDS patients, and the coincidence of increased tuberculosis notifications with the spreading of the HIV epidemic in several African countries. Tuberculosis is the leading cause of death among HIV infected people in Africa.

In populations where HIV co-infection is frequent among TB patients, health services struggle to cope with the large and rising numbers of TB patients. Consequences

include the over-diagnosis of sputum smear-negative pulmonary TB (see, Elliot *et al.* [43]), under-diagnosis of sputum smear-positive pulmonary TB, inadequate supervision of anti-TB chemotherapy (see, [144]), etc.

One study in New York State reported expenditure for HIV-positive TB patients of more than 2.5 times the total cost for HIV-negative TB cases. While use of all categories of health service was significantly higher among the co-infected group, this difference was largely due to a greater use of inpatient service among the co-infected persons (see, Cosler *et al.* [31]).

According to the AVERT website [7] about two billion people, one third of the world's population, are believed to be infected with TB (in 2006). Each year, 8 million people develop active TB, and nearly 2 million people with active TB die. TB and HIV/AIDS are inseparably linked, and these infections occur most frequently in economically deprived regions of the developing world. The immunodeficiency caused by HIV infection reactivates latent TB infection and accelerates the progression of newly acquired TB (Hausler *et al.* [57]).

The HIV/AIDS epidemic is reviving an old problem in well resourced countries and greatly worsening an existing problem in countries leaking resources. There are several important associations between epidemics of HIV and tuberculosis:

- Tuberculosis is harder to diagnose in HIV positive people.
- Tuberculosis progresses faster in HIV_+ infected people.
- Tuberculosis in HIV positive people is more likely to be fatal if undiagnosed or left untreated.
- Tuberculosis occurs earlier in the course of HIV infection than other opportunistic infections.
- Tuberculosis is the only major AIDS-related opportunistic infection that poses a risk to HIV-negative people.

In the next section, we explore some more works that deal with the association of the epidemic of HIV and TB.

1.2 Literature review

The increasing rate of tuberculosis (TB) cases in many countries of Sub-Saharan Africa over the past decade are largely attributing to the human immunodeficiency virus (HIV) epidemic [102, 105]. In this region, more than 20% of new tuberculosis cases had been attributed to HIV infection by the mid 1990s [39]. The cost of managing tuberculosis in HIV-positive TB patients, however, has been speculated to be substantially higher than the cost of care for TB patients without HIV infection [103]. This raises the concern that treating TB patients who are also HIV-positive may be less cost-effective [103].

In [117], Phillips explains, TB infection can be latent or active. In the latent form it is held at bay by the immune system, does not cause illness, and cannot be spread from one person to another. In the active state it can be transmitted to others, and severe illness and death can result if it is not diagnosed and effectively treated. Anyone who is latently infected is at risk of developing active TB later in life if his or her immune system fails. Unlike HIV infection, which is not spread by casual contact, TB infection can be acquired by healthy individuals who inhale mycobacterium tuberculosis. TB is more likely to be spread in crowded living conditions (such as homeless shelters, prisons, or crowded homes) and areas of high prevalence in which uninfected individuals are in close proximity with persons with active TB.

In [9], Bekker and Wood focused in detail on a specific, well-demarcated population that is heavily burdened with the dual epidemics of HIV and TB. They found that the driver of the co-epidemic of both diseases appears to be a high annual risk of mycobacterium tuberculosis infection in the community which might be the result of unrecognized infections coupled with intense social interaction and crowding. They suggested that new non-facility-based interventions will be required, with emphasis on

community-based case finding and contact tracing to decrease the infective TB pool.

A review of the interactions between HIV and TB is done by Fitz Gerald and Houston [46]. They outlined the approach to screening and preventing TB, as well as managing active TB, in the presence of HIV infection. It is concluded that HIV-related TB is much less common in Canada than in many other countries, but it is a potentially serious problem in certain populations such as injection drug users, aboriginal people and disadvantaged inner-city populations. It is also mentioned that physicians caring for patients with HIV must have a high index of suspicion for TB, and those treating patients with TB should consider the possibility of HIV.

Motivated by the striking mismatch between TB and HIV trends reported for Kenya (where HIV is declining while tuberculosis (TB) numbers continue rising), Sánchez *et al.* in [125] conducted a comparative investigation of TB-HIV co-dynamics to determine the likelihood of reported trends and to gain a wide-range perspective on TB-HIV co-epidemiology. They gave two parsimonious explanations: an unaccounted improvement in TB case detection has occurred, or HIV is not declining as reported. The TB-HIV mismatch could be compounded by surveillance biases due to spatial heterogeneity in disease dynamics. Their results highlighted the need to re-evaluate trends of both diseases in Kenya, and identify the most critical epidemiological factors at play.

In [56], Harries *et al.* focused their attention on the prevention of tuberculosis in people with HIV infection. They concentrated on regions with the greatest burden of the HIV, especially sub-Saharan Africa. They argued for aggressive approach to early diagnosis and treatment of HIV infection in affected communities, and propose urgent assessment of frequent testing for HIV and early start of antiretroviral treatment (ART) which resulted in short-term and long-term declines in tuberculosis incidence through individual immune reconstitution and reduced HIV transmission.

In [41], Escombe *el al.* considered a model in Lima (Peru) and reported the use of molecular fingerprinting to investigate patient infectiousness in the current era of HIV infection and multi drug-resistant (MDR) TB. It is found that a small number of inadequately treated MDR TB patients co-infected with HIV were responsible for almost

all TB transmission, and some patients were highly infectious. This result highlights the importance of rapid TB drug-susceptibility testing to allow prompt initiation of effective treatment, and environmental control measures to reduce ongoing TB transmission in crowded health care settings. They mentioned that TB infection control must be prioritized in order to prevent health care facilities from disseminating the drug-resistant TB that they are attempting to treat.

Corbett *et al.* [30] mentioned that directly observed treatment short course (DOTS), the global control strategy aimed at controlling tuberculosis (TB) transmission through prompt diagnosis of symptomatic smear positive disease, has failed to prevent rising tuberculosis incidence rates in Africa brought about by the HIV epidemic. However, they found that rising incidence does not necessarily imply failure to control tuberculosis transmission, which is primarily driven by prevalent infectious disease. They investigated the epidemiology of prevalent and incident TB in a high HIV prevalence population provided with enhanced primary health care. They found that strategies based on prompt investigation of TB symptoms, such as DOTS, may be an effective way of controlling prevalent TB in high HIV prevalence populations. This may translate into effective control of TB transmission despite high TB incidence rates and a period of sub-clinical infectiousness in some patients.

To quantify the impact of HIV infection on the number of tuberculosis cases in San Francisco, DeRiemer *et al.* [35] studied all patients reported with tuberculosis in San Francisco from 1991 to 2002. They determined the case number, case rate, and the fraction of tuberculosis attributable to HIV infection as their measurements. They found that during a period encompassing the resurgence and decline of tuberculosis in San Francisco, a substantial number of the tuberculosis cases were attributable to HIV infection. Co-infection with HIV amplified the local tuberculosis epidemic.

Currie *et al.* [33], aimed to compare the cost, affordability and cost-effectiveness of seven strategies for reducing the burden of TB in countries with high HIV prevalence. A compartmental difference equation model of TB and HIV and recent cost data were used to assess the costs (for year 2003) and effects (TB cases averted, deaths averted,

DALYs gained) of these strategies in Kenya during the period 2004-2023. They concluded that to reduce the burden of TB in high HIV prevalence settings, the immediate goal should be increased to TB case detection rates and, to the extent possible, improve TB cure rates, preferably in combination. Realizing the full potential of ART will require substantial new funding and strengthening of health system capacity so that increased funding can be used effectively.

In [28], Cohen *et al.* developed a mathematical model of TB-HIV co-epidemics to examine the impact of community-wide implementation of isoniazid preventive therapy (IPT) for TB-HIV co-infected individuals on the dynamics of drug-sensitive and resistant TB epidemics. They found that community-wide IPT will reduce the incidence of TB in the short-term but may also speed the emergence of drug-resistant TB. They concluded that community-wide IPT in areas of emerging HIV and drug-resistant TB should be coupled with diagnostic and treatment policies designed to identify and effectively treat the increasing proportion of patients with drug-resistant TB.

A cross-sectional survey of pulmonary TB (PTB) and HIV infection in a community of 13,000 with high HIV prevalence and high TB notification rate and a well-functioning DOTS TB control program was conducted by Wood *et al* [143]. In their study, they performed active case finding for PTB in 762 adults using sputum microscopy and mycobacterium tuberculosis culture, testing for HIV, and a symptom and risk factor questionnaire. Survey findings were correlated with notification data extracted from the TB treatment register. They found that PTB was identified in 9% of HIV-infected individuals, with 5% being previously undiagnosed. Lack of symptoms suggest PTB may contribute to low case-finding rates. DOTS strategy based on passive case finding should be supplemented by active case finding targeting HIV-infected individuals.

The main purpose of the study by Williams *et al.* [142] is to investigate whether, in the face of the HIV epidemic, India's Revised National TB Control Program (RNTCP) can overcome the expected HIV-driven increases in TB incidence, prevalence, and death rates. It is found that HIV has a relatively small impact on the prevalence of TB, a greater impact on the incidence of TB, and an even greater impact on TB mortal-

ity. They explained that the reason behind this is because HIV-positive TB patients progress more rapidly to disease, suffer much higher mortality, and are less infectious than their HIV-negative counterparts, they contribute less to TB transmission. For these reasons, a good DOTS program should be able to reduce the prevalence of TB and hence the overall risk of infection.

Bates *et al.* [12] reviewed a broad range of evidence detailing factors at individual, household, and community levels that influence vulnerability to malaria, tuberculosis, and HIV infection and used this evidence to identify strategies that could improve resilience to these diseases. The first part of their review explores the concept of vulnerability to infectious diseases and examines how age, sex, and genetics can influence the biological response to malaria, tuberculosis, and HIV infection. They highlighted factors that influence processes such as poverty, livelihoods, gender discrepancies, and knowledge acquisition and provided examples of how approaches to altering these processes may have a simultaneous effect on all three diseases.

In [131], Song *et al.* introduced some models that incorporate local and individual interactions in the context of the transmission dynamics of tuberculosis. The multilevel contact structure implicitly assumes that individuals are at risk of infection from close contacts in generalized household (clusters) as well as from casual (random) contacts in the general population. They used epidemiological time scales to reduce the dimensionality of the model and used a singular perturbation approach to corroborate the results of time-scale approximations. Then they discussed the generalized household size on TB dynamics.

Bacaër *et al.* [10] presented a compartmental model for the interaction between HIV and TB epidemics using data from a township where the prevalence of HIV is above 20 % and where the TB notification rate is close to 2,000 per 100,000 per year. They estimated the parameters of the model and studied how various control measures might change the course of these epidemics and they found that condom promotion, increased TB detection, and TB preventive therapy have a clear positive effect.

In [25] Castillo-Chavez and Song provided a detailed review of the work on the dy-

namics and control of TB models mainly concentrate on TB control strategies, optimal vaccination policies, approaches toward the elimination of TB in U.S.A, TB co-infection with HIV/AIDS, drug-resistant TB, responses of the immune system, impacts of demography, the role of public transportation systems, and the impact of contact patterns. They formulated the models as ODEs (both autonomous and non-autonomous systems), PDEs, system of difference equations, system of integro-differential equations, and Markov chain model.

El-Sony in [44] compared the cost of managing HIV-positive and HIV-negative tuberculosis (TB) patients in Sudan. The total cost associated with management of tuberculosis was significantly higher for HIV-positive, as compared with HIV-negative TB patients (US$ 105.08 versus US$ 73.92). This difference was due mainly to greater costs for hospitalization of those HIV-positive, as compared with those HIV-negative (US$ 190.80 versus US$ 141.00). The differences in cost for diagnostic tests, for drugs, for management of adverse reactions and for inter current symptoms were not significant between HIV-positive TB patients and HIV-negative TB patients. He concluded that the management of the HIV-positive TB case was more costly than that of the HIV-negative case in this stage of the HIV/AIDS epidemic in Sudan.

According to the best of our knowledge, Kirschner [72] was among the first few researchers who made mathematical attempts to explain the interaction between the TB, HIV-1, and the immune system by means of ordinary differential equations. The infection with TB can decrease the $CD4^+$ T-cell counts (which is a key marker of AIDS progression) and in turn shortens survival in HIV infected individuals. Another main marker for HIV progression is the viral load. If this load is increased due to the presence of opportunistic infections, the disease progression is much more rapid. In this work, Kirschner explored the effects of drug treatment on the TB infection in the doubly-infected patient.

Kirschner and Marino in [73] presented some results using mathematical models each of which was generated to study the interaction of mycobacterium tuberculosis and the immune system. These models were formulated on the basis of assumptions

regarding system component interactions, enabling them to explore specific aspects at diverse biological scales (e.g. intracellular, cellcell interactions, and cell population dynamics).

Murphy *et al.* [104] presented a model which considers treatment and investigate different strategies for treatment of latent and active TB disease in heterogeneous populations. They illustrated how the presence of a genetically susceptible subpopulation dramatically alters effects of treatment in the same way a core population does in the setting of sexually transmitted diseases. In addition, they evaluated treatment strategies that focus specifically on this subpopulation, and their results indicate that genetically susceptible subpopulations should be accounted for when designing treatment strategies to achieve the greatest reduction in disease prevalence.

In [129] Sharomi *et al.* addressed the synergistic interaction between HIV and mycobacterium tuberculosis using a deterministic model. In the absence of TB infection, the model (HIV-only model) is shown to have a globally asymptotically stable disease-free equilibrium whenever the associated reproduction number is less than unity and has a unique endemic equilibrium whenever this number exceeds unity. On the other hand, the model with TB alone (TB-only model) undergoes the phenomenon of backward bifurcation, where the stable disease-free equilibrium co-exists with a stable endemic equilibrium when the associated reproduction threshold is less than unity. Their analysis of the respective reproduction thresholds showed that the use of a targeted HIV treatment strategy can lead to effective control of HIV below a certain threshold. The full model, with both HIV and TB, is simulated to evaluate the impact of the various treatment strategies. They showed that the HIV-only treatment strategy saves more cases of the mixed infection than the TB-only strategy. Further, for low treatment rates, the mixed-only strategy saves the least number of cases (of HIV, TB, and the co-infection) in comparison to the other strategies. Finally, they showed that the universal strategy saves more cases of the co-infection than any of the other strategies.

Using mathematical models, West and Thompson [141] investigated the magnitude and duration of the effect that the HIV epidemic may have on TB. They developed

models which reflect the transmission dynamics of both TB and HIV, and discussed the relative merits of these models. These models were then linked together to form a model for the combined spread of both diseases. They performed a numerical study to investigate the influence of certain key parameters. The effect that HIV will have on the general population was found to be dependent on the contact structure between the general population and the HIV risk groups, as well as a possible shift in the dynamics associated with TB transmission.

Other relevant works concerning HIV-TB co-infections are [34, 42, 45, 48, 51, 57, 58, 62, 76, 94, 108, 109, 111, 118, 122, 130, 133, 134] whereas those dealing with HIV only are [20, 22, 32, 54, 63, 64, 126] and with TB only are [6, 18, 24, 27, 49, 50, 70, 71, 73, 86, 89, 101, 104, 132, 147].

The special class of numerical methods, namely, nonstandard finite difference methods, used in this thesis are surveyed thoroughly in [112]. A variety of mathematical models for biological systems, mathematical theories and techniques useful in analyzing those models are presented in [3]. Many concepts about differential equations and dynamical systems can be found in [116]. A rigorous mathematical foundation of bifurcation theory is presented in [74]. For more in-depth concepts in mathematical biology, one can also refer to [4, 100]. Finally, the biostatistical information can be seen in [127].

Above literature covers an state-of-the-art review of what is happening in the field. However, it should be noted that more specific research works related to individual models discussed in this thesis are presented in the particular chapters so as to make the chapters self-contained.

1.3 Preliminaries

This section is devoted for main results we are going to use in the subsequent chapters. Readers are advised to refer the corresponding books or papers for the proofs of the results.

1.3.1 Well-posedness for ordinary differential equations

As stated in [19], the differential equation

$$\frac{d\mathbf{x}}{dt} = \mathbf{X}(\mathbf{x}, \mathbf{t}), \tag{1.3.1.1}$$

is said to be well-posed if its solution exists, unique, and continuously depends on its initial values. The following theorems show that if $\mathbf{X}$ satisfies the Lipschitz condition (1.3.1.1), then the differential equation (1.3.1.1) defines a well-posed initial value problem.

Definition 1.3.1.1. ([19])**(Lipschitz condition).** *A family of vector fields* $\mathbf{X}(\mathbf{x}, t)$ *satisfies a Lipschitz condition in a region* $\mathcal{R}$ *of* $(\mathbf{x}, t)$*-space if and only if, for some Lipschitz constant* L*,*

$$|\mathbf{X}(\mathbf{x}, t) - \mathbf{X}(\mathbf{y}, t)| \leq L|\mathbf{x} - \mathbf{y}| \quad \textit{if } (\mathbf{x}, t) \textit{ and } (\mathbf{y}, t) \in \mathcal{R}. \tag{1.3.1.2}$$

Theorem 1.3.1.1. ([19])**(UNIQUENESS THEOREM).** *If the vector fields* $\mathbf{X}(\mathbf{x}, t)$ *satisfy a Lipschitz condition (1.3.1.1) in a domain* $\mathcal{R}$*, there is at most one solution* $\mathbf{x}(t)$ *of the vector differential equation (1.3.1.1) that satisfies a given initial condition* $\mathbf{x}(a) = \mathbf{c}$ *in* $\mathcal{R}$*.*

Theorem 1.3.1.2. ([19])**(CONTINUITY THEOREM 1).** *Let* $\mathbf{x}(t)$ *and* $\mathbf{y}(t)$ *be any two solutions of the vector differential equation (1.3.1.1), where* $\mathbf{X}(\mathbf{x}, t)$ *is continuous and satisfies the Lipschitz condition (1.3.1.1). Then*

$$|\mathbf{x}(a + h) - \mathbf{y}(a + h)| \leq e^{L|h|}|\mathbf{x}(a) - \mathbf{y}(a)|. \tag{1.3.1.3}$$

Theorem 1.3.1.3. ([19])**(CONTINUITY THEOREM 2).** *Let* $\mathbf{x}(t)$ *and* $\mathbf{y}(t)$ *satisfy the differential equations*

$$\begin{aligned} \frac{dx}{dt} &= \mathbf{X}(\mathbf{x}, t), \\ \frac{dy}{dt} &= \mathbf{Y}(\mathbf{y}, t), \end{aligned} \tag{1.3.1.4}$$

respectively, on $a \leq t \leq b$. *Further, let the functions* $\mathbf{X}$ *and* $\mathbf{Y}$ *be defined and continuous in a common domain* D, *and let*

$$|\mathbf{X}(\mathbf{z}, t) - \mathbf{Y}(\mathbf{z}, t)| \leq \epsilon, \quad a \leq t \leq b, \ \ \mathbf{z} \in D. \tag{1.3.1.5}$$

Finally, let $\mathbf{X}(\mathbf{x}, t)$ *satisfy the Lipschitz condition (1.3.1.1). Then*

$$|(\mathbf{x}(t) - (\mathbf{y}(t)| \leq \mathbf{x}(a) - \mathbf{y}(a)|e^{L|t-a|} + \frac{\epsilon}{L}\left(e^{L|t-a|} - 1\right). \tag{1.3.1.6}$$

The function $\mathbf{Y}$ *is not required to satisfy a Lipschitz condition.*

Theorem 1.3.1.4. ([19])**(Comparison Theorem).** *Let* f *and* g *be solutions of the the differential equations*

$$y' = F(x, y) \text{ and } z' = G(x, y) \tag{1.3.1.7}$$

respectively, where $F(x, y) \leq G(x, y)$ *in the strip* $a \leq x \leq b$ *and* F *or* G *satisfies a Lipschitz condition. Let also* $f(a) = g(a)$. *Then* $f(x) \leq g(x)$ *for all* $x \in [a, b]$.

1.3.2 Stability for ordinary differential equations

In this section, we present results which will be used to prove the local stability for systems of ordinary differential equations.

Definition 1.3.2.1. ([137])**(Basic reproduction number).** *The basic reproduction number, denoted* R_0, *is the expected number of secondary cases produced, in a completely*

susceptible population, by a typical infective individual. If $R_0 < 1$, then on average an infected individual produces less than one new infected individual over the course of his infectious period, and the infection cannot grow. Conversely, if $R_0 > 1$, then each infected individual produces, on average, more than one new infection, and the disease can invade the population.

To determine the local stability of the disease free equilibrium of a system of ordinary differential equations, the following theorem will be used.

Theorem 1.3.2.1. ([137]) *Consider the disease transmission model given by (1.3.2.1) with $f(x)$ satisfying conditions (A1)-(A5) given below. If x_0 is a DFE of the model, then x_0 is locally asymptotically stable if $\mathcal{R}_0 < 1$, but unstable if $\mathcal{R}_0 > 1$, where $\mathcal{R}_0$ as is given in Definition 1.3.2.1.*

Define X_s to be the set of all disease free states. That is

$$X_s = \{x \geq 0 | x_i = 0, i = 1, \ldots, m\}.$$

Let $\mathcal{F}_i(x)$ be the rate of appearance of new infections in compartment i, $\mathcal{V}_i^+(x)$ be the i rate of transfer of individuals into compartment i by all other means, and $\mathcal{V}_i^-(x)$ be the i rate of transfer of individuals out of compartment i. It is assumed that each function is continuously differentiable at least twice in each variable. The disease transmission model consists of non-negative initial conditions together with the following system of equations:

$$\dot{x}_i = f_i(x) = \mathcal{F}_i(x) - \mathcal{V}_i(x), \quad i = 1, 2, \ldots, n, \tag{1.3.2.1}$$

where $\mathcal{V}_i(x) = \mathcal{V}_i^-(x) - \mathcal{V}_i^+(x)$ and the functions satisfy assumptions (A1)-(A5) described below. Since each function represents a directed transfer of individuals, they are all non-negative. Thus

(A1) If $x \geq 0$, then $\mathcal{F}_i, \mathcal{V}_i^+, \mathcal{V}_i^- \geq 0$ for $i = 1, \ldots, n$.

(A2) If $x_i = 0$, then $\mathcal{V}_i^- = 0$. In particular, if $x \in X_s$ then $\mathcal{V}_i^-(x) = 0$ for $i = 1, \ldots, m$.

(A3) $\mathcal{F}_i = 0$ for $i > m$.

(A4) If $x \in X_s$ then $\mathcal{F}_i(x) = 0$ and $\mathcal{V}_i^+(x) = 0$ for $i = 1, \ldots, m$.

(A5) If $\mathcal{F}(x)$ is set to zero, then all eigenvalues of $Df(x_0)$ have negative real parts, where $Df(x_0)$ is the Jacobian matrix of system (1.3.2.1) evaluated at x_0.

To determine the local stability of an endemic equilibrium, we will use the following theorem, which depends on the general center manifold theory.

Theorem 1.3.2.2. ([25]) *Consider a general system of ODEs with a parameter ϕ:*

$$\frac{dx}{dt} = f(x, \phi), \quad f : \mathbb{R}^n \times \mathbb{R} \to \mathbb{R}^n \ \text{ and } \ f \in \mathbb{C}^2(\mathbb{R}^n \times \mathbb{R}). \tag{1.3.2.2}$$

Without loss of generality, it is assumed that 0 is an equilibrium for system (1.3.2.2) for all values of the parameter ϕ, that is

$$f(0, \phi) \equiv 0 \text{ for all } \phi. \tag{1.3.2.3}$$

Now, assume

- *$A = D_x f(0,0) = \left(\frac{\partial f_i}{\partial x_j}(0,0)\right)$ is the linearization matrix of system (1.3.2.2) around the equilibrium 0 with ϕ evaluated at 0. Zero is a simple eigenvalue of A and all other eigenvalues of A have negative real parts;*
- *Matrix A has a nonnegative right eigenvector w and a left eigenvector v corresponding to the zero eigenvalue.*

Let f_k be the k-th component of f and

$$a = \sum_{k,i,j=1}^{n} v_k w_i w_j \frac{\partial^2 f_k}{\partial x_i \partial x_j}(0,0), \tag{1.3.2.4}$$

$$b = \sum_{k,i=1}^{n} v_k w_i \frac{\partial^2 f_k}{\partial x_i \partial \phi}(0,0). \tag{1.3.2.5}$$

The local dynamics of (1.3.2.2) around 0 *are totally determined by* a *and* b.

Case I. $a > 0$, $b > 0$: *When* $\phi < 0$ *with* $|\phi| \ll 1$, 0 *is locally asymptotically stable, and there exists a positive unstable equilibrium; when* $0 < \phi \ll 1$, 0 *is unstable and there exists a negative and locally asymptotically stable equilibrium;*

Case II. $a < 0, b < 0$: *When* $\phi < 0$ *with* $|\phi| \ll 1$, 0 *is unstable; when* $0 < \phi \ll 1$, 0 *is locally asymptotically stable, and there exists a positive unstable equilibrium;*

Case III. $a > 0, b < 0$: *When* $\phi < 0$ *with* $|\phi| \ll 1$, 0 *is unstable, and there exists a locally asymptotically stable negative equilibrium; when* $0 < \phi \ll 1$, 0 *is stable, and a positive unstable equilibrium appears;*

Case IV. $a < 0, b > 0$: *When* ϕ *changes from negative to positive,* 0 *changes its stability from stable to unstable. Correspondingly a negative unstable equilibrium becomes positive and locally asymptotically stable.*

Theorem 1.3.2.3. ([3])**(Routh Hurwitz Criteria).** *Given the polynomial,*

$$P(\lambda) = \lambda^n + a_1\lambda^{n-1} + \cdots + a_{n-1}\lambda + a_n, \tag{1.3.2.6}$$

where the coefficients a_i *are real constant,* $i = 1, ...n$, *define the* n *Hurwitz matrices*

using the coefficients a_i of the characteristic polynomial:

$$
\begin{aligned}
H_1 &= (a_1), \\
H_2 &= \begin{pmatrix} a_1 & 1 \\ a_3 & a_2 \end{pmatrix}, \\
H_3 &= \begin{pmatrix} a_1 & 1 & 0 \\ a_3 & a_2 & a_1 \\ a_5 & a_4 & a_3 \end{pmatrix}, \\
H_n &= \begin{pmatrix} a_1 & 1 & 0 & 0 & \cdots & 0 \\ a_3 & a_2 & a_2 & 1 & \cdots & 0 \\ a_5 & a_4 & a_3 & a_2 & \cdots & 0 \\ \vdots & \vdots & \vdots & \vdots & \cdots & \vdots \\ 0 & 0 & 0 & 0 & \cdots & a_n \end{pmatrix},
\end{aligned}
$$

where $a_j = 0$ if $j > n$. All of the roots of the polynomial $P(\lambda)$ are negative or have negative real part iff the determinants of all Hurwitz matrices are positive:

$$\det H_j > 0, \quad j = 1, 2, ..., n.$$

For example, the Routh Hurwitz criteria for polynomials of degree $n = 2, 3$ are

$$
\begin{aligned}
n &= 2 : a_1 > 0 \ \textit{and} \ a_2 > 0. \\
n &= 3 : a_1 > 0, \ \ a_3 > 0, \ \ \textit{and} \ a_1 a_2 > a_3. \\
n &= 4 : a_1 > 0, \ \ a_3 > 0, \ \ a_4 > 0, \textit{and} \ a_1 a_2 a_3 > a_3^2 + a_1^2 a_4.
\end{aligned}
$$

1.3.3 Stability for discrete systems

Theorem 1.3.3.1. ([3]) *Assume that the functions $f(x, y)$ and $g(x, y)$ have continuous first-order partial derivatives in x and y on some open set in $\mathbb{R}^2$ that contains the point $(\bar{x}, \bar{y})$. Then the equilibrium point $(\bar{x}, \bar{y})$ of the nonlinear system*

$$x_{t+1} = f(x_t, y_t),$$
$$y_{t+1} = g(x_t, y_t),$$

is locally asymptotically stable if the eigenvalues of the Jacobian matrix J evaluated at the equilibrium satisfy $|\lambda_i| < 1$ iff

$$Tr(J) < 1 + det(J) < 2.$$

The equilibrium is unstable if $|\lambda_i| > 1$ for at least one i, that is, if any one of the following three inequalities is satisfied:

$$Tr(J) > 1 + det(J),$$

$$Tr(J) < -1 - det(J),$$

or

$$det(J) > 1.$$

Lemma 1.3.3.1. ([21]) *The roots of the second degree polynomial*

$$g(\lambda) = \lambda^2 + a_1\lambda + a_2, \tag{1.3.3.1}$$

satisfy $|\lambda_i| < 1$, $i = 1, 2$, if and only if the following conditions are satisfied:

(i) $g(1) \quad = 1 - a_1 + a_2 > 0,$

(ii) $g(-1) = 1 + a_1 + a_2 > 0$,

(iii) $g(0) \ = |a_2| < 1$.

Lemma 1.3.3.2. ([3])**(Jurry conditions, Schur-Cohn criteria, n=3).** *Consider the characteristic polynomial*

$$p(\lambda) = \lambda^3 + a_1\lambda^2 + a_2\lambda + a_3.$$

The solutions λ_i, $i = 1, 2, 3$, *of* $p(\lambda) = 0$ *satisfy* $|\lambda_i| < 1$ *iff the following three conditions hold:*

(i) $p(1) \ = 1 + a_1 + a_2 + a_3 > 0$,

(ii) $(-1)^3 p(-1) = 1 - a_1 + a_2 - a_3 > 0$,

(iii) $1 - a_3^2 \ > |a_2 - a_3 a_1|$.

1.3.4 Stability for delay differential equations

Theorem 1.3.4.1. ([47]) *Consider the following second order real scalar linear neutral delay equation*

$$\frac{d^2x(t)}{dt^2} + \alpha\frac{d^2x(t-\tau)}{dt^2} + a\frac{dx(t)}{dt} + b\frac{dx(t-\tau)}{dt^2} + cx(t) + dx(t-\tau) = 0, \quad (1.3.4.1)$$

where τ, α, a, b, c *and* d *are real constants. Its corresponding characteristic equation is*

$$\lambda^2 + \alpha\lambda^2 e^{-\lambda\tau} + a\lambda + b\lambda e^{-\lambda\tau} + c + de^{-\lambda\tau} = 0. \quad (1.3.4.2)$$

Assume $|\alpha| < 1$, $c + d \neq 0$ *and* $a^2 + b^2 + (d - \alpha c)^2 \neq 0$. *The number of different positive (negative) imaginary roots of (1.3.4.2) can be zero, one or two only.*

1. *If there are no such roots, then the stability of the zero solution does not change for any* $\tau \geq 0$.

2. *If there is one imaginary root, an unstable zero solution never becomes stable for any* $\tau \geq 0$. *If the zero solution is stable for* $\tau = 0$, *then it is stable up to the time* $\tau_{0,1}$ *which is given by*

$$\tau_{0,1} = \frac{\theta_1}{\omega}, \tag{1.3.4.3}$$

where $0 < \theta_1 < 2\pi$, *and becomes unstable afterwards.*

3. *If there are two imaginary roots,* $i\omega_+$ *and* $i\omega_-$, *such that* $\omega_+ > \omega_- > 0$, *then the stability of the zero solution can change a finite number of times at most as* τ *increased, and eventually it becomes unstable.*

1.3.5 Gamma distribution function

The gamma distribution is a two-parameter family of continuous probability distributions. It has a scale parameter b and a shape parameter n. If n is an integer, then the distribution represents an Erlang distribution, which is the sum of n independent exponentially distributed random variables, each of which has a mean b. The gamma distribution is frequently a probability model for waiting times.

The equation defining the probability density function of a gamma-distributed random variable x is

$$g(x; n, b) = \frac{x^{n-1} e^{-x/b}}{b^n\,(n-1)!} \text{ for } x \geq 0 \text{ and } n,\, b > 0. \tag{1.3.5.1}$$

The mean value is $\bar{x} = nb$, the variance is nb^2, and the peak is $(n-1)b$.

When $n = 1$ gamma distribution reduces to an exponential distribution and (1.3.5.1)

becomes

$$g(x;1,b)=\frac{e^{-x/b}}{b} \text{ for } x\geq 0 \text{ and } b>0, \tag{1.3.5.2}$$

with mean value b and variance b^2.

Theorem 1.3.5.1. ([90]) *If X_1, X_2 are independent Gamma (n_1,b) and Gamma (n_2,b) variates, then $Z=\frac{X_1}{X_1+X_2}$ and $Y=X_1+X_2$ are independent variates with the Beta (n_1,n_2) and the Gamma (n_1+n_2,b) distributions respectively. Conversely, if (Z,Y) are independent variates with the later pair of distributions, then $X_1=YZ$, $X_2=Y(1-Z)$ have the indicated Gamma distributions.*

According to Theorem 1.3.5.1, if n is an integer and we sum n independent Gamma $(1,b)$ random variables, the resultant sum is Gamma (n,b).

Theorem 1.3.5.2. ([124])**(Central Limit Theorem).** *Let X_1, X_2, ..., X_n be a sequence of independent and identically distributed random variables each having mean μ and variance σ^2. Then for n large, the distribution of $X_1+\cdots+X_n$ is approximately normal with mean $n\mu$ and variance $n\sigma^2$.*

According to Theorem 1.3.5.2, when n is large, Gamma distribution can be approximated by the Normal distribution with mean $\mu=nb=\bar{x}$ and variance $\sigma^2=nb^2=\frac{(\bar{x})^2}{n}$, i.e.,

$$g(x;\,n,b)\approx f(x;\,\mu,\sigma^2)=\frac{1}{\sqrt{2\pi\sigma^2}}e^{\frac{-(x-\mu)^2}{2\sigma^2}}.$$

When $n\to\infty$, $\sigma^2=\frac{(\bar{\tau})^2}{n}\to 0$ and then the Normal distribution approaches to a delta function, i.e.,

$$f(x;\,\mu,\sigma^2)=f(x,\bar{x},0)=\delta(x-\bar{x}).$$

Note that the delta function has the properties:

$$\delta(x-\bar{x})=\begin{cases}\infty & x=\bar{x}\\ 0 & x\neq\bar{x}.\end{cases}$$

and

$$\int_{-\infty}^{\infty} \delta(x-\bar{x})dx = 1 \text{ and } \int_{-\infty}^{\infty} y(x)\delta(x-\bar{x})dx = y(\bar{x}).$$

In the next section, we give a brief outline of the thesis.

1.4 Outline of the thesis

This thesis deals with the construction and analysis of robust numerical methods for solving HIV-TB co-infection models. We systematically proceed in this direction by studying first the sub-models (HIV-only and TB-only) and then the full model (HIV-TB). More specific details are provided below.

In Chapter 2, we develop and analyze a mathematical model describing the transmission dynamics of HIV. The model accounts for behavior change, where a response function is considered. This function allowed us to study various responses of the individuals to the HIV prevalence.

The analysis presented in Chapter 2 indicates how the Hill coefficient k can be used to capture different responses of individuals to educational campaigns. The information that we receive by analyzing the model proposed in this chapter suggests that studying this effect can be useful in designing efficient educational campaigns. It is anticipated that such responses also affect the dynamics of TB and therefore in Chapter 3 we investigate this above approach to study a co-infection model of HIV-TB. In this chapter, the model developed in Chapter 2 is combined with a tuberculosis model (TB-only sub-model) to formulate a deterministic model of an HIV and TB co-infection. A bifurcation analysis is also provided for this model.

Detailed numerical simulations for the full model are carried out in Chapter 3 to assess the impact of the response function on the HIV and TB prevalences. Both prevalences were found increasing with k (decreasing with λ_0). This suggests that the way individuals respond to the HIV prevalence not only affecting it but also affects the TB prevalence. Thus, by incorporating behavior change and by taking into consideration

the various responses of individuals to the HIV prevalence, the number of HIV-TB co-infected individuals can be controlled. To this end, the effects of behavior change on the dynamics of HIV-TB co-infections are investigated. What missing, is to explore these effects in a situation where individuals may not react immediately to educational campaigns. Hence, a time delay is considered in the response function. This is studied in Chapter 4.

By considering a distributed delay in the response function, the HIV-only sub-model is studied for the impact of the time needed for the individuals to reduce their risky behaviors on the HIV prevalence. We show that the introduction of the distributed delay in the model leads to Hopf bifurcations around the endemic equilibria of the model. These bifurcations correspond to the existence of periodic solutions that oscillate around the equilibria at given thresholds. Further, we show how the delay can result in more HIV infections causing more increase in the HIV prevalence.

In Chapter 5, we propose competitive unconditionally stable nonstandard finite difference methods (NSFDMs) to solve the HIV mathematical model presented in Chapter 2. We show these the methods are qualitatively stable and the numerical results presented in the chapter confirm the applicability of the proposed NSFDMs for the biological systems.

The methods proposed in Chapter 5 preserved some essential qualitative properties of the continuous model and therefore we extend these methods to solve a TB mathematical model in Chapter 6. Having looked at its competitiveness, we then explore its applicability to solve the full HIV-TB co-infection model in this chapter.

Finally several conclusions are drawn from this study. These are mentioned in Chapter 7 where we also indicate scope of some future research.

Chapter 2

Analysis of an HIV model with behavior change

We develop and analyze a mathematical model for the transmission dynamics of HIV that accounts for behavior change. It is assumed that the contact rate (termed as response function) is a decreasing function of HIV prevalence to reflect a reduction in a risky behavior that results from the awareness of individuals to a higher HIV prevalence. A function of Hill type is considered as a response function. This allows us to study the effect of different responses of individuals to higher HIV prevalence. We study the impact of the response function on its parameters on the dynamics of the model. Although these parameters did not affect the stability of the model equilibria, we will show how they affect the prevalence of the HIV.

2.1 Introduction

Many researchers have studied the impact of the educational campaigns on the HIV and/or AIDS awareness and prevention. For example, by using HIV testing rates as a surrogate marker, Ross and Scott [123] found that television based media campaigns appear to be the most effective way of increasing awareness of HIV, but their effects did not last long. This indicates a need for constant reminder of the dangers of HIV

infection. On the other hand, Oboh and Sani [110] studied the role of radio in the campaign against the spread of HIV/AIDS among farmers in Makurdi local government area of Benue state, Nigeria. They concluded that HIV/AIDS radio programmes enhance farmers interest, listenership and positive change in behavior.

In [15], Bessinger *et al.* indicated that campaigns using multiple media channels may be most effective in improving sexual health knowledge when they examined influences of behavior change communication campaigns on knowledge and use of condoms for prevention of HIV/AIDS and other sexually transmitted infections in target areas of Uganda.

As one of their findings in [135], Tripathi *et al.* showed how preventive campaigns could reduce the spread of the HIV/AIDS disease in a homogeneous population with constant immigration of susceptibles. They noted that the endemicity of the infection is reduced when infectives, after becoming aware of their infection, do not take part in sexual interaction whereas it increases in the absence of screening of unaware infectives.

In [69], Keating *et al.* assessed the effects of a media campaign on HIV/AIDS awareness and prevention. They concluded that exposure to mass media programs about reproductive health and HIV prevention topics can help increase HIV/AIDS awareness and these improvements in HIV/AIDS prevention behavior are likely to require that these programmatic efforts be continued, scaled up, done in conjunction with other interventions, and targeted towards individuals with specific socio-demographic characteristics.

In the above as well as in, among others, see for example, [14, 16, 69, 99, 128, 135, 148] one can see the important role that educational campaigns can play in changing individuals' behavior by increasing their awareness and encouraging them to adopt preventive strategies.

Mathematical modeling has been proven to be a powerful tool in understanding the effects of the behavior change on HIV prevalence. This clearly can be seen, for example, in [10] where Bacaër *et al.* considered an exponentially decreasing function of HIV prevalence for the transmission rate of HIV to reflect behavior changes as HIV

awareness develops in the HIV$_-$ population.

In their model [11], Baryarama *et al.* used variable force of infection allowing for incorporation of behavior change from behavioral surveillance data. They showed that the dramatic decline in HIV prevalence in Uganda in the early 1990s was only possible through drastic declines in the force of infection which could be attributed to reductions in probability of transmission per sexual act probably due to increased selective condom use among high risk sexual partnerships.

Chen [26] presented an epidemic model of HIV transmission with self-protective behavior and preferred mixing. It is shown that if the degree of preferred mixing is increased, the disease prevalence can decrease in the high-risk subpopulation while the situation is reversed for the low-risk subpopulation.

Gregson *et al.* [52], examined changes in HIV prevalence and sexual behavior in Eastern Zimbabwe between 1998 and 2003. They found that HIV prevalence fell most steeply among men aged 17 to 29 years and women aged 15 to 24 years and in more educated groups. They reported that HIV incidence was higher in those who had multiple sexual partners than in those who reported a single partner. The risk rose progressively with increasing number of sexual partners reported for women. They also found that, for men, consistent condom use reduced the risk of HIV infection. In addition, it is found that delaying sexual activities has its impact on the HIV infection.

Theoretical studies of the effect of behavior change on the spread of HIV/AIDS can be found, among others, in [29, 52, 60, 106, 146].

From the above, we have seen how HIV educational campaigns impact behavior of individuals, which in turn can alter the prevalence of HIV. But individuals responses to these campaigns may change from one setting to another. This was the case in [123, 138], where the effect of media campaigns did not last long indicating a need for constant reminder of the dangers of HIV infection as pointed out by the authors.

In the view of the above discussion, in this chapter we develop and analyze a mathematical model for the transmission dynamics of HIV that accounts for behavior change. The contact rate is modeled by a decreasing function of HIV prevalence to

reflect a reduction in risky behavior that results from the awareness of individuals to a higher HIV prevalence. For this, a function of Hill type is considered as a response function that allow us to study the impact of the way individuals respond to a high HIV prevalence on the dynamics of the model. We investigate the impact of this function with respect to its parameters on the system equilibria, the HIV prevalence and the bifurcation behavior of the model.

We show that the stability of the system equilibria is completely determined by the basic reproduction number R_0^{HIV}. The system is shown to exhibit a forward bifurcation where only a stable disease free equilibrium (DFE) exists if $R_0^{HIV} < 1$ and a unique stable endemic equilibrium (EE) exists if and only if $R_0^{HIV} > 1$. Furthermore, the DFE is found globally asymptotically stable if $R_0^{HIV} < 1$. We also show that the parameters of the response function (k and λ_0 which denote the Hill coefficient and behavior change respectively) alter the value of endemic equilibrium and hence the prevalence. The HIV prevalence is found increasing with k (decreasing with λ_0).

The rest of this chapter is organized as follows. The mathematical model is described in the next section. In Section 2.3 we present the mathematical analysis of this model. We carry out some numerical simulations in Section 2.4. Section 2.5 is devoted to discussion on these results.

2.2 Model description

The model of our interest is an SI model describing the transmission dynamics of HIV epidemic where S and I represent the susceptible and infectious subpopulations respectively. It is assumed that, at any time t, new recruits enter the susceptible class at a constant rate B. Upon effective contact with an infectious individual at time t, a susceptible individual acquires infection and moves into the I class of infectious individuals. The effective contact rate at time t is equal to $f(H(t))$. To reflect a reduction in risky behavior that results from the awareness of individuals to a higher HIV prevalence, the function $f(H)$ is assumed to be a decreasing function of the HIV

prevalence H. Furthermore, we denote the natural death rate by μ_1, and the mortality rate of infectious by μ_2. The equations describing this model are then given by

$$\begin{aligned} \frac{dS(t)}{dt} &= B - \mu_1 S(t) - f(H(t))H(t)S(t), \\ \frac{dI(t)}{dt} &= f(H(t))H(t)S(t) - \mu_2 I(t), \end{aligned} \tag{2.2.0.1}$$

with

$$H(t) = \frac{I(t)}{S(t) + I(t)}. \tag{2.2.0.2}$$

For the purpose of our study, we choose $f(H)$ to be a function of Hill type

$$f(H) = \frac{d}{1 + \lambda_0 H^k}, \quad k \geq 1. \tag{2.2.0.3}$$

The compartmental diagram 2.2.0.1 below shows the evolution of the disease and Table 2.2.0.1 contains values of the parameters used in the model. While k is chosen to be a positive integer, all other values are taken from [10].

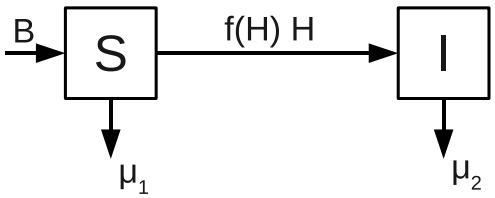

Figure 2.2.0.1: Flows between the compartments of the HIV model

Table 2.2.0.1: Description and values of parameters used in system (2.2.0.1)

Description	Parameter	Value
Birth rate	B	200/year
Natural death rate	μ_1	0.02/year
Mortality rate	μ_2	0.25/year
Maximum contact rate	d	0.7/year
Behavior change	λ_0	5.9
Hill coefficient	k	variable

Proposition 2.2.1. *The response function (2.2.0.3) has an inflection point given by*

$$H_{infl} = \left(\frac{k-1}{\lambda_0(k+1)}\right)^{\frac{1}{k}},$$

which is positive and increasing with k. Moreover,

$$H_{infl} \leq 1 \text{ if and only if } \lambda_0 \geq \frac{k-1}{k+1}.$$

Proof. To prove this proposition, we note that the first and second derivatives of $f(H)$ with respect to H are given by

$$f'(H) = -\frac{d\lambda_0 k H^k}{(1+\lambda_0 H^k)^2 H},$$

and

$$f''(H) = \frac{d\lambda_0 k H^k(\lambda_0 H^k(k+1)+1-k)}{(1+\lambda_0 H^k)^3 H^2}.$$

From these equations, we can see that $f'(H) < 0$ for any k, and $f''(H) \leq 0$ if and only if $\lambda_0 \leq (k-1)/(k+1)$.

By equating the last equation to zero, we obtain

$$H_{infl}(k) = \left(\frac{k-1}{\lambda_0(k+1)}\right)^{\frac{1}{k}}.$$

Clearly, $H_{infl}(k)$ satisfies $0 \leq H_{infl}(k) < 1$ since k is a positive integer.

To show that $H_{infl}(k)$ is an increasing function of k, we show that its derivative with respect to k is positive. Indeed,

$$H'_{infl}(k) = \frac{1}{k^2}\left(\frac{k-1}{\lambda_0(k+1)}\right)^{\frac{1}{k}}\left[\frac{2k}{\lambda_0(k^2-1)} - \ln\left(\frac{k-1}{\lambda_0(k+1)}\right)\right] > 0.$$

This completes the proof. □

Figure 2.2.0.2 below confirms what we have already mentioned in the above proposition. We first note that for small values of k, the response function decreases rapidly as soon as the prevalence start increasing because the inflection point is at zero in this case. This would be the case when the educational campaigns are more effective. As k increases, the inflection point of the prevalence moves to the right (higher prevalence) causing slower response until the prevalence reaches this point and then it starts declining rapidly. This would be the situation where educational campaigns take a longer time before it starts having some impact on the transmission of the disease.

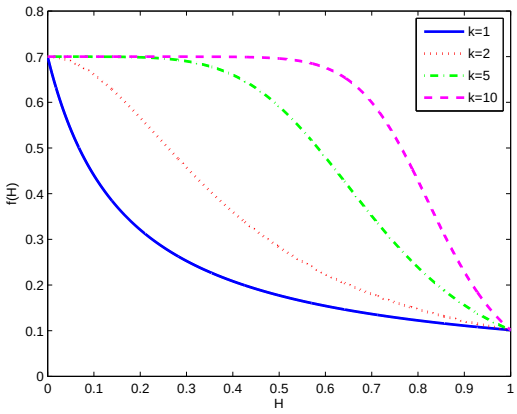

Figure 2.2.0.2: The response function $f(H)$ plotted for different values of Hill coefficient k.

The effect of λ_0 (the parameter describing behavior change) on the response function is shown in Figure 2.2.0.3. When the value of λ_0 equals zero, only the maximum

contact rate, d, governs the transmission of the disease because there is no change in the behavior. When λ_0 increases, this reflects reduction in the individuals' risky behavior, therefore the transmission decreases.

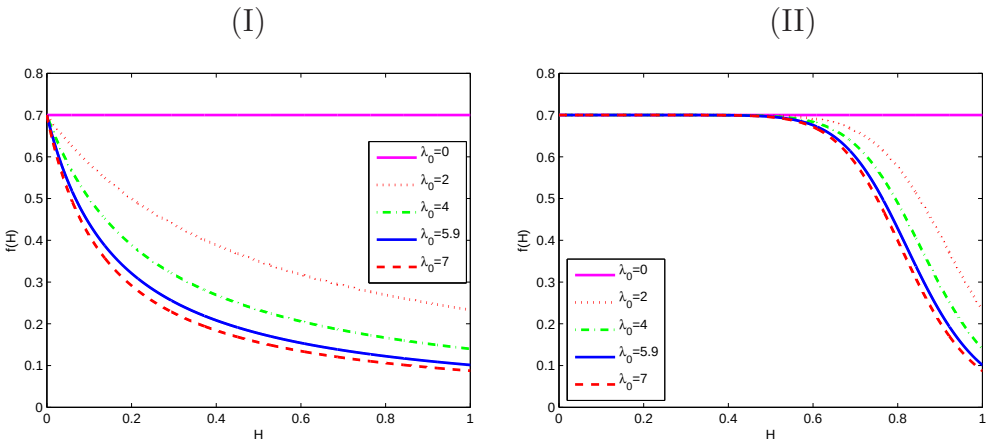

Figure 2.2.0.3: The response function $f(H)$ plotted for different values of λ_0. In (I) $k = 1$ and in (II) $k = 10$.

2.3 Mathematical analysis of the model

In this section we establish some mathematical results for system (2.2.0.1). We start by showing that the model is well-posed. In addition, we find basic reproduction number and equilibria and discuss their stability properties.

2.3.1 Well-posedness.

We show that system (2.2.0.1) is a well-posed, that is, its solution exists, it is unique, and continuously depends on the data (initial values). In view of the results presented in Section 1.3.1, it suffices to show that the system satisfies Lipschitz condition given in Definition 1.3.1.1.

Proposition 2.3.1. *System (2.2.0.1) has a unique solution that continuously depends on initial values.*

Proof. Let

$$\mathbf{X}(\mathbf{x},t)=\begin{bmatrix} f_1(\mathbf{x}(t)) \\ f_2(\mathbf{x}(t)) \end{bmatrix},$$

such that $f_1(\mathbf{x}(t))$ and $f_2(\mathbf{x}(t))$ represent the right hand sides of equations (2.2.0.1) and let $\mathbf{x}(\mathbf{t}),\mathbf{y}(\mathbf{t})$ be in some region $\mathcal{R}=\mathbb{R}^2$ where

$$\mathbf{x}(\mathbf{t})=\begin{bmatrix} S(t) \\ I(t) \end{bmatrix},$$

and

$$\mathbf{y}(\mathbf{t})=\begin{bmatrix} \check{S}(t) \\ \check{I}(t) \end{bmatrix}.$$

Now for system (2.2.0.1), we have

$$\begin{aligned}
|\mathbf{X}(\mathbf{x},t)-\mathbf{X}(\check{\mathbf{x}},t)| &= \left|\begin{bmatrix} f_1(\mathbf{x}(t)) \\ f_2(\mathbf{x}(t)) \end{bmatrix}-\begin{bmatrix} f_1(\check{\mathbf{x}}(t)) \\ f_2(\check{\mathbf{x}}(t)) \end{bmatrix}\right|, \\
&= \left|\begin{bmatrix} \mu_1(\check{S}-S)+f(\check{H})\check{H}\check{S}-f(H)H)S \\ \mu_2(\check{I}-I)+f(\check{H})\check{H}\check{S}-f(H)H)S \end{bmatrix}\right|, \\
&\leq \left|\begin{bmatrix} \mu_1(\check{S}-S) \\ \mu_2(\check{I}-I) \end{bmatrix}\right|+\left|\begin{bmatrix} f(\check{H})\check{H}\check{S}-f(H)H)S \\ f(\check{H})\check{H}\check{S}-f(H)H)S \end{bmatrix}\right|, \\
&\leq \begin{bmatrix} \mu_1 & 0 \\ 0 & \mu_2 \end{bmatrix}\left|\begin{bmatrix} S-\check{S} \\ I-\check{I} \end{bmatrix}\right|.
\end{aligned}$$

Thus, we have

$$|\mathbf{X}(\mathbf{x},t)-\mathbf{X}(\mathbf{y},t)|\leq L|\mathbf{x}-\mathbf{y}|, \tag{2.3.1.1}$$

where $L=\mu_1\mu_2$. This completes the proof. □

Remark 2.3.1.1. Since $S(t) > 0$ and $I(t) \geq 0$, it is easy to show that $0 < H < 1$ and $0 < f(H) < d$. Hence, we could establish the above proposition because of the boundedness of the state variables, H and $f(H)$.

2.3.2 Positively-invariant region

It is important to prove that the state variables $S(t)$ and $I(t)$ of system (2.2.0.1) are nonnegative for all time $t > 0$ since we are dealing with a human population. For this, we state and prove the next proposition.

Proposition 2.3.2. *If the initial conditions $S(0)$ and $I(0)$ are non-negative, then the corresponding solution $(S(t), I(t))$ of the system (2.2.0.1) is non-negative for all $t > 0$. Moreover,*

$$\lim_{t\to\infty} N(t) \leq \frac{B}{\mu_1}. \tag{2.3.2.1}$$

If in addition $N(0) \leq B/\mu_1$, then $N(t) \leq B/\mu_1$. In particular, the region

$$\mathcal{D}_H = \left\{(S, I) \in \mathbb{R}^2_+ : S + I \leq \frac{B}{\mu_1}\right\},$$

is positively-invariant.

Proof. Denote by t_{max} the upper bound of the maximum interval of existence corresponding to $(S(t), I(t))$. To show that the solution is positive and bounded in $[0, +\infty[$, it is sufficient to show the positivity and boundedness results in $[0, t_{max}[$. Let

$$t_1 = \sup\{0 \leq t < t_{max} : S \text{ and } I \text{ are positive on } [0, t]\}.$$

Since $S(0)$ and $I(0)$ are non-negative, we have $t_1 > 0$. If $t < t_{max}$, then by using the variation of constants formula to the first equation of system (2.2.0.1), we have

$$S(t_1) = S(0)e^{-\mu_1 t_1 - \int_0^{t_1} f(H(v))H(v)dv} + B\int_0^{t_1} e^{-\mu_1(t_1-u) - \int_u^{t_1} f(H(v))H(v)dv}du > 0. \tag{2.3.2.2}$$

If $t_1 < t_{max}$, then from (2.3.2.2), we have $S(t_1)$ is positive. Similarly we can show that

the other state variable is also positive at t_1. This contradicts the fact that t_1 is the supremum because at least one of the variable should be equal to zero at t_1. Therefore $t_1 = t_{max}$ and the solution is positive on its maximal interval of existence $[0, t_{max}[$.

Now we show that the solution is bounded on $[0, t_{max}[$. By using Theorem 1.3.1.4 and by accounting for the positivity of the solution on $[0, t_{max}[$, we obtain from (2.2.0.1)

$$N(0)e^{-\mu_2 t} + \frac{B}{\mu_2}\left(1 - e^{-\mu_2 t}\right) \leq N(t) \leq N(0)e^{-\mu_1 t} + \frac{B}{\mu_1}\left(1 - e^{-\mu_1 t}\right). \qquad (2.3.2.3)$$

Therefore $N(t)$ is bounded on $[0, t_{max}[$. Hence $t_{max} = \infty$ which proves the global existence and the positivity results.

Concerning the invariance properties, it is easy to obtain from (2.3.2.3) that if $N(0) \leq B/\mu_1$ then $N(t) \leq B/\mu_1$. This establishes the invariance of $\mathcal{D}_H$ as required. The result (2.3.2.1) follows immediately from (2.3.2.3). □

In the view of Proposition 2.3.2 above, we conclude that system (2.2.0.1) is epidemiologically feasible in $\mathcal{D}_H$.

2.3.3 Basic reproduction number (R_0^{HIV})

For this model, we denote the basic reproduction number (see Definition 1.3.2.1) by R_0^{HIV}. If $R_0^{HIV} < 1$, then on average, an infected individual produces less than one new infected individual over the course of its infectious period, and the infection cannot grow. Conversely, if $R_0^{HIV} > 1$, then each infected individual produces, on average, more than one new infection, and the disease can invade the population.

By using the next generation matrix method [137], we will find the basic reproduction number, R_0^{HIV}, for system (2.2.0.1). To start with, we note that this system can

be re-written as

$$\begin{aligned}\frac{dI(t)}{dt} &= \frac{dIS}{\left(1+\lambda_0\left(\frac{I}{S+I}\right)^k\right)(S+I)} - \mu_2 I,\\ \frac{dS(t)}{dt} &= B - \mu_1 S - \frac{dIS}{\left(1+\lambda_0\left(\frac{I}{S+I}\right)^k\right)(S+I)}.\end{aligned} \tag{2.3.3.1}$$

By using the same notations as in [137], we define

$$\mathcal{F} = \begin{pmatrix} \frac{dIS}{\left(1+\lambda_0\left(\frac{I}{S+I}\right)^k\right)(S+I)} \\ 0 \end{pmatrix},$$

and

$$\mathcal{V} = \begin{pmatrix} \mu_2 I \\ -B+\mu_1 S + \frac{dIS}{\left(1+\lambda_0\left(\frac{I}{S+I}\right)^k\right)(S+I)} \end{pmatrix}.$$

Hence, we obtain $F = d$ and $V = \mu_2$. Thus, the basic reproduction number, R_0^{HIV}, for system (2.2.0.1) is the spectral radius of the operator $(FV)^{-1}$ [137]. That is

$$R_0^{HIV} = \frac{d}{\mu_2}. \tag{2.3.3.2}$$

2.3.4 Equilibria and stability analysis

In this section, we find the equilibria of system (2.2.0.1) and we determine their stability properties.

By solving system (2.2.0.1) at the equilibrium, we obtain

$$H^*(\mu_2\lambda_0 H^{*k} + dH^* + \mu_2(1 - R_0^{HIV})) = 0, \tag{2.3.4.1}$$

where

$$H^* = \frac{I^*}{S^* + I^*}, \tag{2.3.4.2}$$

is the prevalence at the equilibrium.

The solution $H^* = 0$ of (2.3.4.1) corresponds to the disease free equilibrium

$$E_0^* = \left(\frac{B}{\mu_1}, 0\right).$$

Moreover, any endemic equilibrium is given by

$$E^* = \left(\frac{B(1-H^*)}{\mu_1(1-H^*) + \mu_2 H^*}, \frac{BH^*}{\mu_1(1-H^*) + \mu_2 H^*}\right),$$

where H^* is a positive solution of the equation

$$\mu_2 \lambda_0 H^{*k} + dH^* + \mu_2(1 - R_0^{HIV}) = 0. \tag{2.3.4.3}$$

Thus, we have the following proposition.

Proposition 2.3.3. *For any value of the Hill coefficient, k, system (2.2.0.1) exhibits a transcritical bifurcation. Moreover, at the equilibrium, the HIV prevalence, H^*, is an increasing function of Hill coefficient, k, and a decreasing function of the behavior change λ_0.*

Proof. To start with, we write the left hand side of equation (2.3.4.3) as a function of H^* as follows

$$\mathcal{U}(H^*) = \mu_2 \lambda_0 H^{*k} + dH^* + \mu_2(1 - R_0^{HIV}). \tag{2.3.4.4}$$

If $R_0^{HIV} \leq 1$, then H^* has no positive roots. When $R_0^{HIV} > 1$, we have

$$\mathcal{U}(0) = \mu_2(1 - R_0^{HIV}) < 0$$

and

$$\mathcal{U}(1) = \mu_2(\lambda_0 + 1) > 0.$$

Hence, $\mathcal{U}$ has at least one root in $(0, 1)$. Moreover, this root is unique (we denote it by $H^*(k, \lambda_0)$) due to the monotonicity of $\mathcal{U}$ with respect to H^* since we have

$$\mathcal{U}'(H^*) = k\mu_2\lambda_0 H^{*k-1} + d > 0.$$

Next, we explore the variation of $H^*(k, \lambda_0)$ with respect to Hill coefficient k and behavior change λ_0.

From equation (2.3.4.4), we obtain

$$\frac{\partial H^*(k, \lambda_0)}{\partial k} = -\frac{\partial \mathcal{U}}{\partial k} \Big/ \frac{\partial \mathcal{U}}{\partial H^*}$$

and

$$\frac{\partial H^*(k, \lambda_0)}{\partial \lambda_0} = -\frac{\partial \mathcal{U}}{\partial \lambda_0} \Big/ \frac{\partial \mathcal{U}}{\partial H^*}.$$

Therefore,

$$\frac{\partial H^*(k, \lambda_0)}{\partial k} = -\frac{\mu_2\lambda_0 H^{*k} \ln(H^*)}{k\mu_2\lambda_0 H^{*k-1} + d} > 0$$

and

$$\frac{\partial H^*(k, \lambda_0)}{\partial \lambda_0} = -\frac{\mu_2 H^{*k}}{k\mu_2\lambda_0 H^{*k-1} + d} < 0.$$

Therefore, $H^*(k, \lambda_0)$ is an increasing function of k and a decreasing function of λ_0. □

2.3.4.1 Local stability of the disease free equilibrium

In this section, we discuss the local stability of the disease free equilibrium of system (2.2.0.1).

Theorem 2.3.4.1. *The disease free equilibrium of system (2.2.0.1), E_0^*, is locally asymptotically stable if $R_0^{HIV} < 1$ and unstable if $R_0^{HIV} > 1$.*

Proof. The Jacobian matrix of the system (2.2.0.1) evaluated at the disease free equilibrium, E_0^*, is

$$J(E_0^*) = \begin{pmatrix} -\mu_1 & -d \\ 0 & -(\mu_2 - d) \end{pmatrix}.$$

Being a triangular matrix, the eigenvalues of the above matrix are the entries along the main diagonal, i.e.,

$$\begin{aligned} \lambda_1 &= -\mu_1, \\ \lambda_2 &= -(\mu_2 - d), \\ &= \mu_2 \left(R_0^{HIV} - 1 \right). \end{aligned}$$

Thus, λ_1 is always negative. The second eigenvalue, λ_2, is negative if $R_0^{HIV} < 1$ and positive if $R_0^{HIV} > 1$. Therefore, by Theorem 1.3.2.3, the required result is established. □

2.3.4.2 Global stability of the disease free equilibrium

In the following result, we show that the disease free equilibrium of system (2.2.0.1) is globally asymptotically stable in $\mathcal{D}_H$ if $R_0^{HIV} < 1$.

Theorem 2.3.4.2. *The disease free equilibrium of system (2.2.0.1), E_0^*, is globally asymptotically stable in $\mathcal{D}_H$ if $R_0^{HIV} < 1$.*

Proof. By substituting $x = B/\mu_1 - S \geq 0$ and $y = I \geq 0$ for all t, in (2.2.0.1), we

obtain the following system

$$\begin{aligned}\frac{dx(t)}{dt} &= f(z(t))z(t)\left(\frac{B}{\mu_1}-x(t)\right)-\mu_1 x(t),\\ \frac{dy(t)}{dt} &= f(z(t))z(t)\left(\frac{B}{\mu_1}-x(t)\right)-\mu_2 y(t),\end{aligned} \tag{2.3.4.5}$$

where in this case

$$z(t)=\frac{y(t)}{\left(\frac{B}{\mu_1}-x(t)\right)+y(t)}.$$

We note that $(0,0)$ is an equilibrium of the system (2.3.4.5). It must be noted that the global stability of $(0,0)$ for system (2.3.4.5) implies the global stability of the disease free equilibrium $E_0^*=\left(\frac{B}{\mu_1},0\right)$ for system (2.2.0.1) in $\mathcal{D}_H$. To show this, we note that

$$\begin{aligned} f(z(t))-\mu_2 &= \frac{-\mu_2(1-R_0^{HIV})-\mu_2\lambda_0 z^k(t)}{1+\lambda_0 z^k(t)},\\ &< -\mu_2(1-R_0). \end{aligned} \tag{2.3.4.6}$$

From the second equation of system (2.3.4.5), we have

$$\begin{aligned}\frac{dy(t)}{dt} &= f(z(t))\left(\frac{\frac{B}{\mu_1}-x(t)}{\frac{B}{\mu_1}-x(t)+y(t)}\right)y(t)-\mu_2 y(t),\\ &< \left[f(z(t))-\mu_2\right]y(t),\\ &< -\mu_2\left(1-R_0^{HIV}\right)y(t),\end{aligned} \tag{2.3.4.7}$$

for $y(t)>0$. By using Theorem 1.3.1.4, we obtain

$$y(t) < y(0)e^{-\mu_2\left(1-R_0^{HIV}\right)t}. \tag{2.3.4.8}$$

Therefore, if $R_0^{HIV} < 1$, it follows that $y(t) \to 0$ as $t \to \infty$.
From the first equation of system (2.3.4.5), we have

$$\begin{aligned}\frac{dx(t)}{dt} &= f(z(t))\left(\frac{\frac{B}{\mu_1} - x(t)}{\frac{B}{\mu_1} - x(t) + y(t)}\right) y(t) - \mu_1 x(t),\\ &< \mu_2 y(t) - \mu_1 x(t),\\ &< \mu_2 y(0) e^{-\mu_2\left(1-R_0^{HIV}\right)t - \mu_1 x(t)},\end{aligned}$$

where we have used (4.3.3.7) in the last step of the above inequality. This inequality can be written as

$$\frac{d}{dt}x(t) + \mu_1 x(t) < \mu_2 y(0) e^{-\mu_2\left(1-R_0^{HIV}\right)t}.$$

Again by using Theorem 1.3.1.4, the solution of the above inequality satisfies

$$x(t) < e^{-\mu_1 t}x(0) + \mu_2 y(0) e^{-\mu_1 t}\int_0^t e^{\left(\mu_1 - \mu_2\left(1-R_0^{HIV}\right)\right)s} ds.$$

Then

$$x(t) < \begin{cases} e^{-\mu_1 t}x(0) + \frac{\mu_2 y(0)}{\mu_1 - \mu_2\left(1-R_0^{HIV}\right)}\left(e^{-\mu_2\left(1-R_0^{HIV}\right)t} - e^{-\mu_1 t}\right), & \text{if } \mu_1 \neq \mu_2\left(1-R_0^{HIV}\right),\\ e^{-\mu_1 t}x(0) + \mu_2 y(0) t e^{-\mu_1 t}, & \text{if } \mu_1 = \mu_2(1-R_0^{HIV}).\end{cases}$$

It should be noted that the solution $x(t)$ is bounded above by an exponentially decaying function as $t \to \infty$. Hence, $x \to 0$ as $t \to \infty$. Thus, we have proved $(0,0)$ is globally stable for system (2.3.4.5) in $\mathcal{D}_H$. Therefore, $E_0^* = \left(\frac{B}{\mu_1}, 0\right)$ is globally asymptotically stable for system (2.2.0.1) in $\mathcal{D}_H$. □

In the following part of the analysis, the value of Hill coefficient k is considered as 1. Other cases when $k \geq 2$ are investigated numerically in Section 2.4.1.

2.3.4.3 Local stability of the endemic equilibrium

The stability of the endemic equilibrium of system (2.2.0.1) is given in the following result.

Theorem 2.3.4.3. *The endemic equilibrium, E^*, of system (2.3.3.1) is locally asymptotically stable if $R_0^{HIV} > 1$ and unstable if $R_0^{HIV} < 1$.*

Proof. The Jacobian matrix of the system (2.2.0.1) evaluated at the endemic equilibrium

$$E^* = \left(\frac{B(1+\lambda_0)}{(\mu_1(1+\lambda_0) + \mu_2\left(R_0^{HIV}-1\right)}, \frac{B(R_0^{HIV}-1)}{\mu_1(1+\lambda_0) + \mu_2(R_0^{HIV}-1)} \right), \tag{2.3.4.9}$$

is

$$J(E^*) = \begin{pmatrix} -\frac{\mu_1\left(R_0^{HIV}\right)^2 + \mu_1\left(R_0^{HIV}\right)^2\lambda_0 + d\left(R_0^{HIV}\right)^2 - 2dR_0^{HIV} + d}{(1+\lambda_0)\left(R_0^{HIV}\right)^2} & -\frac{d}{\left(R_0^{HIV}\right)^2} \\ \\ \frac{(R_0^{HIV}-1)^2 d}{(1+\lambda_0)\left(R_0^{HIV}\right)^2} & -\frac{\mu_2\left(R_0^{HIV}\right)^2 - d}{\left(R_0^{HIV}\right)^2} \end{pmatrix}. \tag{2.3.4.10}$$

The characteristic equation associated with the above matrix is given by

$$\lambda^2 + A_1\lambda + A_2 = 0, \tag{2.3.4.11}$$

where

$$A_1 = \frac{\mu_1\left(R_0^{HIV}\right)^2\lambda_0 + dR_0^{HIV}\left(R_0^{HIV}-1\right) + \mu_1\left(R_0^{HIV}\right)^2 + \mu_2\lambda_0 R_0^{HIV}\left(R_0^{HIV}-1\right)}{\left(R_0^{HIV}\right)^2(1+\lambda_0)}, \tag{2.3.4.12}$$

and

$$A_2 = \frac{\mu_1\mu_2 R_0^{HIV}\left(R_0^{HIV}-1\right) + \lambda_0\mu_1\mu_2 R_0^{HIV}\left(R_0^{HIV}-1\right) + d\mu_2\left(R_0^{HIV}-1\right)^2}{R_0^2(1+\lambda_0)} \tag{2.3.4.13}$$

It should be noted that both A_1 and A_2 are greater that zero if $R_0^{HIV} > 1$. Hence, from Theorem 1.3.2.3, the eigenvalues of the Jacobian matrix are negative or have negative

real parts. The required result therefore follows. □

2.4 Numerical results and simulations

In order to study the dynamics of system (2.2.0.1), we perform some numerical simulations. Parameters values used in these simulations are given in Table 2.2.0.1. Note that in Section 2.3, we have shown the stability properties of the system when Hill coefficient $k = 1$. In the following section, we provide the numerical stability properties of the system when Hill coefficient $k \geq 2$.

2.4.1 Numerical stability of the endemic equilibria for Hill coefficient $k \geq 2$

In this section, we tabulate the equilibria and corresponding eigenvalues associated with the Jacobian matrices for the system (2.2.0.1) for different values of k. It should be noted that when solving system (2.2.0.1) for its equilibria for $k = 2, 3, ..., 10$, it always has the disease free equilibrium $E_0^* = (10000, 0)$ and k endemic equilibria (for the set of parameter values mentioned in Table 2.2.0.1 which give $R_0^{HIV} > 1$), but only one endemic equilibrium is relevant for each value of k.

Table 2.4.1.1: Endemic equilibria and their eigenvalues for system (2.2.0.1) for $k \geq 2$.

k	S^*	I^*	λ_1	λ_2
2	1280	1744	−0.1998	−0.0890
3	1019	1796	−0.2903	−0.0876
4	866	1827	−0.3652	−0.0881
5	763	1847	−0.4288	−0.0889
6	689	1862	−0.4832	−0.0897
7	633	1873	−0.5296	−0.0904
8	589	1882	−0.5690	−0.0910
9	553	1889	−0.6022	−0.0916
10	523	1895	−0.6298	−0.0922

It is clear from the above tabular results that the eigenvalues in each case of $k = 2, 3, ..., 10$ are negative. We therefore have the following remark.

Remark 2.4.1.1. For $k = 2, 3, 4, ..., 10$, the system (2.2.0.1) has a disease free equilibrium when $R_0^{HIV} < 1$ and it possesses a number of endemic equilibria as presented above in Table 2.4.1.1 when $R_0^{HIV} > 1$. Each of these endemic equilibria is locally asymptotically stable if $R_0^{HIV} > 1$.

2.4.2 Numerical simulations

In Figure 2.4.2.1, we show that system (2.2.0.1) exhibits a transcritical bifurcation, where there exists only stable disease free equilibrium if $R_0^{HIV} < 1$ and a stable endemic equilibrium as well as unstable disease free equilibrium if $R_0^{HIV} > 1$.

The dependence of the endemic equilibria of the system on the parameters of the response function, Hill coefficient k and behavior change parameter λ_0, is shown in the Figures 2.4.2.2 and 2.4.2.3.

The HIV prevalence H as a function of Hill coefficient and behavior change, is shown in Figure 2.4.2.4, where we can see that the prevalence is a increasing (decreasing) function of the Hill coefficient k (behavior change λ_0).

In the Figures 2.4.2.5 and 2.4.2.6, the profile of the prevalence in the period of time is shown for different values of k and λ_0, where it can be seen that the prevalence increases when k increases (decreases when λ_0 increases). When the prevalence is high (large k or small λ_0), we note that it reaches a peak in the first few years before it stabilizes.

The solution profile for the susceptible and infectious individuals for the disease free equilibrium is given in Figure 2.4.2.7, while for the endemic equilibrium it is shown in the Figures 2.4.2.8 and 2.4.2.9. These simulations are performed for different values of k and λ_0.

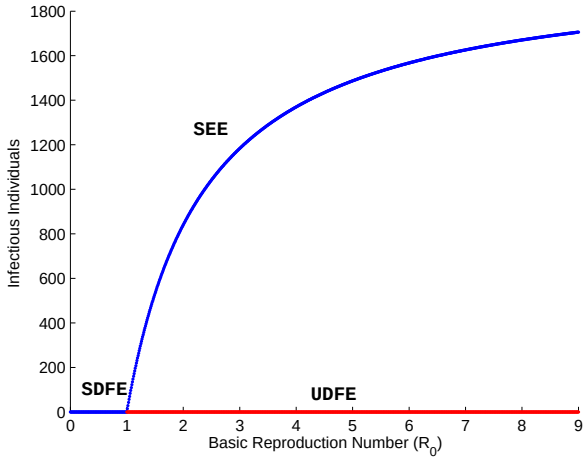

Figure 2.4.2.1: Bifurcation diagram: SDFE stands for stable disease free equilibrium, UDFE stands for unstable disease free equilibrium and SEE stands for stable endemic equilibrium.

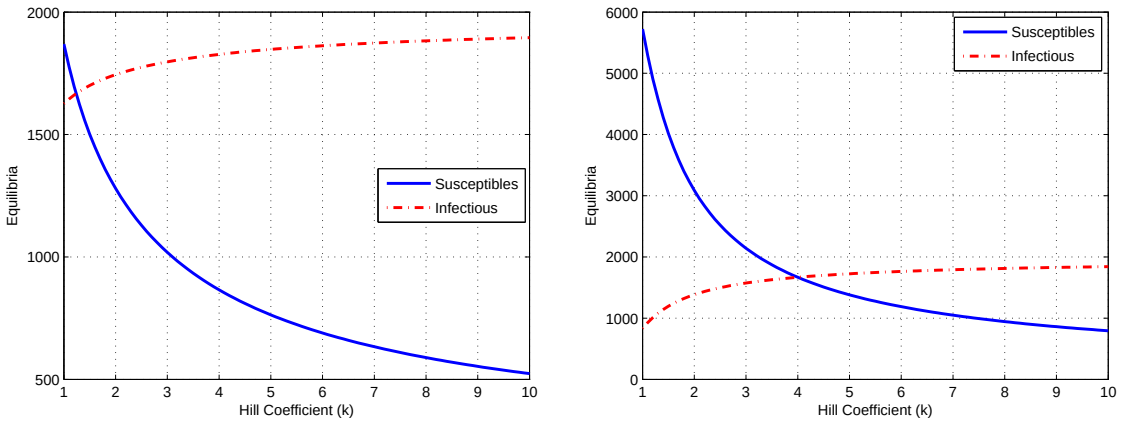

Figure 2.4.2.2: Equilibrium points of system (2.2.0.1) as a function of k when $\lambda_0 = 5.9$ (left figure) and $\lambda_0 = 40$ (right figure).

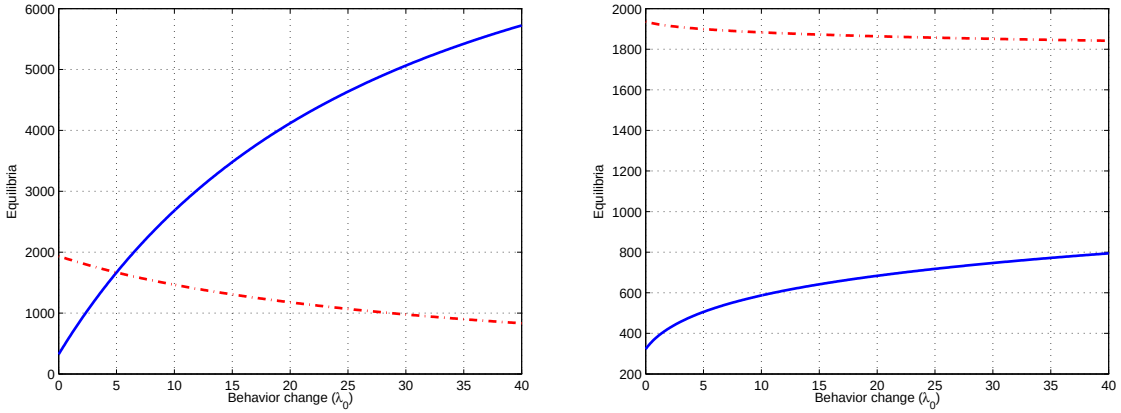

Figure 2.4.2.3: Equilibrium points of system (2.2.0.1) as a function of λ_0 when $k = 1$ (left figure) and $k = 10$ (right figure).

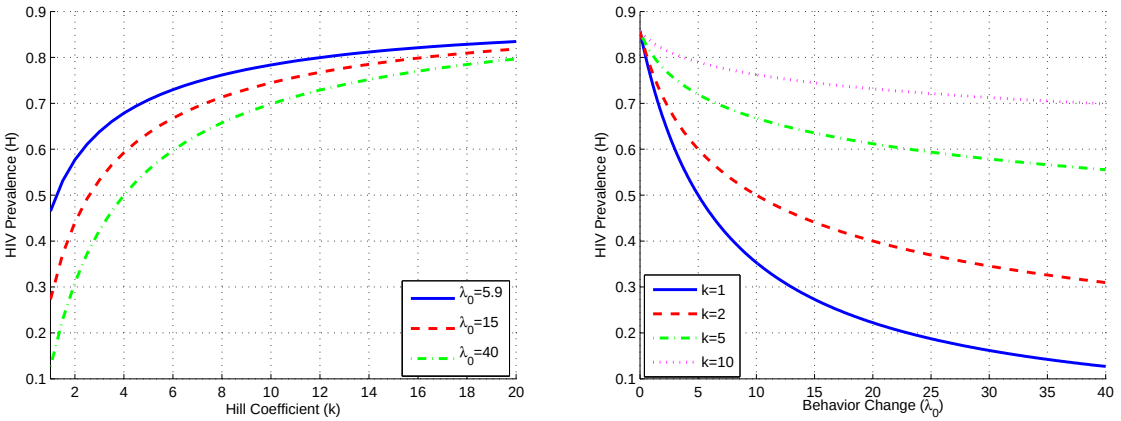

Figure 2.4.2.4: The prevalence of HIV as a function of k (left figure) and as a function of λ_0 (right figure).

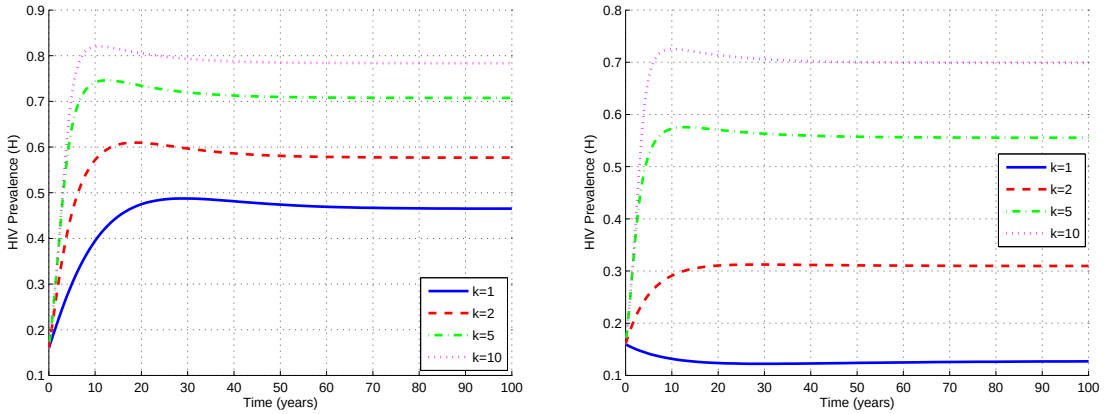

Figure 2.4.2.5: The prevalence of HIV as a function of time t for various values of k and with $\lambda_0 = 5.9$ (left figure) and $\lambda_0 = 40$ (right figure).

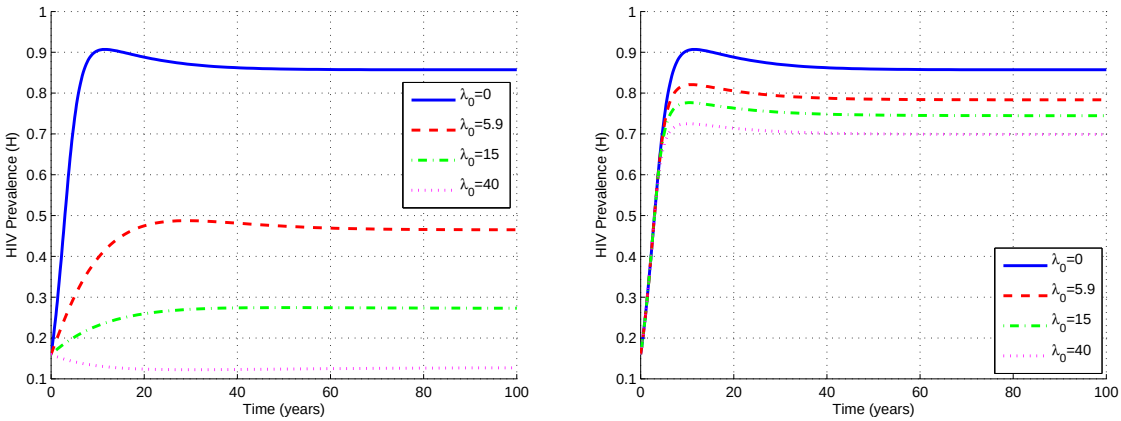

Figure 2.4.2.6: The prevalence of HIV as a function of time t for various values of λ_0 and with $k = 1$ (left figure) and $k = 10$ (right figure).

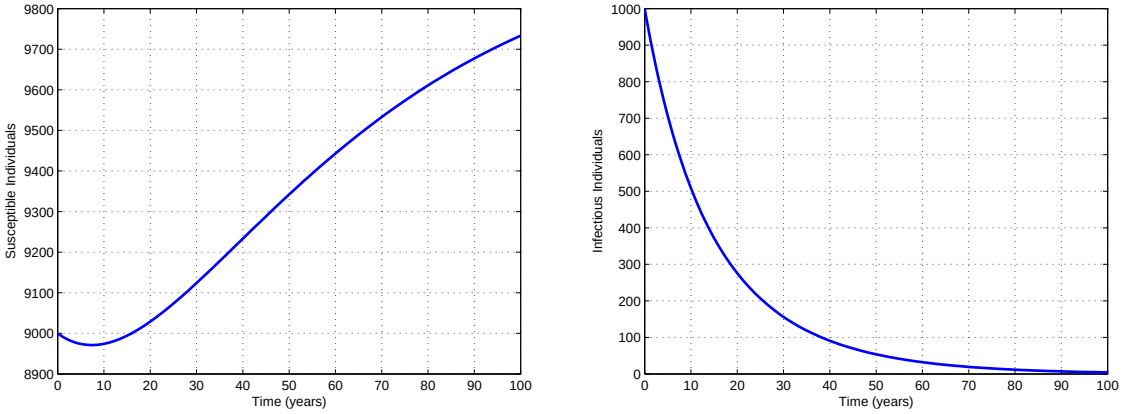

Figure 2.4.2.7: Profiles of solutions [susceptibles ($S(t)$): left figure and infectious individuals ($I(t)$): right figure] when $d = 0.05$ ($R_0^{HIV} < 1$) and with $k = 1$, $\lambda_0 = 5.9$ and initial conditions $(S(0), I(0)) = (9000, 1000)$.

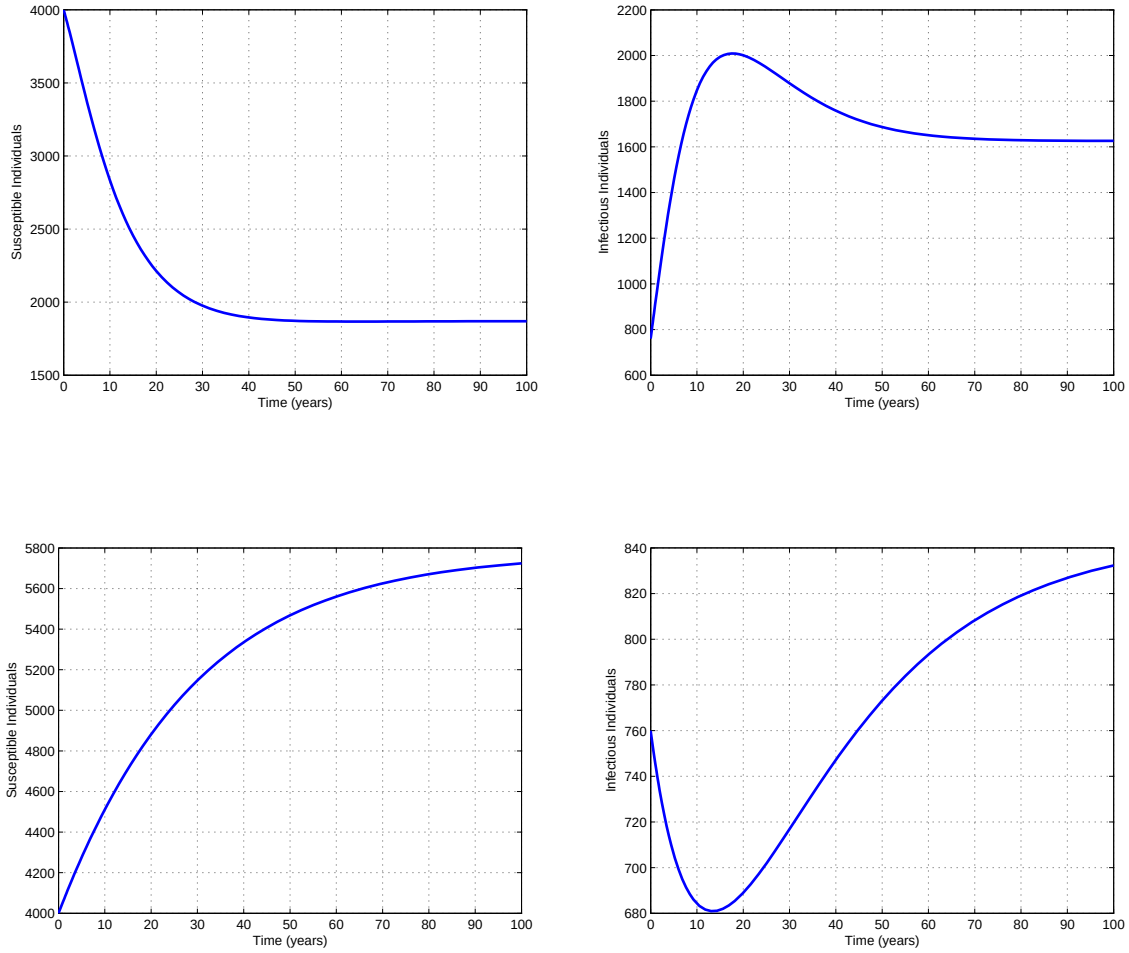

Figure 2.4.2.8: Profiles of solutions [susceptibles ($S(t)$): left column and infectious individuals ($I(t)$): right column] when $k = 1$, $\lambda_0 = 5.9$ (first row), $\lambda_0 = 40$ (second row) and with initial conditions $(S(0), I(0)) = (4000, 760)$.

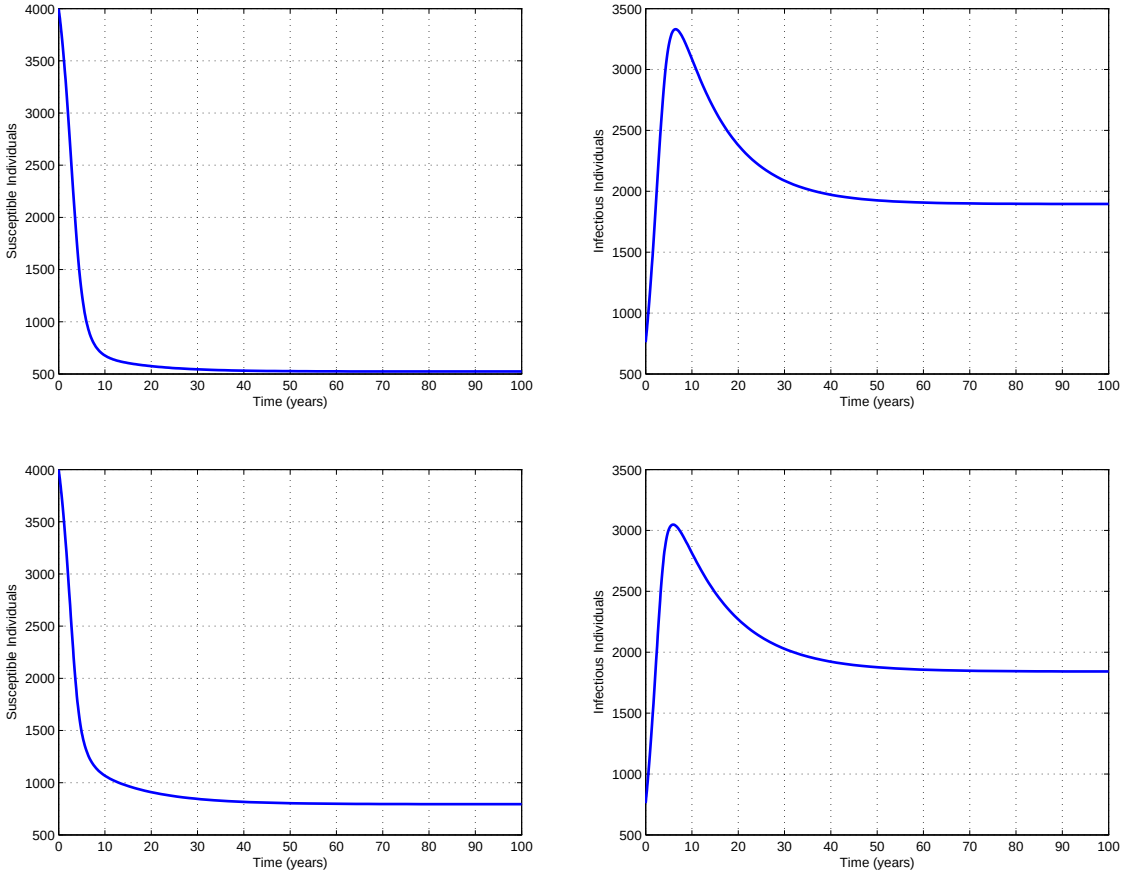

Figure 2.4.2.9: Profiles of solutions [susceptibles ($S(t)$): left column and infectious individuals ($I(t)$): right column] when $k = 10$, $\lambda_0 = 5.9$ (first row), $\lambda_0 = 40$ (second row) and with initial conditions $(S(0), I(0)) = (4000, 760)$.

2.5 Summary and discussion

In this chapter, a mathematical model of the transmission dynamics of HIV is developed and analyzed. The population in this model is classified into susceptibles and infectious subgroups. The system is analyzed mathematically with regard to well-posedness, positivity, invariant region, boundedness of solutions. We also analyzed the system's equilibria and their stability. We found that the basic reproduction number completely determines the dynamics of the system around the models' equilibria. If $R_0^{HIV} < 1$,

only the disease-free equilibrium exists and it is globally asymptotically stable. If $R_0^{HIV} > 1$, then only one stable endemic equilibrium exists.

We found that although the Hill coefficient k and the parameter responsible for behavior change, λ_0, are not affecting the stability of the system equilibria, they affected the values of the endemic equilibria and hence the HIV prevalence. The HIV prevalence is found increasing with k and decreasing with λ_0.

The analysis in this chapter indicates how the Hill coefficient k can be used to capture different responses of individuals to educational campaigns. The information that we receive by analyzing the model proposed in this chapter suggests that studying this effect can be useful in designing efficient educational campaigns. It is anticipated that such responses also affect the dynamics of TB and therefore in next chapter we investigate the above approach to study a co-infection model of HIV-TB.

Chapter 3

Analysis of an HIV-TB co-infection model with behavior change

We consider a deterministic model for the co-infection of HIV and TB that accounts for behavior change. It is a combination of the tuberculosis (TB) sub-model presented in [10] and the HIV model developed in Chapter 2. The resulting model accounts, in addition to behavior change, for modeling different responses of individuals to HIV prevalence. This is achieved by the Hill coefficient in the response function. Using the center manifold theory, we show that the full (HIV-TB co-infection) model exhibits backward bifurcation. Numerical simulations of this full model are carried out to show that the two diseases co-exist and the way individuals respond to the HIV prevalence does not only affect the HIV prevalence but it also affects the TB prevalence.

3.1 Introduction

The co-infection of HIV and TB presents an immediate and grave public health and socioeconomic threat, particularly in the developing countries. According to the website of WHO, millions of people had been infected with both HIV since the beginning of the pandemic; 95% of them were in the developing countries. This association between the two diseases is evident from the high incidence of tuberculosis among HIV-infected

individuals and the high occurrence of TB among AIDS patients.

Mathematical modeling has been proven to be a powerful tool in understanding the dynamics of many models arising in biology. Although there are many of such studies on HIV and TB epidemics as single diseases, only few researchers studied the co-infection of HIV-TB on population level. Some of these works can be found in [17, 88, 121, 129, 141]. Unlike these studies, where the contact rate of HIV is considered as a constant, other researchers studied the impact of considering a variable contact rate of HIV by inclusion of behavior change, to possibly prevent the HIV transmissions, on the dynamics of their co-infected models. This effect is studied by many researchers, for example [11, 26, 29, 52, 60, 106], when modeling HIV as a single disease. However, only few authors considered this when modeling the co-epidemics of HIV-TB.

In [10], Bacaër *et al.* considered an exponentially decreasing function of HIV prevalence for the contact rate of HIV to reflect behavior change as HIV awareness develops in the HIV_- population. Also, Long *et al.* [79] considered in their model a contact rate as a function of the average number of sexual partners, the average condom usage rate and infectivity allowing for variable contact rate as sexual behavior patterns and infectivity change as HIV progresses to AIDS. However, non of these co-infected models addressed the issue of how individuals respond to a higher HIV prevalence will affect the model dynamics. The various responses from individuals are not widely addressed, and hence, we believe it is important to study how they affect the HIV prevalence in the presence of TB. We also wanted to know if these responses can affect the TB prevalence as well.

Therefore, in this chapter we analyze a mathematical model for the transmission dynamics of the joint epidemics of HIV-TB taking into account the impacts of the response function (modeled by a type of Hill function). We also investigate the effects of this function with respect to its respective parameters on the system equilibria, the HIV and TB prevalences and the bifurcation behavior of the system.

We have shown that the disease free equilibrium is globally asymptotically stable if the basic reproduction number R_0 is less than unity independent of the parameters

of the response function. These parameters are found to alter the value of the endemic equilibrium of the full model. Further, they also have an impact not only on the HIV prevalence but also on the TB prevalence. Furthermore, we have shown that the full HIV-TB co-infection model exhibits a backward bifurcation.

We have organized this chapter as follows. The Model description is presented in Section 3.2. In Section 3.4 we present the mathematical analysis of the model. We carry out some numerical results and simulations in Section 3.5. Finally, in Section 3.6, we discuss these results.

3.2 Model description

The mathematical model of HIV-TB confection of our interest combines two states for HIV (HIV_- and HIV_+) with three states for TB (susceptible (S_i), latent (E_i) and infectious individuals (I_i), $i = 1, 2$. The subscript 1 refers to HIV_- individuals and the subscript 2 refers to HIV_+ individuals. The original model has been modified by considering the HIV model that we have developed and fully analyzed in Chapter 2. This will allow us to consider various responses of individuals to higher HIV prevalence.

The evolution of both diseases is given in the compartmental diagram 3.3. The descriptions and values for the time-invariant parameters of the model (as presented in [10]) are given in the following table.

Table 3.2.0.1: Description and values of parameters used in system (3.2.0.1).

Description	HIV_-	Value	HIV_+	Value
Mortality rate	μ_1	0.02/year	μ_2	0.1/year
TB mortality rate	m_1	0.25/year	m_2	1.6/year
MTB infections rate	k_1	11.4/year	k_2	$k_1 \times 2/3$
Fast route rate	p_1	11%	p_2	30%
Slow route rate	a_1	0.0003/year	a_2	0.08/year
Reinfection rate	q_1	$0.7p_1$	q_2	$0.75p_2$
Recovery rate	β_1	0.25/year	β_2	0.4/year
Detection rate	γ_1	0.74/year	γ_2	3.0/year
Treatment rate	ε_1	80%	ε_2	80%
Births rate	B	200/year		
Contact rate	d	0.7/year		
Behavior change parameter	λ_0	5.9		
Hill coefficient	k	Variable		
Initial year	t_0	1984		

Using the above notations, the governing model is described by the following non-linear system of ordinary differential equations:

$$\begin{aligned}
\frac{dS_1}{dt} &= B - S_1\left(\frac{k_1I_1 + k_2I_2}{N}\right) - \mu_1 S_1 - f(H)HS_1,\\
\frac{dE_1}{dt} &= ((1-p_1)S_1 - q_1E_1)\left(\frac{k_1I_1 + k_2I_2}{N}\right) - (a_1+\mu_1)E_1 + b_1I_1 - f(H)HE_1,\\
\frac{dI_1}{dt} &= (p_1S_1 + q_1E_1)\left(\frac{k_1I_1 + k_2I_2}{N}\right) - (b_1+m_1)I_1 + a_1E_1 - f(H)HI_1,\\
\frac{dS_2}{dt} &= -S_2\left(\frac{k_1I_1 + k_2I_2}{N}\right) - \mu_2 S_2 + f(H)HS_1,\\
\frac{dE_2}{dt} &= ((1-p_2)S_2 - q_2E_2)\left(\frac{k_1I_1 + k_2I_2}{N}\right) - (a_2+\mu_2)E_2 + b_2I_2 + f(H)HE_1,\\
\frac{dI_2}{dt} &= (p_2S_2 + q_2E_2)\left(\frac{k_1I_1 + k_2I_2}{N}\right) - (b_2+m_2)I_2 + a_2E_2 + f(H)HI_1,
\end{aligned} \tag{3.2.0.1}$$

where

$$N = S_1 + E_1 + I_1 + S_2 + E_2 + I_2, \tag{3.2.0.2}$$

is the total number of population, and

$$H = \frac{S_2 + E_2 + I_2}{N}, \tag{3.2.0.3}$$

is the HIV prevalence.

The function $f(H)$, which represents the transmission rate of HIV, is considered as the following function of Hill type (as in the previous chapter)

$$f(H) = \frac{d}{1 + \lambda_0 H^k}, \quad k \geq 1, \tag{3.2.0.4}$$

where k is the Hill coefficient. It should be noted that the above function is chosen as a decreasing function of H to reflect reduction in risky behavior resulting from the awareness of individuals to a higher HIV prevalence.

3.3 TB-only sub-model

Associated with the full model (3.2.0.1) is the following tuberculosis (TB) sub-model (when there is no HIV infections):

$$\begin{aligned}
\frac{dS_1}{dt} &= B - S_1\left(\frac{k_1 I_1}{N_2}\right) - \mu_1 S_1, \\
\frac{dE_1}{dt} &= ((1-p_1)S_1 - q_1 E_1)\left(\frac{k_1 I_1}{N_2}\right) - (a_1 + \mu_1)E_1 + b_1 I_1, \\
\frac{dI_1}{dt} &= (p_1 S_1 + q_1 E_1)\left(\frac{k_1 I_1}{N_2}\right) - (b_1 + m_1)I_1 + a_1 E_1,
\end{aligned} \tag{3.3.0.5}$$

where

$$N_2 = S_1 + E_1 + I_1. \tag{3.3.0.6}$$

The evolution of the TB disease is given in the following compartmental diagram.

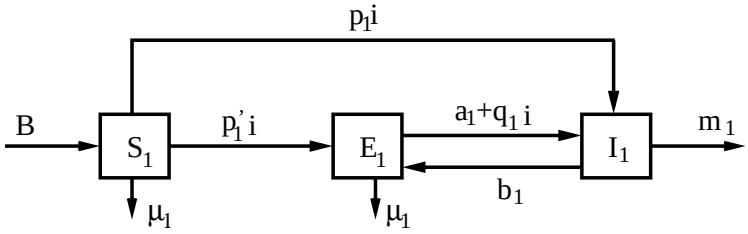

Figure 3.3.0.1: Flows between the compartments of the TB-only model $i = k_1 I_1/N_2$ and $p' = 1 - p_1$.

The following results determine the basic qualitative features of the continuous model (3.3.0.5). Main results remain the same as presented in [10], and hence, we will provide only the proof of some of them which are not provided in [10]. More detailed analysis can be found in that work.

It is important to prove that the state variables $S_1(t)$, $E_1(t)$ and $I_1(t)$ of system (3.3.0.5) are nonnegative for all time $t > 0$ since we are dealing with human population. For this, we state and prove the next proposition.

Proposition 3.3.1. *If $S_1(0)$, $E_1(0)$ and $I_1(0)$ are non-negative, then so are $S_1(t)$, $E_1(t)$ and $I_1(t)$ for all $t > 0$. Moreover,*

$$\lim_{t\to\infty} N_2(t) \leq \frac{B}{\gamma_1}, \tag{3.3.0.7}$$

where $\gamma_1 = \min(\mu_1, m_1)$. Furthermore, if in addition $N(0) \leq B/\gamma_1$, then $N_2(t) \leq B/\gamma_1$. In particular, the region

$$\mathcal{D}_T = \left\{ (S_1(0),\, E_1(0),\, I_1(0)) \in \mathbb{R}^3_+ : S_1 + E_1 + I_1 \leq \frac{B}{\gamma_1} \right\},$$

is positively-invariant.

Proof. We denote by t_{max} the upper bound of the maximum interval of existence corresponding to $(S_1(t), E_1(t), I_1(t))$. To show that the solution is positive and bounded in $[0, +\infty[$, it is sufficient to show that it is positive and bounded in $[0, t_{max}[$.

Let

$$t_1 = \sup\{0 \leq t < t_{max} : S_1, E_1 \text{ and } I_1 \text{ are positive on } [0, t]\}.$$

Since $S_1(0)$, $E_1(0)$ and $I_1(0)$ are non-negative then $t_1 > 0$. If $t_1 < t_{max}$ then by using the variation of constants formula to the first equation of system (3.2.0.1), we have

$$S_1(t_1) = S_1(0)e^{-\mu_1 t_1 - \int_0^{t_1} \zeta_1(v)dv} + B\int_0^{t_1} e^{-\mu_1(t_1-u) - \int_u^{t_1} \zeta_1(v)dv} du > 0, \qquad (3.3.0.8)$$

where

$$\zeta_1(t) = \frac{k_1 I_1(t)}{N_2(t)}.$$

If $t_1 < t_{max}$, then from (3.3.0.8), we have $S_1(t_1)$ is positive. It can be shown in a similar manner that the other variables are also positive at t_1. This contradicts the fact that t_1 is the supremum because at least one of the variable should be equal to zero at t_1. Therefore $t_1 = t_{max}$ and the solution is positive on its maximal interval of existence $[0, t_{max}[$.

Next, we show that the solution is bounded on $[0, t_{max}[$. By using Theorem 1.3.1.4 and by accounting for the positivity of the solution on $[0, t_{max}[$, we obtain from the equations of system (3.3.0.5)

$$\begin{aligned} \frac{dN_2}{dt} &= B - \mu_1(S_1 + E_1) - m_1 I_1, \\ &\leq B - \gamma_1 N_2(t), \end{aligned} \qquad (3.3.0.9)$$

where $\gamma_1 = \min(\mu_1, m_1)$.
Hence,

$$0 \leq N_2(t) \leq N(0)e^{-\gamma_1 t} + \frac{B}{\gamma_1}\left(1 - e^{-\gamma_1 t}\right), \qquad (3.3.0.10)$$

Therefore $N_2(t)$ is bounded on $[0, t_{max}[$. Hence $t_{max} = \infty$ which proves the global existence and the positivity results.

Concerning the invariance properties, it is easy to obtain from (3.3.0.10) that if $N_2(0) \leq B/\gamma_1$, then $N_2(t) \leq B/\gamma_1$. This establishes the invariance of $\mathcal{D}_T$ as required. The result (3.3.0.7) follows immediately from (3.3.0.10). □

The basic reproduction number of system (3.3.0.5), denoted by R_0^{TB}, is given by

$$R_0^{TB} = \frac{k_1(a_1 + p_1\mu_1)}{a_1m_1 + m_1\mu_1 + \mu_1b_1}. \tag{3.3.0.11}$$

Furthermore, explicit form of the equilibria of system (3.3.0.5) are not obtainable. Alternatively, we write them in terms of the force of infection of TB,

$$\lambda_T^* = \frac{k_1I_1^*}{S_1^* + E_1^* + I_1^*}, \tag{3.3.0.12}$$

as follows

$$S_1^* = \frac{B}{\lambda_T^* + \mu_1}, \tag{3.3.0.13}$$

$$E_1^* = \frac{B\lambda_T^*(b_1 + m_1(1 - p_1))}{(\lambda_T^* + \mu_1)\left[m_1q_1\lambda_T^* + (a_1m_1 + m_1\mu_1 + \mu_1b_1)\right]}, \tag{3.3.0.14}$$

$$I_1^* = \frac{B\lambda_T^*(a_1 + p_1\mu_1 + q_1\lambda_T^*)}{(\lambda_T^* + \mu_1)\left[m_1q_1\lambda_T^* + (a_1m_1 + m_1\mu_1 + \mu_1b_1\right]}. \tag{3.3.0.15}$$

Thus, evaluation of equilibria for system (3.3.0.5) results into the following characteristic equation

$$\lambda_T^*((\lambda_T^*)^2 + A_1\lambda_T^* + A_2) = 0, \tag{3.3.0.16}$$

where

$$A_1 = \frac{a_1 + b_1 + (1 - p_1)m_1 + p_1\mu_1}{q_1} + m_1 - k_1, \tag{3.3.0.17}$$

and

$$A_2 = \frac{(\mu_1 b_1 + m_1\mu_1 + m_1 a_1)(1 - R_0^{TB})}{q_1}. \tag{3.3.0.18}$$

The following theorem gives the conditions for which the equation (3.3.0.16) will have nonnegative roots, and hence the nonnegative equilibria of system (3.3.0.5).

Theorem 3.3.0.1. *(i) Equation (3.3.0.16) always has the solution $\lambda_T^* = 0$, which is corresponding to the disease free equilibrium $E_0^* = (B/\mu_1, 0, 0)$.*
(ii) If $R_0^{TB} < 1$ and $q_1 > p_1$, then equation (3.3.0.16) has, in addition to the disease free equilibrium, two positive solutions, and hence system (3.3.0.5) has two positive endemic equilibria (a case of backward bifurcation).
(iii) If $R_0^{TB} > 1$, then system (3.3.0.5) has exactly one endemic equilibrium (a case of forward bifurcation).

Remark 3.3.0.1. As pointed out in [10], realistically q_1 is always less than p_1. Hence, system (3.3.0.5) have only the disease free equilibrium if $R_0^{TB} < 1$ and exactly one endemic equilibrium if $R_0^{TB} > 1$.

It can easily be proved that these equilibria have the following stability properties:

Theorem 3.3.0.2. *The disease free equilibrium of system (3.3.0.5), E_0^*, is locally asymptotically stable if $R_0^{TB} < 1$ and unstable if $R_0^{TB} > 1$.*

Theorem 3.3.0.3. *If $p_1 > q_1$, then the unique endemic equilibrium of system (3.3.0.5), E^*, is locally asymptotically stable provided that $R_0^{TB} > 1$ but close to 1.*

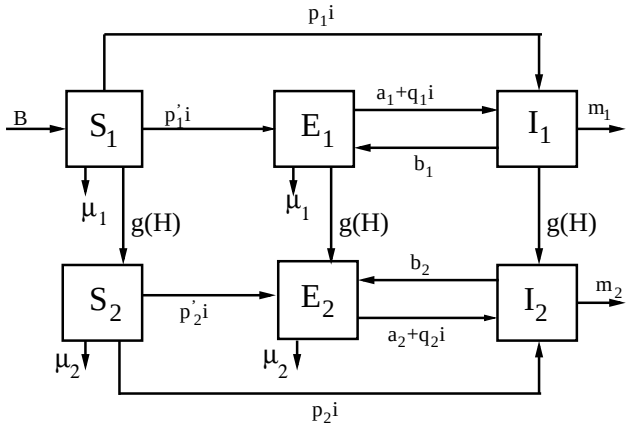

Figure 3.3.0.2: Flows between the compartments describing the HIV-TB dynamics $i = (k_1 I_1 + k_2 I_2)/N$, $g(H) = f(H)H$, $p_1' = (1 - p_1)$, $p_2' = (1 - p_2)$.

3.4 Mathematical analysis of the full model

In this section we present some properties that system (3.2.0.1) satisfies. Furthermore, we determine basic reproduction number and equilibria and their stability properties.

3.4.1 Well-posedness

Using results of Section 1.3.1, we show that system (3.2.0.1) is well-posed, that is, its solution exists, unique, and continuously depends on the initial values. It suffices to show that the system satisfies the Lipschitz condition given in Definition 1.3.1.1.

Proposition 3.4.1. *System (3.2.0.1) has a unique solution that is continuously depend on its initial values.*

Proof. Let

$$\mathbf{X}(\mathbf{x}, t) = [f_1(\mathbf{x}(t)), f_2(\mathbf{x}(t)), f_3(\mathbf{x}(t)), f_4(\mathbf{x}(t)), f_5(\mathbf{x}(t)), f_6(\mathbf{x}(t))]^T,$$

where $\mathbf{x}(t) = [S_1(t), E_1(t), I_1(t), S_2(t), E_2(t), I_2(t)]^T$ such that $f_1(\mathbf{x}(t))$, $f_2(\mathbf{x}(t))$, $f_3(\mathbf{x}(t))$, $f_4(\mathbf{x}(t))$, $f_5(\mathbf{x}(t))$ and $f_6(\mathbf{x}(t))$ represent the right hand sides of system (3.2.0.1) and

let $\mathbf{x(t)}$ and $\check{\mathbf{x}}\mathbf{(t)}$ be in some region $\mathcal{R} = \mathbb{R}^6$ where

$$\check{\mathbf{x}}(t) = \left[\check{S}_1(t), \check{E}_1(t), \check{I}_1(t), \check{S}_1(t), \check{E}_1(t), \check{I}_1(t)\right]^T.$$

Then system (3.2.0.1) can be written as follows

$$|\mathbf{X}(\mathbf{x},t) - \mathbf{X}(\check{\mathbf{x}},t)| = \left|\left|\begin{bmatrix} f_1(\mathbf{x}(t)) \\ f_2(\mathbf{x}(t)) \\ f_3(\mathbf{x}(t)) \\ f_4(\mathbf{x}(t)) \\ f_5(\mathbf{x}(t)) \\ f_6(\mathbf{x}(t)) \end{bmatrix} - \begin{bmatrix} f_1(\check{\mathbf{x}}(t)) \\ f_2(\check{\mathbf{x}}(t)) \\ f_3(\check{\mathbf{x}}(t)) \\ f_4(\check{\mathbf{x}}(t)) \\ f_5(\check{\mathbf{x}}(t)) \\ f_6(\check{\mathbf{x}}(t)) \end{bmatrix}\right|\right|,$$

$$= \left|\left|\begin{bmatrix} -\mu_1(S_1 - \check{S}_1) \\ -(a_1+\mu_1)(E_1 - \check{E}_1) + b_1(I_1 - \check{I}_1) \\ a_1(E_1 - \check{E}_1) - (b_1+m_1)(I_1 - \check{I}_1) \\ -\mu_2(S_2 - \check{S}_2) \\ -(a_2+\mu_2)(E_2 - \check{E}_2) + b_2(I_2 - \check{I}_2) \\ a_2(E_2 - \check{E}_2) - (b_2+m_2)(I_2 - \check{I}_2) \end{bmatrix} + \begin{bmatrix} \mathcal{J}_1 \\ \mathcal{J}_2 \\ \mathcal{J}_3 \\ \mathcal{J}_4 \\ \mathcal{J}_5 \\ \mathcal{J}_6 \end{bmatrix}\right|\right|,$$

$$\leq \left|\left|\begin{bmatrix} -\mu_1(S_1 - \check{S}_1) \\ -(a_1+\mu_1)(E_1 - \check{E}_1) + b_1(I_1 - \check{I}_1) \\ a_1(E_1 - \check{E}_1) - (b_1+m_1)(I_1 - \check{I}_1) \\ -\mu_2(S_2 - \check{S}_2) \\ -(a_2+\mu_2)(E_2 - \check{E}_2) + b_2(I_2 - \check{I}_2) \\ a_2(E_2 - \check{E}_2) - (b_2+m_2)(I_2 - \check{I}_2) \end{bmatrix}\right|\right|,$$

$$= \begin{bmatrix} -\mu_1 & 0 & 0 & 0 & 0 & 0 \\ 0 & -(a_1+\mu_1) & b_1 & 0 & 0 & 0 \\ 0 & a_1 & -(b_1+m_1) & 0 & 0 & 0 \\ 0 & 0 & 0 & -\mu_2 & 0 & 0 \\ 0 & 0 & 0 & 0 & -(a_2+\mu_2) & b_2 \\ 0 & 0 & 0 & 0 & a_2 & -(b_2+m_2) \end{bmatrix} \left\| \begin{bmatrix} S_1-\check{S}_1 \\ E_1-\check{E}_1 \\ I_1-\check{I}_1 \\ S_2-\check{S}_1 \\ E_2-\check{E}_1 \\ I_2-\check{I}_1 \end{bmatrix} \right\|,$$

where

$$\begin{aligned}
\mathcal{J}_1 &= \check{S}_1\check{r}(\check{I}_1,\check{I}_2) - S_1 r(I_1,I_2) + f(\check{H})\check{H}\check{S}_1 - f(H)HS_1, \\
\mathcal{J}_2 &= -((1-p_1)\check{S}_1 - q_1\check{E}_1)\check{r}(\check{I}_1,\check{I}_2) + ((1-p_1)S_1 - q_1E_1)r(I_1,I_2) \\
&\quad + f(\check{H})\check{H}\check{E}_1 - f(H)HE_1, \\
\mathcal{J}_3 &= -(p_1\check{S}_1 + q_1\check{E}_1)\check{r}(\check{I}_1,\check{I}_2) + (p_1S_1 + q_1E_1)r(I_1,I_2) + f(\check{H})\check{H}\check{I}_1 - f(H)HI_1, \\
\mathcal{J}_4 &= -f(\check{H})\check{H}\check{S}_1 + f(H)HS_1 + \check{S}_2\check{r}(\check{I}_1,\check{I}_2) - S_2 r(I_1,I_2), \\
\mathcal{J}_5 &= -((1-p_2)\check{S}_2 - q_2\check{E}_2)\check{r}(\check{I}_1,\check{I}_2) + ((1-p_2)S_2 - q_2E_2)r(I_1,I_2) \\
&\quad - f(\check{H})\check{H}\check{E}_1 + f(H)HE_1, \\
\mathcal{J}_6 &= -(p_2\check{S}_2 + q_2\check{E}_2)\check{r}(\check{I}_1,\check{I}_2) + (p_2S_2 + q_2E_2)r(I_1,I_2) - f(\check{H})\check{H}\check{I}_1 + f(H)HI_1,
\end{aligned}$$

with

$$r(I_1,I_2) = \frac{k_1I_1 + k_2I_2}{N} \quad \text{and} \quad \check{r}(\check{I}_1,\check{I}_2) = \frac{k_1\check{I}_1 + k_2\check{I}_2}{\check{N}},$$

where

$$\check{N} = \check{S}_1 + \check{E}_1 + \check{I}_1 + \check{S}_2 + \check{E}_2 + \check{I}_2.$$

Thus, we have

$$|\mathbf{X}(\mathbf{x},t) - \mathbf{X}(\mathbf{y},t)| \leq L|\mathbf{x}-\mathbf{y}|, \tag{3.4.1.1}$$

where L is a Lipschitz constant representing the norm of the matrix

$$\begin{pmatrix} -\mu_1 & 0 & 0 & 0 & 0 & 0 \\ 0 & -(a_1+\mu_1) & b_1 & 0 & 0 & 0 \\ 0 & a_1 & -(b_1+m_1) & 0 & 0 & 0 \\ 0 & 0 & 0 & -\mu_2 & 0 & 0 \\ 0 & 0 & 0 & 0 & -(a_2+\mu_2) & b_2 \\ 0 & 0 & 0 & 0 & a_2 & -(b_2+m_2) \end{pmatrix}.$$

This completes the proof. □

Remark 3.4.1.1. *As in the previous chapter, it is should be noted that we could prove the above because of the boundness of the state variables of the system and that of H and $f(H)$.*

3.4.2 Positively-invariant region

It is important to prove that the state variables $S_1(t)$, $E_1(t)$, $I_1(t)$, $S_2(t)$, $E_2(t)$ and $I_2(t)$ of system (3.2.0.1) are nonnegative for all time $t > 0$ since we are dealing with human population. For this, we state and prove the next proposition.

Proposition 3.4.2. *If $S_1(0)$, $E_1(0)$, $I_1(0)$, $S_2(0)$, $E_2(0)$ and $I_2(0)$ are non-negative, then so are $S_1(t)$, $E_1(t)$, $I_1(t)$, $S_2(t)$, $E_2(t)$ and $I_2(t)$ for all $t > 0$. Moreover,*

$$\lim_{t\to\infty} N(t) \leq \frac{B}{\gamma}, \tag{3.4.2.1}$$

where $\gamma = \min(\mu_1, m_1, \mu_2, m_2)$. If in addition $N(0) \leq B/\gamma$, then $N(t) \leq B/\gamma$. In particular, the region

$$\mathcal{D} = \left\{ (S_1(0),\, E_1(0),\, I_1(0),\, S_2(0),\, E_2(0),\, I_2(0)) \in \mathbb{R}^6_+ : S_1 + E_1 + I_1 + S_2 + E_2 + I_2 \leq \frac{B}{\gamma} \right\},$$

is positively-invariant.

Proof. We denote by t_{max} the upper bound of the maximum interval of existence corresponding to $(S(t), I(t))$. To show that the solution is positive and bounded in $[0, +\infty[$, it is sufficient to show the positivity and boundedness results in $[0, t_{max}[$. Let

$$t_1 = \sup\{0 \leq t < t_{max} : S_1, E_1, I_1, S_2, E_2 \text{ and } I_2 \text{ are positive on } [0, t]\}.$$

Since $S_1(0)$, $E_1(0)$, $I_1(0)$, $S_2(0)$, $E_2(0)$ and $I_2(0)$ are non-negative then $t_1 > 0$. If $t_1 < t_{max}$ then by using the variation of constants formula to the first equation of system (3.2.0.1), we have

$$S_1(t_1) = S_1(0)e^{-\mu_1 t_1 - \int_0^{t_1} \zeta(v)dv} + B\int_0^{t_1} e^{-\mu_1(t_1-u) - \int_u^{t_1} \zeta(v)dv}du > 0, \qquad (3.4.2.2)$$

where

$$\zeta(t) = \mu_1 + f(H(t))H(t) + \frac{k_1 I_1(t) + k_2 I_2(t)}{N(t)}.$$

If $t_1 < t_{max}$, then from (3.4.2.2), we have $S_1(t_1)$ is positive. It can be shown in the same manner that the other variables are also positive at t_1. This contradicts the fact that t_1 is the supremum because at least one of the variable should be equal to zero at t_1. Therefore $t_1 = t_{max}$ and the solution is positive on its maximal interval of existence $[0, t_{max}[$.

Next, we show that the solution is bounded on $[0, t_{max}[$. By using Theorem 1.3.1.4 and by accounting for the positivity of the solution on $[0, t_{max}[$, we obtain from the equations of system (3.2.0.1)

$$\begin{aligned} \frac{dN}{dt} &= B - \mu_1(S_1 + E_1) - m_1 I_1 - \mu_2(S_2 + E_2) - m_2 I_2, \\ &\leq B - \gamma N(t), \end{aligned} \qquad (3.4.2.3)$$

where $\gamma = \min(\mu_1, m_1, \mu_2, m_2)$.

Hence,

$$0 \leq N(t) \leq N(0)e^{-\gamma t} + \frac{B}{\gamma}\left(1 - e^{-\gamma t}\right), \tag{3.4.2.4}$$

Therefore $N(t)$ is bounded on $[0, t_{max}[$. Hence $t_{max} = \infty$ which proves the global existence and the positivity results.

Concerning the invariance properties, it is easy to obtain from (3.4.2.4) that if $N(0) \leq \frac{B}{\gamma}$ then $N(t) \leq \frac{B}{\gamma}$. This establishes the invariance of $\mathcal{D}$ as required. The results on (3.4.2.1) follows immediately from (3.4.2.4). □

3.4.3 Basic reproduction number (R_0)

To obtain the basic reproduction number, R_0, for the full model (3.2.0.1), we again apply the next generation matrix approach [137]. For this, we re-write the system in the following order

$$\begin{aligned}
\frac{dE_1}{dt} &= ((1-p_1)S_1 - q_1E_1)\left(\frac{k_1I_1 + k_2I_2}{N}\right) - (a_1+\mu_1)E_1 + b_1I_1 - f(H)HE_1,\\
\frac{dI_1}{dt} &= (p_1S_1 + q_1E_1)\left(\frac{k_1I_1 + k_2I_2}{N}\right) - (b_1+m_1)I_1 + a_1E_1 - f(H)HI_1,\\
\frac{dE_2}{dt} &= ((1-p_2)S_2 - q_2E_2)\left(\frac{k_1I_1 + k_2I_2}{N}\right) - (a_2+\mu_2)E_2 + b_2I_2 + f(H)HE_1,\\
\frac{dI_2}{dt} &= (p_2S_2 + q_2E_2)\left(\frac{k_1I_1 + k_2I_2}{N}\right) - (b_2+m_2)I_2 + a_2E_2 + f(H)HI_1,\\
\frac{dS_2}{dt} &= -S_2\left(\frac{k_1I_1 + k_2I_2}{N}\right) - \mu_2S_2 + f(H)HS_1,\\
\frac{dS_1}{dt} &= B - S_1\left(\frac{k_1I_1 + k_2I_2}{N}\right) - \mu_1S_1 - f(H)HS_1.
\end{aligned} \tag{3.4.3.1}$$

Thus, we have

$$\mathcal{F} = \begin{pmatrix} \frac{(1-p_1)S_1(k_1I_1+k_2I_2)}{S_1+E_1+I_1+S_2+E_2+I_2} \\ \frac{(p_1S_1+q_1E_1)(k_1I_1+k_2I_2)}{S_1+E_1+I_1+S_2+E_2+I_2} \\ \frac{(1-p_2)S_2(k_1I_1+k_2I_2)}{S_1+E_1+I_1+S_2+E_2+I_2} + f(H)HE_1 \\ \frac{(p_2S_2+q_2E_2)(k_1I_1+k_2I_2)}{(S_1+E_1+I_1+S_2+E_2+I_2)} + f(H)HI_1 \\ 0 \\ f(H)HS_1 \end{pmatrix},$$

and

$$\mathcal{V} = \begin{pmatrix} \frac{q_1E_1(k_1I_1+k_2I_2)}{S_1+E_1+I_1+S_2+E_2+I_2} + (a_1+\mu_1)E_1 - b_1I_1 + f(H)HE_1 \\ (b_1+m_1)I_1 - a_1E_1 + f(H)HI_1 \\ \frac{q_2E_2(k_1I_1+k_2I_2)}{S_1+E_1+I_1+S_2+E_2+I_2} + (a_2+\mu_2)E_2 - b_2I_2 \\ (b_2+m_2)I_2 - a_2E_2 \\ \frac{S_1(k_1I_1+k_2I_2)}{S_1+E_1+I_1+S_2+E_2+I_2} - B + \mu_1S_1 + f(H)HS_1 \\ \frac{S_2(k_1I_1+k_2I_2)}{S_1+E_1+I_1+S_2+E_2+I_2} + \mu_2S_2. \end{pmatrix}.$$

The infected compartments are E_1, I_1, E_2, I_2 and S_2. Therefore, the matrices F and V for the new infection terms and the remaining transfer terms are respectively given by

$$F = \begin{pmatrix} 0 & (1-p_1)k_1 & 0 & (1-p_1)k_2 & 0 \\ 0 & p_1k_1 & 0 & p_1k_2 & 0 \\ 0 & 0 & 0 & 0 & 0 \\ 0 & 0 & 0 & 0 & 0 \\ 0 & 0 & d & d & d \end{pmatrix},$$

and

$$V = \begin{pmatrix} a_1+\mu_1 & -b_1 & 0 & 0 & 0 \\ -a_1 & b_1+m_1 & 0 & 0 & 0 \\ 0 & 0 & a_2+\mu_2 & -b_2 & 0 \\ 0 & 0 & -a_2 & b_2+m_2 & 0 \\ 0 & 0 & 0 & 0 & \mu_2 \end{pmatrix}.$$

Therefore,

$$FV^{-1} = \begin{pmatrix} \frac{(1-p_1)k_1a_1}{b_1\mu_1+m_1a_1+m_1\mu_1} & \frac{(1-p_1)k_1(a_1+\mu_1)}{b_1\mu_1+m_1a_1+m_1\mu_1} & \frac{(1-p_1)k_2a_2}{b_2\mu_2+m_2a_2+m_2\mu_2} & \frac{(1-p_1)k_2(a_2+\mu_2)}{b_2\mu_2+m_2a_2+m_2\mu_2} & 0 \\ \frac{p_1k_1a_1}{b_1\mu_1+m_1a_1+m_1\mu_1} & \frac{p_1k_1(a_1+\mu_1)}{b_1\mu_1+m_1a_1+m_1\mu_1} & \frac{p_1k_2a_2}{b_2\mu_2+m_2a_2+m_2\mu_2} & \frac{p_1k_2(a_2+\mu_2)}{b_2\mu_2+m_2a_2+m_2\mu_2} & 0 \\ 0 & 0 & 0 & 0 & 0 \\ 0 & 0 & 0 & 0 & 0 \\ 0 & 0 & \frac{d(b_2+m_2)+da_2}{b_2\mu_2+m_2a_2+m_2\mu_2} & \frac{d(a_2+\mu_2)+db_2}{b_2\mu_2+m_2a_2+m_2\mu_2} & \frac{d}{\mu_2} \end{pmatrix}.$$

The dominant eigenvalues of the above matrix are

$$R_0^{HIV} = \frac{d}{\mu_2}, \tag{3.4.3.2}$$

which is the basic reproduction number for the HIV sub-model (2.2.0.1), and

$$R_0^{TB} = \frac{k_1(a_1+p_1\mu_1)}{a_1m_1+m_1\mu_1+\mu_1b_1}, \tag{3.4.3.3}$$

which is the basic reproduction number for the TB sub-model (3.3.0.5). Therefore, the basic reproduction number of the full model (3.2.0.1), denoted R_0, is given by

$$R_0 = \max\left\{R_0^{TB}, R_0^{HIV}\right\}. \tag{3.4.3.4}$$

3.4.4 Equilibria and stability analysis

To find equilibria of system (3.2.0.1), we denote any endemic equilibrium by $E^* = (S_1^*, E_1^*, I_1^*, S_2^*, E_2^*, I_2^*)$. By noting that

$$N^* = S_1^* + E_1^* + I_1^* + S_2^* + E_2^* + I_2^*, \tag{3.4.4.1}$$

and

$$H^* = \frac{S_2^* + E_2^* + I_2^*}{N^*}, \tag{3.4.4.2}$$

the forces of TB and HIV infections at the equilibrium are given by

$$\lambda_T^* = \frac{k_1 I_1^* + k_2 I_2^*}{N^*}, \tag{3.4.4.3}$$

and

$$\lambda_H^* = \frac{dH^*}{1 + \lambda (H^*)^k}, \tag{3.4.4.4}$$

respectively. Thus, the system (3.2.0.1) can be written in the following form

$$\begin{aligned}
\frac{dS_1}{dt} &= B - S_1\lambda_T^* - \mu_1 S_1 - \lambda_H^* S_1,\\
\frac{dE_1}{dt} &= ((1-p_1)S_1 - q_1 E_1)\lambda_T^* - (a_1+\mu_1)E_1 + b_1 I_1 - \lambda_H^* E_1,\\
\frac{dI_1}{dt} &= (p_1 S_1 + q_1 E_1)\lambda_T^* - (b_1+m_1)I_1 + a_1 E_1 - \lambda_H^* I_1,\\
\frac{dS_2}{dt} &= -S_2\lambda_T^* - \mu_2 S_2 + \lambda_H^* S_1,\\
\frac{dE_2}{dt} &= ((1-p_2)S_2 - q_2 E_2)\lambda_T^* - (a_2+\mu_2)E_2 + b_2 I_2 + \lambda_H^* E_1,\\
\frac{dI_2}{dt} &= (p_2 S_2 + q_2 E_2)\lambda_T^* - (b_2+m_2)I_2 + a_2 E_2 + \lambda_H^* I_1.
\end{aligned} \tag{3.4.4.5}$$

By equating the right hand side of system (3.4.4.5) to zero, we obtain the following endemic equilibrium in terms of the forces of infection λ_T^* and λ_T^*

$$\begin{aligned}
S_1^* &= \frac{B}{\lambda_T^* + \mu_1 + \lambda_H^*}, \\
E_1^* &= \frac{S_1^* \lambda_T^* (b_1 + (1-p_1)(m_1 + \lambda_H^*))}{(\mu_1 + \lambda_H^*)(b_1 + m_1 + \lambda_H^*) + (\lambda_T^* q_1 + a_1)(m_1 + \lambda_H^*)}, \\
I_1^* &= \frac{S_1^* \lambda_T^* p_1 + (\lambda_T^* q_1 + a_1) E_1^*}{b_1 + m_1 + \lambda_H^*}, \\
S_2^* &= \frac{\lambda_H^* S_1^*}{\lambda_T^* + \mu_2}, \\
E_2^* &= \frac{S_2^* \lambda_T^* (b_2 + m_2(1-p_2)) + b_2 \lambda_H^* I_1^* + \lambda_H^* E_1^* (b_2 + m_2)}{\mu_2 (b_2 + m_2) + m_2 (q_2 \lambda_T^* + a_2)}, \\
I_2^* &= \frac{S_2^* \lambda_T^* p_2 + \lambda_T^* q_2 E_2^* + a_2 E_2^* + \lambda_H^* I_1^*}{b_2 + m_2}.
\end{aligned}$$

By substituting these expressions into equations (3.4.4.3) and (3.4.4.4), we can see that the forces of infection λ_T^* and λ_H^* are the solution of the following nonlinear system

$$\begin{aligned}
F(\lambda_T^*, \lambda_H^*) &= 0, \\
G(\lambda_T^*, \lambda_H^*) &= 0,
\end{aligned} \tag{3.4.4.6}$$

where

$$\begin{aligned}
F(\lambda_T^*, \lambda_H^*) &= \lambda_T^* N^*(\lambda_T^*, \lambda_H^*) - \{k_1 I_1^*(\lambda_T^*, \lambda_H^*) + k_2 I_2^*(\lambda_T^*, \lambda_H^*)\}, \\
G(\lambda_T^*, \lambda_H^*) &= \lambda_H^* \left\{1 + \lambda_0 (H^*(\lambda_T^*, \lambda_H^*))^k\right\} - d H^*(\lambda_T^*, \lambda_H^*).
\end{aligned} \tag{3.4.4.7}$$

It should be noted that the solution $\lambda_T^* = 0$ and $\lambda_H^* = 0$ corresponds to the disease free equilibrium

$$E_0^* = \left(\frac{B}{\mu_1}, 0, 0, 0, 0, 0\right), \tag{3.4.4.8}$$

whereas the solution $\lambda_T^* = 0$ with $\lambda_H^* > 0$ corresponds to the endemic equilibrium of the HIV sub-model (2.2.0.1) and the solution $\lambda_H^* = 0$ with $\lambda_T^* > 0$ corresponds to

the endemic equilibrium of the TB sub-model (3.3.0.5). If $\lambda_T^* > 0$ and $\lambda_H^* > 0$, then this solution correspond to the endemic equilibrium of both diseases of the full model (3.2.0.1).

The system (3.4.4.6) is highly nonlinear in λ_T^* and λ_H^* and hence explicit solutions are not obtainable. Therefore, in Section 3.5, the endemic equilibria of system (3.2.0.1) will be obtained by numerically solving the system (3.2.0.1).

3.4.4.1 Local stability of the disease free equilibrium

In this section, we give the stability properties of the disease free equilibrium of system (3.2.0.1). We will make use of Theorem 1.3.2.1 to establish the following result.

Theorem 3.4.4.1. *The disease free equilibrium of system (3.2.0.1), E_0^*, is locally asymptotically if $R_0 < 1$ and unstable if $R_0 > 1$.*

Proof. To start with, we write $x = [S_1, E_1, I_1, S_2, E_2, I_2]^t$ where $x_1 = S_1$, $x_2 = E_1$, $x_3 = I_1$, $x_4 = S_2$, $x_5 = E_2$, and $x_6 = I_2$ with each $x_i \geq 0$, $i = 1, \cdots, 6$, and $N = x_1 + x_2 + x_3 + x_4 + x_5 + x_6$ is the total population. Then, we re-write system (3.2.0.1) as follows

$$\begin{aligned}
\frac{dx_2}{dt} &= ((1-p_1)x_1 - q_1x_2)\left(\frac{k_1x_3 + k_2x_6}{N}\right) - (a_1+\mu_1)x_2 + b_1I_1 - f(W)Wx_2,\\
\frac{dx_3}{dt} &= (p_1x_1 + q_1x_2)\left(\frac{k_1x_3 + k_2x_6}{N}\right) - (b_1+m_1)x_3 + a_1x_2 - f(W)Wx_3,\\
\frac{dx_5}{dt} &= ((1-p_2)x_4 - q_2x_5)\left(\frac{k_1x_3 + k_2x_6}{N}\right) - (a_2+\mu_2)x_5 + b_2x_6 + f(W)Wx_2,\\
\frac{dx_6}{dt} &= (p_2x_4 + q_2x_5)\left(\frac{k_1x_3 + k_2x_6}{N}\right) - (b_2+m_2)x_6 + a_2x_5 + f(W)Wx_3,\\
\frac{dx_4}{dt} &= -x_4\left(\frac{k_1x_3 + k_2x_6}{N}\right) - \mu_2x_4 + f(W)Wx_1,\\
\frac{dx_1}{dt} &= B - x_1\left(\frac{k_1x_3 + k_2x_6}{N}\right) - \mu_1x_1 - f(W)Wx_1,
\end{aligned} \tag{3.4.4.9}$$

with

$$W = \frac{x_4 + x_5 + x_6}{x_1 + x_2 + x_3 + x_4 + x_5 + x_6}, \tag{3.4.4.10}$$

where the function f as given before. The set of all disease free states, X_s, is given by $X_s = \{x \geq 0, x_i = 0, i = 1\}$.

The system (3.4.4.9) can be represented by

$$x_i' = f_i(x) = \mathcal{P}_i(x) - \mathcal{Q}_i(x), \quad i = 1, \cdots 6, \tag{3.4.4.11}$$

or

$$x' = f(x) = \mathcal{P}(x) - \mathcal{Q}(x), \tag{3.4.4.12}$$

where

$$\mathcal{P} = \begin{pmatrix} \frac{(1-p_1)x_1(k_1x_3+k_2x_6)}{x_1+x_2+x_3+x_4+x_5+x_6} \\ \frac{(p_1x_1+q_1x_2)(k_1x_3+k_2x_6)}{x_1+x_2+x_3+x_4+x_5+x_6} \\ \frac{(1-p_2)x_4(k_1x_3+k_2x_6)}{x_1+x_2+x_3+x_4+x_5+x_6} + f(W)Wx_2 \\ \frac{(p_2x_4+q_2x_5)(k_1x_3+k_2x_6)}{x_1+x_2+x_3+x_4+x_5+x_6} + f(W)Wx_3 \\ 0 \\ f(W)Wx_1 \end{pmatrix},$$

and

$$\mathcal{Q} = \begin{pmatrix} \frac{q_1x_2(k_1x_3+k_2x_6)}{x_1+x_2+x_3+x_4+x_5+x_6} + (a_1+\mu_1)x_2 - b_1x_3 + f(W)Wx_2 \\ (b_1+m_1)x_3 - a_1x_2 + f(W)Wx_3 \\ \frac{q_2x_5(k_1x_3+k_2x_6)}{x_1+x_2+x_3+x_4+x_5+x_6} + (a_2+\mu_2)x_5 - b_2x_6 \\ (b_2+m_2)x_6 - a_2x_5 \\ \frac{x_4(k_1x_3+k_2x_6)}{x_1+x_2+x_3+x_4+x_5+x_6} + \mu_2x_4 \\ -B + \frac{x_1(k_1x_3+k_2x_6)}{x_1+x_2+x_3+x_4+x_5+x_6} + \mu_1x_1 + f(W)Wx_1 \end{pmatrix}.$$

The matrix $\mathcal{Q}$ can be written as $\mathcal{Q} = \mathcal{Q}^- - \mathcal{Q}^+$, where

$$\mathcal{Q}^- = \begin{pmatrix} \frac{q_1 x_2(k_1 x_3 + k_2 x_6)}{x_1+x_2+x_3+x_4+x_5+x_6} + (a_1+\mu_1)x_2 + f(W)Wx_2 \\ (b_1+m_1)x_3 + f(W)Wx_3 \\ \frac{q_2 x_5(k_1 x_3 + k_2 x_6)}{x_1+x_2+x_3+x_4+x_5+x_6} + (a_2+\mu_2)x_5 \\ (b_2+m_2)x_6 \\ \frac{x_4(k_1 x_3 + k_2 x_6)}{x_1+x_2+x_3+x_4+x_5+x_6} + \mu_2 x_4 \\ \frac{x_1(k_1 x_3 + k_2 x_6)}{x_1+x_2+x_3+x_4+x_5+x_6} + \mu_1 x_1 + f(W)Wx_1 \end{pmatrix},$$

and

$$\mathcal{Q}^+ = \Big(b_1 x_3, a_1 x_2, b_2 x_6, a_2 x_5, 0, B\Big)^T. \tag{3.4.4.13}$$

Now, we verify that $\mathcal{P}, \mathcal{Q}^-$ and $\mathcal{Q}^+$ satisfy the five axioms of Theorem 1.3.2.1. We note that

- If $x_i \geq 0$, $i = 1, \cdots, 6$ then $\mathcal{P}_i \geq 0$, $\mathcal{Q}_i^- \geq 0$ and $\mathcal{Q}_i^+ \geq 0$ for $i = 1, \cdots, 6$ and therefore axiom (A1) holds.
- If $x_i = 0$ then $\mathcal{Q}_i^- = 0$, $i = 1, \cdots, 6$. Hence, axiom (A2) also holds.
- Since $\mathcal{P}_i = 0$, $i = 1, \cdots, 5$ then axiom (A3) is satisfied.
- At the disease free equilibrium $(B/\mu_1, 0, 0, 0, 0, 0)$, we find that $\mathcal{P}_i = 0$, $i = 1, \cdots, 5$ and thus axiom (A4) is satisfied.

- Setting $\mathcal{P}(x)$ to zero, we obtain the following system

$$\begin{aligned}
\frac{dx_2}{dt} &= -q_1 x_2 \left(\frac{k_1 x_3 + k_2 x_6}{N}\right) - (a_1 + \mu_1)x_2 + b_1 x_3 - f(W)W x_2, \\
\frac{dx_3}{dt} &= -(b_1 + m_1)x_3 + a_1 x_2 - f(W)W x_3, \\
\frac{dx_5}{dt} &= -q_2 x_5 \left(\frac{k_1 x_3 + k_2 x_6}{N}\right) - (a_2 + \mu_2)x_5 + b_2 x_6, \\
\frac{dx_6}{dt} &= -(b_2 + m_2)x_6 + a_2 x_5, \\
\frac{dx_4}{dt} &= -x_4 \left(\frac{k_1 x_3 + k_2 x_6}{N}\right) - \mu_2 x_4, \\
\frac{dx_1}{dt} &= B - x_1 \left(\frac{k_1 x_3 + k_2 x_6}{N}\right) - \mu_1 x_1 - f(W)W x_1.
\end{aligned}$$

The Jacobian matrix at the disease free equilibrium, $Df(E_0^*)$, of the above system is given by

$$Df(E_0^*) = \begin{pmatrix}
-\mu_1 & 0 & -k_1 & -d & -d & -(k_2 + d) \\
0 & -(a_1 + \mu_1) & b_1 & 0 & 0 & 0 \\
0 & a_1 & -(b_1 + m_1) & 0 & 0 & 0 \\
0 & 0 & 0 & -\mu_2 & 0 & 0 \\
0 & 0 & 0 & 0 & -(a_2 + \mu_2) & b_2 \\
0 & 0 & 0 & 0 & a_2 & -(b_2 + m_2)
\end{pmatrix}.$$

The characteristic equation associated with the above matrix is

$$\begin{aligned}
(\lambda + \mu_1)(\lambda + \mu_2)(\lambda^2 + (a_1 + \mu_1 + b_1 + m_1)\lambda + a_1 m_1 + m_1\mu_1 + \mu_1 b_1) \times \\
(\lambda^2 + (a_2 + \mu_2 + b_2 + m_2)\lambda + a_2 m_2 + m_2\mu_2 + \mu_2 b_2) = 0. \quad (3.4.4.14)
\end{aligned}$$

The first and second roots are given by

$$\lambda_1 = -\mu_1, \quad (3.4.4.15)$$

and

$$\lambda_2 = -\mu_2, \tag{3.4.4.16}$$

respectively. The third and fourth roots are the solutions of the equation

$$\lambda^2 + (a_1 + \mu_1 + b_1 + m_1)\lambda + a_1 m_1 + m_1\mu_1 + \mu_1 b_1 = 0, \tag{3.4.4.17}$$

and by using Theorem 1.3.2.3, these roots are negative or have negative real parts. The fifth and sixth roots are the solutions of the equation

$$\lambda^2 + (a_2 + \mu_2 + b_2 + m_2)\lambda + a_2 m_2 + m_2\mu_2 + \mu_2 b_2 = 0, \tag{3.4.4.18}$$

and by using Theorem 1.3.2.3 they are negative or have negative real parts. Therefore, all eigenvalues of the Jacobian matrix $Df(E_0^*)$ are negative or have negative real parts. Thus, axiom (A5) holds.

Since the five axioms of Theorem 1.3.2.1 are satisfied, then the disease free equilibrium of system (3.2.0.1) is locally asymptotically stable if $R_0 < 1$ and unstable if $R_0 > 1$. □

3.4.4.2 Analysis of backward bifurcation

It is shown from Theorem 3.4.4.1 that the DFE of the full model (3.2.0.1) is locally asymptotically stable if $R_0 < 1$. However, this equilibrium may not be globally asymptotically stable in $\mathcal{D}$ for $R_0 < 1$, which means stable DFE can co-exist with a stable endemic equilibrium when $R_0 < 1$ (a case of backward bifurcation). Therefore, the classical requirement of having the basic reproduction number less than unity is not sufficient for eradicating the disease. The possibility of this for system (3.2.0.1) is investigated below. It must be pointed out that R_0^{TB} and R_0^{HIV} are disjoint. Hence, two cases are considered. We firstly assume $R_0 = R_0^{TB} > R_0^{HIV}$ and secondly we will assume $R_0 = R_0^{HIV} > R_0^{TB}$. Using Theorem 1.3.2.2 for each case, we state and prove

the following two results.

Theorem 3.4.4.2. *If $R_0 = R_0^{TB} > R_0^{HIV}$, then for any value of Hill coefficient, k, the full model (3.2.0.1) undergoes*

- *a forward bifurcation if $p_1 < 1$, i.e., if $R_0 > 1$ the unique endemic equilibrium guaranteed by Theorem 1.3.2.2, is locally asymptotically stable but only for values of R_0 that are greater than and close to 1, and*
- *a backward bifurcation at $R_0 = 1$ whenever the following inequalities hold:*

$$a = \frac{-6\vartheta a_1 \mu_1^3 (a_2 m_2 + m_2\mu_2 + \mu_2 b_2)(a_1 + p_1\mu_1)\phi_1}{B} > 0, \tag{3.4.4.19}$$

and

$$b = 3a_1\mu_1(1-p_1)(a_1 + p_1\mu_1)(a_2 m_2 + m_2\mu_2 + \mu_2 b_2) > 0, \tag{3.4.4.20}$$

where

$$\vartheta = (a_1 + p_1\mu_1)(1-p_1) + ((1-p_1)m_1 + b_1)(q_1 + (1-p_1)). \tag{3.4.4.21}$$

Proof. By using the same notations as in Theorem 3.4.4.1 and noting that $k_2 = \frac{2}{3}k_1$, and letting $k_1 = \phi_1$ be the bifurcation parameter, we re-write system (3.2.0.1) in the form

$$\frac{dx}{dt} = F(x),$$

where $F = (f_1, f_2, f_3, f_4, f_5, f_6)^T$ and $x = (x_1, x_2, x_3, x_4, x_5, x_6)^T$, with

$$\begin{aligned}
\frac{dx_1}{dt} &= f_1 = B - \phi_1 x_1 \left(\frac{x_3 + \frac{2}{3}x_6}{N}\right) - \mu_1 x_1 - f(W)Wx_1,\\
\frac{dx_2}{dt} &= f_2 = \phi_1((1-p_1)x_1 - q_1 x_2)\left(\frac{x_3 + \frac{2}{3}x_6}{N}\right) - (a_1+\mu_1)x_2 + b_1 x_3 - f(W)Wx_2,\\
\frac{dx_3}{dt} &= f_3 = \phi_1(p_1 x_1 + q_1 x_2)\left(\frac{x_3 + \frac{2}{3}x_6}{N}\right) - (b_1+m_1)x_3 + a_1 x_2 - f(W)Wx_3,\\
\frac{dx_4}{dt} &= f_4 = -\phi_1 x_4 \left(\frac{x_3 + \frac{2}{3}x_6}{N}\right) - \mu_2 x_4 + f(W)Wx_1,\\
\frac{dx_5}{dt} &= f_5 = \phi_1((1-p_2)x_4 - q_2 x_5)\left(\frac{x_3 + \frac{2}{3}x_6}{N}\right) - (a_2+\mu_2)x_5 + b_2 x_6 + f(W)Wx_2,\\
\frac{dx_6}{dt} &= f_6 = \phi_1(p_2 x_4 + q_2 x_5)\left(\frac{x_3 + \frac{2}{3}x_6}{N}\right) - (b_2+m_2)x_6 + a_2 x_5 + f(W)Wx_3,
\end{aligned}$$

where H is given by (3.4.4.10). By evaluating the Jacobian matrix of the above system at the DFE, we obtain

$$Df(E_0^*) = \begin{pmatrix}
-\mu_1 & 0 & -\phi_1 & -d & -d & -\frac{2}{3}\phi_1 - d\\
0 & -(a_1+\mu_1) & (1-p_1)\phi_1 + b_1 & 0 & 0 & \frac{2}{3}(1-p_1)\phi_1\\
0 & a_1 & p_1\phi_1 - (b_1+m_1) & 0 & 0 & \frac{2}{3}p_1\phi_1\\
0 & 0 & 0 & -\mu_2 + d & d & d\\
0 & 0 & 0 & 0 & -(a_2+\mu_2) & b_2\\
0 & 0 & 0 & 0 & a_2 & -(b_2+m_2)
\end{pmatrix}.$$

Consider the case when $R_0 = 1$ (e.g., $R_0^{HIV} < R_0^{TB} = 1$). This gives

$$\phi_1 = \frac{a_1 m_1 + m_1\mu_1 + \mu_1 b_1}{a_1 + p_1\mu_1}. \tag{3.4.4.22}$$

Substituting (3.4.4.22) in the above matrix and calculating the eigenvalues, we obtain

$$\lambda_1 = 0, \tag{3.4.4.23}$$

$$\lambda_2 = -\mu_1, \tag{3.4.4.24}$$

$$\lambda_3 = -\mu_2\left(1-\frac{d}{\mu_2}\right) = -\mu_2\left(1-R_0^{HIV}\right), \tag{3.4.4.25}$$

$$\lambda_4 = -\frac{a_1b_1+(1-p_1)a_1m_1+(a_1+\mu_1)(a_1+p_1\mu_1)}{a_1+p_1\mu_1}, \tag{3.4.4.26}$$

$$\lambda_5 = -\frac{1}{2}\left[(a_2+\mu_2+b_2+m_2)-\sqrt{\mathcal{L}}\right], \tag{3.4.4.27}$$

$$\lambda_6 = -\frac{1}{2}\left[(a_2+\mu_2+b_2+m_2)+\sqrt{\mathcal{L}}\right], \tag{3.4.4.28}$$

where

$$\mathcal{L} = (a_2+\mu_2)^2+2b_2(a_2-\mu_2)-2m_2(a_2+\mu_2)+(b_2+m_2)^2.$$

From Lemma 3.4.4.1 below, the eigenvalue λ_5 is negative or have negative real part. Hence, we have zero as a simple eigenvalue of $Df(E_0^*)$ and all other eigenvalues are negative or have negative real parts. Thus, Theorem 1.3.2.2 can be used.

Computations of eigenvectors of $Df(E_0^*)$:

The matrix $Df(E_0^*)$ has a left eigenvector given by $\nu = [\nu_1, \nu_2, \nu_3, \nu_4, \nu_5, \nu_6]$, where $\nu_1 = 0$, $\nu_2 = 3a_1(a_2m_2 + m_2\mu_2 + \mu_2b_2)$, $\nu_3 = 3(a_2m_2 + m_2\mu_2 + \mu_2b_2)(a_1 + \mu_1)$, $\nu_4 = 0$, $\nu_5 = 2a_2(a_1m_1 + m_1\mu_1 + \mu_1b_1)$ and $\nu_6 = 2(a_1m_1 + m_1\mu_1 + \mu_1b_1)(a_2 + \mu_2)$. Further, the matrix has a right eigenvector given by $\omega = [\omega_1, \omega_2, \omega_3, \omega_4, \omega_5, \omega_6]^T$, where $\omega_1 = -(a_1m_1 + m_1\mu_1 + \mu_1b_1)$, $\omega_2 = \mu_1((1 - p_1)m_1 + b_1)$, $\omega_3 = \mu_1(a_1 + p_1\mu_1)$ and $\omega_4 = \omega_5 = \omega_6 = 0$.

Computations of a and b:

To compute a and b, we note that after some manipulations, it can be shown that

$$a = \frac{-6\vartheta a_1\mu_1^3(a_2m_2 + m_2\mu_2 + \mu_2b_2)(a_1 + p_1\mu_1)\phi_1}{B},$$

and

$$b = 3a_1\mu_1(1 - p_1)(a_1 + p_1\mu_1)(a_2m_2 + m_2\mu_2 + \mu_2b_2), \tag{3.4.4.29}$$

where ϑ as in 3.4.4.21. It should be noted that $a < 0$ and $b > 0$ if $p_1 < 1$. Thus, it follows from Theorem 1.3.2.2, that the system (3.2.0.1) undergoes a forward bifurcation at $R_0 = 1$ if $p_1 < 1$. Hence, the first result stated in the theorem is obtained. Moreover, the system undergoes a backward bifurcation at $R_0 = 1$ whenever $a > 0$ and $b > 0$. □

Lemma 3.4.4.1. *The eigenvalue λ_5 is negative or have negative real part.*

Proof. From the expression of λ_5 in (3.4.4.27), the result is directly obtained if $\mathcal{L} \leq 0$. If $\mathcal{L} > 0$, we must prove

$$\left[(a_2 + \mu_2 + b_2 + m_2) - \sqrt{\mathcal{L}}\right] > 0.$$

We prove it by contradiction and therefore assume by contradiction that

$$\left[(a_2 + \mu_2 + b_2 + m_2) - \sqrt{\mathcal{L}}\right] \leq 0.$$

This can be written as

$$(a_2+\mu_2+b_2+m_2)^2 \leq (a_2+\mu_2)^2 + 2b_2(a_2-\mu_2) - 2m_2(a_2+\mu_2) + (b_2+m_2)^2,$$

which can be further simplified to

$$a_2+\mu_2+b_2+m_2 \leq -(a_2+\mu_2+b_2+m_2),$$

or

$$2(a_2+\mu_2+b_2+m_2) = 0.$$

This contradicts the fact that all the parameter of the system are positive. Thus,

$$\left[(a_2+\mu_2+b_2+m_2) - \sqrt{\mathcal{L}}\right] > 0,$$

and hence $\lambda_5 < 0$. □

Theorem 3.4.4.3. *If $R_0 = R_0^{HIV} > R_0^{TB}$, then for any value of Hill coefficient, k, the full model (3.2.0.1) undergoes*

- *a forward bifurcation if*

$$k_1 < \frac{a_1+\mu_1+b_1+m_1}{p_1}, \tag{3.4.4.30}$$

  i.e., if $R_0 > 1$ the endemic equilibrium is locally asymptotically stable but only for R_0 close to 1, and

- *a backward bifurcation at $R_0 = 1$ whenever the following inequality holds:*

$$\tilde{a} = -\mu_1^2(a_2m_2 + m_2\mu_2 + \mu_2b_2)(\mu_2 - \phi_2) > 0. \tag{3.4.4.31}$$

Proof. We consider in this case $R_0 = 1$ (e.g., $R_0^{TB} < R_0^{HIV} = 1$). Let $d = \phi_2$ be the

bifurcation parameter. Solving $R_0 = 1$ gives

$$\phi_2 = \mu_2. \tag{3.4.4.32}$$

Evaluating the Jacobian matrix of system (3.4.4.22) at the DFE when we consider (3.4.4.32), we obtain

$$Df(E_0^*) = \begin{pmatrix} -\mu_1 & 0 & -k_1 & -\phi_2 & -\phi_2 & -\frac{2}{3}k_1 - \phi_2 \\ 0 & -(a_1+\mu_1) & (1-p_1)k_1 + b_1 & 0 & 0 & \frac{2}{3}(1-p_1)k_1 \\ 0 & a_1 & p_1k_1 - (b_1+m_1) & 0 & 0 & \frac{2}{3}p_1k_1 \\ 0 & 0 & 0 & -\mu_2+\phi_2 & \phi_2 & \phi_2 \\ 0 & 0 & 0 & 0 & -(a_2+\mu_2) & b_2 \\ 0 & 0 & 0 & 0 & a_2 & -(b_2+m_2) \end{pmatrix}.$$

Substituting (3.4.4.32) in the above matrix and calculating the eigenvalues, we obtain $\tilde{\lambda}_1 = 0$, $\tilde{\lambda}_2 = -\mu_1$, $\tilde{\lambda}_3 = \lambda_5$, $\tilde{\lambda}_4 = \lambda_6$, $\tilde{\lambda}_5 = -\frac{1}{2}\left[(a_1+\mu_1+b_1+m_1-p_1k_1) - \sqrt{\mathcal{K}}\right]$ and $\tilde{\lambda}_6 = -\frac{1}{2}\left[(a_1+\mu_1+b_1+m_1-p_1k_1) + \sqrt{\mathcal{K}}\right]$, where λ_5 and λ_6 as given in (3.4.4.27) and (3.4.4.28) respectively, and

$$\begin{aligned} \mathcal{K} &= ((a_1+\mu_1) - (b_1+m_1))^2 + p_1^2k_1^2 - 2p_1k_1(a_1+m_1+b_1) + \\ &\quad 2k_1(a_1+p_1\mu_1) + 2a_1k_1. \end{aligned} \tag{3.4.4.33}$$

It is clear that the eigenvalue $\tilde{\lambda}_6$ is negative or have negative real part if the inequality (3.4.4.30) holds. From Lemma 3.4.4.2 below, we note that the sign of $\tilde{\lambda}_5$ negative or have negative real part. Hence, we have zero as a simple eigenvalue of $Df(E_0^*)$ and all other eigenvalues are negative or have negative real parts. Thus, Theorem 1.3.2.2 can be used.

Computations of eigenvectors of $Df(E_0^*)$:

The matrix $Df(E_0^*)$ has a left eigenvector given by $\tilde{\nu} = [\tilde{\nu}_1, \tilde{\nu}_2, \tilde{\nu}_3, \tilde{\nu}_4, \tilde{\nu}_5, \tilde{\nu}_6]$, where $\tilde{\nu}_1 = \tilde{\nu}_2 = \tilde{\nu}_3 = 0$, $\tilde{\nu}_4 = a_2m_2 + m_2\mu_2 + \mu_2b_2$, $\tilde{\nu}_5 = \mu_2(a_2+b_2+m_2)$ and $\tilde{\nu}_6 = \mu_2(a_2+b_2+\mu_2)$.

Further, the matrix has a right eigenvector given by $\tilde{\omega} = [\tilde{\omega}_1, \tilde{\omega}_2, \tilde{\omega}_3, \tilde{\omega}_4, \tilde{\omega}_5, \tilde{\omega}_6]^T$, where $\tilde{\omega}_1 = -\mu_2$, $\tilde{\omega}_2 = \tilde{\omega}_3 = 0$, $\tilde{\omega}_4 = \mu_1$ and $\tilde{\omega}_5 = \tilde{\omega}_6 = 0$.

Computations of $\tilde{a}$ and $\tilde{b}$:

Same as before, it can be shown that

$$\tilde{a} = -\mu_1^2(a_2m_2 + m_2\mu_2 + \mu_2b_2)(\mu_2 - \phi_2) \tag{3.4.4.34}$$

and

$$\tilde{b} = \mu_1(a_2m_2 + m_2\mu_2 + \mu_2b_2). \tag{3.4.4.35}$$

It should be noted $\tilde{b} > 0$ is always satisfied. If $\tilde{a} < 0$, then from Theorem 1.3.2.2, the system (3.2.0.1) undergoes a forward bifurcation at $R_0 = 1$, and hence the first result stated in the theorem is obtained. Further, the system undergoes a backward bifurcation at $R_0 = 1$ whenever $\tilde{a} > 0$. □

Lemma 3.4.4.2. *The eigenvalue $\tilde{\lambda}_5$ is negative or have negative real part if the inequality (3.4.4.30) holds.*

Proof. Looking at the expression for $\tilde{\lambda}_5$ mentioned earlier, the result is directly obtained if $\mathcal{K} \leq 0$. Now, if $\mathcal{K} > 0$, then we must show that

$$(a_1 + \mu_1 + b_1 + m_1 - p_1k_1) - \sqrt{\mathcal{K}} > 0.$$

Assume by contradiction that

$$(a_1 + \mu_1 + b_1 + m_1 - p_1k_1) - \sqrt{\mathcal{K}} \leq 0.$$

This can be written as

$$(a_1 + \mu_1 + b_1 + m_1 - p_1k_1)^2 \leq \mathcal{K}$$

which can be further simplified to

$$-4a_1k_1 + 4b_1\mu_1 + 4m_1\mu_1 + 4m_1a_1 - 4p_1k_1\mu_1 \leq 0,$$

or

$$(a_1m_1 + m_1\mu_1 + \mu_1b_1)\left(1 - \frac{k_1(a_1 + p_1\mu_1)}{a_1m_1 + m_1\mu_1 + \mu_1b_1}\right) \leq 0,$$

$$\Rightarrow (a_1m_1 + m_1\mu_1 + \mu_1b_1)\left(1 - R_0^{TB}\right) \leq 0,$$

which can not be true because in this case we have $R_0^{TB} < 1$. Thus,

$$\left[(a_2 + \mu_2 + b_2 + m_2) - \sqrt{\mathcal{K}}\right] > 0,$$

and hence $\tilde{\lambda}_5 < 0$ if the inequality (3.4.4.30) holds. □

3.5 Numerical simulations

In this section, we present numerical simulations for the model (3.2.0.1) to examine the impact of the response function with regard to its parameters k and λ_0 on the model dynamics and on the HIV and TB prevalences. Unless otherwise stated, the parameters used in the simulations are as presented in Table 3.2.0.1.

To study the dynamics of the full model (3.2.0.1), we vary the values of the associated basic reproduction numbers R_0^{HIV} and R_0^{TB}. When $R_0^{HIV} < 1$ and $R_0^{TB} < 1$, (e.g., $R_0 < 1$), the solution of the system converges to the disease free equilibrium (DFE) (in agreement with Theorem (3.4.4.1)), as shown in Figure 3.5.0.1, or the endemic equilibrium (EE). Therefore, for certain values of some parameters (to meet the requirements of Theorem (3.4.4.2)), the full model exhibits backward bifurcation. That is, some solutions converge to a DFE and others to an EE when the basic reproduction number R_0 is less than unity. This phenomenon is shown in Figure 3.5.0.2. We must point out that the results in the second figure agree with Theorem (3.4.4.2).

(I)

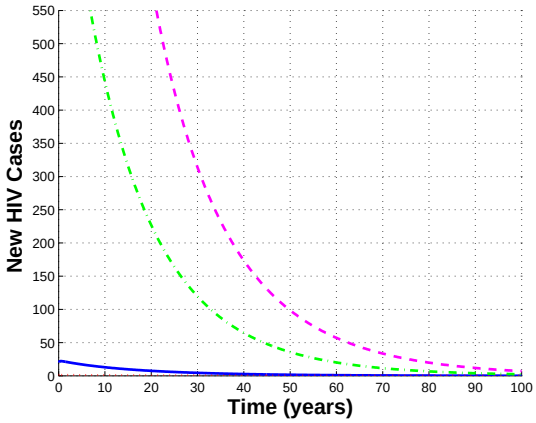

(II)

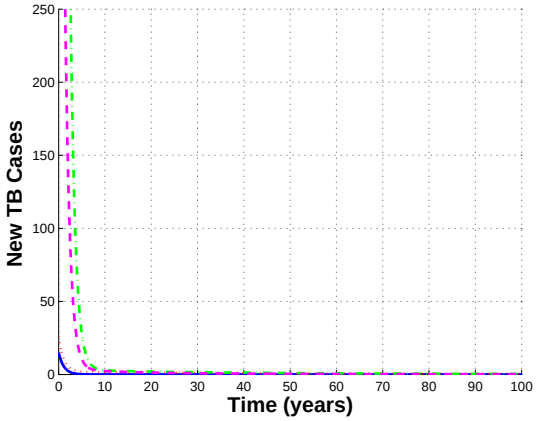

(III)

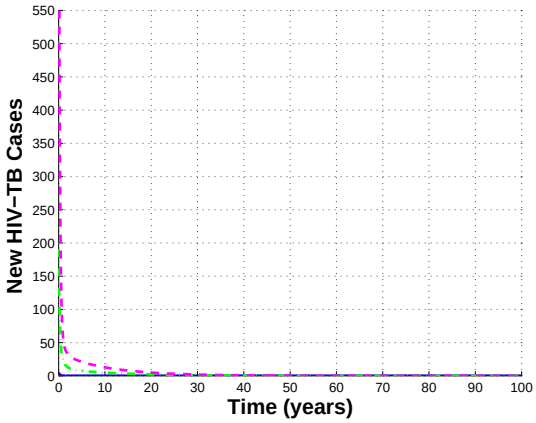

Figure 3.5.0.1: Solution of the full system (3.2.0.1) for different initial conditions and $k = 10$ when $R_0^{HIV} = 0.2$ and $R_0^{TB} = 0.5$ so that $R_0 = 0.5$. (I) New TB cases, (II) New HIV cases and (III) New HIV-TB cases.

(I)

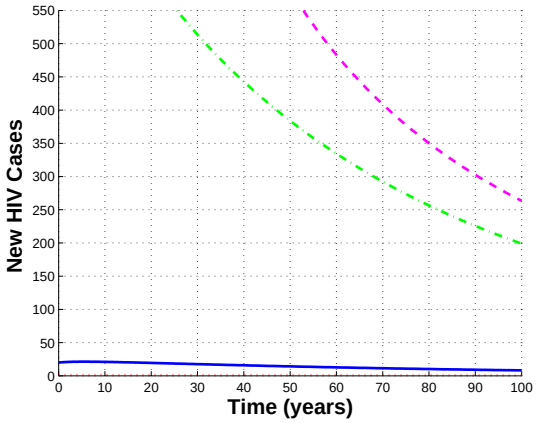

(II)

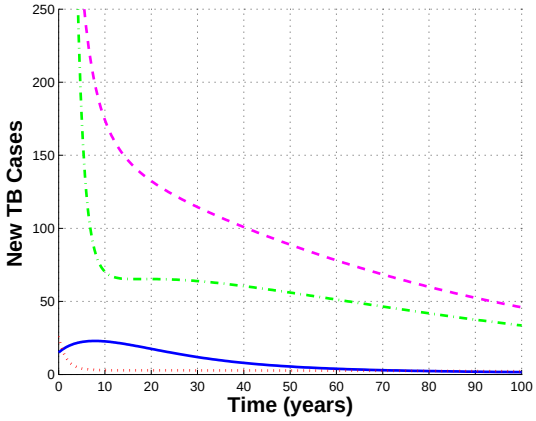

(III)

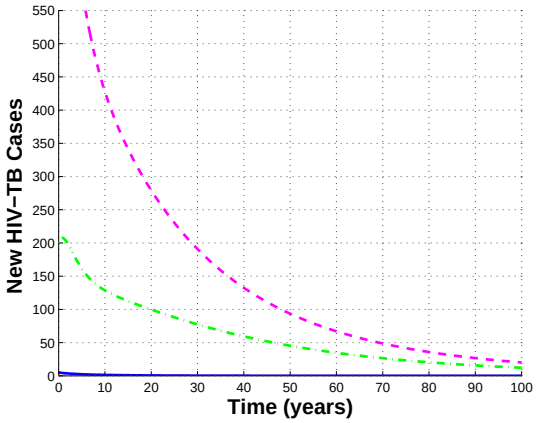

Figure 3.5.0.2: Solution of the full system (3.2.0.1). Backward bifurcation diagrams for different initial conditions and $p_1 = 1.5$, $q_1 = 0.13$, $b_2 = 0.2$, $m_2 = 0.1$ and $k = 10$ with $R_0^{HIV} = 0.89$ and $R_0^{TB} = 0.97$ so that $R_0 = 0.97$. (I) New TB cases, (II) New HIV cases and (III) New HIV-TB cases.

Figure 3.5.0.3 and Figure 3.5.0.4 below show the profiles of the DFE ($R_0 < 1$) and the EE ($R_0 > 1$) of system (3.2.0.1) respectively. Figure 3.5.0.3 shows the endemicity when the model is driven by both diseases. Further, Figure 3.5.0.5 shows the endemic equilibrium of the full model when it is driven by the TB epidemic, which corresponds to the endemic equilibrium of the TB-only sub-model whereas Figure 3.5.0.6 shows the endemic equilibrium of the full model when it is driven by the HIV epidemics, which corresponds to the endemic equilibrium of the HIV-only sub-model.

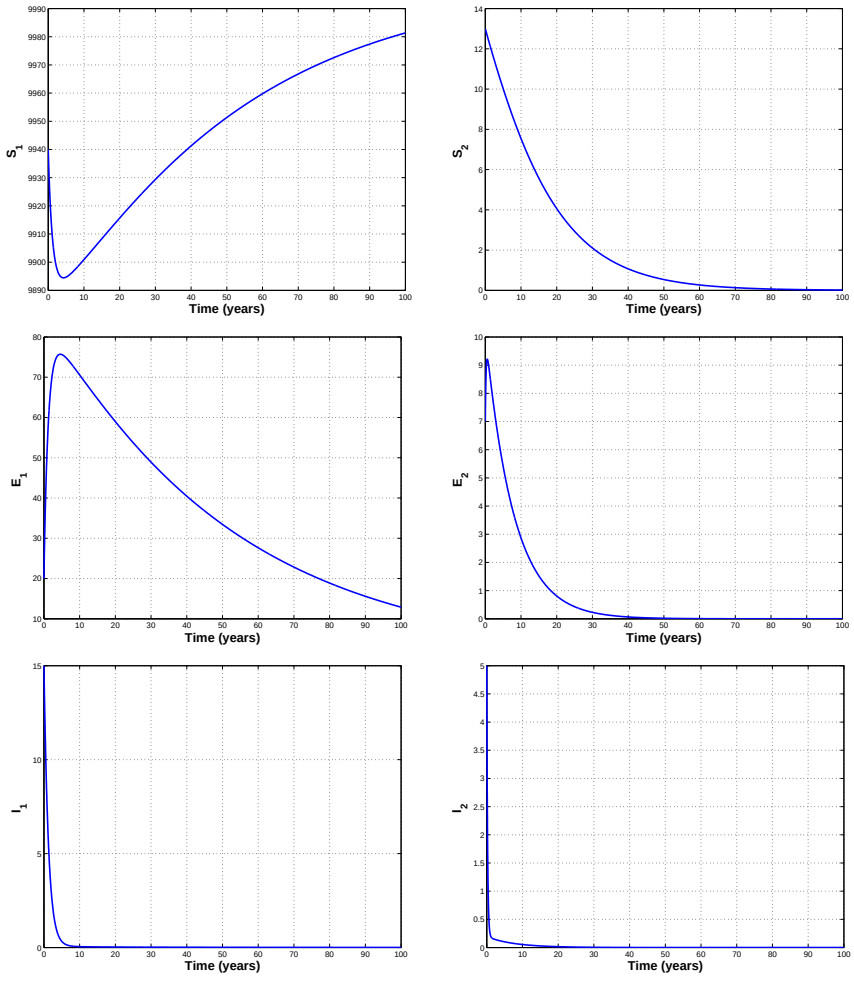

Figure 3.5.0.3: The DFE of system (3.2.0.1) when $R_0^{HIV} < 1$ ($d = 0.03$), $R_0^{TB} < 1$ ($k_1 = 2.6$) with $k = 1$ and initial conditions as $(S_1(0), E_1(0), I_1(0), S_2(0), E_2(0), I_2(0)) = (9940, 20, 15, 13, 7, 5)$.

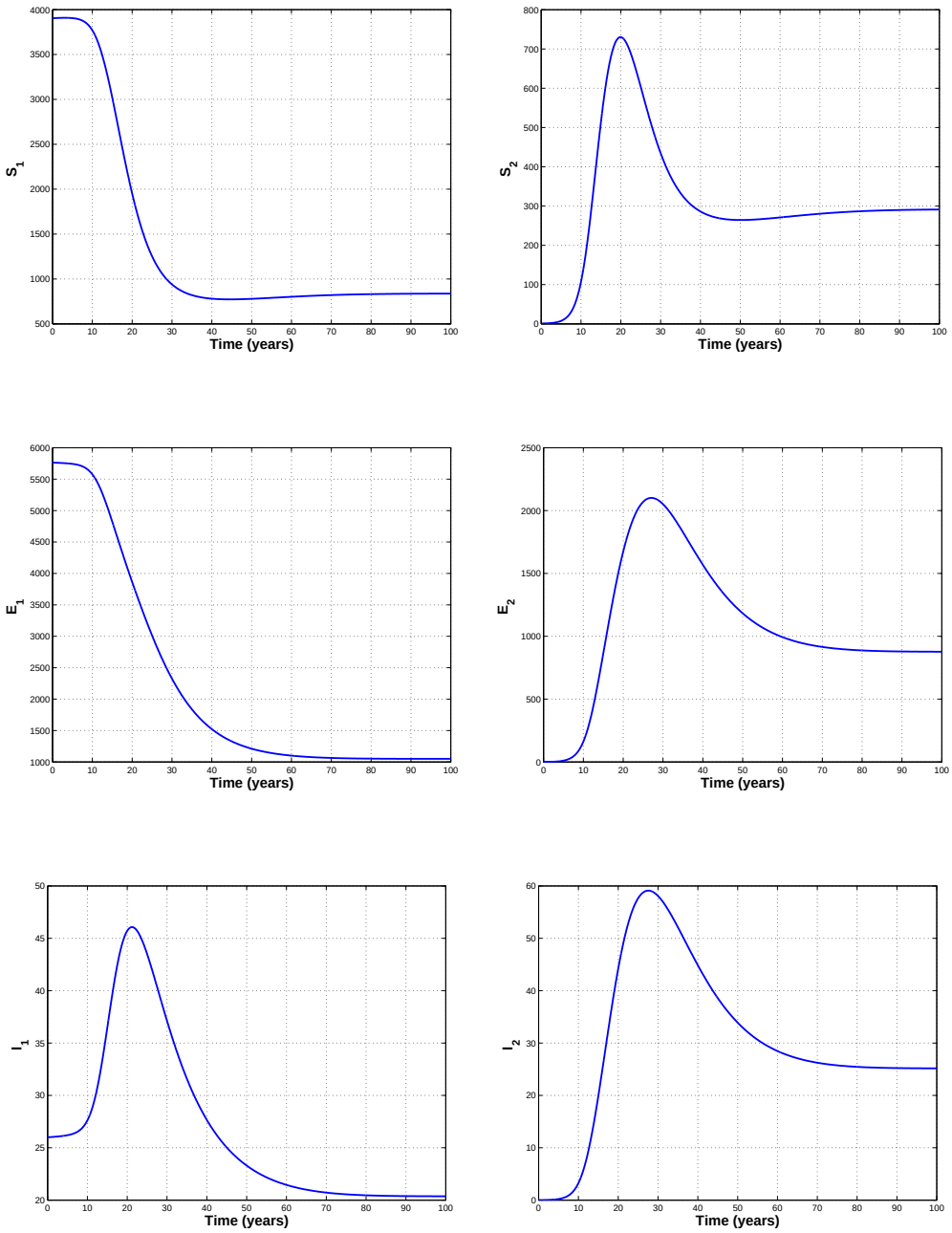

Figure 3.5.0.4: Solution of system (3.2.0.1) at the endemic equilibrium when $R_0^{HIV} > 1$ ($d = 0.7$), $R_0^{TB} > 1$ ($k_1 = 11.4$) with $k = 1$ and initial conditions as $(S_1(0), E_1(0), I_1(0), S_2(0), E_2(0), I_2(0)) = (3904, 5764, 26, 1, 0, 0)$.

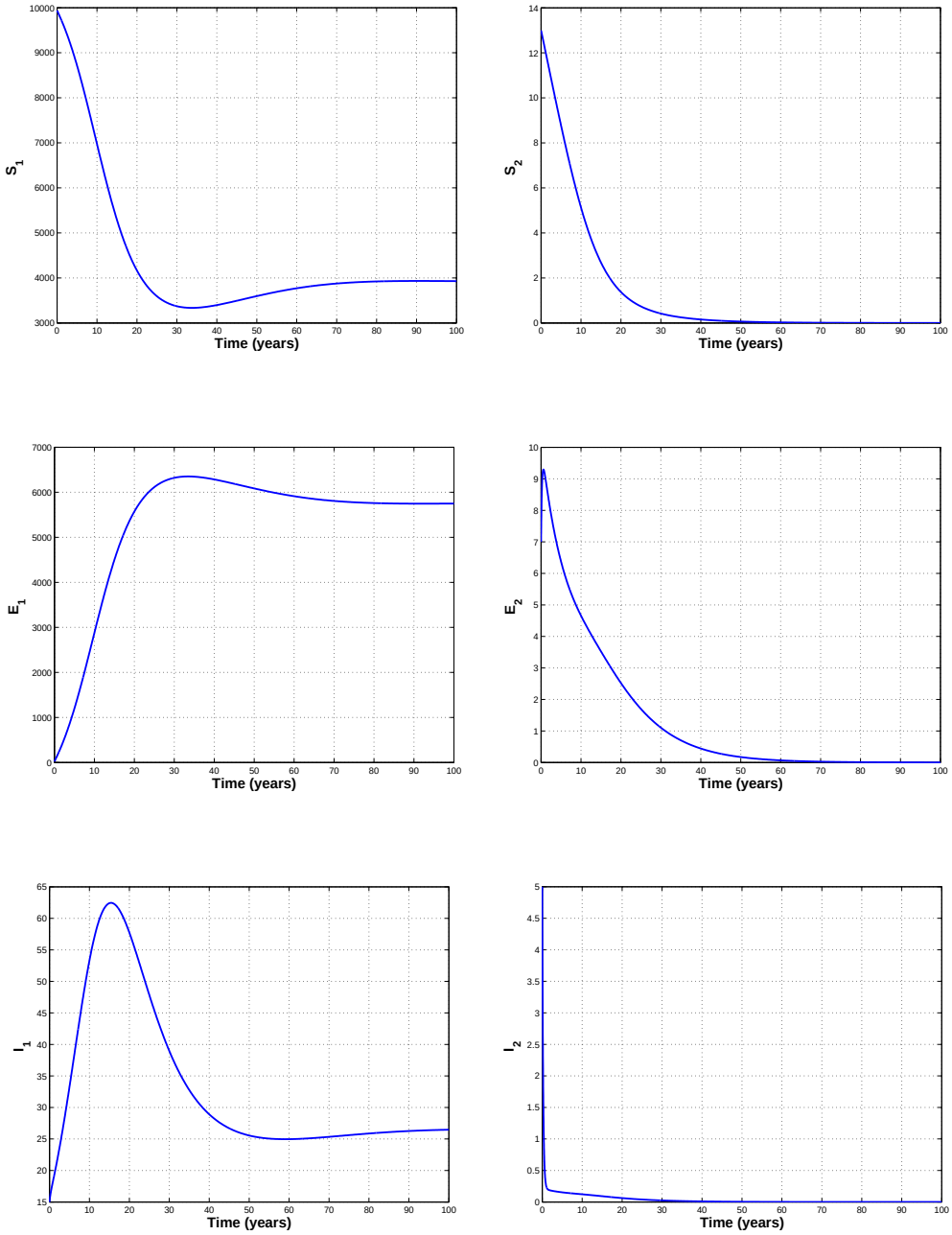

Figure 3.5.0.5: Solution of system (3.2.0.1) when $R_0^{HIV} < 1$ ($d = 0.03$) and $R_0^{TB} > 1$ ($k_1 = 11.4$) with $k = 1$ and initial conditions as $(S_1(0), E_1(0), I_1(0), S_2(0), E_2(0), I_2(0)) = (9940, 20, 15, 13, 7, 5)$.

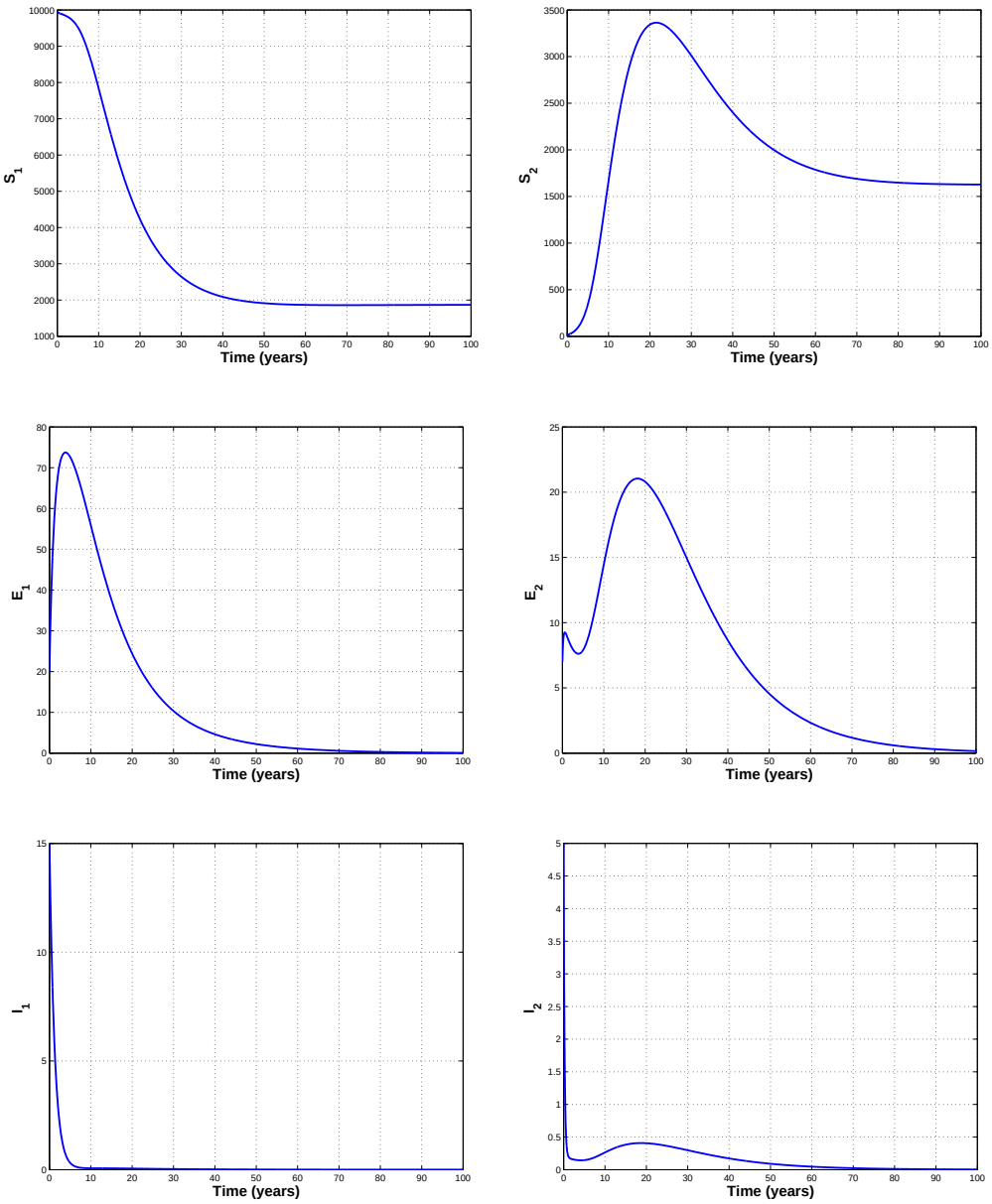

Figure 3.5.0.6: Solution of system (3.2.0.1) when $R_0^{HIV} > 1$ ($d = 0.7$) and $R_0^{TB} < 1$ ($k_1 = 2.6$) with $k = 1$ and initial conditions as $(S_1(0), E_1(0), I_1(0), S_2(0), E_2(0), I_2(0)) = (9940, 20, 15, 13, 7, 5)$.

In the following two figures we plotted the endemic equilibrium of the full model (3.2.0.1) as a function of the Hill coefficient k and the behavior change parameter λ_0. In Figure 3.5.0.7, it can be seen that the number of HIV infectious individuals increases with k (as for larger k individuals respond slowly to the HIV prevalence as mentioned

in Chapter 2). Therefore, the number of co-infected individuals also increases with k unlike the impact of behavior change parameter in which case the HIV infection reduces with λ_0 and hence we expect less individuals who leave the upper compartments to the lower ones in Figure 3.5.0.8. This clearly reduces the co-infected individuals.

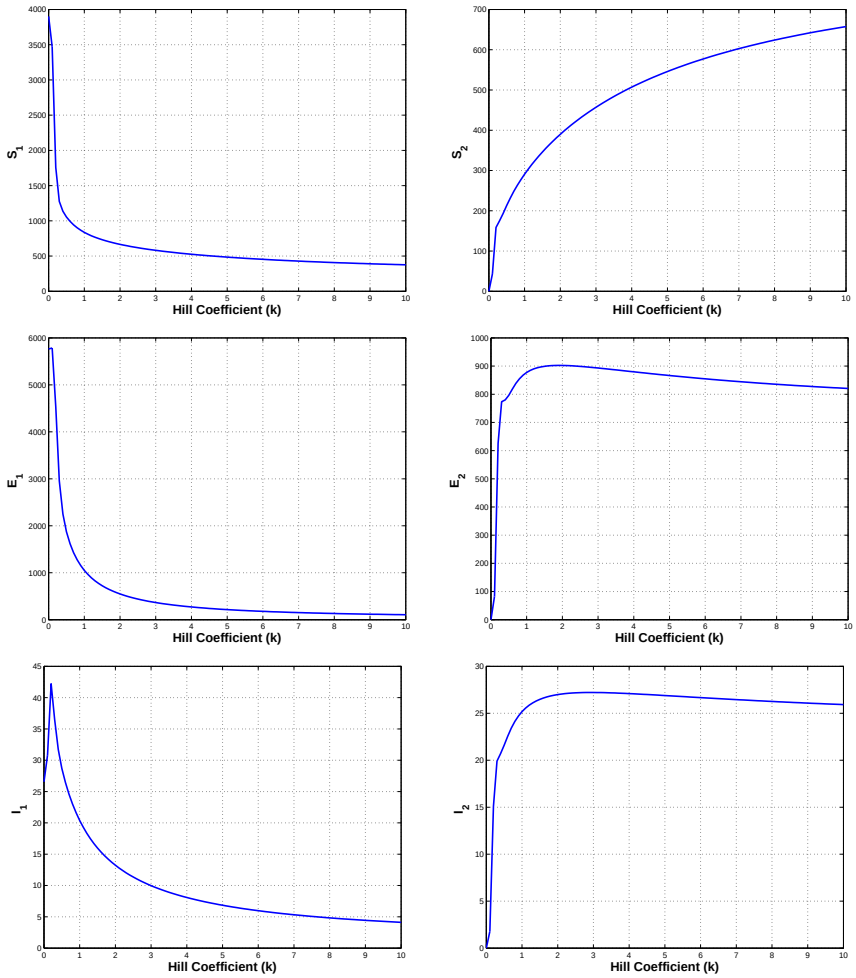

Figure 3.5.0.7: The endemic equilibrium of system (3.2.0.1) as a function of k.

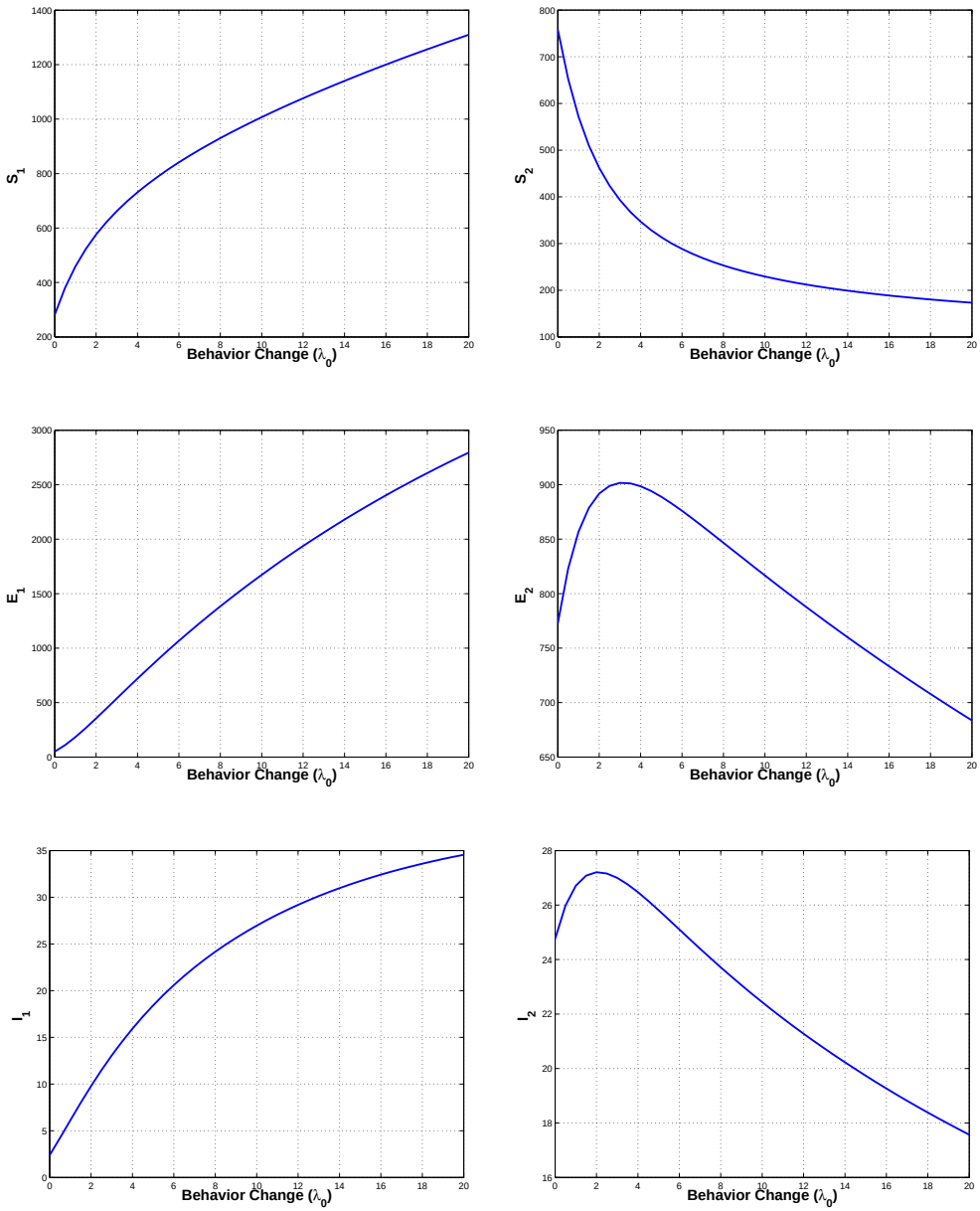

Figure 3.5.0.8: The endemic equilibrium of system (3.2.0.1) as a function of λ_0 with $k = 1$.

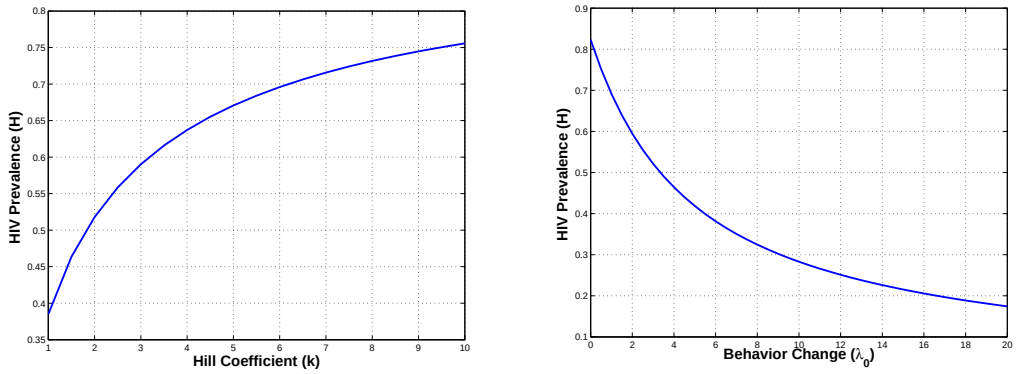

Figure 3.5.0.9: The HIV prevalence as a function of k (left figure) and λ_0 ($k = 1$) (right figure) at the endemic equilibrium.

The HIV prevalence H as a function of k and λ_0 at the endemic is shown in Figure 3.5.0.9 above, where we can see that the prevalence increases with k (decreases with λ_0). In Figure 3.5.0.10 below, the HIV prevalence is plotted for different values of k and λ_0 against time t. The value and the shape of the peak of the prevalences changes with the values of these parameters, however, when the system stabilizes, only the value of the prevalence changes.

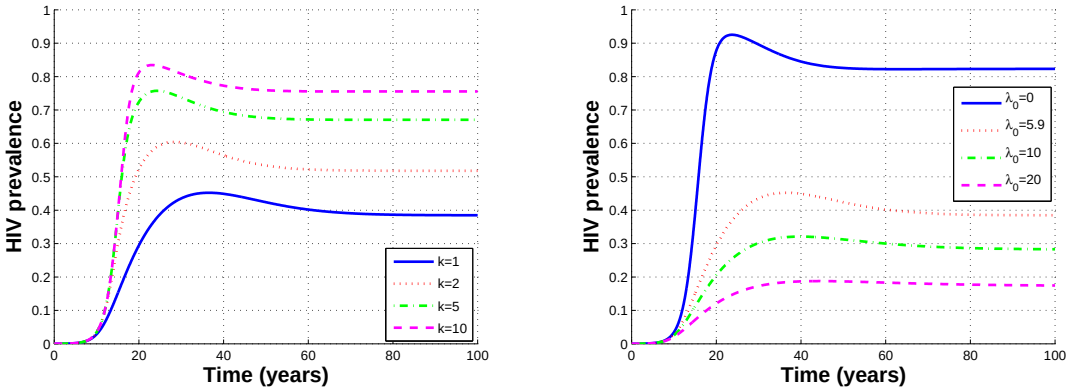

Figure 3.5.0.10: The HIV prevalence for different values of k (left figure) and λ_0 ($k = 1$) (right figure).

To study the impact of the k and λ_0 on the TB prevalence we plotted it as a function of these two parameters at the endemic equilibrium as shown in Figure 3.5.0.11 below.

While the TB prevalence increases with k, it also increases for values of λ_0 satisfying $\lambda_0 < \lambda_0^* = 2.2$ and after this threshold it decreases rapidly.

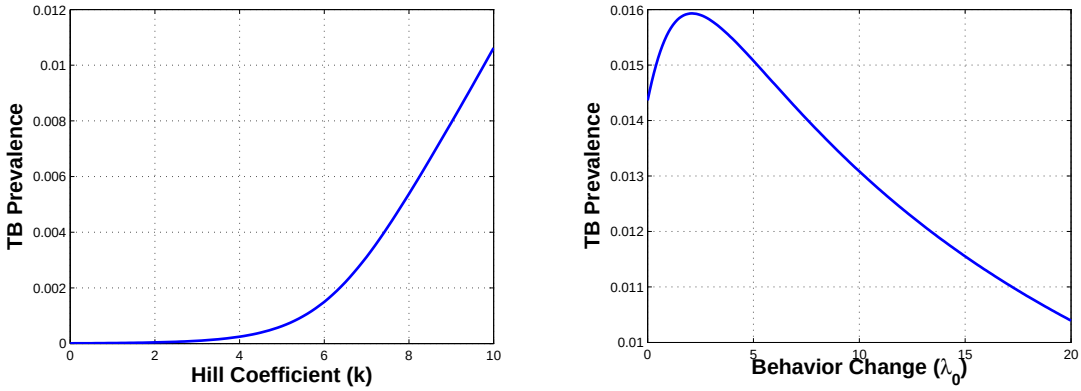

Figure 3.5.0.11: The TB prevalence as a function of k (left figure) and λ_0 (when $k = 1$) (right figure) at the endemic equilibrium.

Figure 3.5.0.12 below, shows the profile of the TB prevalence when is plotted for different values of k and λ_0 against time t. The value and the shape of the peak of the prevalence in each case changes with the values of these parameters and eventually when the system stabilizes, only the value of the prevalence changes.

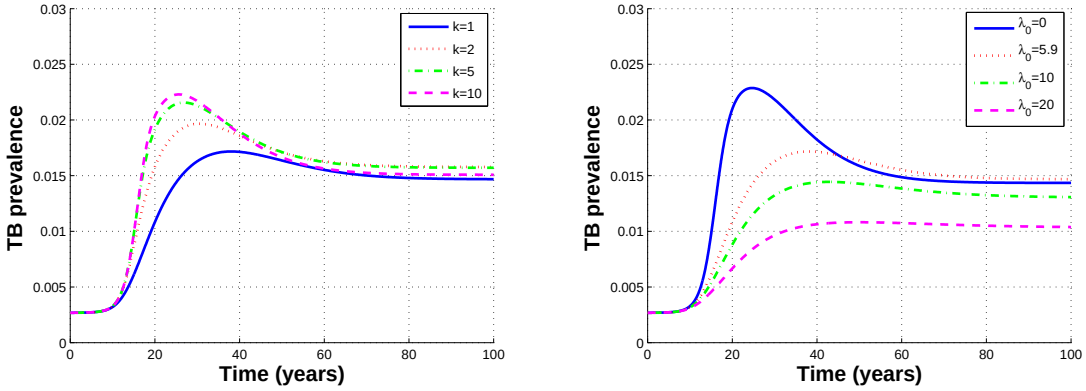

Figure 3.5.0.12: The TB prevalence for different values of k (left figure) and λ_0 (when $k = 1$) (right figure).

3.6 Summary and discussion

In this chapter, we considered a deterministic model for the transmission dynamics of the joint epidemics of HIV and TB in a population. We studied the impact of the incorporation of Hill function (the response function: allowing for various responses of individuals to an HIV prevalence) on the dynamics of the model. The full HIV-TB model is shown to have a locally-asymptotically stable disease free equilibrium when its basic reproduction number R_0 (described by the maximum of the basic reproduction numbers of the two sub-models HIV and TB) is less than unity, and unstable if R_0 is greater than unity. By using Theorem 1.3.2.2, it was shown that the full model undergoes the phenomenon of backward bifurcation when the associated basic reproduction number R_0 is greater than and close to 1 and some of the model parameters meet some criteria.

Numerical simulations of the full model were carried out to show that the two diseases co-exist whenever R_0 exceeds unity (Figure 3.5.0.4). If the basic reproduction number associated with the HIV-only sub-model is less than unity and the one associated with the TB- only sub-model is greater than unity, then the full model is driven by the TB and hence we obtain the endemic equilibrium of the TB-only sub-model (3.5.0.5).

Further numerical simulations of the full model were carried out to assess the impact of the response function in its parameters: Hill coefficient k and behavior change λ_0 on the HIV and TB prevalences (Figures 3.5.0.9, 3.5.0.10, 3.5.0.11 and 3.5.0.12). Both prevalences were found increasing with k (decreasing with λ_0). This suggests that the way individuals respond to the HIV prevalence not only affecting it but also it affects the TB prevalence. Thus, by incorporating behavior change and by taking into consideration the various responses of individuals to the HIV prevalence, the HIV infections can be controlled which leads also to controlling the co-infected individuals.

In the next chapter, we study the effect of the time needed for individuals to reduce their risky behaviors on the dynamics of the HIV infections.

Chapter 4

Analysis of an HIV model with distributed delay and behavior change

In Chapter 2, we studied the effect of the response function on the transmission dynamics of the HIV-only sub-model. In this chapter, we consider the same model and incorporate a distributed delay representing the time needed for individuals to reduce their risky behavior. We study (both mathematically and numerically) the impact of the distributed delay on the dynamics of the model. Threshold values for the delay at which the system destabilizes and periodic solutions can arise through Hopf bifurcation are determined.

4.1 Introduction

To possibly prevent HIV infections, efforts are focused on scaling up public awareness and knowledge about HIV through educational campaigns. We have seen from Chapter 2 how the educational campaigns can reduce the HIV prevalence by encouraging people to adopt safer behaviors. In addition to that, the incorporation of behavior change allow mathematical models to be more realistic in modeling the epidemics of HIV. It captures

different reactions of individuals to educational campaigns. This was the case in many studies as mentioned in the introduction of Chapter 2. Further, in that chapter, we studied the impact of different responses of individuals on the transmissions of HIV. What is missing, is to study the effect of the time individuals may take until their responses take place. It should be noted that even "the best "response would not be effective if it is too late. Hence, we also want to study the effect of the time needed for individuals to reduce their risky behaviors on the HIV prevalence.

In view of the above, in this chapter we consider the HIV-only sub-model (2.2.0.1) which is developed and analyzed in Chapter 2. We allow for incorporation of a distributed delay (modeled by gamma function) taking into account the model also includes a response function. We also investigate the effects of the two functions in their respective parameters on the system equilibria, the HIV prevalence and the bifurcation behavior of the system.

We have shown that, in the presence of the delay, the parameters of the response function (Hill coefficient k and behavior change λ_0) alter the value of endemic equilibrium and hence the prevalence of HIV. Further, the disease free equilibrium is found globally asymptotically stable independent of the parameters of gamma function (mean delay $\bar{\tau}$ and shape parameter n). Furthermore, while it is shown that n has very little impact on the prevalence, $\bar{\tau}$ is found affecting the HIV prevalence specially when it is high. Moreover, when $\bar{\tau}$ passes through specific critical values, the endemic equilibrium loses its stability and Hopf bifurcation occurs.

The rest of the chapter is organized as follows. The model is presented in the next section. In Section 4.3 we present the mathematical analysis of the model. We carry out some numerical results and simulations in Section 4.4. Section 4.5 is devoted to discussion on results.

4.2 Model description

We consider the model presented in Chapter 2 and incorporate a distributed delay. The resulting model then reads

$$\begin{aligned}\frac{dS(t)}{dt} &= B - \mu_1 S(t) - \int_0^\infty g(\tau) f(H(t-\tau)) d\tau H(t) S(t),\\ \frac{dI(t)}{dt} &= \int_0^\infty g(\tau) f(H(t-\tau)) d\tau H(t) S(t) - \mu_2 I(t),\end{aligned} \tag{4.2.0.1}$$

with H and $f(H)$ are as described in Chapter 2. We choose the probability distribution, denoted by $g(\tau)$, to be a gamma distribution function. That is

$$g(\tau) \equiv g_{n,\bar{\tau}}(\tau) = \frac{n^n \tau^{n-1}}{(n-1)!\bar{\tau}^n} e^{-\frac{n\tau}{\bar{\tau}}}, \tag{4.2.0.2}$$

where $\bar{\tau}$ is the mean delay and $\frac{\bar{\tau}^2}{n}$ is the variance. The value of n is assumed to be positive integer, $n \geq 1$. It is worth noting that when $n = 1$, the distribution reduces to an exponential distribution, while when $n \to \infty$, the distribution approaches a delta function $\delta(t-\tau)$ (see, results of Section 1.3.5). The values of B, μ_1, μ_2, d and λ_0 are presented in Table 2.2.0.1 and the other parameters are assumed to be positive.

The effect of the shape parameter n and the mean delay $\bar{\tau}$ on the shape and peak of gamma distribution function can be seen in Figure 4.2.0.1 below. In (I), while n sets the width of the distribution from being wide when n is small to being very narrow when n is large, it also increases the peak when n increases. In (II), when the mean delay $\bar{\tau}$ increases, the peak of gamma distribution function decreases and moves with the mean delay in addition to affecting the width of the distribution to be larger when we increase $\bar{\tau}$.

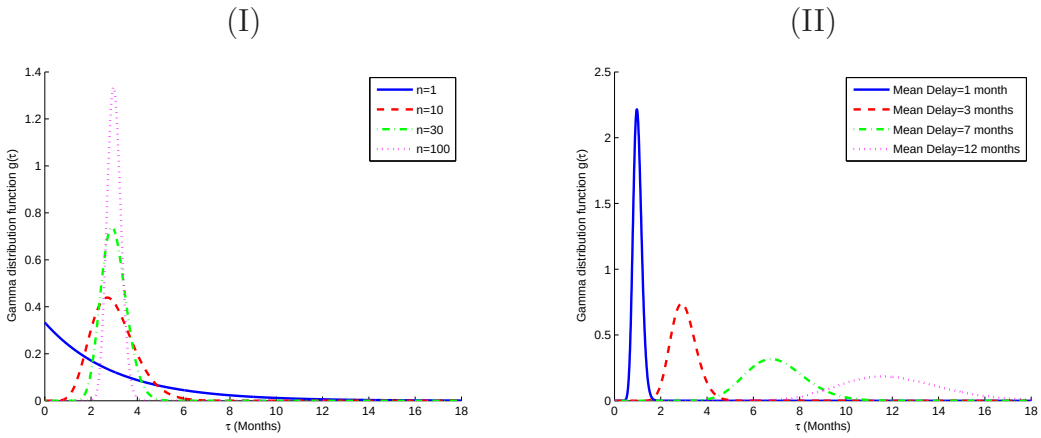

Figure 4.2.0.1: Gamma distribution function plotted for: (I) different values of n with $\bar{\tau} = 3$ and (II) different values of $\bar{\tau}$ with $n = 30$.

4.3 Mathematical analysis of the model

In this section we present some mathematical properties that system (4.2.0.1) satisfies in addition to determining its equilibria and basic reproduction number. We then explore the effect of the delay on the stability of equilibria.

4.3.1 Well-posedness

To show the well-posedness of system (4.2.0.1), we define, for each $\alpha > 0$, the following fading memory space UC_α ([75]):

$$UC_\alpha = \{\Theta \in C(]-\infty, 0], \mathbb{R}^2) : \|\Theta\|_\alpha = \sup_{\tau \leq 0} \|\Theta(\tau)\|_{\mathbb{R}^2} e^{\alpha\tau} < \infty, \\ \Theta(\tau) \text{ is uniformly continuous on }]-\infty, 0]\} \tag{4.3.1.1}$$

endowed with the norm

$$\|\Theta\|_\alpha = \sup_{\tau \leq 0} \|\Theta(\tau)\|_{\mathbb{R}^2} e^{\alpha\tau}.$$

By [55], the existence, uniqueness and continuity of solutions of system (4.2.0.1) are guaranteed in UC_α.

4.3.2 Positively-invariant region

It is important to prove that the state variables $S(t)$ and $I(t)$ of system (4.2.0.1) are nonnegative for all time $t > 0$ since we are dealing with human population. For this, we state and prove the next proposition.

Proposition 4.3.1. *If the initial condition is in UC_α^+, then the corresponding solution $(S(t), I(t))$ of the system (4.2.0.1) is non-negative for all $t > 0$. Moreover,*

$$\lim_{t\to\infty} N(t) \leq \frac{B}{\mu_1}. \tag{4.3.2.1}$$

Furthermore, if in addition $N(0) \leq B/\mu_1$, then $N(t) \leq B/\mu_1$. In particular, the region

$$\mathcal{D}_0 = \left\{ \Theta = (\phi, \psi) \text{ in } UC_\alpha^+ \text{ such that } \phi(0) + \psi(0) \leq \frac{B}{\mu_1} \right\}$$

is positively-invariant, where

$$UC_\alpha^+ = \{\Theta = (\phi, \psi) \text{ in } UC_\alpha \text{ such that } \phi, \psi \text{ are positive in }]-\infty, 0]\}.$$

Proof. Denote by t_{max} the upper bound of the maximum interval of existence corresponding to $(S(t), I(t))$. To show that the solution is positive and bounded in $[0, +\infty[$, it is sufficient to show the positivity and boundedness results in $[0, t_{max}[$. Let

$$t_1 = \sup\{0 \leq t < t_{max} : S \text{ and } I \text{ are positive on } [0, t]\}.$$

Since $S(0)$ and $I(0)$ are non-negative then $t_1 > 0$. If $t < t_{max}$, then by using the variation of constants formula to the first equation of system (4.2.0.1), we have

$$S(t) = S(0)e^{-\mu_1 t - \int_0^t G(v)H(v)dv} + B\int_0^t e^{-\mu_1(t-u) - \int_u^t G(v)H(v)dv} du > 0, \tag{4.3.2.2}$$

where

$$G(t) = \int_0^\infty g_{n,\bar{\tau}}(\tau) f(H(t-\tau)) d\tau.$$

To prove that $G(t)$ is well defined, we prove that $H(t-\tau)$ is in $[0,1]$ for each $t \in]0, t_1[$ and $\tau \in]-\infty, 0]$. In fact, we have $t-\tau \in]-\infty, t] \subset]-\infty, t_1]$ which together with the positivity of the initial condition imply that $S(t-\tau)$ and $I(t-\tau)$ are positive. Hence, $H(t-\tau)$ is in $[0,1]$.

If $t_1 < t_{max}$, then from (4.3.2.2), we have $S(t_1)$ is positive. It can be shown in similar manner that the other variable is also positive at t_1. This contradicts the fact that t_1 is the supremum because at least one of the variable should be equal to zero at t_1. Therefore $t_1 = t_{max}$ and the solution is positive on its maximal interval of existence $[0, t_{max}[$.

Next, we show that the solution is bounded on $[0, t_{max}[$. By using Theorem 1.3.1.4 and by accounting for the positivity of the solution on $[0, t_{max}[$, we obtain from the two equations of system (4.2.0.1)

$$N(0)e^{-\mu_2 t} + \frac{B}{\mu_2}(1 - e^{-\mu_2 t}) \leq N(t) \leq N(0)e^{-\mu_1 t} + \frac{B}{\mu_1}(1 - e^{-\mu_1 t}). \qquad (4.3.2.3)$$

Therefore $N(t)$ is bounded on $[0, t_{max}[$. Hence $t_{max} = \infty$ which proves the global existence and the positivity results.

Concerning the invariance properties, it is easy to obtain from (4.3.2.3) that if $N(0) \leq B/\mu_1$ then $N(t) \leq B/\mu_1$. This establishes the invariance of $\mathcal{D}_0$ as required. The result (4.3.2.1) follows immediately from (4.3.2.3). □

In the view of Proposition 4.3.1 above, we conclude that system (4.2.0.1) is epidemiologically feasible in $\mathcal{D}_0$.

4.3.3 Equilibria, basic reproduction number and stability

To find the equilibria of system (4.2.0.1), we first note that the equilibria of this system remain the same as those of the system without delay since from (4.2.0.1) we have $\int_0^\infty g(\tau)d\tau = 1$ ([107]). However, for convenience, we denote the disease free and endemic equilibria for the model in this chapter by $\bar{E}_0$ and $\bar{E}$, respectively.

Thus, we have the following proposition without proof as it is already in Section 2.3.4.

Proposition 4.3.2. *For any value of the Hill coefficient, k, system (4.2.0.1) exhibits a transcritical bifurcation. Moreover, at the equilibrium, the HIV prevalence, $\bar{H}$, is an increasing function of Hill coefficient, k, and a decreasing function of the behavior change λ_0.*

In the following analysis, we consider $k = 1$. The case when $k > 1$ will be investigated numerically in Section 4.4.1.

From the Definition 1.3.2.1, the basic reproduction number is the product of the infection rate and the mean duration of the infection. This gives d/μ_2 as the basic reproduction number for system (4.2.0.1) wich is the same basic reproduction number of the continuous model (2.2.0.1). Therefore, we use the same notation for both models. That is

$$R_0^{HIV} = \frac{d}{\mu_2}. \tag{4.3.3.1}$$

For $k = 1$, the unique endemic equilibrium for system (4.2.0.1) is given by

$$\bar{E} = \left(\frac{B(1+\lambda_0)}{\mu_1(1+\lambda_0) + \mu_2\left(R_0^{HIV} - 1\right)}, \frac{B\left(R_0^{HIV} - 1\right)}{\mu_1(1+\lambda_0) + \mu_2\left(R_0^{HIV} - 1\right)} \right).$$

One should note that this equilibrium exists only if $R_0^{HIV} > 1$.

Next, we give a detailed analysis for the asymptotic stability of each equilibrium of system (4.2.0.1).

Let $(\bar{S}, \bar{I})$ be any equilibrium of the system. Then, the associated transcendental characteristic equation of system (4.2.0.1) at $(\bar{S}, \bar{I})$ is given by

$$\lambda^2 + a_1\lambda + a_2\lambda\mathcal{H}(\lambda, \bar{\tau}) + a_3 + a_4\mathcal{H}(\lambda, \bar{\tau}) = 0, \tag{4.3.3.2}$$

where

$$\begin{aligned} a_1 &= \mu_1 + \mu_2 - \frac{d(\bar{S} - \bar{I})}{\bar{S} + (1 + \lambda_0)\bar{I}}, \\ a_2 &= \frac{d\lambda_0\bar{S}\bar{I}}{(\bar{S} + (1 + \lambda_0)\bar{I})^2}, \\ a_3 &= \mu_1\mu_2 - \frac{d(\mu_1\bar{S}^2 - \mu_2\bar{I}^2)}{(\bar{S} + (1 + \lambda_0)\bar{I})(\bar{S} + \bar{I})}, \\ a_4 &= \frac{d\lambda_0\bar{S}\bar{I}(\mu_1\bar{S} + \mu_2\bar{I})}{(\bar{S} + (1 + \lambda_0)\bar{I})^2(\bar{S} + \bar{I})}, \end{aligned}$$

and

$$\mathcal{H}(\lambda, \bar{\tau}) = \int_0^\infty g_{n,\bar{\tau}}(\tau)e^{-\lambda\tau}d\tau.$$

4.3.3.1 Local stability of the disease free equilibrium

For the stability of system (4.2.0.1) at the disease free equilibrium, $\bar{E}_0$, we sate and prove the following result.

Theorem 4.3.3.1. *The disease free equilibrium of system (4.2.0.1), $\bar{E}_0$, is locally asymptotically stable if $R_0^{HIV} < 1$ and unstable if $R_0^{HIV} > 1$ independently of the mean delay $\bar{\tau}$ and the shape parameter n.*

Proof. At the disease free equilibrium $\bar{E}_0$, the characteristic equation (4.3.3.2) reduces

to

$$\lambda^2 + \left(\mu_1 + \mu_2\left(1 - R_0^{HIV}\right)\right)\lambda + \mu_1\mu_2\left(1 - R_0^{HIV}\right) = 0.$$

Therefore by Theorem 1.3.2.3, the required results are obtained. □

4.3.3.2 Global stability of the disease free equilibrium

In the following theorem, we discuss the global asymptotical stability of the DFE.

Theorem 4.3.3.2. *The disease free equilibrium of system (4.2.0.1), $\bar{E}_0$, is globally asymptotically stable in $\mathcal{D}_0$ if $R_0^{HIV} < 1$.*

Proof. By substituting $x = B/\mu_1 - S \geq 0$ and $y = I \geq 0$ for all t, in (4.2.0.1), we obtain the following system

$$\begin{aligned} \frac{dx(t)}{dt} &= \int_0^\infty g(\tau)f(z(t-\tau))d\tau z(t)\left(\frac{B}{\mu_1} - x(t)\right) - \mu_1 x(t), \\ \frac{dy(t)}{dt} &= \int_0^\infty g(\tau)f(z(t-\tau))d\tau z(t)\left(\frac{B}{\mu_1} - x(t)\right) - \mu_2 y(t), \end{aligned} \tag{4.3.3.3}$$

where

$$z(t) = \frac{y(t)}{\left(\frac{B}{\mu_1} - x(t)\right) + y(t)}.$$

System (4.3.3.3) has $(0,0)$ as an equilibrium. It must be noted that the global stability of $(0,0)$ for system (4.3.3.3) implies the global stability of the disease free equilibrium $\bar{E}_0 = \left(\frac{B}{\mu_1}, 0\right)$ for system (4.2.0.1) in $\mathcal{D}_0$. To show this, we note that

$$\begin{aligned} f(z(t-\tau)) - \mu_2 &= \frac{-\mu_2\left(1 - R_0^{HIV}\right) - \mu_2\lambda_0 z^k(t-\tau)}{1 + \lambda_0 z^k(t-\tau)}, \\ &< -\mu_2\left(1 - R_0^{HIV}\right). \end{aligned} \tag{4.3.3.4}$$

Thus, we have

$$\int_0^\infty g(\tau)f(z(t-\tau))d\tau - \mu_2 < -\mu_2\left(1 - R_0^{HIV}\right). \tag{4.3.3.5}$$

From the second equation of system (4.3.3.3), we have

$$\begin{aligned}
\frac{dy(t)}{dt} &= \int_0^\infty g(\tau)f(z(t-\tau))d\tau \left(\frac{\frac{B}{\mu_1} - x(t)}{\frac{B}{\mu_1} - x(t) + y(t)}\right) y(t) - \mu_2 y(t), \\
&< \left[\int_0^\infty g(\tau)f(z(t-\tau))d\tau - \mu_2\right] y(t), \\
&< -\mu_2\left(1 - R_0^{HIV}\right) y(t),
\end{aligned} \tag{4.3.3.6}$$

for $y(t) > 0$. By using results on differential inequalities [19], we obtain

$$y(t) < y(0)e^{-\mu_2\left(1-R_0^{HIV}\right)t}. \tag{4.3.3.7}$$

Therefore, if $R_0^{HIV} < 1$, it follows that $y(t) \to 0$ as $t \to \infty$.

Now from the first equation of system (4.3.3.3), we have

$$\begin{aligned}
\frac{dx(t)}{dt} &= \int_0^\infty g(\tau)f(z(t-\tau))d\tau \left(\frac{\frac{B}{\mu_1} - x(t)}{\frac{B}{\mu_1} - x(t) + y(t)}\right) y(t) - \mu_1 x(t), \\
&< \mu_2 y(t) - \mu_1 x(t), \\
&< \mu_2 y(0)e^{-\mu_2\left(1-R_0^{HIV}\right)t - \mu_1 x(t)},
\end{aligned}$$

where we have used (4.3.3.7) in the last step of the above inequality. This inequality can be written as

$$\frac{d}{dt}x(t) + \mu_1 x(t) < \mu_2 y(0)e^{-\mu_2\left(1-R_0^{HIV}\right)t}.$$

By using Theorem 1.3.1.4, the solution of the above inequality satisfies

$$x(t) < e^{-\mu_1 t}x(0) + \mu_2 y(0)e^{-\mu_1 t}\int_0^t e^{\left(\mu_1 - \mu_2\left(1-R_0^{HIV}\right)\right)s}ds.$$

Then

$$x(t) < \begin{cases} e^{-\mu_1 t}x(0) + \frac{\mu_2 y(0)}{\mu_1 - \mu_2\left(1-R_0^{HIV}\right)}\left(e^{-\mu_2\left(1-R_0^{HIV}\right)t} - e^{-\mu_1 t}\right), & \text{if } \mu_1 \neq \mu_2\left(1-R_0^{HIV}\right), \\ e^{-\mu_1 t}x(0) + \mu_2 y(0) t e^{-\mu_1 t}, & \text{if } \mu_1 = \mu_2\left(1-R_0^{HIV}\right). \end{cases}$$

It should be noted that the solution $x(t)$ is bounded above by exponentially decaying function as $t \to \infty$. Hence, $x \to 0$ as $t \to \infty$. Thus, we have proved that $(0,0)$ is globally stable for system (4.3.3.3) in $\mathcal{D}_0$. Therefore, $\bar{E}_0 = \left(\frac{B}{\mu_1}, 0\right)$ is globally asymptotically stable for system (4.2.0.1) in $\mathcal{D}_0$. □

4.3.3.3 Local stability of the endemic equilibrium

In this section we study the effect of the delay on the local stability of the endemic equilibrium, $\bar{E}$, of system (4.2.0.1). Throughout this section we consider $R_0^{HIV} > 1$. MacDonald [85] stated that the conditions for the stability for any n is the same as for the case $n \to \infty$. When $n \to \infty$, we have $\mathcal{H}(\lambda, \bar{\tau}) = e^{-\lambda\bar{\tau}}$ reducing the characteristic equation (4.3.3.2) to that obtained in the case of the discrete delay, i.e.,

$$\lambda^2 + a_1\lambda + a_2\lambda e^{-\lambda\bar{\tau}} + a_3 + a_4 e^{-\lambda\bar{\tau}} = 0, \tag{4.3.3.8}$$

where

$$\begin{aligned} a_1 &= \frac{\mu_1(1+\lambda_0) + \mu_2(R_0^{HIV}-1)}{1+\lambda_0}, \\ a_2 &= \frac{\lambda_0(R_0^{HIV}-1)\mu_2}{R_0^{HIV}(1+\lambda_0)}, \\ a_3 &= \frac{\mu_2(R_0^{HIV}-1)}{\lambda_0 + R_0^{HIV}}a_1, \\ a_4 &= \frac{\lambda_0}{R_0^{HIV}}a_3. \end{aligned}$$

When $\bar{\tau} = 0$, equation (4.3.3.8) reduces to

$$\lambda^2 + (a_1+a_2)\lambda + (a_3+a_4) = 0. \tag{4.3.3.9}$$

If $R_0^{HIV} > 1$, then the coefficients $a_i's > 0$. Therefore, by using Theorem 1.3.2.3, the roots of equation (4.3.3.9) are negative or have negative real parts. Thus we have proved the following proposition.

Proposition 4.3.3. *When there is no delay, the endemic equilibrium of (4.2.0.1) is locally asymptotically stable if* $R_0^{HIV} > 1$.

Next, we consider $\bar{\tau}$ as a bifurcation parameter to study the stability of the endemic equilibrium $\bar{E}$ of system (4.2.0.1) and the existence of Hopf bifurcation. By using Theorem 1.3.4.1, we establish the proposition below, where the conditions at which stability switches of the endemic equilibrium occur are determined.

Proposition 4.3.4. *There is a stability switch of the endemic equilibrium of system (4.2.0.1) if and only if equation (4.3.3.13) below has at least one positive root (i.e., ($d_2 < 0$) or ($d_2 = 0$ and $d_1 < 0$) or ($d_2 > 0$, $d_1 < 0$ and $\Delta > 0$) where d_2, d_1 and Δ are respectively given by (4.3.3.14), (4.3.3.15) and (4.3.3.18)) below.*

Proof. Assume $\lambda = i\omega$ and, without loss of generality, assume $\omega > 0$ is a root of (4.3.3.8) for some $\bar{\tau} > 0$. It should be noted that $a_3 + a_4 \neq 0$, which implies that $\omega \neq 0$. Thus, we have

$$a_2\omega\, sin\,\omega\bar{\tau} - \omega^2 + a_3 + a_4\, cos\,\omega\bar{\tau} + (a_2\omega\, cos\,\omega\bar{\tau} + a_1\omega - a_4\, sin\,\omega\bar{\tau})i = 0, \quad (4.3.3.10)$$

or equivalently, ω satisfies the following equations

$$a_2\omega\, sin\,\omega\bar{\tau} + a_4\, cos\,\omega\bar{\tau} = \omega^2 - a_3, \quad (4.3.3.11)$$

$$a_2\omega\, cos\,\omega\bar{\tau} - a_4\, sin\,\omega\bar{\tau} = -a_1\omega. \quad (4.3.3.12)$$

Squaring both sides of each equation above and then adding them we obtain

$$\omega^4 + d_1\omega^2 + d_2 = 0, \quad (4.3.3.13)$$

where

$$\begin{aligned} d_1 &= a_1^2 - a_2^2 - 2a_3, \\ &= \mu_1^2 + \frac{2\left(R_0^{HIV}-1\right)^2 \mu_2\mu_1}{\left(1+\lambda_0\right)\left(\lambda_0+R_0^{HIV}\right)} + \frac{\left(R_0^{HIV}-1\right)^2\left(R_0^{HIV}-\lambda_0\right)\left(\left(R_0^{HIV}\right)^2+\lambda_0^2\right)}{\left(R_0^{HIV}\right)^2\left(1+\lambda_0\right)^2\left(\lambda_0+R_0^{HIV}\right)} \\ &\quad -\frac{2\mu_2^2}{\left(1+\lambda_0\right)^2\left(\lambda_0+R_0^{HIV}\right)} \end{aligned} \tag{4.3.3.14}$$

and

$$\begin{aligned} d_2 &= a_3^2 - a_4^2, \\ &= \frac{\left(R_0^{HIV}-\lambda_0\right)\mu_2^2\left(R_0^{HIV}-1\right)^2\left(\mu_1\left(1+\lambda_0\right)+\mu_2\left(R_0^{HIV}-1\right)\right)^2}{\left(R_0^{HIV}\right)^2\left(\lambda_0+R_0^{HIV}\right)\left(1+\lambda_0\right)^2}. \end{aligned} \tag{4.3.3.15}$$

The roots of equation (4.3.3.13) are

$$\omega_1^2 = \frac{-d_1+\sqrt{\Delta}}{2} \tag{4.3.3.16}$$

and

$$\omega_2^2 = \frac{-d_1-\sqrt{\Delta}}{2}, \tag{4.3.3.17}$$

where

$$\Delta = d_1^2 - 4d_2. \tag{4.3.3.18}$$

To determine the sign of the derivative of $Re\lambda(\bar{\tau})$, from equation (4.3.3.8), we have

$$\left(2\lambda + a_2e^{-\lambda\bar{\tau}} - a_2\lambda\bar{\tau}e^{-\lambda\bar{\tau}} + a_1 - a_4\bar{\tau}e^{-\lambda\bar{\tau}}\right)\frac{d\lambda(\bar{\tau})}{d\bar{\tau}} - a_4\lambda e^{-\lambda\bar{\tau}} - a_2\lambda^2e^{-\lambda\bar{\tau}} = 0.$$

After rearranging, we obtain

$$\begin{aligned}\left(\frac{d\lambda}{d\bar{\tau}}\right)^{-1} &= \frac{(2\lambda+a_1)e^{\lambda\bar{\tau}}+a_2}{\lambda(a_2\lambda+a_4)}-\frac{\bar{\tau}}{\lambda},\\ &= -\frac{(2\lambda+a_1)}{\lambda(\lambda^2+a_1\lambda+a_3)}+\frac{a_2}{\lambda(a_2\lambda+a_4)}-\frac{\bar{\tau}}{\lambda}.\end{aligned}$$

Thus, we have

$$\begin{aligned}sign\left\{\left(\frac{dRe(\lambda)}{d\bar{\tau}}\right)^{-1}\right\}_{\lambda=i\omega} &= sign\left\{Re\left(\frac{d\lambda}{d\bar{\tau}}\right)^{-1}\right\}_{\lambda=i\omega},\\ &= sign\left\{d_1+2\omega^2\right\},\\ &= \begin{cases}\sqrt{\Delta} & \text{if } \omega=\omega_1\\ -\sqrt{\Delta} & \text{if } \omega=\omega_2.\end{cases}\end{aligned}$$

Therefore, for the equation (4.3.3.13), either

- it has no positive root, and hence no stability switch occurs, or
- it has exactly one positive root given by ω_1^2, where the crossing of the imaginary axis is from left to right as $\bar{\tau}$ increases and hence there exists a stability switch, where in this case necessarily $(d_2<0)$ or $(d_2=0$ and $d_1<0)$, or
- in addition to ω_1^2 it has another positive root ω_2^2, where the crossing at ω_2 is from right to left as $\bar{\tau}$ increase, and hence there is no stability switch at this root. In this case necessarily $d_2>0$, $d_1<0$ and $\Delta>0$.

Thus, equation (4.3.3.13) has one or two positive roots. In each case, there is a crossing of the imaginary axis from left to right as $\bar{\tau}$ increases and hence stability switches occur at some critical values of $\bar{\tau}$. □

In the following, we determine the thresholds of the delay at which the Hopf bifurcation occurs.

If ω_1 is the only positive root of (4.3.3.13), then from (4.3.3.11) and (4.3.3.12), we have

$$sin\,\omega\bar{\tau} = \frac{a_1a_4\omega - a_2\omega(a_3-\omega^2)}{a_2^2\omega^2+a_4^2},$$
$$cos\,\omega\bar{\tau} = -\frac{a_4(a_3-\omega^2)+a_1a_2\omega^2}{a_2^2\omega^2+a_4^2}.$$

By substituting $\theta_1 = \omega_1\bar{\tau}$, $0 < \theta_1 \leq 2\pi$, the above two equations can be written

$$sin\,\theta_1 = \frac{a_1a_4\omega_1 - a_2\omega_1(a_3-\omega_1^2)}{a_2^2\omega_1^2+a_4^2},$$
$$cos\,\theta_1 = -\frac{a_4(a_3-\omega_1^2)+a_1a_2\omega_1^2}{a_2^2\omega_1^2+a_4^2}.$$

Hence, from the last equation we have

$$\theta_1 = arccos\left(-\frac{a_4(a_3-\omega_1^2)+a_1a_2\omega_1^2}{a_2^2\omega_1^2+a_4^2}\right), \quad 0 < \theta_1 \leq \pi. \tag{4.3.3.19}$$

Therefore, at ω_1 we have

$$\bar{\tau}_{0,1} = \frac{\theta_1}{\omega_1}. \tag{4.3.3.20}$$

If, in addition to ω_1, equation (4.3.3.13) has other positive root ω_2, then there exists $\bar{\tau}_{0,2}$ such that

$$\bar{\tau}_{0,2} = \frac{\theta_2}{\omega_2}, \tag{4.3.3.21}$$

where

$$\theta_2 = arccos\left(-\frac{a_4(a_3-\omega_2^2)+a_1a_2\omega_2^2}{a_2^2\omega_2^2+a_4^2}\right), \quad 0 < \theta_2 \leq \pi. \tag{4.3.3.22}$$

By using the Propositions 4.3.3 and 4.3.4 above, we establish the following result for the local stability of the unique endemic equilibrium, $\bar{E}$, of system (4.2.0.1).

Theorem 4.3.3.3. *If $R_0^{HIV} > 1$, then*

I. For $\bar{\tau} = 0$, the endemic equilibrium is locally asymptotically stable.

II. As $\bar{\tau}$ increases, the endemic equilibrium is locally asymptotically stable for $\bar{\tau} \leq \bar{\tau}_{0,1}$ and becomes unstable when $\bar{\tau}$ passes through $\bar{\tau}_{0,1}$.

III. At $\bar{\tau} = \bar{\tau}_{0,1}$ system (4.2.0.1) exhibits a Hopf bifurcation; that is, a family of periodic solutions bifurcates from $\bar{E}$ as $\bar{\tau}$ passes through the critical value $\bar{\tau}_{0,1}$.

Biologically, the results of the above theorem mean that there is a critical value for the time $\bar{\tau}$ needed for individuals to change their risky behaviors. That time determines the stability of the endemic equilibrium $\bar{E}$.

In the above analysis, we have determined the conditions for the stability of the disease free equilibrium for any n when we consider gamma distribution, while we could determine the stability conditions for the endemic equilibrium for the discrete delay case only, that is when $n \to \infty$. Therefore, following MacDonald [85], we have the theorem:

Theorem 4.3.3.4. *The stability results obtained in Theorem (4.3.3.3) for the case of the discrete delay are applicable to the case of the continuous delay.*

4.4 Numerical results and simulations

In this section, we investigate the impact of the parameters: Hill coefficient k and behavior change λ_0 of the response function $f(H)$ and the parameters: $\bar{\tau}$ and n of gamma function on the endemic equilibria of system (4.2.0.1). In addition to this, the impact of these parameters on the HIV prevalence is also studied. Moreover, the impact of the delay on stability of the endemic equilibria and on the HIV prevalence when $k \geq 2$ is also provided.

4.4.1 Numerical stability analysis for Hill coefficient $k \geq 2$

In Section 4.3.3, the impact of the delay on the stability of the equilibria of system (4.2.0.1) were investigated analytically when Hill coefficient $k = 1$. The possible existence of pure imaginary eigenvalues will be examined numerically in this section for values of Hill coefficient $k \geq 2$. Thus, the roots of equation (4.3.3.13) will be investigated numerically when $k \geq 2$. When $k = 1$, the discriminant (4.3.3.18) is always negative for any $\bar{\tau} > 0$, and hence the equation has no positive solutions. This agrees well with the results of Proposition 4.3.4.

Now, for larger k, the equation (4.3.3.8) has the form

$$\lambda^2 + \tilde{a}_1\lambda + \tilde{a}_2\lambda e^{-\lambda\bar{\tau}} + \tilde{a}_3 + \tilde{a}_4 e^{-\lambda\bar{\tau}} = 0, \tag{4.4.1.1}$$

where the coefficients $\tilde{a}_i,\ i = 1...4$, have to be calculated numerically. Associated with this equation is the following fourth order equation in ω

$$(\omega^2)^2 + \tilde{d}_1\omega^2 + \tilde{d}_2 = 0, \tag{4.4.1.2}$$

with

$$\tilde{d}_1 = \tilde{a}_1^2 - \tilde{a}_2^2 - 2\tilde{a}_3, \tag{4.4.1.3}$$

$$\tilde{d}_2 = \tilde{a}_3^2 - \tilde{a}_4^2, \tag{4.4.1.4}$$

and

$$\tilde{\Delta} = \tilde{d}_1^2 - 4\tilde{d}_2. \tag{4.4.1.5}$$

Remark 4.4.1.1. For each $k \geq 2$, system (4.2.0.1) has exactly one endemic equilibrium guaranteed by Proposition 4.3.2. If $R_0^{HIV} > 1$, then each of these endemic equilibria is locally asymptotically stable when $\bar{\tau} = 0$. Moreover, when $\bar{\tau} > 0$, system (4.2.0.1) exhibits Hopf bifurcations.

When $\bar{\tau} = 0$, the eigenvalues for each endemic equilibrium when $k \geq 2$ are calculated for $R_0^{HIV} > 1$. In each case, these eigenvalues are negative or have negative real parts. This gives the required result when there is no delay.

In the following, we consider $\bar{\tau}$ in the range from $\bar{\tau} = 1$ month to $\bar{\tau} = 15$ years. In each case we have $\tilde{a}_3 + \tilde{a}_4 \neq 0$, which implies that $\omega \neq 0$.

Now, when $k = 2$ months, we have $\tilde{\Delta} > 0$, $\tilde{d}_1 < 0$ and $\tilde{d}_2 > 0$ for $\bar{\tau} > 0$. Hence, we have two positive solutions for the equation (4.4.1.2), where

$$sign\left\{\left(\frac{dRe(\lambda)}{d\bar{\tau}}\right)^{-1}\right\}_{\lambda=i\omega_1} > 0 \tag{4.4.1.6}$$

and

$$sign\left\{\left(\frac{dRe(\lambda)}{d\bar{\tau}}\right)^{-1}\right\}_{\lambda=i\omega_2} > 0. \tag{4.4.1.7}$$

Hence, there is stability switch of the endemic equilibrium $(\bar{S}, \bar{I}) = (1280, 1744)$ at $\bar{\tau}_{0,1} = 23.8$ months and $\bar{\tau}_{0,2} = 151.7$ months corresponding to $\omega_1 = 0.1037$ and $\omega_2 = 0.0203$ respectively. Therefore, Hopf bifurcations occur as $\bar{\tau}$ passes through $\bar{\tau}_{0,1}$ and $\bar{\tau}_{0,2}$.

When we solve equation (4.4.1.2) for $3 \leq k \leq 8$, we always have $\tilde{d}_2 < 0$ for $\bar{\tau} > 0$. Hence, we have one positive solution ω for each k with

$$sign\left\{\left(\frac{dRe(\lambda)}{d\bar{\tau}}\right)^{-1}\right\}_{\lambda=i\omega} > 0.$$

Therefore, there is stability switch of the endemic equilibrium for each k and Hopf bifurcations occur as $\bar{\tau}$ passes through the critical values $\bar{\tau}_{0,1}$.

When $k = 9$, 10, we have $\tilde{\Delta} > 0$, $\tilde{d}_1 < 0$ and $\tilde{d}_2 > 0$ for $\bar{\tau} > 0$. Hence, we have two

positive solutions in each case for equation (4.4.1.2), where

$$sign\left\{\left(\frac{dRe(\lambda)}{d\bar{\tau}}\right)^{-1}\right\}_{\lambda=i\omega_1} > 0 \tag{4.4.1.8}$$

and

$$sign\left\{\left(\frac{dRe(\lambda)}{d\bar{\tau}}\right)^{-1}\right\}_{\lambda=i\omega_2} > 0. \tag{4.4.1.9}$$

Therefore, there is a stability switch of each endemic equilibrium and Hopf bifurcations occur as $\bar{\tau}$ passes through the critical values $\bar{\tau}_{0,1}$ and $\bar{\tau}_{0,2}$ for each k.

From the above, it is clear how the delay affects the stability of the endemic equilibria for different values of Hill coefficient k. For the values of the parameters given in Table 2.2.0.1, the stability of the endemic equilibrium is not affected by the delay when $k = 1$, while there is a stability switch for each endemic equilibrium when $2 \leq k \leq 10$ as we have one or two positive solutions for the equation (4.4.1.2) and the crossing of the imaginary axis is from left to right giving rise to Hop bifurcations to occur as the delay passes through the critical values $\bar{\tau}_{0,1}$ or $\bar{\tau}_{0,2}$ which are defined for each k.

4.4.2 Numerical simulations

To study the impact of the delay on the HIV prevalence, we make use of Matlab solver *ode15s* to integrate the equations of system (4.2.0.1). Because of the nature of the delay considered in this model, we extend the Matlab solver *ode15s* in a special manner. A Matlab quadrature routine *quadgk*, which supports infinite intervals, is invoked to calculate the infinite integral. It should be noted that the MATLAB solver *dde23* (designed to solve delay differential equations) can not be used in this case, simply because here we are dealing with a problem having an infinite delay.

We will vary the values of some parameters whereas the other parameters used in the simulations are taken from Table 2.2.0.1.

In Figure 4.4.2.1, it is shown that the number of susceptibles (infectious individuals)

decreases (increases) with the value of Hill coefficient k. In contrast to this, it is shown that the number of susceptibles (infectious individuals) increases (decreases) with the value of behavior change parameter λ_0.

In Proposition 4.3.2, we have shown that, at an equilibrium, the prevalence increases when k is increased and decreases when λ_0 is increased. This is shown in Figure 4.4.2.2.

Figure (4.4.2.3) below, shows how the profile of the HIV prevalence varies with time t for different values of the parameters of the response function k and λ_0.

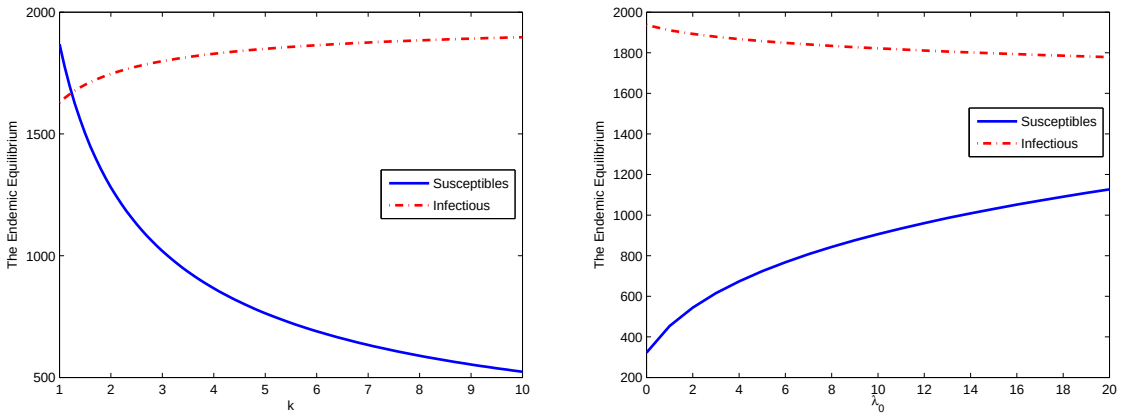

Figure 4.4.2.1: The endemic equilibrium of system (4.2.0.1) as k (left figure) and λ_0 (when $k = 5$) (right figure) with $n = 30$ and $\bar{\tau} = 3$ months.

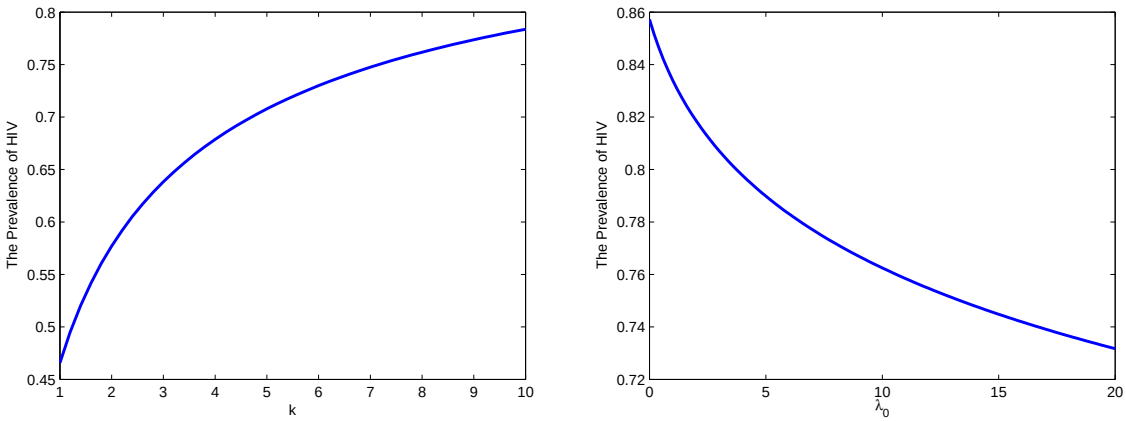

Figure 4.4.2.2: The prevalence of HIV at the endemic equilibrium as function of k (left figure) and λ_0 (when $k = 10$) (right figure) with $n = 30$ and $\bar{\tau} = 3$ months.

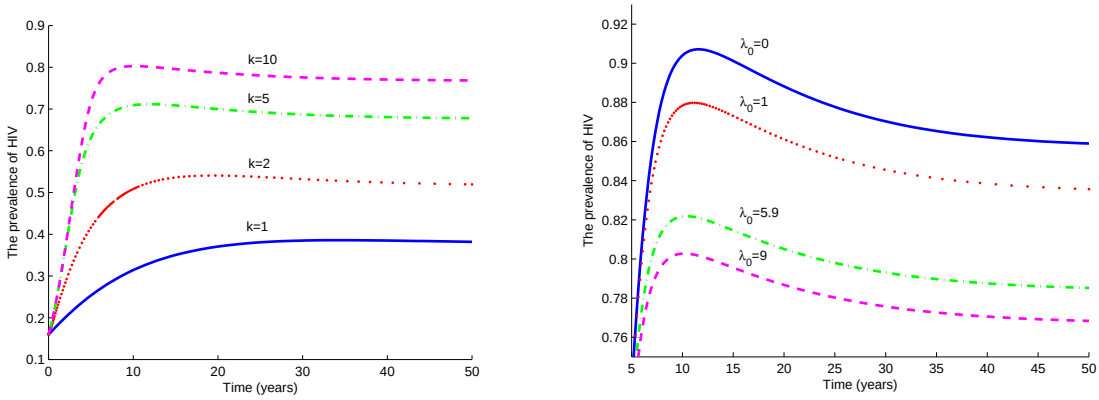

Figure 4.4.2.3: The HIV prevalence against time t for different values of k (left figure) and different values of λ_0 (right figure) with $n = 30$ and $\bar{\tau} = 3$ months.

Next, we investigate the impact of the parameters of gamma function, the mean delay $\bar{\tau}$ and the shape parameter n, on the HIV prevalence.

As it can be seen from Figure 4.4.2.4, the mean delay has a small effect on the prevalence for small value of k (corresponding to a situation where the response is quick) while $\bar{\tau}$ affects the value and the shape of the prevalence peak before the prevalence stabilizes. It should be noted that this occurs for larger values of k (corresponding to a situation where the response is slow).

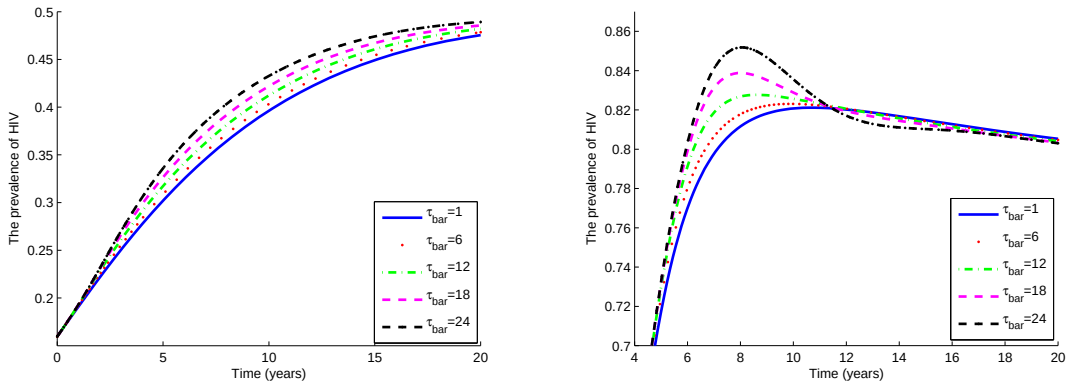

Figure 4.4.2.4: The effect of $\bar{\tau}$ on the HIV prevalence when $k = 1$ (left figure) and when $k = 10$ (right figure) with $n = 30$.

In the next two figures, we have plotted the HIV prevalence for different values of the shape parameter n with various values of k and λ_0 taking into consideration slow and quick responses of individuals to the HIV prevalence (controlled by k).

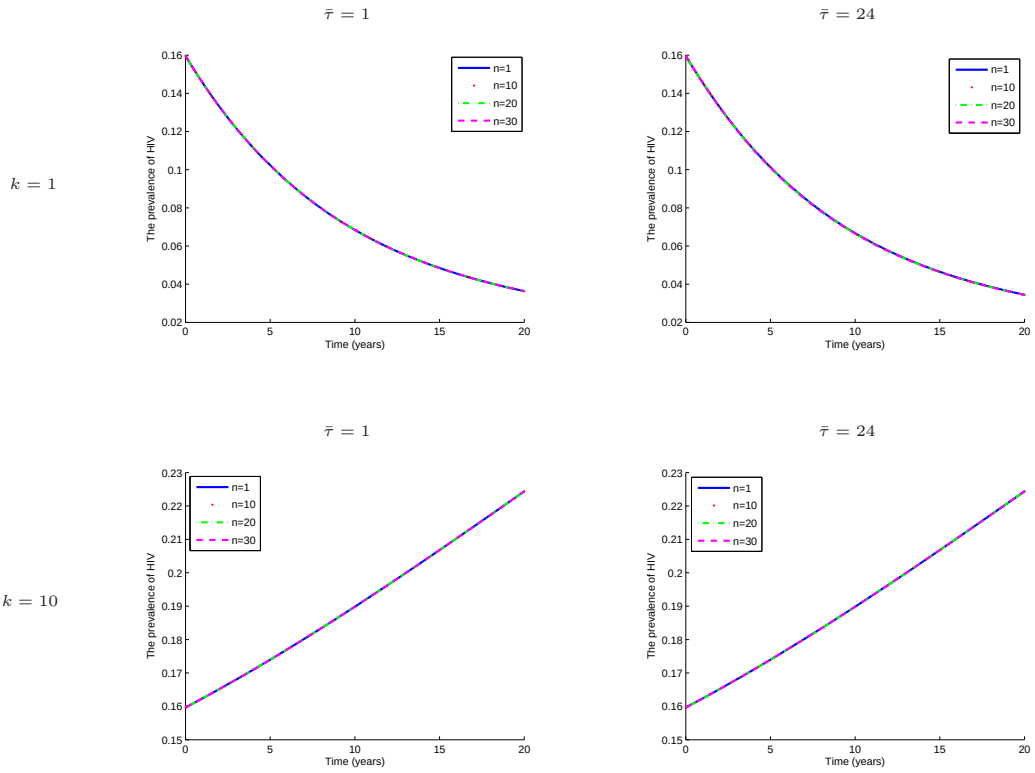

Figure 4.4.2.5: The effect of n on the HIV prevalence when $d = 0.15$ and $\lambda_0 = 40$ with different values of k and $\bar{\tau}$.

By decreasing the value of the maximum contact rate d and increasing the value of the behavior change parameter λ_0, to keep the prevalence at low values (more realistically), it can be seen from Figure 4.4.2.5, that the shape parameter has no effect on the HIV prevalence if individuals respond quickly (small k) or slowly (large k). This remains the same even if we use different values of the mean delay $\bar{\tau}$ in these simulations.

For larger values of the prevalence, as in Figure 4.4.2.6, we can see that if $\bar{\tau}$ is small, then n has no impact on the prevalence whether the response is quick or slow (left column). When $\bar{\tau}$ is larger, then n starts to have an impact on the HIV prevalence

(right column).

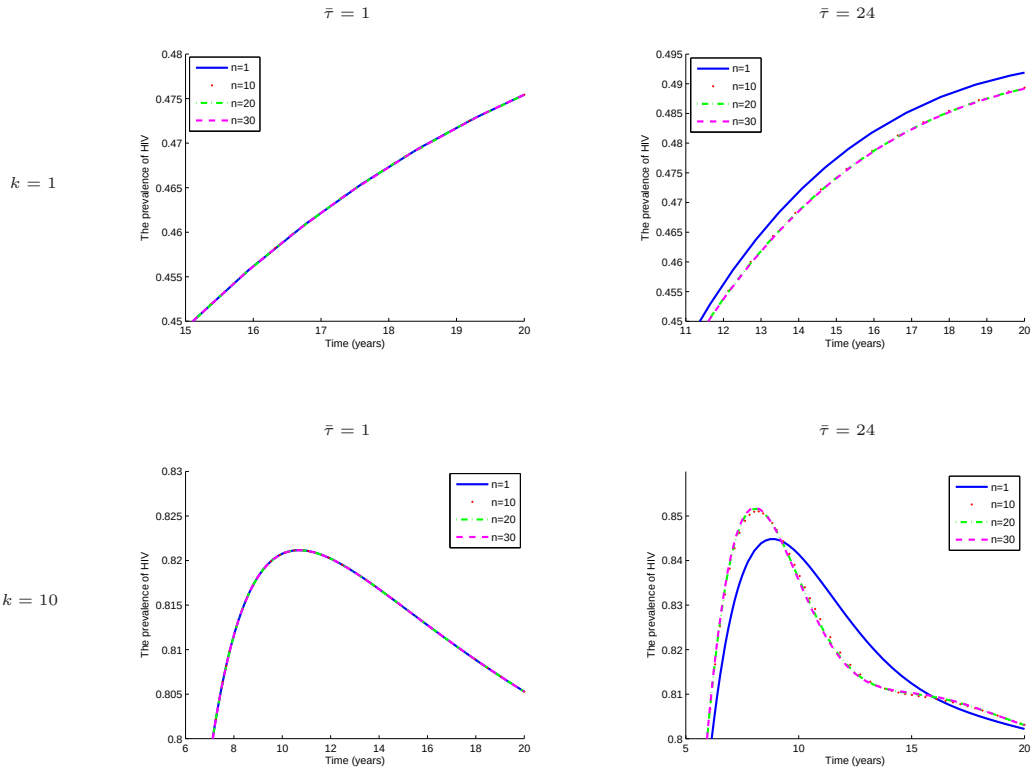

Figure 4.4.2.6: The effect of n on the HIV prevalence when $d = 0.7$ and $\lambda_0 = 5.9$ with different values of k and $\bar{\tau}$.

4.5 Summary and discussion

In this chapter we developed and analyzed an HIV mathematical model that accounts for behavior change. The contact rate is modeled by the response function, which is a decreasing function of the HIV prevalence to reflect a reduction in risky behavior that results from the awareness of individuals to a higher HIV prevalence.

We explored the impact of introducing a distributed delay, which represents the time needed for the individuals to reduce their risky behaviors, on the stability of the model equilibria. The disease free equilibrium is found globally asymptotically stable when $R_0^{HIV} < 1$ and unstable when $R_0^{HIV} > 1$ independent of the mean delay $\bar{\tau}$ and the

shape parameter n. We showed that the introduction of the distributed delay in the model leads to a Hopf bifurcation around the endemic equilibrium of the model. This bifurcation corresponds to the existence of periodic solutions that oscillate around the endemic equilibrium at given thresholds.

Further, we showed how the incorporation of the delay affected the HIV prevalence. In situations where individuals do not respond until the HIV prevalence reaches a high value (modeled by a large value of Hill coefficient k, i.e., $k = 10$), this resulted in more HIV infections causing more increase in the HIV prevalence.

On the other hand, in situations where individuals respond very quickly to the HIV prevalence (modeled by a small value of Hill coefficient k, i.e., $k = 1$), the delay is found to have little impact on the prevalence as in this case when individuals delay their response will not result in more infections. These effects can be seen in Figure 4.4.2.4.

In the next chapter, we design special class of numerical methods to solve the mathematical model of HIV transmissions dynamics presented in Chapter 2. These methods are then extended to solve the full model.

Chapter 5

An unconditionally stable nonstandard finite difference method for the HIV model

We design and analyze an unconditionally stable nonstandard finite difference method for the mathematical model of HIV transmission dynamics presented in Chapter 2. The dynamics of this model are studied using the qualitative theory of dynamical systems. These qualitative features of the continuous model are preserved by the numerical method that we propose in this chapter. This method also preserves positivity of the solution which is one of the essential requirements when modeling epidemic diseases. Furthermore, we show that the numerical method is elementary stable. Robust numerical results confirming theoretical investigations are provided. Comparisons are also made with the other conventional approaches that are routinely used for such problems.

5.1 Introduction

In this chapter, we design a special class of numerical methods, known as nonstandard finite difference methods (NSFDMs). Dimitrov and Kojouharov [38] pointed out that

numerical methods one uses to approximate the solutions of dynamical systems, are expected to be consistent with the original differential systems, and should be stable and convergent. The methods that we develop in this chapter meet these criteria in addition to other essential properties. These NSFDMs are explored by many researchers to solve problems in the biological sciences and other areas. Below, we mention a few of them.

Arenas *et al.* [8] developed a nonstandard numerical scheme for a SIRS seasonal epidemiological model for Respiratory Syncytial Virus (RSV). They compared their method with some well-known explicit methods and carried out some simulations with data from Gambia and Finland. They showed that the forward Euler and fourth order Runge-Kutta schemes do not converge unless the step-size used in the numerical simulations for these two methods is less than a critical step-size $h_c = 0.1$.

General two-dimensional autonomous dynamical systems and their standard numerical discretizations are considered in [36]. In this work, Dimitrov *et al.* designed and analyzed nonstandard stability-preserving finite-difference schemes based on the explicit and implicit Euler and the second-order Runge-Kutta methods. The methods proposed in that paper can be applicable for solving arbitrary two-dimensional autonomous dynamical systems. In another work ([37]), these authors formulated positive and elementary stable nonstandard finite-difference methods to solve a general class of Rosenzweig-MacArthur predator-prey systems which involve a logistic intrinsic growth of the prey population. Their methods preserve the positivity of solutions and the stability of the equilibria for arbitrary step-sizes, while the approximations obtained by the other numerical methods experience difficulties in preserving either the stability or the positivity of the solutions or both.

In [54], Gumel *et al.* investigated a class of NSFDMs for solving systems of differential equations arising in mathematical biology. They showed that their methods can often give numerical results that are asymptotically consistent with those of the corresponding continuous model by using a number of case studies in human epidemiology and ecology.

Some fundamentals concepts and applications of nonstandard finite different scheme for the solution of an initial value problem of ordinary differential equations are presented in [61] by Ibijola *et al.* They stated the reason why nonstandard methods are needed despite the fact that we have numerous standard methods available by pointing out that one of the shortcomings of standard methods is that qualitative properties of the exact solution are not usually transferred to the numerical solution.

In [65] Jódar *et al.* explain how to construct two competitive implicit finite difference schemes for a deterministic mathematical model associated with the evolution of influenza in human population. They obtained numerical simulations with different sets of initial conditions, parameters values, time step-sizes.

Villanueva *et al.*[139] developed (and analyzed numerically) nonstandard finite difference schemes which is free of numerical instabilities, to obtain the numerical solution of a mathematical model of infant obesity with constant population size. This model consists of a system of coupled nonlinear ordinary differential equations describing the dynamics of overweight and obese populations. The numerical results presented in this paper showed that their methods have better convergence properties as compared to the classical Euler or the fourth-order Runge-Kutta methods and the MATLAB routines in the sense that these routines give negative values for some of the state variables.

The relationship between a continuous dynamical system and numerical methods to solve it, viewed as discrete dynamical systems, is studied by Anguelov *et al.* [5]. In this work, the authors further categorize the term 'dynamic consistency' as the 'topological dynamic consistency' and proposed a topologically dynamically consistent nonstandard finite difference method.

Applications of these NSFDMs for singularly perturbed problems can be seen in [66, 80, 81, 82, 83, 97, 113, 114, 115]. However, an exhaustive account of work that use such methods is provided in the survey article by Patidar [112].

We develop in this chapter some NSFDMs for numerical solution of the system (2.2.0.1) presented in Chapter 2. To keep the methods fully explicit, we will use

the forward difference approximations for the first derivative terms. The nonlocal approximations will be used to tackle the nonlinear terms. In some cases, we will also make use of denominator functions which are little complex functions of the time step-size than the classical one. Furthermore, we will show that these NSFDMs preserve some key properties of the corresponding continuous model. It should be noted that the proposed schemes are unconditionally stable.

This chapter is organized as follows. In the next section, we design and analyze a numerical method to solve the model proposed in Chapter 2. Further numerical analysis as well as some numerical simulations are presented in Section 5.3. A thorough discussion on the results is presented in Section 5.4.

5.2 Construction and analysis of the NSFDM

In this section, we design a nonstandard finite difference method (NSFDM) that satisfies the positivity of the state variables involved in the system (2.2.0.1) presented in Chapter 2. It is important that a numerical method preserves this property when used to solve differential models arising in population biology because these state variables represent subpopulations which never take negative values.

To keep this chapter self-contained, we recall the following model presented in Chapter 2:

$$\begin{aligned} \frac{dS(t)}{dt} &= B - f(H(t))H(t)S(t) - \mu_1 S(t), \\ \frac{dI(t)}{dt} &= f(H(t))H(t)S(t) - \mu_2 I(t), \end{aligned} \tag{5.2.0.1}$$

where

$$H(t) = \frac{I(t)}{N(t)}, \tag{5.2.0.2}$$

with $N(t) = S(t) + I(t)$ as the total number of population, and

$$f(H) = \frac{d}{1 + \lambda_0 H^k}, \quad k \geq 1. \tag{5.2.0.3}$$

The descriptions of the state variables and other time-invariant parameters as well as their values are mentioned in Chapter 2.

To construct the NSFDM, we discretize the system (5.2.0.1) based on the approximation of the temporal derivatives by a generalized first order forward method. To begin with, the time domain $[0, T]$ is partitioned through the discrete time levels $t_n = n\ell$, where $\ell > 0$ is the time step-size. We then have

For $S(t) \in \mathbb{C}^1(\mathbb{R})$, the discrete derivative is defined by

$$\frac{dS(t)}{dt} = \frac{S(t + \ell) - S(t)}{\psi(\ell)} + \mathcal{O}(\psi(\ell)) \text{ as } \ell \to 0, \tag{5.2.0.4}$$

where $\psi(\ell)$ is a denominator function ([91, 93]) which is a real-valued function and satisfies

$$\psi(\ell) = \ell + \mathcal{O}(\ell^2), \text{ for all } \ell > 0. \tag{5.2.0.5}$$

The discrete derivative for $I(t)$ is obtained analogously whereas the non-derivative terms are approximated locally, i.e., at the base time level.

Denoting the approximations of $S(n\ell)$ and $I(n\ell)$ by S^n and I^n, respectively, where $n = 0, 1, 2, ...$; the NSFDM reads

$$\begin{aligned} \frac{S^{n+1} - S^n}{\psi(\ell)} &= B - \mu_1 S^{n+1} - f(H^n) H^n S^{n+1}, \\ \frac{I^{n+1} - I^n}{\psi(\ell)} &= f(H^n) H^n S^{n+1} - \mu_2 I^{n+1}, \end{aligned} \tag{5.2.0.6}$$

where discretizations for H and $f(H)$ are given by

$$H^n = \frac{I^n}{S^n + I^n} \tag{5.2.0.7}$$

and

$$f(H^n) = \frac{d}{1 + \lambda_0 (H^n)^k}, \tag{5.2.0.8}$$

respectively.

Remark 5.2.0.1. It is to be noted that besides the use of a non-classical denominator function, we have also used some non-local discretizations. As is mentioned in the literature (see, e.g., [92, 112]) a finite difference method is termed as a nonstandard finite difference method if either we use a denominator function or a non-local approximation. In view of this, when $\psi(\ell) = \ell$, the above method will be referred to as "NSFDM-I". However, if the denominator function $\psi(\ell)$ is different than ℓ, the method will be referred to as "NSFDM-II". In this work, this function is considered as $(e^{\mu_2 \ell} - 1)/\mu_1,\ \mu_2 > \mu_1$.

Simplifying (5.2.0.6), we obtain

$$\begin{aligned} S^{n+1} &= \frac{S^n + \psi(\ell) B}{1 + \psi(\ell) \left\{ f(H^n) H^n + \mu_1 \right\}}, \\ I^{n+1} &= \frac{I^n + \psi(\ell) f(H^n) H^n S^{n+1}}{1 + \mu_2 \psi(\ell)}. \end{aligned} \tag{5.2.0.9}$$

The positivity of the solution reflects from the above method (5.2.0.9), because if the initial values $S(0)$ and $I(0)$ are non-negative, then the right hand side of (5.2.0.9) admits no negative terms for any of $n = 0, 1, 2, 3, ...$

In the following section we determine the stability properties of system (5.2.0.6), and we verify that

(i) the continuous and the discrete models have the same equilibria, and

(ii) both models possess similar qualitative features near these equilibria.

5.2.1 Fixed points and stability analysis

We study in this section the stability and convergence properties of the fixed points of the proposed NSFDM numerical method (5.2.0.6).

We begin by noting that the fixed points $(\hat{S}, \hat{I})$ of system (5.2.0.6) can be found by solving

$$\begin{aligned} F(\hat{S}, \hat{I}) &= \hat{S}, \\ G(\hat{S}, \hat{I}) &= \hat{I}, \end{aligned} \tag{5.2.1.1}$$

where $F(\hat{S}, \hat{I})$ and $G(\hat{S}, \hat{I})$ can be obtained by considering the right hand sides in (5.2.0.9), i.e.,

$$\begin{aligned} F(\hat{S}, \hat{I}) &= \frac{\hat{S} + \psi(\ell)B}{1 + \psi(\ell)\left\{f(\hat{H})\hat{H} + \mu_1\right\}}, \\ G(\hat{S}, \hat{I}) &= \frac{\hat{I} + \psi(\ell)f(\hat{H})\hat{H}\hat{S}}{1 + \mu_2\psi(\ell)}, \end{aligned} \tag{5.2.1.2}$$

where

$$\hat{H} = \frac{\hat{I}}{\hat{S} + \hat{I}}. \tag{5.2.1.3}$$

Solving (5.2.1.1), we obtain the following equation for $\hat{H}$:

$$\hat{H}\left(\mu_2\lambda_0\hat{H}^k + d\hat{H} + \mu_2\left(1 - R_0^{HIV}\right)\right) = 0. \tag{5.2.1.4}$$

In the above equation, $\hat{H} = 0$ corresponds to the disease free equilibrium

$$\hat{E}_0 = \left(\frac{B}{\mu_1}, 0\right), \tag{5.2.1.5}$$

whereas the system may have more than one endemic equilibrium which can be written

in the following implicit form:

$$\hat{E} = \left(\frac{B(1-\hat{H})}{\mu_1(1-\hat{H}) + \mu_2\hat{H}}, \frac{B\hat{H}}{\mu_1(1-\hat{H}) + \mu_2\hat{H}} \right), \tag{5.2.1.6}$$

in which $\hat{H}$ corresponds to the positive solutions of the characteristic equation

$$\mu_2\lambda_0\hat{H}^k + d\hat{H} + \mu_2\left(1 - R_0^{HIV}\right) = 0. \tag{5.2.1.7}$$

The form of the above equation is similar to the characteristic equation for the continuous systems (5.2.0.1) given by (2.3.4.3). Therefore, both systems (5.2.0.1) and (5.2.0.6) have the same characteristic equation and expressions of equilibria. Hence, we have the following result.

Remark 5.2.1.1. For any k, the continuous system (5.2.0.1) and the discrete system (5.2.0.6) have the same equilibria. Furthermore, when $k = 1$, then in addition to above disease free equilibrium, the system (5.2.0.6) has the following endemic equilibrium

$$\hat{E} = \left(\frac{B(1+\lambda_0)}{(\mu_1(1+\lambda_0) + \mu_2\left(R_0^{HIV} - 1\right)}, \frac{B\left(R_0^{HIV} - 1\right)}{\mu_1(1+\lambda_0) + \mu_2\left(R_0^{HIV} - 1\right)} \right), \tag{5.2.1.8}$$

which exists only if $R_0^{HIV} > 1$.

The next theorems give us the stability properties only when $k = 1$. However, it is difficult to find the endemic equilibria for system (5.2.0.6) in closed form when $k \geq 2$, we will be investigating them numerically. This will be shown in Section 5.3.1. Moreover, we will show that both systems (the discrete as well as the continuous) behave similarly near their equilibria.

Theorem 5.2.1.1. *Let $\psi(\ell)$ be a real-valued function such that $\psi(\ell) = \ell + O(\ell^2)$. If $R_0^{HIV} < 1$, then system (5.2.0.6) is unconditionally (i.e.,regardless of the step-size ℓ) locally asymptotically stable at the disease free equilibrium, $\hat{E}_0 = (B/\mu_1, 0)$, and unstable otherwise.*

Proof. The Jacobian matrix of the system (5.2.0.6) evaluated at the disease free equilibrium, $\hat{E}_0$, is

$$J(\hat{E}_0) = \begin{pmatrix} \frac{1}{1+\psi(\ell)\mu_1} & -\frac{\psi(\ell)d}{1+\psi(\ell)\mu_1} \\ 0 & \frac{1+\psi(\ell)d}{1+\psi(\ell)\mu_2} \end{pmatrix}.$$

Being a triangular matrix, its eigenvalues are the entries along the main diagonal, i.e.,

$$\lambda_1 = \frac{1}{1+\psi(\ell)\mu_1},$$

and

$$\lambda_2 = \frac{1+\psi(\ell)d}{1+\psi(\ell)\mu_2}.$$

It should be noted that the inequality $|\lambda_1| < 1$ always holds. However, $|\lambda_2| < 1$ if $d < \mu_2$, i.e., if $\mu_2\left(R_0^{HIV} - 1\right) < 0$, which is always true since $R_0^{HIV} < 1$ for the disease free equilibrium. Hence, the spectral radius is strictly less than unity in magnitude if $R_0^{HIV} < 1$ for all ℓ, and then using Theorem 2.10 in [3], the required result is obtained. □

Theorem 5.2.1.2. *The endemic equilibrium of system (5.2.0.6), $\hat{E}$, is unconditionally locally asymptotically stable if $R_0^{HIV} > 1$.*

Proof. The Jacobian matrix of the system (5.2.0.6) evaluated at the endemic equilibrium

$$\hat{E} = \left(\frac{B(1+\lambda_0)}{(\mu_1(1+\lambda_0) + \mu_2\left(R_0^{HIV} - 1\right)}, \frac{B\left(R_0^{HIV} - 1\right)}{\mu_1(1+\lambda_0) + \mu_2\left(R_0^{HIV} - 1\right)} \right),$$

is

$$J(\hat{E}) = \begin{pmatrix} \frac{R_0^{HIV}(1+\lambda_0)+\psi(\ell)\mu_2\left(R_0^{HIV}-1\right)}{R_0^{HIV}\left((1+\psi(\ell)\mu_1)(1+\lambda_0)+\psi(\ell)\mu_2\left(R_0^{HIV}-1\right)\right)} & -\frac{\mu_2(1+\lambda_0)\psi(\ell)}{R_0^{HIV}\left((1+\psi(\ell)\mu_1)(1+\lambda_0)+\psi(\ell)\mu_2\left(R_0^{HIV}-1\right)\right)} \\ \\ \frac{\mu_2\left(R_0^{HIV}-1\right)^2\psi(\ell)}{R_0^{HIV}(1+\psi(\ell)\mu_2)(1+\lambda_0)} & \frac{R_0^{HIV}+\psi(\ell)\mu_2}{R_0^{HIV}(1+\psi(\ell)\mu_2)} \end{pmatrix},$$

which can be written in the following form

$$J(\hat{E}) = \begin{pmatrix} b_1 & -b_2 \\ b_3 & b_4 \end{pmatrix},$$

where

$$\begin{aligned} b_1 &= \frac{a_1 + a_2}{a_1 a_3 + R_0^{HIV} a_2}, \\ b_2 &= \frac{a_4}{a_1 a_3 + R_0^{HIV} a_2}, \\ b_3 &= \frac{a_2\left(R_0^{HIV} - 1\right)}{a_5 a_7}, \\ b_4 &= \frac{a_6}{a_7}, \end{aligned}$$

with

$$\begin{aligned} a_1 &= R_0^{HIV}(1 + \lambda_0), \\ a_2 &= \psi(\ell)\mu_2\left(R_0^{HIV} - 1\right), \\ a_3 &= 1 + \psi(\ell)\mu_1, \\ a_4 &= \mu_2(1 + \lambda_0)\psi(\ell), \\ a_5 &= 1 + \lambda_0, \\ a_6 &= R_0^{HIV} + \psi(\ell)\mu_2, \\ a_7 &= R_0^{HIV}(1 + \psi(\ell)\mu_2). \end{aligned}$$

Since we have $R_0^{HIV} > 1$, it should be noted that $a_i > 0$, $1 \leq i \leq 7$, $0 < b_1$, $b_4 < 1$ and

b_2, $b_3 > 0$.

The characteristic equation associated with the above matrix is given by

$$g(\lambda) = \lambda^2 - A_1\lambda + A_2 = 0, \tag{5.2.1.9}$$

where

$$\begin{aligned} A_1 &= b_1 + b_4 > 0, \\ A_2 &= b_1 b_4 + b_2 b_3 > 0. \end{aligned}$$

From equation (5.2.1.9), we have

$$\begin{aligned} g(1) &= 1 - A_1 + A_2, \\ &= (1 - b_1)(1 - b_4) + b_2 b_3, \\ &> 0, \end{aligned} \tag{5.2.1.10}$$

as both b_1 and b_4 are less than unity. Also

$$\begin{aligned} g(-1) &= 1 + A_1 + A_2, \\ &> 0, \end{aligned} \tag{5.2.1.11}$$

since both A_1 and A_2 are greater than zero. Moreover, we have

$$\begin{aligned} |g(0)| &= |A_2|, \\ &= \left| \frac{\nu_1 + \nu_2}{\nu_1 + R_0^{HIV}\nu_2 + \nu_3} \right| < 1, \end{aligned} \tag{5.2.1.12}$$

since we have $R_0^{HIV} > 1$, and

$$\begin{aligned}
\nu_1 &= R_0^{HIV}(1+\lambda_0) > 0, \\
\nu_2 &= \psi(\ell)\mu_2(R_0^{HIV}+\lambda_0) + (\psi(\ell))^2\mu_2^2\left(R_0^{HIV}-1\right) > 0, \\
\nu_3 &= \psi(\ell)\mu_1 R_0^{HIV}(1+\lambda_0)(1+\psi(\ell)\mu_2) > 0.
\end{aligned}$$

From (5.2.1.10), (5.2.1.11) and (5.2.1.12), the conditions of Lemma 1.3.3.1 hold. Therefore, the eigenvalues of the associated Jacobian matrix in this case are strictly less than unity in modulus when $R_0^{HIV} > 1$ for all step-sizes ℓ. Hence, the numerical method (5.2.0.6) is unconditionally stable at its endemic equilibrium $\hat{E}$. □

Remark 5.2.1.2. From the results in this section, we can conclude that both models (the continuous (5.2.0.1) as well as the discrete one (5.2.0.6)) have the same equilibria, and they behave qualitatively similar near these equilibria. Therefore, the nonstandard finite difference method (5.2.0.6) is elementary stable.

5.3 Numerical results and simulations

In this section, we present some numerical simulations using the proposed NSFDMs. The numerical results that we obtain support our theoretical results. The methods are also tested for convergence. We numerically show that both of these methods (NSFDM-I and NSFDM-II) are elementary stable when the Hill coefficient $k \geq 2$. A number of different numerical simulations are carried out and comparisons are made with other well-known numerical methods for various time step-sizes ℓ. Parameters values used in the simulations are presented in Table 2.2.0.1 (which gives $R_0^{HIV} > 1$). Some of these parameters are varied to test the robustness of the methods. As is mentioned before in Section 5.2.1, for $k \geq 2$, we attempt to investigate the stability of the endemic equilibria numerically as shown below in Table 5.3.1.1 and Table 5.3.1.2.

5.3.1 Numerical stability analysis of the fixed points

The spectral radii of the Jacobian matrices corresponding to the endemic equilibria of the numerical method for different values of Hill coefficient k and the time step-size ℓ are tabulated in this section. We recall from Remark 5.2.1.1, the equilibria of both systems (5.2.0.1) and (5.2.0.6) remain the same for any value of k.

Table 5.3.1.1: The spectral radii of the Jacobian matrices corresponding to the fixed points of NSFDM-I for $k \geq 2$.

k	$\ell = 0.01$	$\ell = 0.5$	$\ell = 1$	$\ell = 10$	$\ell = 20$	$\ell = 100$
2	0.998864	0.945832	0.896589	0.431238	0.241651	0.034112
3	0.998706	0.938325	0.882257	0.352413	0.136550	0.177431
4	0.998608	0.933664	0.873359	0.303474	0.071299	0.266411
5	0.998546	0.930702	0.867703	0.272367	0.029823	0.322969
6	0.998508	0.928864	0.864195	0.253071	0.004094	0.358054
7	0.998486	0.927820	0.862201	0.242107	0.010524	0.377988
8	0.998476	0.927359	0.861322	0.237270	0.016973	0.386782
9	0.998476	0.927340	0.861285	0.237065	0.017247	0.387155
10	0.998482	0.927659	0.861895	0.240424	0.012768	0.381048

Table 5.3.1.2: The spectral radii of the Jacobian matrices corresponding to the fixed points of NSFDM-II for $k \geq 2$.

k	$\ell = 0.01$	$\ell = 0.5$	$\ell = 1$	$\ell = 10$	$\ell = 20$	$\ell = 100$
2	0.994338	0.767892	0.607976	0.018925	0.102996	0.137513
3	0.993553	0.735724	0.553645	0.160140	0.255862	0.295163
4	0.993066	0.715752	0.519913	0.247812	0.350768	0.393039
5	0.992756	0.703058	0.498472	0.303540	0.411093	0.455252
6	0.992564	0.695183	0.485172	0.338109	0.448515	0.493845
7	0.992455	0.690708	0.477615	0.357751	0.469777	0.515773
8	0.992407	0.688735	0.474282	0.366415	0.479157	0.525446
9	0.992405	0.688651	0.474140	0.366783	0.479555	0.525856
10	0.992438	0.690022	0.476455	0.360766	0.473041	0.519139

It can be seen from these two tables above, that all the spectral radii are less than one in magnitude irrespective of the time step-size used in the simulations. Hence, each of these fixed points is locally asymptotically stable if $R_0^{HIV} > 1$ for $k = 2, 3, ..., 10$. Thus, we have the following result.

Remark 5.3.1.1. For $k = 2, 3, ..., 10$, each fixed point of system (5.2.0.6) is locally asymptotically stable if $R_0^{HIV} > 1$. Moreover, the system is unconditionally elementary

stable.

5.3.2 Numerical simulations for the disease free equilibrium

The disease free equilibrium (DFE) is calculated using the proposed NSFDMs along with other numerical methods conventionally used. A thorough comparison of these methods is presented for many different scenarios. The maximum transmission rate, d, is very important from the biological point of view and hence its value will be varied in a certain range while keeping $R_0^{HIV} < 1$ (as needed for DFE).

In Section 2.3.4.1, we have shown that system (5.2.0.1) has asymptotically stable disease free equilibrium if $R_0^{HIV} < 1$. The numerical value of this DFE is given by $E_0^* = (10000, 0)$. The initial condition considered in this part of the simulations is taken as $(S(0), I(0)) = (9900, 100)$, unless otherwise mentioned.

In order to check whether these numerical methods converge to the theoretical value of the DFE, we require a tolerance value. To this end, for susceptibles we consider its value as 1% of the susceptible population whereas we consider 20 individuals as the tolerance value for the infectious population.

Although all the numerical methods converge to the disease free equilibrium, E_0^*, for any time step-size used when $d = 0.07$, we can see from Figure 5.3.2.1 that only the NSFDM-II achieves much better convergence.

In Table 5.3.2.1, it is shown that when $d = 0.09$, only the NSFDM-II converges to the correct disease free equilibrium, E_0^*, for different values of the step-size. This is also shown in Figure 5.3.2.2 and in Figure 5.3.2.3.

To see the robustness of the NSFDMs with respect to the initial conditions, the results are presented in Table 5.3.2.2. In this table we also put the results obtained by fourth order Runge-Kutta method and the MATLAB solver *ode45*. It can be seen that the NSFDM-II converge for all initial conditions whereas the others do not. This also can be seen from Figure 5.3.2.4.

As far as the positivity of the solutions obtained by these methods is concerned,

we note that the Euler method does not preserve this property although it converges for a wide range of the step-sizes and initial conditions. See, Figure 5.3.2.5. However, NSFDMs always preserves this property.

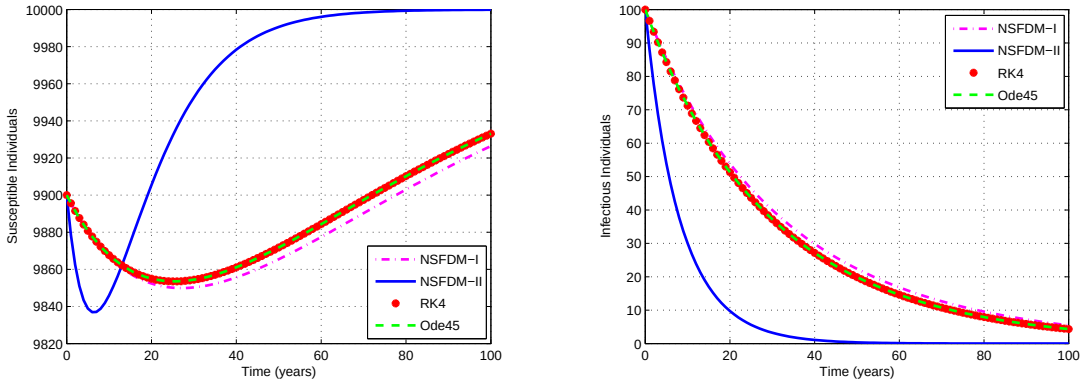

Figure 5.3.2.1: Profiles of solutions [susceptibles ($S(t)$): left figure and infectious individuals ($I(t)$): right figure] obtained by using different numerical methods for $\ell = 1$ when $d = 0.07$.

Table 5.3.2.1: Results obtained by different numerical methods when $d = 0.09$.

ℓ	ode45	RK4	NSFDM-I	NSFDM-II
0.01	Divergent	Divergent	Divergent	Convergent
0.1	Divergent	Divergent	Divergent	Convergent
0.5	Divergent	Divergent	Divergent	Convergent
1	Divergent	Divergent	Divergent	Convergent
4	Divergent	Divergent	Divergent	Convergent
6	Divergent	Divergent	Divergent	Convergent

The disease free equilibrium is given by: $(S^*, I^*) = (10000, 0)$.

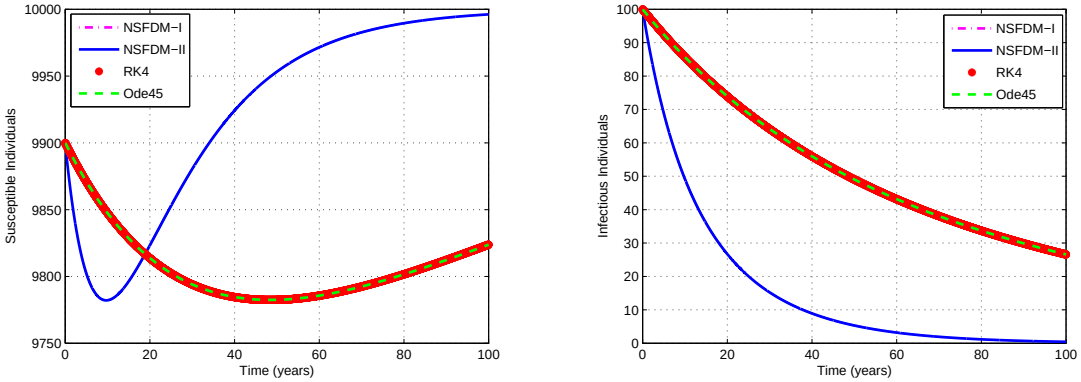

Figure 5.3.2.2: Profiles of solutions [susceptibles ($S(t)$): left column and infectious individuals ($I(t)$): right column] obtained by using different numerical methods for $\ell = 0.01$ when $d = 0.09$.

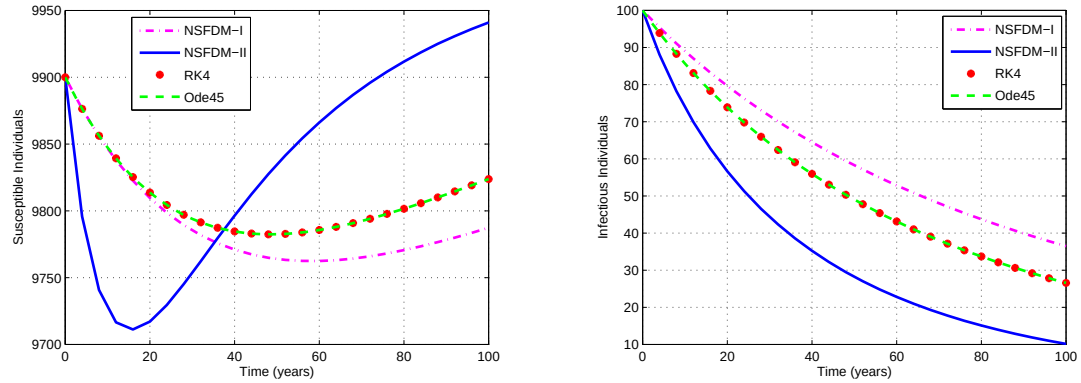

Figure 5.3.2.3: Profiles of solutions [susceptibles ($S(t)$): left column and infectious individuals ($I(t)$): right column] obtained by using different numerical methods for $\ell = 4$ when $d = 0.09$.

Table 5.3.2.2: Results obtained by different numerical methods for different initial conditions when $\ell = 1$ and $d = 0.07$.

$S(0)$	$I(0)$	ode45	RK4	NSFDM-I	NSFDM-II
9950	50	Convergent	Convergent	Convergent	Convergent
9900	100	Convergent	Convergent	Convergent	Convergent
9850	150	Convergent	Convergent	Divergent	Convergent
9800	200	Divergent	Divergent	Divergent	Convergent
7000	3000	Divergent	Divergent	Divergent	Convergent
2000	8000	Divergent	Divergent	Divergent	Convergent

The disease free equilibrium is given by: $(S^*, I^*) = (10000, 0)$.

$(S(0), I(0)) = (9950, 50)$

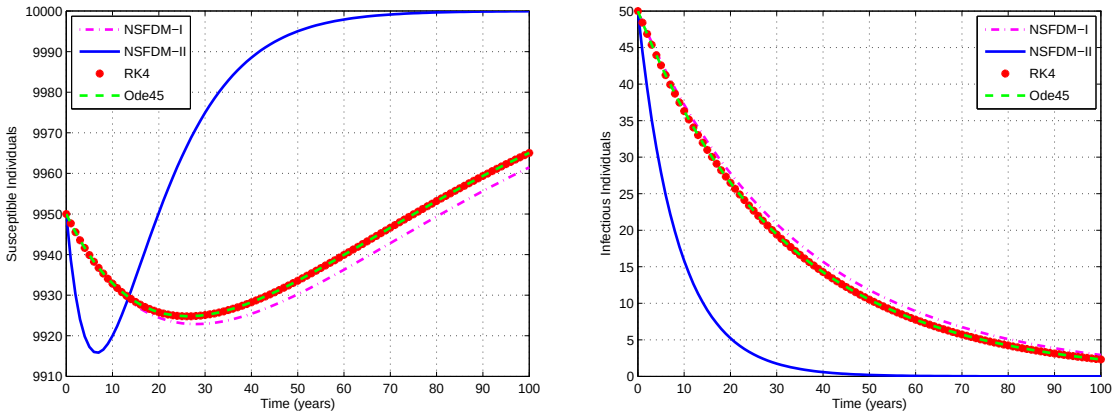

$(S(0), I(0)) = (5000, 5000)$

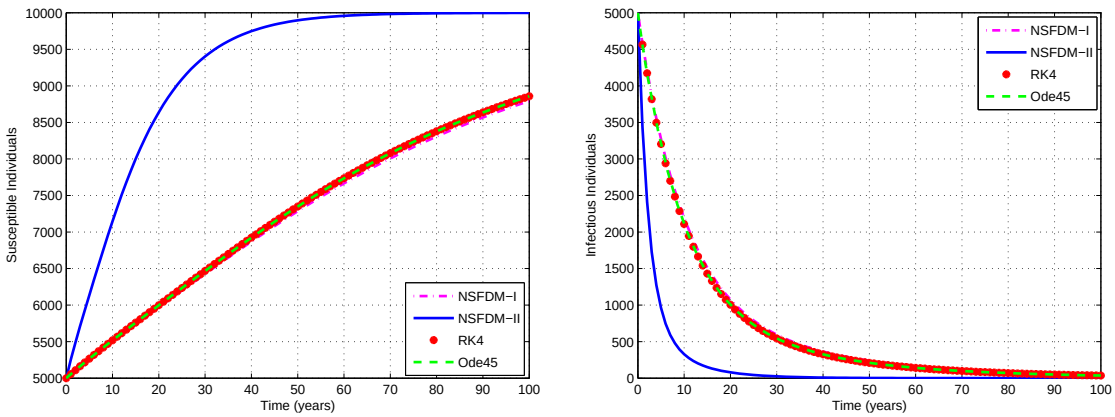

$(S(0), I(0)) = (2000, 8000)$

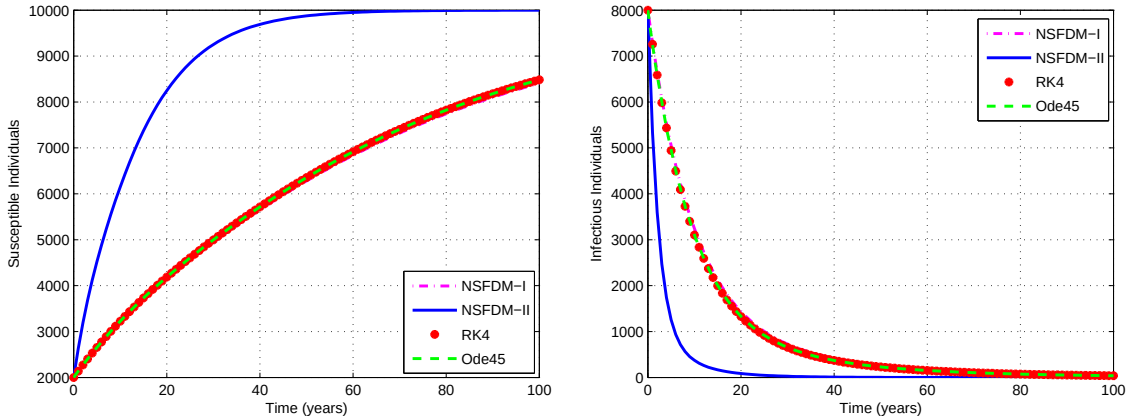

Figure 5.3.2.4: Profiles of solutions [susceptibles ($S(t)$): left column and infectious individuals ($I(t)$): right column] obtained by using different numerical methods when $\ell = 1$ and $d = 0.07$.

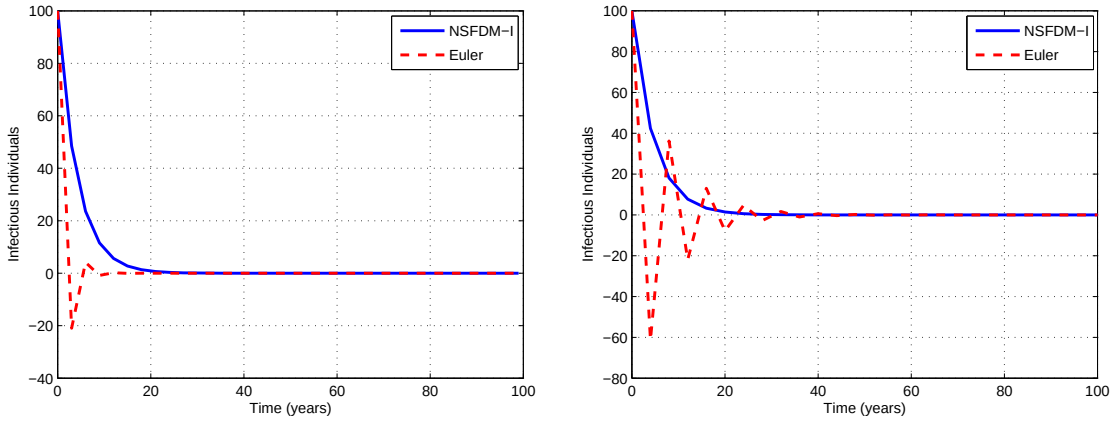

Figure 5.3.2.5: Profiles of solutions for infectious individuals ($I(t)$) obtained by the NSFDM-I and Euler method when $d = 0.05$, $\mu_2 = 0.45$ and $\ell = 3$ (left figure), $\ell = 4$ (right figure).

5.3.3 Numerical simulations for the endemic equilibria

In this section, we study the convergence behavior of the numerical methods to the endemic equilibria. We provide the results for various values of the Hill coefficient k.

5.3.3.1 Case I: Hill coefficient $k = 1$

When $k = 1$, the unique endemic equilibrium, E^*, of system (5.2.0.1) is locally asymptotically stable if $d > \mu_2$ ($R_0^{HIV} > 1$). In this section, the tolerance values are 1% and 10% for S^* and I^*, respectively.

It can be seen from Figure 5.3.3.1, Figure 5.3.3.2, 5.3.3.3 and 5.3.3.5 that all numerical methods converge almost to the endemic equilibrium E^* when $d > \mu_2$. However, the NSFDM-II converges more accurately.

Furthermore, all the numerical methods converge to the correct endemic equilibrium for any initial conditions used. However, when d close to μ_2 (which means that R_0^{HIV} close to 1), only the NSFDM-II could achieve convergence for a wide range of the initial conditions. This is shown in Table 5.3.3.1 as well as in Figure 5.3.3.5.

Again as in the case of DFE, the preservation of the positivity of the solutions is

observed only for NSFDM-I. The Euler method failed to do so although it converges asymptotically to the correct endemic equilibrium. This is depicted in Figure 5.3.3.6 below.

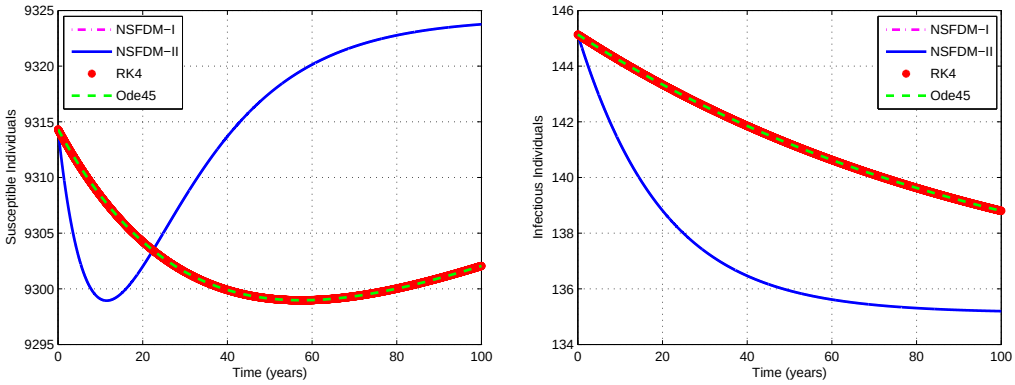

Figure 5.3.3.1: Profiles of solutions [susceptibles ($S(t)$): left column and infectious individuals ($I(t)$): right column] obtained by using different numerical methods when $d = 0.11$ and with $\ell = 0.01$ and initial conditions $S(0), I(0)) = (9314, 145)$.

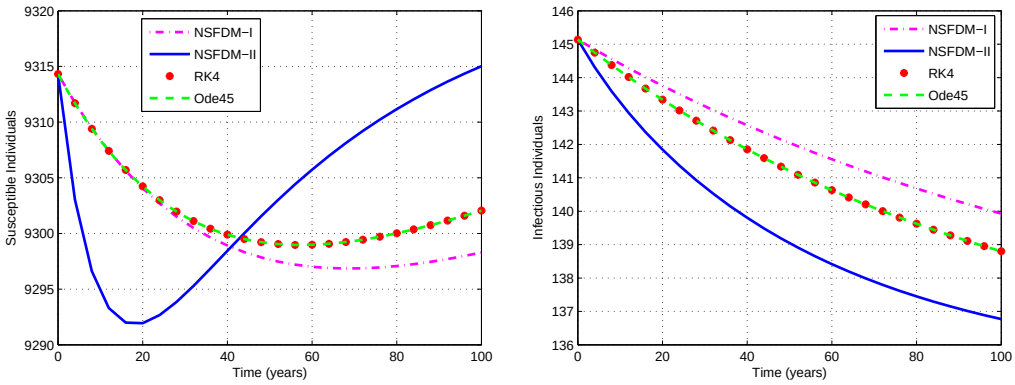

Figure 5.3.3.2: Profiles of solutions [susceptibles ($S(t)$): left column and infectious individuals ($I(t)$): right column] obtained by using different numerical methods when $d = 0.11$ and with $\ell = 4$ and initial conditions $S(0), I(0)) = (9314, 145)$.

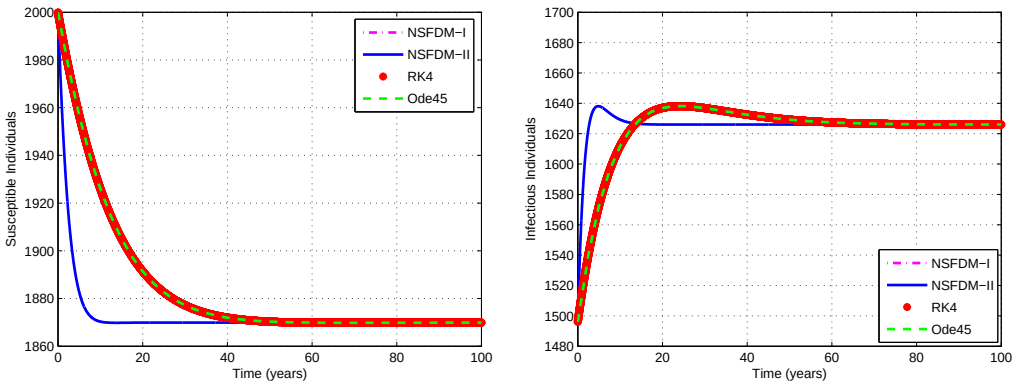

Figure 5.3.3.3: Profiles of solutions [susceptibles ($S(t)$): left column and infectious individuals ($I(t)$): right column] obtained by using different numerical methods when $d = 0.7$ and with $\ell = 0.01$ and initial conditions $S(0), I(0)) = (2000, 1496)$.

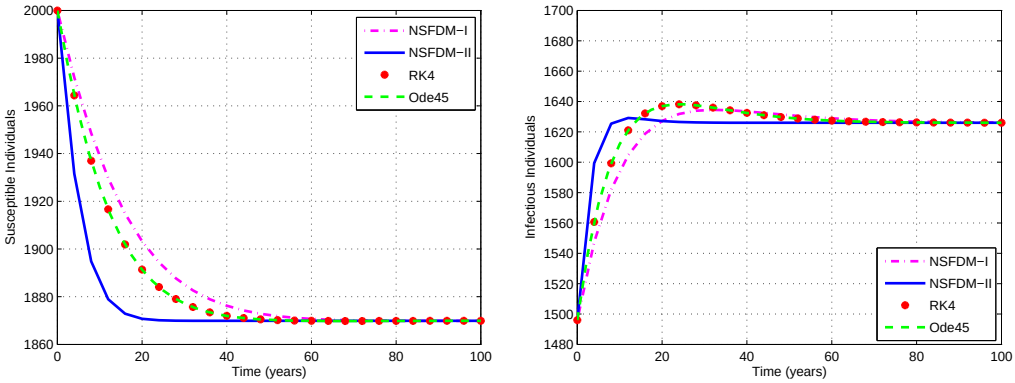

Figure 5.3.3.4: Profiles of solutions [susceptibles ($S(t)$): left column and infectious individuals ($I(t)$): right column] obtained by using different numerical methods when $d = 0.7$ and with $\ell = 4$ and initial conditions $S(0), I(0)) = (2000, 1496)$.

Table 5.3.3.1: Results obtained by different numerical methods for different initial conditions when $\ell = 1$ and $d = 0.11$.

$S(0)$	$I(0)$	ode45	RK4	NSFDM-I	NSFDM-II
9318	141	Convergent	Convergent	Convergent	Convergent
9314	145	Convergent	Convergent	Convergent	Convergent
9267	192	Divergent	Divergent	Divergent	Convergent
8275	1184	Divergent	Divergent	Divergent	Convergent
6280	3179	Divergent	Divergent	Divergent	Convergent
3324	6135	Divergent	Divergent	Divergent	Convergent

The disease free equilibrium is given by: $(S^*, I^*) = (9324, 135)$.

$$(S(0), I(0)) = (9267, 192)$$

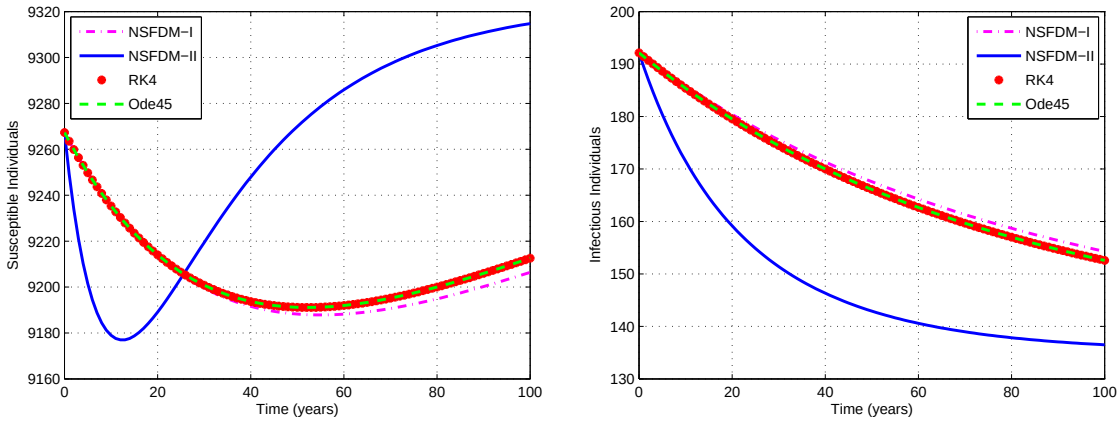

$$(S(0), I(0)) = (3324, 6135)$$

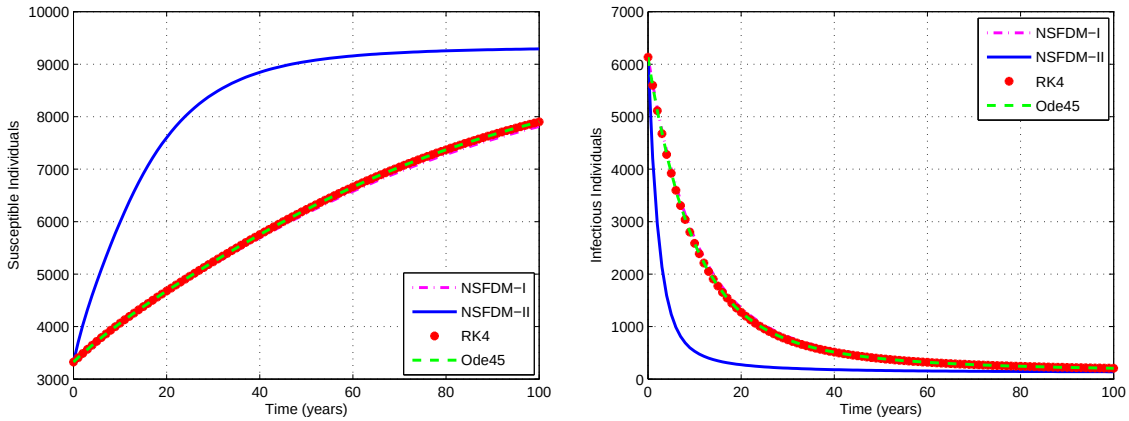

Figure 5.3.3.5: Profiles of solutions [susceptibles ($S(t)$): left column and infectious individuals ($I(t)$): right column] obtained by using different numerical methods when $d = 0.11$ and with $\ell = 1$.

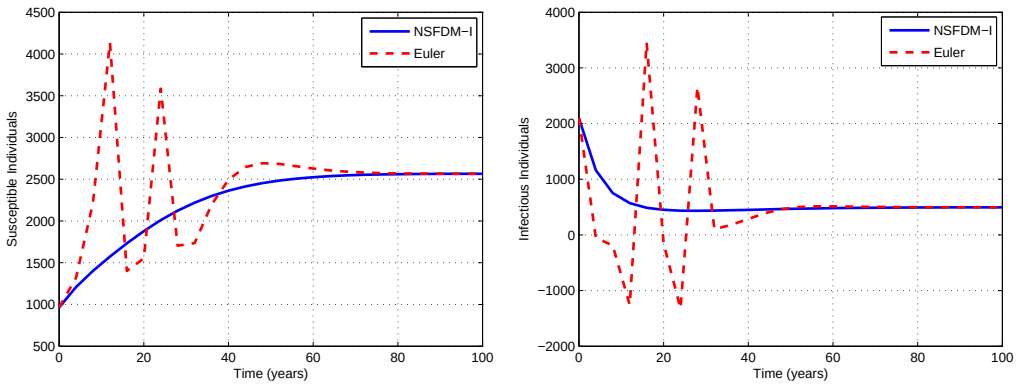

Figure 5.3.3.6: Profiles of solutions [susceptibles ($S(t)$): left column and infectious individuals ($I(t)$): right column] obtained by the NSFDM-I and Euler method when $d = 0.7$, $\mu_2 = 0.3$, initial conditions as $(S(0), I(0)) = (965, 2096)$ and $\ell = 4$.

5.3.3.2 Case II: Hill coefficient $k > 1$

In this section, simulation results are presented for different numerical methods for a range of $k > 1$. As in the previous case, the tolerance value for S^* is taken as 1%. However, for $k > 1$, there will be sufficient fluctuations in the dynamics of the infectious population and therefore we would not take the tolerance as 10% in this case; and hence 1% tolerance would suffice for I^*. It can be seen that all the methods mentioned in the tables converge for small step-sizes. However, when the step-sizes are larger then only NSFDMs converge to the correct endemic equilibrium. This is shown in tables 5.3.3.2, 5.3.3.3 and 5.3.3.4. Furthermore, figures 5.3.3.7, 5.3.3.8 and 5.3.3.9 below, show how the different numerical methods converge to the equilibrium in each case when the step-size is 1. While all these methods converge, we see that convergence is oscillatory in the case of *ode45* (see Figure 5.3.3.9). NSFDM-II also oscillates in the transient face but converge much before the other methods. However, NSFDM-I has the best performance.

Table 5.3.3.2: Results obtained by different numerical methods for $k = 2$ and initial conditions as $(S(0), I(0)) = (1324, 1700)$ with different step-sizes.

ℓ	ode45	RK4	NSFDM-I	NSFDM-II
0.01	Convergent	Convergent	Convergent	Convergent
1	Convergent	Convergent	Convergent	Convergent
4	Convergent	Convergent	Convergent	Convergent
8	Convergent	Convergent	Convergent	Convergent
12	Failed	Convergent	Convergent	Convergent
15	Failed	Divergent	Convergent	Convergent
20	Failed	Divergent	Convergent	Convergent

In this case, the endemic equilibrium is given by: $(S^*, I^*) = (1280, 1744)$.

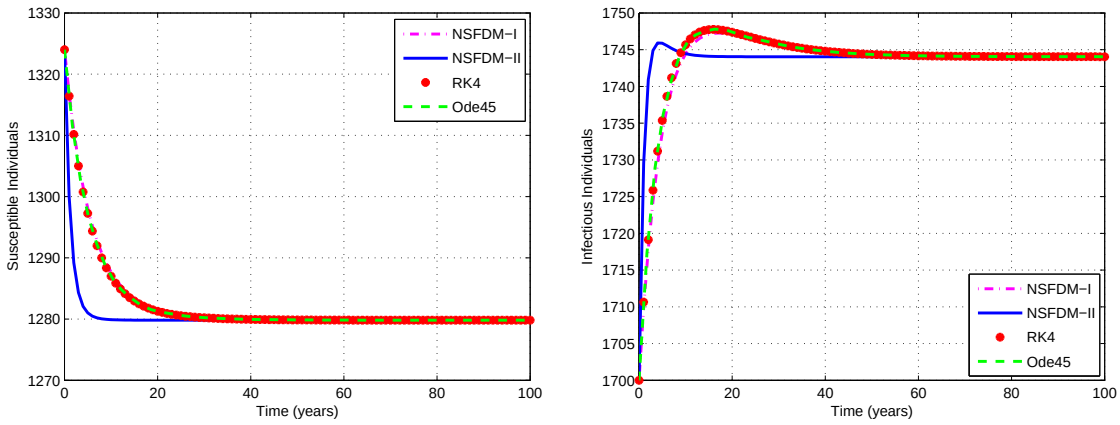

Figure 5.3.3.7: Profiles of solutions [susceptibles $(S(t))$: left column and infectious individuals $(I(t))$: right column] obtained by using different numerical methods when $k = 2$ and with initial conditions $(S(0), I(0)) = (1324, 1700)$ and $\ell = 1$.

Table 5.3.3.3: Results obtained by different numerical methods for $k = 5$ and initial conditions as $(S(0), I(0)) = (810, 1800)$ with different step-sizes.

ℓ	ode45	RK4	NSFDM-I	NSFDM-II
0.01	Convergent	Convergent	Convergent	Convergent
1	Convergent	Convergent	Convergent	Convergent
3	Convergent	Convergent	Convergent	Convergent
4	Failed	Convergent	Convergent	Convergent
6	Failed	Convergent	Convergent	Convergent
10	Failed	Divergent	Convergent	Convergent
15	Failed	Divergent	Convergent	Convergent
20	Failed	Divergent	Convergent	Convergent

In this case, the endemic equilibrium is given by: $(S^*, I^*) = (763, 1847)$.

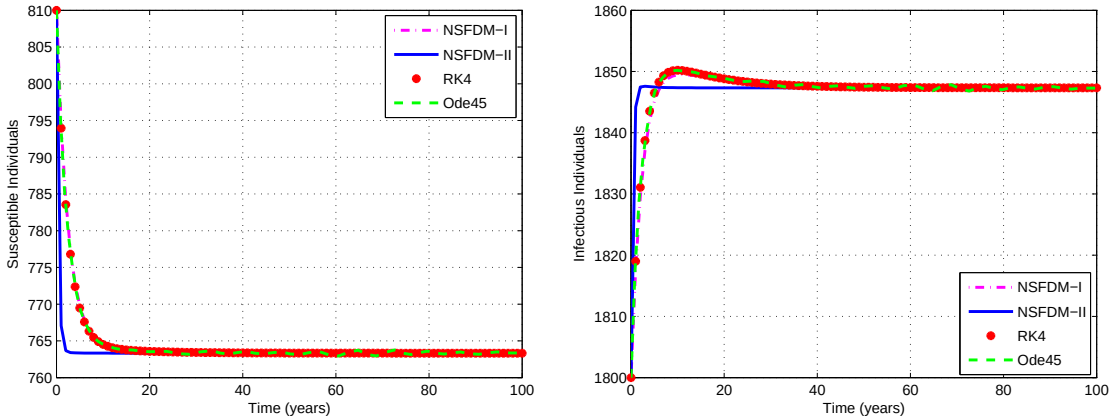

Figure 5.3.3.8: Profiles of solutions [susceptibles ($S(t)$): left column and infectious individuals ($I(t)$): right column] obtained by using different numerical methods when $k = 5$ and with initial conditions $(S(0), I(0)) = (810, 1800)$ and $\ell = 1$.

Table 5.3.3.4: Results obtained by different numerical methods for $k = 10$ and initial conditions as $(S(0), I(0)) = (500, 1918)$ with different step-sizes.

ℓ	ode45	RK4	NSFDM-I	NSFDM-II
0.01	Convergent	Convergent	Convergent	Convergent
1	Convergent	Convergent	Convergent	Convergent
3	Failed	Convergent	Convergent	Convergent
4	Failed	Convergent	Convergent	Convergent
6	Failed	Divergent	Convergent	Convergent
10	Failed	Divergent	Convergent	Convergent
15	Failed	Divergent	Convergent	Convergent
20	Failed	Divergent	Convergent	Convergent

In this case, the endemic equilibrium is given by: $(S^*, I^*) = (523, 1895)$.

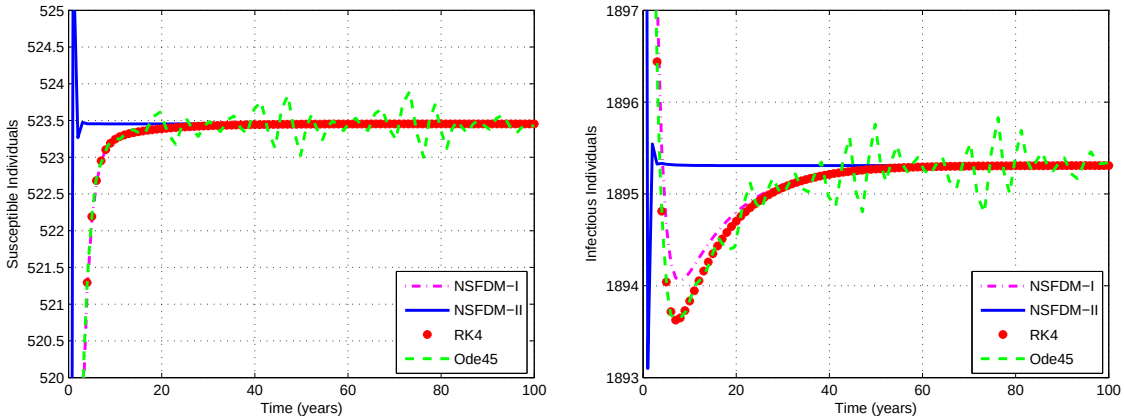

Figure 5.3.3.9: Profiles of solutions [susceptibles ($S(t)$): left column and infectious individuals ($I(t)$): right column] obtained by using different numerical methods when $k = 10$ and with initial conditions $(S(0), I(0)) = (500, 1918)$ and $\ell = 1$.

5.4 Summary and discussion

In this chapter, an unconditionally stable nonstandard finite difference method is proposed for solving a mathematical model of HIV represented by a nonlinear system of ordinary differential equations. The proposed method is very competitive. It is qualitatively stable, that is, it produces results which are dynamically consistent with those of the continuous system.

Numerical results presented in Section 5.3 confirm the applicability of the proposed NSFDMs for the biological systems. These methods preserve the positivity of solutions and the stability properties of the equilibria for arbitrary step-sizes, while the solutions obtained by other numerical methods experience difficulties in either preserving the positivity of the solutions or in converging to the correct equilibria. Furthermore, since large step-sizes can be used, these methods saves the computations time and memory.

It should be noted that when numerical simulations using a particular method are performed for a set of parameters that usually fit the model well then the method normally tends to converge. However, a slight change in the values of these parameters

can make some methods unreliable. In reality, one might expect (with a very little probability) some situations, for example, disease outbreaks in a community, when at a particular time there may be more infectious individuals than susceptibles. To test whether the numerical methods capture this dynamics, we have provided some more numerical simulations, see, tables 5.3.2.2, 5.3.3.1 and figures 5.3.2.4, 5.3.3.5. It is clear from these results that NSFDMs could mimic the relevant dynamics whereas the other numerical methods failed to do so.

In view of the fact that the numerical method presented in this chapter is dynamically consistent with the continuous HIV model, we use this approach to solve a TB model and then extend the overall method to solve the full HIV-TB model. This is done in the next chapter.

Chapter 6

A nonstandard finite difference method for the HIV-TB model

In this chapter, we construct nonstandard finite difference methods (NSFDMs) to solve a mathematical model of HIV-TB co-infection. We use the ideas explored in the previous chapter for the HIV model and then begin by designing a NSFDM for the TB-only sub-model resulting from the co-infected model when there is no HIV infections. The dynamics of the TB and HIV-TB models are studied numerically using the qualitative theory of dynamical systems.

6.1 Introduction

In the previous chapter, we have thoroughly reviewed the applications of NSFDMs for systems of differential equations. The governing models describe problems in mathematical biology and other different areas. These methods showed their superiority in preserving the positivity (when compared to other well known numerical methods) of the state variables of the systems under study. This is an essential requirement when simulating systems especially those arising in biology. Apart from the works mentioned in Chapter 5, some more research in this field can be found in [1, 2, 40, 78, 95, 119].

In this chapter, we construct NSFDMs to solve the mathematical model of HIV-TB

co-infection (3.2.0.1) presented in Chapter 3. We first consider the TB-only sub-model (3.3.0.5) and design a NSFDM to solve it. We show that the numerical methods are elementary stable. To show the robustness of the proposed methods, comparisons with other conventional methods are made.

The rest of the chapter is organized as follows. NSFDMs for the TB-only sub-model and for the full model are constructed in Sections 6.2 and 6.3, respectively. For each of these methods, we investigate the fixed points and discuss their stability. Thorough numerical results are also presented for each case. Finally a discussion on these results as well as on the summary of main findings is given in Section 6.4.

6.2 Construction of the NSFDM for the TB-only sub-model

In this section, we design a nonstandard finite difference method (NSFDM) for the TB-only sub-model (3.3.0.5). By considering the same partition of the time domain and approximation of the temporal derivatives as in Chapter 5, the NSFDM for this system reads

$$\begin{aligned}
\frac{{S_1}^{n+1}-{S_1}^{n}}{\psi_1(\ell)} &= B-\frac{k_1{S_1}^{n+1}{I_1}^{n}}{{S_1}^{n}+{E_1}^{n}+{I_1}^{n}}-\mu_1{S_1}^{n+1},\\
\frac{{E_1}^{n+1}-{E_1}^{n}}{\psi_2(\ell)} &= \frac{((1-p_1){S_1}^{n+1}-q_1{E_1}^{n+1})k_1{I_1}^{n}}{S_1^n+E_1^n+I_1^n}-(a_1+\mu_1){E_1}^{n+1}+b_1{I_1}^{n}, \quad (6.2.0.1)\\
\frac{{I_1}^{n+1}-{I_1}^{n}}{\psi_3(\ell)} &= \frac{(p_1{S_1}^{n+1}+q_1{E_1}^{n+1})k_1{I_1}^{n}}{S_1^n+E_1^n+I_1^n}-b_1{I_1}^{n}-m_1{I_1}^{n+1}+a_1{E_1}^{n+1}.
\end{aligned}$$

It is to be noted that we have used some non-local approximations for the nonlinear terms. Also the denominator functions above are respectively taken as $\psi_1(\ell)=1-e^{-\mu_1\ell}$, $\psi_2(\ell)=1-e^{-(a_1+\mu_1)\ell}$ and $\psi_3(\ell)=1-e^{-m_1\ell}$.

Simplifying (6.2.0.1), we obtain

$$S_1{}^{n+1} = \frac{S_1{}^n + \psi_1(\ell)B}{1 + \psi_1(\ell)\left\{\frac{k_1 I_1{}^n}{S_1{}^n + E_1{}^n + I_1{}^n} + \mu_1\right\}},$$

$$E_1{}^{n+1} = \frac{E_1{}^n + \psi_2(\ell)\left\{\frac{(1-p_1)S_1{}^{n+1}k_1 I_1{}^n}{S_1{}^n + E_1{}^n + I_1{}^n} + b_1 I_1{}^n\right\}}{1 + \psi_2(\ell)\left\{\frac{q_1 k_1 I_1{}^n}{S_1{}^{n+1} + E_1{}^n + I_1{}^n} + a_1 + \mu_1\right\}}, \tag{6.2.0.2}$$

$$I_1{}^{n+1} = \frac{(1 - \psi_3(\ell)b_1)I_1{}^n + \psi_3(\ell)\left\{\frac{(p_1 S_1{}^{n+1} + q_1 E_1{}^{n+1})k_1 I_1{}^n}{S_1{}^n + E_1{}^n + I_1{}^n} + a_1 E_1{}^{n+1}\right\}}{1 + \psi_3(\ell)m_1}.$$

The positivity of the solution reflects from the above method (6.2.0.2) because if the initial conditions $S_1(0)$, $E_1(0)$ and $I_1(0)$ are non-negative, then the right hand side of (6.2.0.2) admits no negative terms for any of $n = 0, 1, 2, 3, ...$ because $0 < p_1 < 1$ and $0 < \psi_3(\ell)b_1 < 1$.

In the following section we determine the stability properties of system (6.2.0.1), and we verify that

(i) the continuous and the discrete models have the same equilibria, and

(ii) both models posses similar qualitative features near these equilibria.

6.2.1 Fixed points and stability analysis

We study in this section the stability and convergence properties of the fixed points of the proposed NSFDM.

We begin by noting that the fixed points $(\hat{S}_1, \hat{E}_1, \hat{I}_1)$ of system (6.2.0.1) can be

found by solving

$$\begin{aligned} F_1(\hat{S}_1, \hat{E}_1, \hat{I}_1) = &\quad \hat{S}_1, \\ F_2(\hat{S}_1, \hat{E}_1, \hat{I}_1) = &\quad \hat{E}_1, \\ F_3(\hat{S}_1, \hat{E}_1, \hat{I}_1) = &\quad \hat{I}_1, \end{aligned} \tag{6.2.1.1}$$

where $F_1(\hat{S}_1, \hat{E}_1, \hat{I}_1)$, $F_2(\hat{S}_1, \hat{E}_1, \hat{I}_1)$ and $F_3(\hat{S}_1, \hat{E}_1, \hat{I}_1)$ can be obtained by considering the right hand sides in (6.2.0.2), i.e.,

$$F_1(\hat{S}_1, \hat{E}_1, \hat{I}_1) = \frac{\hat{S}_1 + \psi_1(\ell)B}{1 + \psi_1(\ell)\left\{k_1\hat{\lambda}_T + \mu_1\right\}},$$

$$F_2(\hat{S}_1, \hat{E}_1, \hat{I}_1) = \frac{\hat{E}_1 + \psi_2(\ell)\left\{(1-p_1)\hat{S}_1 k_1\hat{\lambda}_T + b_1\hat{I}_1\right\}}{1 + \psi_2(\ell)\left\{q_1k_1\hat{\lambda}_T + a_1 + \mu_1\right\}},$$

$$F_3(\hat{S}_1, \hat{E}_1, \hat{I}_1) = \frac{(1-\psi_3(\ell)b_1)\hat{I}_1 + \psi_3(\ell)\left\{(p_1\hat{S}_1 + q_1\hat{E}_1)k_1\hat{\lambda}_T + a_1\hat{E}_1\right\}}{1 + \psi_3(\ell)m_1},$$

where

$$\hat{\lambda}_T = \frac{k_1\hat{I}_1}{\hat{S}_1 + \hat{E}_1 + \hat{I}_1}. \tag{6.2.1.2}$$

Solving (6.2.1.1), we obtain the following equation for $\hat{\lambda}_T$

$$\hat{\lambda}_T((\hat{\lambda}_T)^2 + \hat{A}_1\hat{\lambda}_T + \hat{A}_2) = 0. \tag{6.2.1.3}$$

In the above equation, $\hat{\lambda}_T$ corresponds to the disease free equilibrium

$$\hat{E}_0 = \left(\frac{B}{\mu_2}, 0, 0\right), \tag{6.2.1.4}$$

whereas the system may have more than one endemic equilibrium which can be written in the following implicit form:

$$\begin{aligned}
\hat{S}_1 &= \frac{B}{\hat{\lambda}_T + \mu_1}, \\
\hat{E}_1 &= \frac{B\hat{\lambda}_T(b_1 + m_1(1-p_1))}{(\hat{\lambda}_T + \mu_1)\left[m_1 q_1 \hat{\lambda}_T + (a_1 m_1 + m_1\mu_1 + \mu_1 b_1)\right]}, \\
\hat{I}_1 &= \frac{B\lambda_T^*(a_1 + p_1\mu_1 + q_1\hat{\lambda}_T)}{(\hat{\lambda}_T + \mu_1)\left[m_1 q_1 \hat{\lambda}_T + (a_1 m_1 + m_1\mu_1 + \mu_1 b_1\right]},
\end{aligned}$$

in which $\hat{\lambda}_T$ corresponds to the positive solutions of the characteristic equation

$$(\hat{\lambda}_T)^2 + \hat{A}_1\hat{\lambda}_T + \hat{A}_2 = 0, \tag{6.2.1.5}$$

where

$$\hat{A}_1 = \frac{a_1 + b_1 + (1-p_1)m_1 + p_1\mu_1}{q_1} + m_1 - k_1, \tag{6.2.1.6}$$

and

$$\hat{A}_2 = \frac{(\mu_1 b_1 + m_1\mu_1 + m_1 a_1)(1 - R_0^{TB})}{q_1}, \tag{6.2.1.7}$$

where R_0^{TB} is the basic reproduction number associated with system (3.3.0.5). The form of the above equation is similar to the characteristic equation for the continuous systems (3.3.0.5). Therefore, both systems (3.3.0.5) and (6.2.0.1) have the same characteristic equation and expressions of equilibria. Hence, we have the following result.

Remark 6.2.1.1. The continuous system (3.3.0.5) and the discrete system (6.2.0.1) have the same equilibria.

Next, we determine the stability properties of the equilibria of system (6.2.0.1). The Jacobian matrix of the system (6.2.0.1) evaluated at the disease free equilibrium,

$\hat{E}_0$, is

$$J(\hat{E}_0) = \begin{pmatrix} \frac{1}{1+\psi_1(\ell)\mu_1} & 0 & -\frac{k_1\psi_1(\ell)}{1+\psi_1(\ell)\mu_1} \\ 0 & \frac{1}{1+\psi_2(\ell)(a_1+\mu_1)} & \frac{\psi_2(\ell)((1-p_1)k_1+b_1)}{1+\psi_2(\ell)(a_1+\mu_1)} \\ 0 & \frac{\psi_3(\ell)a_1}{1+\psi_3(\ell)m_1} & \frac{1-\psi_3(\ell)b_1+\psi_3(\ell)p_1k_1}{1+\psi_3(\ell)m_1} \end{pmatrix},$$

which has the following characteristic equation

$$g(\lambda) \equiv (\hat{\lambda})^3 - \hat{B}_1(\hat{\lambda})^2 + \hat{B}_2\hat{\lambda} + \hat{B}_3 = 0, \tag{6.2.1.8}$$

where

$$\begin{aligned} \hat{B}_1 &= \frac{1}{(1+\psi_3(\ell)m_1)(1+\psi_2(\ell)(a_1+\mu_1))(1+\psi_1(\ell)\mu_1)} \\ &\times[\mu_1((a_1+\mu_1)((b_1-p_1k_1)\psi_3(\ell)-1)\psi_2(\ell)+(b_1-p_1k_1-m_1)\psi_3(\ell) \\ &-2)\psi_1(\ell)-((p_1k_1-b_1+m_1)(a_1+\mu_1)\psi_3(\ell) \\ &+2\mu_1+2a_1)\psi_2(\ell)-(p_1k_1+2m_1-b_1)\psi_3(\ell)-3], \end{aligned}$$

$$\begin{aligned}\hat{B}_2 &= \frac{1}{(1+\psi_3(\ell)m_1)(1+\psi_2(\ell)a_1+\psi_2(\ell)\mu_1)(1+\psi_1(\ell)\mu_1)}\\ &\times[\mu_1((b_1a_1+(1-p_1)k_1a_1)\psi_3(\ell)\psi_2(\ell)+(b_1-p_1k_1)\psi_3(\ell)-1)\psi_1(\ell)\\ &+(((b_1-p_1k_1)(2a_1+\mu_1)+k_1a_1))\psi_3(\ell)-(a_1+\mu_1))\psi_2(\ell)\\ &+(2(b_1-p_1k_1)-m_1)\psi_3(\ell)-3],\end{aligned}$$

and

$$\hat{B}_3 = \frac{\psi_3(\ell)[b_1-p_1k_1+\psi_2(\ell)((1-p_1)k_1a_1+b_1a_1)]-1}{(1+\psi_3(\ell)m_1)(1+\psi_2(\ell)(a_1+\mu_1))(1+\psi_1(\ell)\mu_1)}.$$

From Lemma 1.3.3.2, the roots of equation (6.2.1.8) satisfy $|\lambda_i| < 1,\ i = 1,\ 2,\ 3$, if and only if the following conditions are satisfied

(i) $g(1) \quad = 1+\hat{B}_1+\hat{B}_2+\hat{B}_3 > 0,$

(ii) $(-1)^3 g(-1) = 1-\hat{B}_1+\hat{B}_2-\hat{B}_3 > 0,$

(iii) $1-(\hat{B}_3)^2 \ > |\hat{B}_2-\hat{B}_3\hat{B}_1|.$

From the above, we note that the nature of the eigenvalues is difficult to determine for general parameters due to the complexity of the analytic expressions. To this end, we will determine the stability of the fixed points of system (6.2.0.1) numerically in Section 6.2.2.2.

6.2.2 Numerical results and simulations

We present some numerical simulations using the proposed NSFDM in this section. The method is also tested for convergence. We numerically show that the NSFDM is

elementary stable. A number of different numerical simulations are carried out and comparisons are made with other well-known numerical methods for various time step-sizes ℓ. Values of parameter used in the simulations are presented in Table 3.2.0.1. Some of these parameters are varied to test the robustness of the methods. As is mentioned earlier, we attempt to investigate numerically the stability of system endemic equilibria. This is shown below in Table 6.2.2.1.

6.2.2.1 Numerical stability analysis of the endemic equilibria

In this section, we tabulate the endemic equilibria and their corresponding eigenvalues associated with the Jacobian matrices for the continuous system (3.3.0.5) for different values of the MTB infection rate k_1. It should be noted that when solving system (3.3.0.5) for its endemic equilibria when $k_1 > k^*$, it always has the disease free equilibrium $E_0^* = (10000, 0, 0)$ and many other endemic equilibria (for the set of parameter values presented in Table 3.2.0.1 which give $(R_0^{TB} > 1)$), but only one endemic equilibrium is relevant for each value of k. This is given in the following table.

Table 6.2.2.1: Basic reproduction number R_0^{TB}, endemic equilibria and corresponding eigenvalues of system (3.3.0.5) when $k_1 > k^*$ $(R_0^{TB} > 1)$.

k_1	R_0^{TB}	S_1^*	E_1^*	I_1^*	λ_1	λ_2	λ_3
9	1.03	9308	672	2	-0.019996	-0.004193	-0.139858
11.4	1.30	3904	5764	27	$-0.059384 + 0.0570030i$	$-0.059384 - 0.0570030\,i$	-0.020278
20	2.28	33	1554	673	-5.963690	-0.106799	-0.383086
50	5.70	6	298	776	-35.940955	-2.598809	-0.197387

At each equilibrium in the above table, the eigenvalues are negative or have negative real parts. We therefore have the following result.

Remark 6.2.2.1. For $k_1 > k^*$, the system (3.3.0.5) has a disease free equilibrium and it possesses a number of endemic equilibria as presented above in Table 6.2.2.1. Each of these endemic equilibria is locally asymptotically stable if $k_1 > k^*$ $\left(R_0^{TB} > 1\right)$.

6.2.2.2 Numerical stability analysis of the fixed points

In this section, we tabulate the spectral radii of the Jacobian matrices corresponding to the fixed points of the numerical method for different values of the MTB infection rate k_1 and the time step-size ℓ as shown in tables 6.2.2.2 and 6.2.2.3. We recall from Remark 6.2.1.1 that the equilibria of both systems (3.3.0.5) and (6.2.0.1) remain the same.

Table 6.2.2.2: The spectral radii of the Jacobian matrices corresponding to the disease free equilibriums of the NSFDM for $k_1 < k^*$ ($R_0^{TB} < 1$).

	The spectral radii when		
ℓ	$k_1 = 1$	$k_1 = 5$	$k_1 = 8$
0.01	0.999996	0.999996	0.999998
0.5	0.999801	0.999825	0.999909
1	0.999604	0.999651	0.999819
7	0.997394	0.997708	0.998819
10	0.996388	0.996825	0.998368
20	0.993450	0.994256	0.997072
100	0.983133	0.985260	0.992721

Table 6.2.2.3: The spectral radii of the Jacobian matrices corresponding to the endemic equilibria of the NSFDM for $k_1 > k^*$ $\left(R_0^{TB} > 1\right)$.

	The spectral radii when		
ℓ	$k_1 = 9$	$k_1 = 11.4$	$k_1 = 20$
0.01	0.999999	0.999996	0.999975
0.5	0.999952	0.999796	0.998777
1	0.999905	0.999594	0.997579
7	0.999383	0.997334	0.984988
10	0.999151	0.996308	0.979745
20	0.998499	0.993320	0.965996
100	0.996452	0.982835	0.930802

It can be seen from the two tables above, that all the spectral radii are less than one in magnitude irrespective of the time step-size used in the simulations. Hence, by Theorem 1.3.3.1 we have the following result.

Remark 6.2.2.2. The disease free equilibrium for system (6.2.0.1) is unconditionally locally asymptotically stable $k_1 < k^*$ ($R_0^{TB} < 1$), whereas each endemic equilibrium of

system (6.2.0.1) is locally asymptotically stable if $k_1 > k^*$ $\left(R_0^{TB} > 1\right)$. Moreover, the system is unconditionally elementary stable.

6.2.2.3 Numerical simulations for the disease free equilibrium

The disease free equilibrium (DFE) is calculated using the proposed NSFDM along with other numerical methods conventionally used. A thorough comparison of these methods is presented for many different scenarios.

The MTB infection rate, k_1, is very important from biological point of view and hence its value will be varied in a certain range while keeping $R_0^{TB} < 1$ (as needed for DFE).

In Section 3.3, we have shown that system (3.3.0.5) has asymptotically stable disease free equilibrium if $k_1 < k^*$ $(R_0^{TB} < 1)$. The numerical value of this DFE is given by $E_0^* = (10000, 0, 0)$.

In order to check whether these numerical methods converge to the theoretical value of the DFE, we require a tolerance value. To this end, for susceptibles we consider its value as 1% of the susceptible population whereas we consider 10 and 1 individuals as the tolerances values for the latent and infectious populations respectively.

In Table 6.2.2.4, it is shown that all numerical methods converge to the correct disease free equilibrium $E_0^* = (10000, 0, 0)$ for small step-size ℓ when $k_1 = 1$. The NSFDM is shown to converge for larger ℓ while other methods diverge or fail. The convergence of the different numerical methods for step-size $\ell = 0.5$ can be seen in Figure 6.2.2.1. Moreover, for some values of the step-size ℓ, the fourth order Runge-Kutta method does not preserve the positivity of the solutions as it can be seen in figures 6.2.2.2 and 6.2.2.3. The MATLAB solver *ode45* failed to produce the solutions in this case.

When the value of k_1 is increased to 5, then from Table 6.2.2.5 and Figure 6.2.2.4, we can see that all the numerical methods converge to the correct disease free equilibrium for larger step-size ℓ than used in the previous simulations. Moreover, the NSFDM converge for any step-size used while other methods diverge or fail.

A comparison between the NSFDM and Runge-Kutta methods in Figure 6.2.2.5 shows that latter methods does not preserve the positivity of the model state variables.

Table 6.2.2.6 as well as Figure 6.2.2.6 show that, when $k_1 = 8$, only the NSFDM converges while other methods diverge even for small step-size ℓ.

As far as the positivity of the solutions obtained by these methods is concerned, we note that the Euler method does not preserve this property although it converges for a wide range of the step-sizes and initial conditions. See, Figure 6.2.2.7. However, the NSFDM always preserves this property.

Table 6.2.2.4: Results obtained by different numerical methods for $k_1 = 1$ ($R_0^{TB} < 1$) and initial conditions as $(S(0), E_1(0), I_1(0)) = (9995, 3, 2)$ with different step-sizes.

ℓ	*ode45*	RK4	NSFDM
0.01	Convergent	Convergent	Convergent
0.5	Convergent	Convergent	Convergent
2	Failed	Convergent	Convergent
7	Failed	Divergent	Convergent
10	Failed	Divergent	Convergent

The disease free equilibrium is: $(S_1^*, E_1^*, I_1^*) = (10000, 0, 0)$.

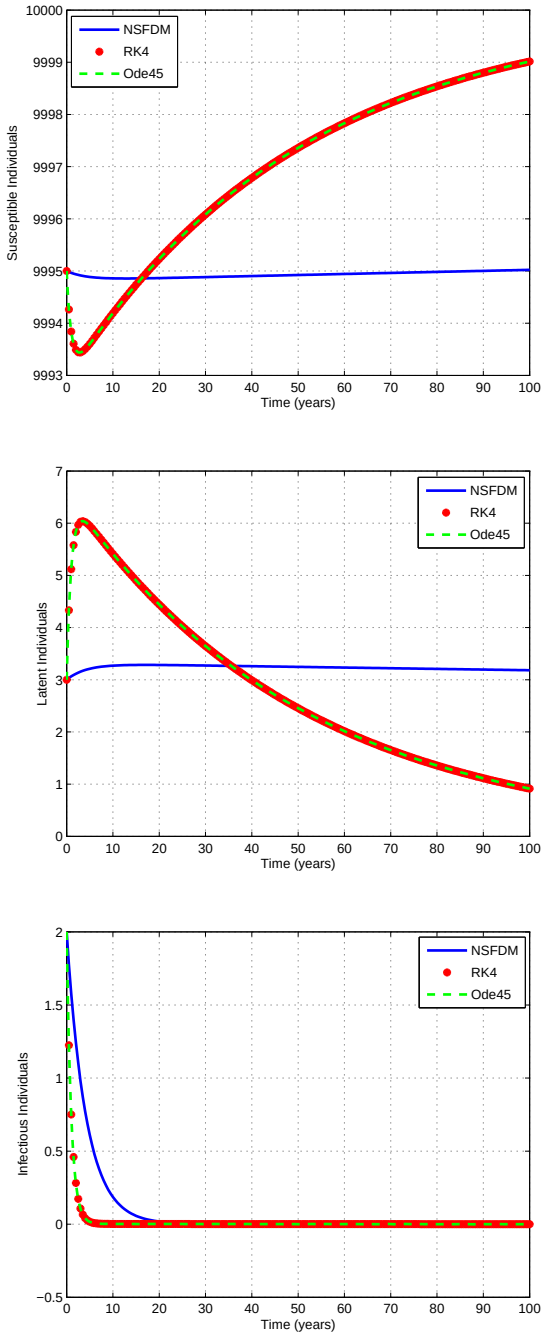

Figure 6.2.2.1: Profiles of solutions [susceptibles ($S_1(t)$): top figure, latent ($E_1(t)$): middle figure and infectious individuals ($I_1(t)$): bottom figure] obtained by using different numerical methods when $k_1 = 1$ and with initial conditions $(S_1(0), E_1(0), I_1(0)) = (9995, 3, 2)$ and $\ell = 0.5$.

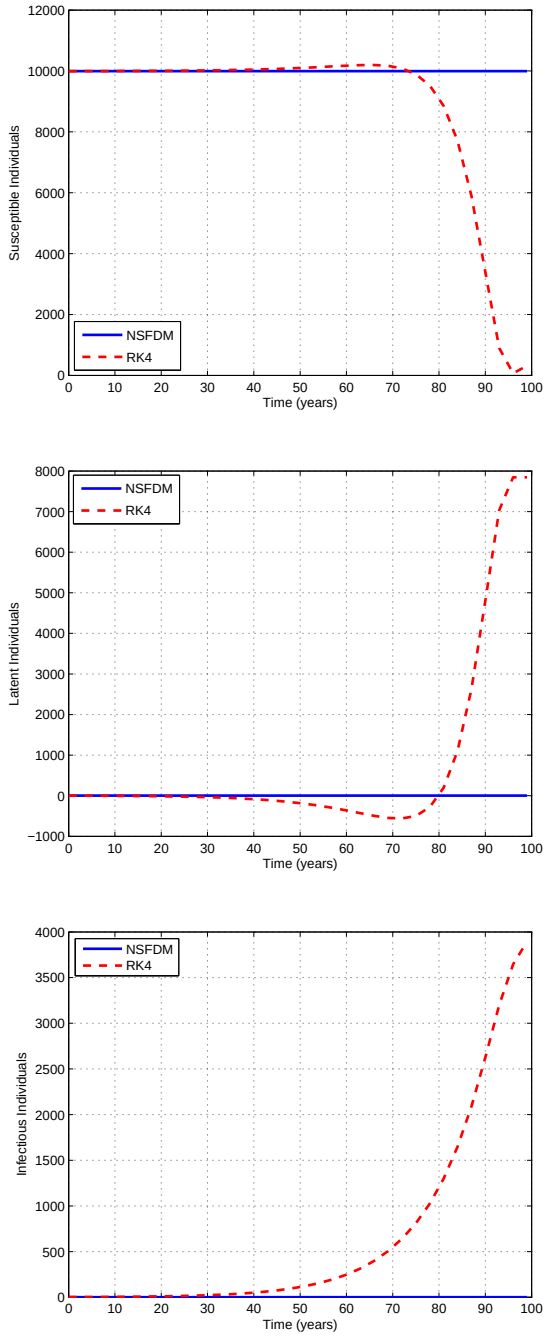

Figure 6.2.2.2: Profiles of solutions [susceptibles ($S_1(t)$): top figure, latent ($E_1(t)$): middle figure and infectious individuals ($I_1(t)$): bottom figure] obtained by using different numerical methods when $k_1 = 1$ and with initial conditions $(S_1(0), E_1(0), I_1(0)) = (9995, 3, 2)$ and $\ell = 3$.

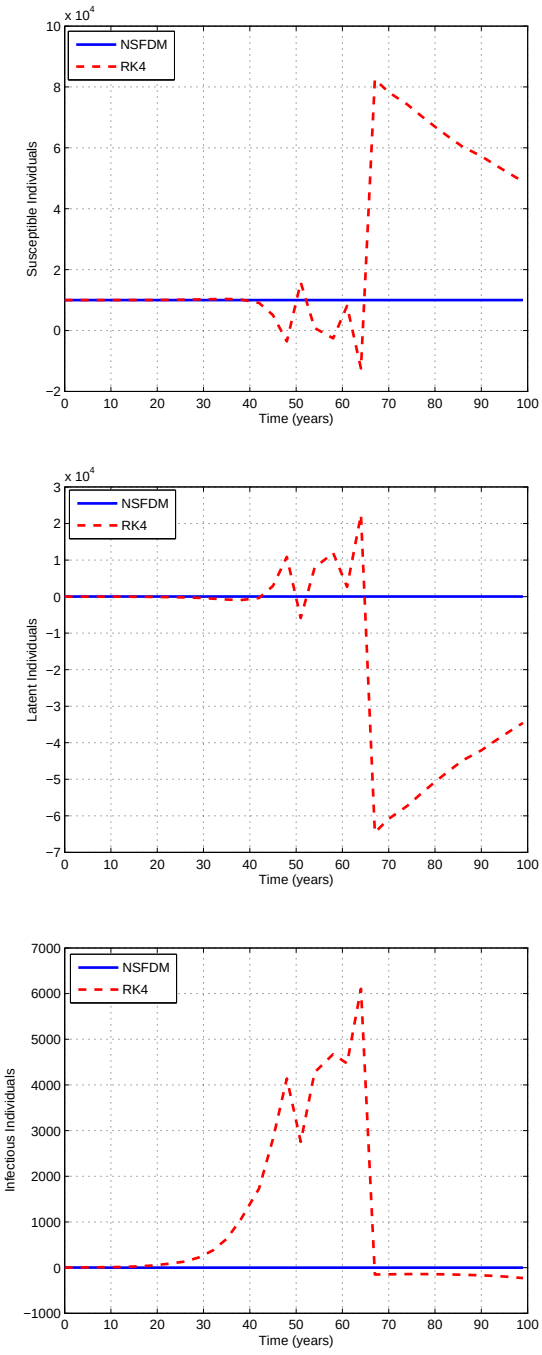

Figure 6.2.2.3: Profiles of solutions [susceptibles ($S_1(t)$): top figure, latent ($E_1(t)$): middle figure and infectious individuals ($I_1(t)$): bottom figure] obtained by using different numerical methods when $k_1 = 1$ and with initial conditions $(S_1(0), E_1(0), I_1(0)) = (9995, 3, 2)$ and $\ell = 3.2$.

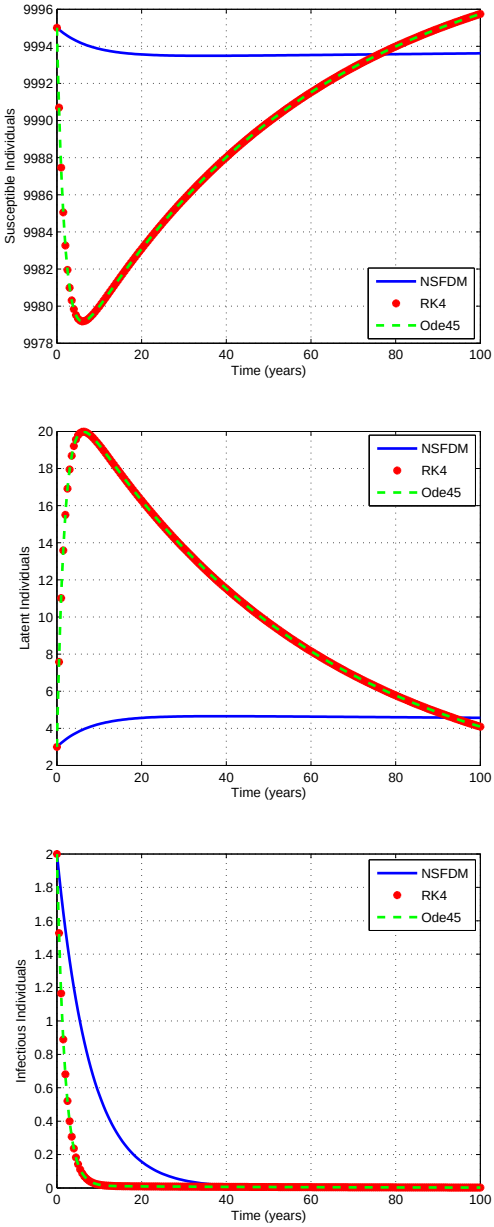

Figure 6.2.2.4: Profiles of solutions [susceptibles ($S_1(t)$): top figure, latent ($E_1(t)$): middle figure and infectious individuals ($I_1(t)$): bottom figure] obtained by using different numerical methods when $k_1 = 5$ and with initial conditions $(S_1(0), E_1(0), I_1(0)) = (9995, 3, 2)$ and $\ell = 0.5$.

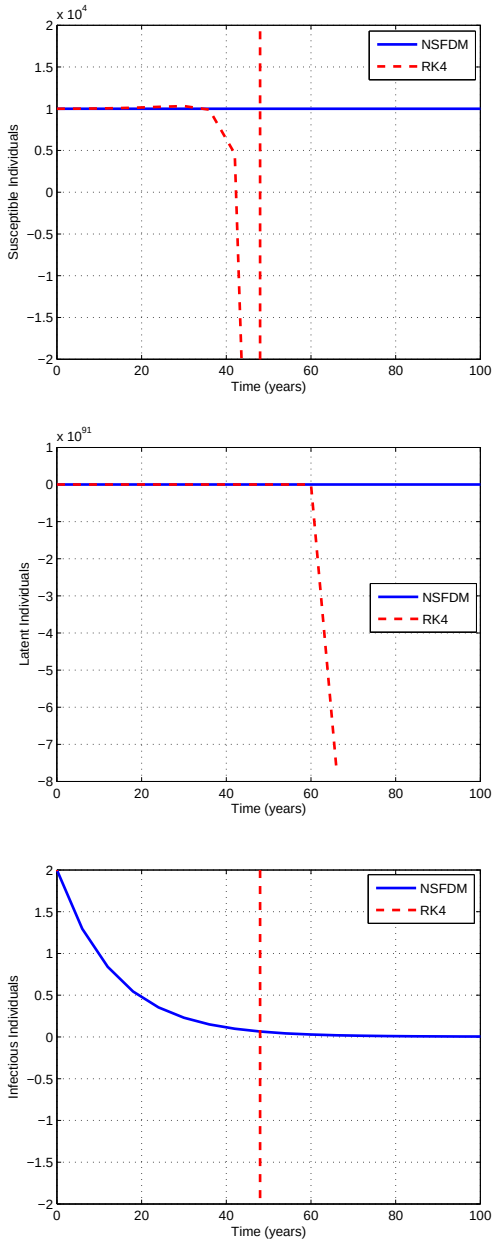

Figure 6.2.2.5: Profiles of solutions [susceptibles ($S_1(t)$): top figure, latent ($E_1(t)$): middle figure and infectious individuals ($I_1(t)$): bottom figure] obtained by using the NSFDM and fourth order Runge-Kutta method when $k_1 = 5$ and with initial conditions $(S_1(0), E_1(0), I_1(0)) = (9995, 3, 2)$ and $\ell = 6$.

Table 6.2.2.5: Results obtained by different numerical methods for $k_1 = 5$ ($R_0^{TB} < 1$) and initial conditions as $(S(0), E_1(0), I_1(0)) = (9995, 3, 2)$ with different step-sizes.

ℓ	*ode45*	RK4	NSFDM
0.01	Convergent	Convergent	Convergent
0.5	Convergent	Convergent	Convergent
2	Failed	Convergent	Convergent
6	Failed	Divergent	Convergent
10	Failed	Divergent	Convergent
15	Failed	Divergent	Convergent

The disease free equilibrium is: $(S_1^*, E_1^*, I_1^*) = (10000, 0, 0)$.

Table 6.2.2.6: Results obtained by different numerical methods for $k_1 = 8$ ($R_0^{TB} < 1$) and initial conditions as $(S(0), E_1(0), I_1(0)) = (9995, 3, 2)$ with different step-sizes.

ℓ	*ode45*	RK4	NSFDM
0.01	Divergent	Divergent	Convergent
0.5	Divergent	Divergent	Convergent
1	Divergent	Divergent	Convergent

The disease free equilibrium is: $(S_1^*, E_1^*, I_1^*) = (10000, 0, 0)$.

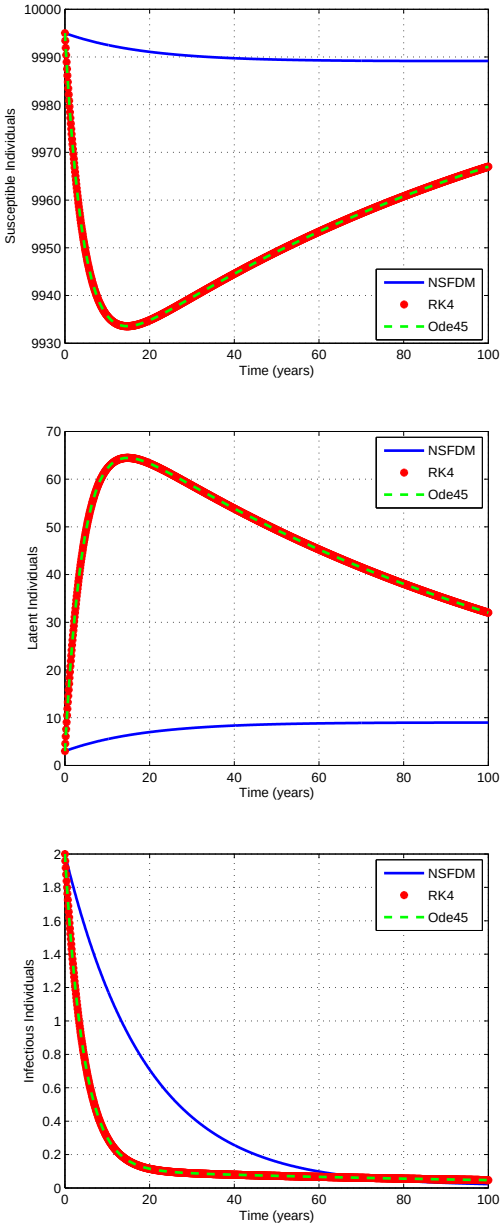

Figure 6.2.2.6: Profiles of solutions [susceptibles ($S_1(t)$): top figure, latent ($E_1(t)$): middle figure and infectious individuals ($I_1(t)$): bottom figure] obtained by using different numerical methods when $k_1 = 8$ and with initial conditions $(S_1(0), E_1(0), I_1(0)) = (9995, 3, 2)$ and $\ell = 0.1$.

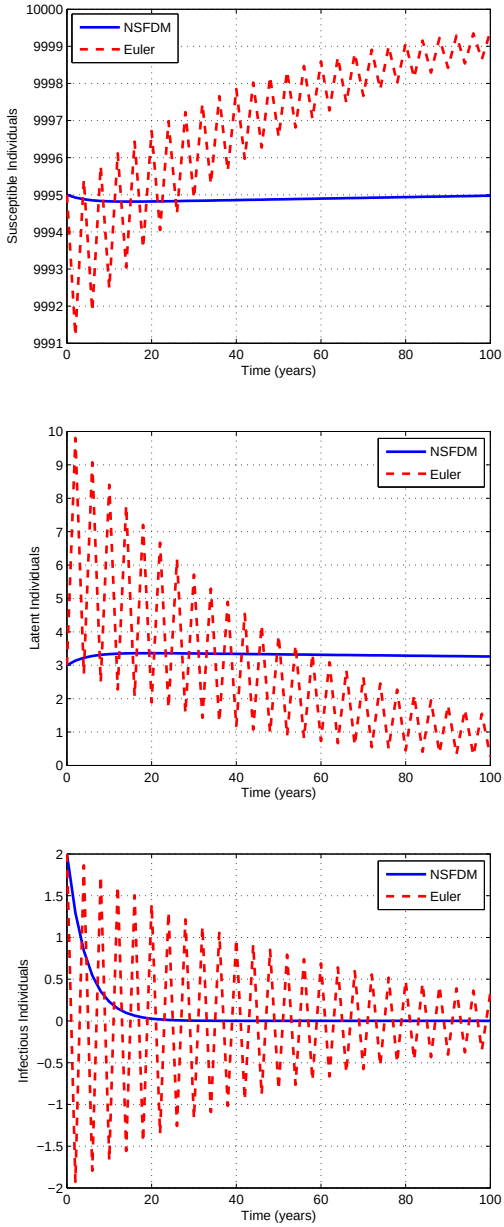

Figure 6.2.2.7: Profiles of solutions [susceptibles ($S_1(t)$): top figure, latent ($E_1(t)$): middle figure and infectious individuals ($I_1(t)$): bottom figure] obtained by using the NSFDM and Euler methods when $k_1 = 1$ and with initial conditions $(S_1(0), E_1(0), I_1(0)) = (9995, 3, 2)$ and $\ell = 2$.

6.2.2.4 Numerical simulations for the endemic equilibria

In this section, we study the convergence behavior of the numerical methods to the endemic equilibria. We provide the results for various values of the MTB infection rate k_1 while keeping $k_1 > k^* \left(R_0^{TB} > 1\right)$.

For each k_1, the endemic equilibrium of system (3.3.0.5), E^*, is locally asymptotically stable if $k_1 > k^* \left(R_0^{TB} > 1\right)$.

The tolerance values for this set of simulations are 1%, 10% and 50% for S_1^*, E_1^* and I_1^*, respectively.

In Table 6.2.2.7 as well as in Figure 6.2.2.8, we can see that only the NSFDM converges to the correct endemic equilibrium E^* when $k_1 = 9$ for small or large step-size ℓ. The other methods diverge or fail when larger step-sizes are used.

When $k_1 = 11.4$, all numerical methods converge for any step-size ℓ used to the correct endemic equilibrium. This is shown in Figure 6.2.2.9 when $\ell = 0.5$.

When $k_1 = 20$, all numerical methods converge to the right endemic equilibrium E^* as it is obvious from Table 6.2.2.8 and Figure 6.2.2.10 for small step-size ℓ. While other methods either diverge or fail for larger step-size, the NSFDM continues to converge.

Table 6.2.2.7: Results obtained by different numerical methods for $k_1 = 9 \left(R_0^{TB} > 1\right)$ and initial conditions as $(S(0), E_1(0), I_1(0)) = (9298, 679, 5)$ with different step-sizes.

ℓ	*ode45*	RK4	NSFDM
0.01	Divergent	Divergent	Convergent
0.5	Divergent	Divergent	Convergent
7	Divergent	Divergent	Convergent
10	Failed	Divergent	Convergent

In this case endemic equilibrium is given by: $(S_1^*, E_1^*, I_1^*) = (9308, 672, 2)$.

Table 6.2.2.8: Results obtained by different numerical methods for $k_1 = 20 \left(R_0^{TB} > 1\right)$ and initial conditions as $(S(0), E_1(0), I_1(0)) = (28, 1589, 643)$ with different step-sizes.

ℓ	*ode45*	RK4	NSFDM
0.01	Convergent	Convergent	Convergent
0.5	Failed	Divergent	Convergent
7	Failed	Divergent	Convergent
10	Failed	Divergent	Convergent

In this case endemic equilibrium is given by: $(S_1^*, E_1^*, I_1^*) = (33, 1554, 673)$.

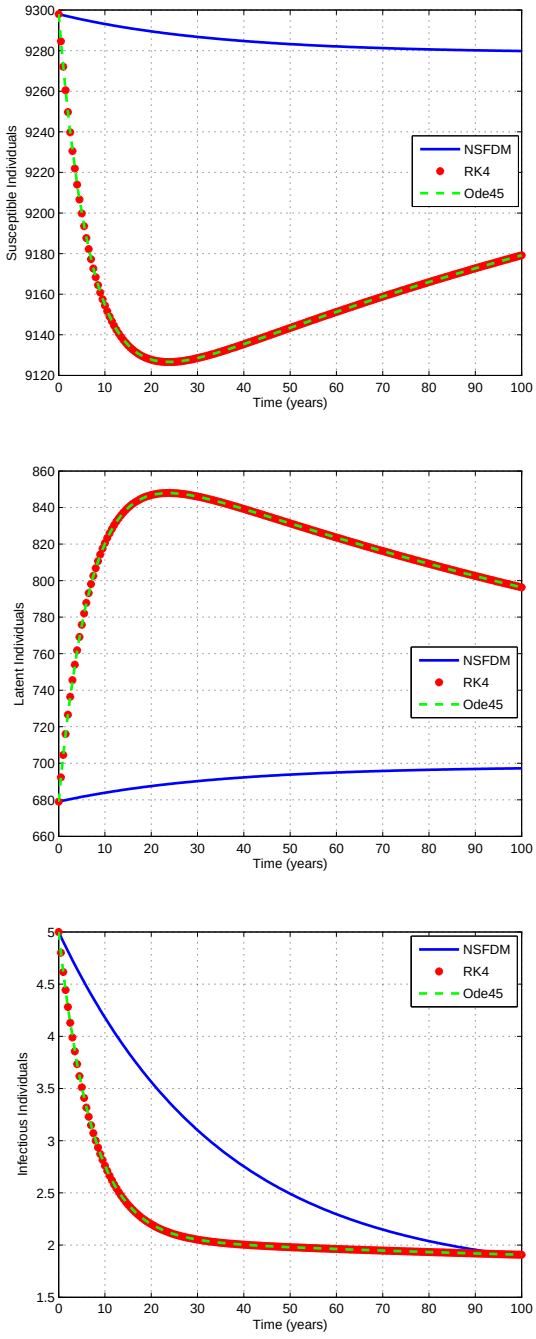

Figure 6.2.2.8: Profiles of solutions [susceptibles ($S_1(t)$): top figure, latent ($E_1(t)$): middle figure and infectious individuals ($I_1(t)$): bottom figure] obtained by using different numerical methods when $k_1 = 9$ and with initial conditions $(S_1(0), E_1(0), I_1(0)) = (9298, 679, 5)$ and $\ell = 0.5$.

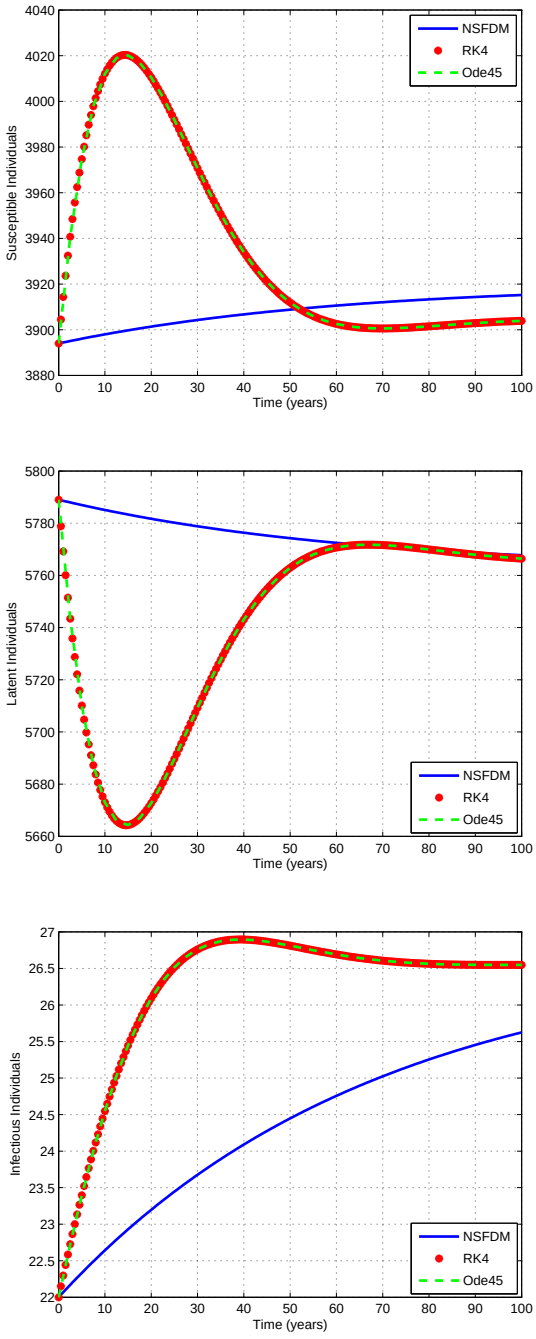

Figure 6.2.2.9: Profiles of solutions [susceptibles ($S_1(t)$): top figure, latent ($E_1(t)$): middle figure and infectious individuals ($I_1(t)$): bottom figure] obtained by using different numerical methods when $k_1 = 11.4$ and with initial conditions $(S_1(0), E_1(0), I_1(0)) = (3894, 5789, 22)$ and $\ell = 0.5$.

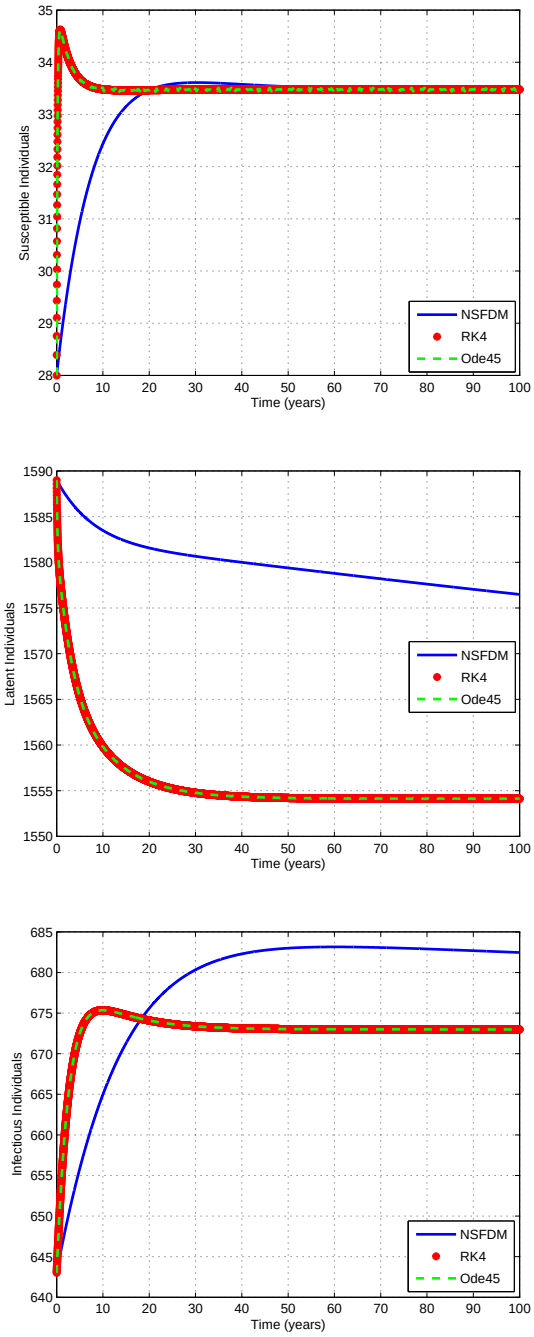

Figure 6.2.2.10: Profiles of solutions [susceptibles ($S_1(t)$): top figure, latent ($E_1(t)$): middle figure and infectious individuals ($I_1(t)$): bottom figure] obtained by using different numerical methods when $k_1 = 20$ and with initial conditions $(S_1(0), E_1(0), I_1(0)) = (28, 1589, 643)$ and $\ell = 0.01$.

6.3 Construction of the NSFDM for the full HIV-TB model

A nonstandard finite difference method (NSFDM) for the system (3.2.0.1) is designed in this section. By using the same method presented in Section 6.2 above, we discretize the system (3.2.0.1) as

$$\begin{aligned}
\frac{S_1^{n+1}-S_1^n}{\psi_1(\ell)} &= B - S_1^{n+1}\left(\frac{1_1 I_1^n + k_2 I_2^n}{N^n}\right) - \mu_1 S_1^{n+1} - f(H^n)H^n S_1^{n+1},\\
\frac{E_1^{n+1}-E_1^n}{\psi_2(\ell)} &= \left((1-p_1)S_1^{n+1} - q_1 E_1^{n+1}\right)\left(\frac{k_1 I_1^n + k_2 I_2^n}{N^n}\right) - (a_1+\mu_1)E_1^{n+1} + b_1 I_1^n\\
&\quad - f(H^n)H^n E_1^{n+1},\\
\frac{I_1^{n+1}-I_1^n}{\psi_3(\ell)} &= \left(p_1 S_1^n + q_1 E_1^{n+1}\right)\left(\frac{k_1 I_1^n + k_2 I_2^n}{N^n}\right) - b_1 I_1^n - m_1 I_1^{n+1} + a_1 E_1^{n+1}\\
&\quad - f(H^n)H^n I_1^{n+1},\\
\frac{S_2^{n+1}-S_2^n}{\psi_4(\ell)} &= -S_2^{n+1}\left(\frac{k_1 I_1^n + k_2 I_2^n}{N^n}\right) - \mu_2 S_2^{n+1} + f(H^n)H^n S_1^{n+1},\\
\frac{E_2^{n+1}-E_2^n}{\psi_5(\ell)} &= \left((1-p_2)S_2^{n+1} - q_2 E_2^{n+1}\right)\left(\frac{k_1 I_1^n + k_2 I_2^n}{N^n}\right) - (a_2+\mu_2)E_2^{n+1} + b_2 I_2^n\\
&\quad + f(H^n)H^n E_1^{n+1},\\
\frac{I_2^{n+1}-I_2^n}{\psi_6(\ell)} &= \left(p_2 S_2^{n+1} + q_2 E_2^{n+1}\right)\left(\frac{k_1 I_1^n + k_2 I_2^n}{N^n}\right) - b_2 I_2^n - m_2 I_2^{n+1} + a_2 E_2^{n+1}\\
&\quad + f(H^n)H^n I_1^{n+1},
\end{aligned} \tag{6.3.0.1}$$

where discretizations for N, H and $f(H)$ are given by

$$N^n = S_1^n + E_1^n + I_1^n + S_2^n + E_2^n + I_2^n, \tag{6.3.0.2}$$

$$H^n = \frac{S_2^n + E_2^n + I_2^n}{N^n} \tag{6.3.0.3}$$

and

$$f(H^n) = \frac{d}{1+\lambda_0(H^n)^k}, \tag{6.3.0.4}$$

respectively.

As before, we note that the nonlocal approximations are used for the nonlinear terms and the following denominator functions are used: $\psi_1(\ell) = \frac{e^{\mu_1\ell}-1}{\mu_1}$, $\psi_2(\ell) = \frac{e^{(a_1+\mu_1)\ell}-1}{a_1+\mu_1}$, $\psi_3(\ell) = \frac{1-e^{-m_1\ell}}{b_1}$, $\psi_4(\ell) = \frac{e^{\mu_2\ell}-1}{\mu_2}$, $\psi_5(\ell) = \frac{e^{(a_2+\mu_2)\ell}-1}{a_2+\mu_2}$ and $\psi_6(\ell) = \frac{1-e^{-m_2\ell}}{b_2}$.

Simplifying (6.3.0.1), we obtain

$$\begin{aligned}
S_1^{n+1} &= \frac{S_1^n + \psi_1(\ell)B}{1+\psi_1(\ell)\left\{\frac{k_1I_1^n+k_2I_2^n}{N^n} + \mu_1 + f(H^n)H^n\right\}},\\
E_1^{n+1} &= \frac{E_1^n + \psi_2(\ell)\left\{\frac{(1-p_1)S_1^{n+1}(k_1I_1^n+k_2I_2^n)}{N^n} + b_1I_1^n\right\}}{1+\psi_2(\ell)\left\{\frac{q_1(k_1I_1^n+k_2I_2^n)}{N^n} + a_1 + \mu_1 + f(H^n)H^n)\right\}},\\
I_1^{n+1} &= \frac{(1-\psi_3(\ell)b_1)I_1^n + \psi_3(\ell)\left\{\frac{(p_1S_1^{n+1}+q_1E_1^{n+1})(k_1I_1^n+k_2I_2^n)}{N^n} + a_1E_1^{n+1})\right\}}{1+\psi_3(\ell)\left\{m_1 + f(H^n)H^n\right\}},\\
S_2^{n+1} &= \frac{S_2^n + \psi_4(\ell)S_1^{n+1}f(H^n)H^n}{1+\psi_4(\ell)\left\{\frac{k_1I_1^{n+1}+k_2I_2^n}{N^n} + \mu_2\right\}},
\end{aligned} \tag{6.3.0.5}$$

$$E_2{}^{n+1} = \frac{E_2{}^n + \psi_5(\ell)\left\{\frac{(1-p_2)S_2{}^{n+1}(k_1I_1{}^{n+1}+k_2I_2{}^n)}{N^n} + b_2I_2{}^n + E_1{}^{n+1}f(H^n)H^n)\right\}}{1+\psi_5(\ell)\left\{\frac{q_2(k_1I_1{}^{n+1}+k_2I_2{}^n)}{N^n} + a_2 + \mu_2\right\}},$$

$$\begin{aligned}
I_2{}^{n+1} = {} & \frac{(1-\psi_6(\ell)b_2)I_2^n}{1+m_2\psi_6(\ell)} + \frac{\psi_6(\ell)}{1+m_2\psi_6(\ell)}\times\\
& \left\{\frac{(p_2S_2{}^{n+1}+q_2E_2{}^{n+1})(k_1I_1{}^{n+1}+k_2I_2{}^n)}{N^n} + a_2E_2{}^{n+1} + I_1{}^{n+1}f(H^n)H^n)\right\}.
\end{aligned}$$

The positivity of the solution reflects from the above method (6.3.0.5) because if the initial conditions $S_1(0)$, $E_1(0)$, $I_1(0)$, $S_2(0)$, $E_2(0)$ and $I_2(0)$ are non-negative, then the right hand side of (6.3.0.5) admits no negative terms for any of $n = 0, 1, 2, 3, ...$ because $0 < p_1 < 1$, $0 < p_2 < 1$, $0 < \psi_3(\ell)b_1 < 1$ and $0 < \psi_6(\ell)b_2 < 1$.

In the following section we determine the stability properties of system (6.3.0.1), and we verify that

(i) the continuous and the discrete models have the same equilibria, and

(ii) both models posses similar qualitatively features near these equilibria.

6.3.1 Fixed points and stability analysis

We study in this section the stability and convergence properties of the fixed points of the proposed NSFDM.

We begin by noting that the fixed points $(\hat{S}_1, \hat{E}_1, \hat{I}_1, \hat{S}_2, \hat{E}_2, \hat{I}_2)$ of system (6.3.0.1) can be found by solving

$$\begin{aligned}
\hat{f}_1(\hat{S}_1, \hat{E}_1, \hat{I}_1, \hat{S}_2, \hat{E}_2, \hat{I}_2) &= \hat{S}_1, \\
\hat{f}_2(\hat{S}_1, \hat{E}_1, \hat{I}_1, \hat{S}_2, \hat{E}_2, \hat{I}_2) &= \hat{E}_1, \\
\hat{f}_3(\hat{S}_1, \hat{E}_1, \hat{I}_1, \hat{S}_2, \hat{E}_2, \hat{I}_2) &= \hat{I}_1, \\
\hat{f}_4(\hat{S}_1, \hat{E}_1, \hat{I}_1, \hat{S}_2, \hat{E}_2, \hat{I}_2) &= \hat{S}_2, \\
\hat{f}_5(\hat{S}_1, \hat{E}_1, \hat{I}_1, \hat{S}_2, \hat{E}_2, \hat{I}_2) &= \hat{E}_2, \\
\hat{f}_6(\hat{S}_1, \hat{E}_1, \hat{I}_1, \hat{S}_2, \hat{E}_2, \hat{I}_2) &= \hat{I}_2,
\end{aligned} \tag{6.3.1.1}$$

where $\hat{F}_i(\hat{S}_1, \hat{E}_1, \hat{I}_1, \hat{S}_2, \hat{E}_2, \hat{I}_2)$, $i = 1, 2, ..., 6$, can be obtained by considering the right

hand sides in (6.3.0.5), i.e.,

$$\begin{aligned}
\hat{f}_1(\hat{S}_1,\hat{E}_1,\hat{I}_1,\hat{S}_2,\hat{E}_2,\hat{I}_2) &= \frac{\hat{S}_1+\psi_1(\ell)B}{1+\psi_1(\ell)\left\{\hat{\lambda}_T+\mu_1+\hat{\lambda}_H\right\}},\\
\hat{f}_2(\hat{S}_1,\hat{E}_1,\hat{I}_1,\hat{S}_2,\hat{E}_2,\hat{I}_2) &= \frac{\hat{E}_1+\psi_2(\ell)\left\{(1-p_1)\hat{S}_1\hat{\lambda}_T+b_1\hat{I}_1\right\}}{1+\psi_2(\ell)\left\{q_1\hat{\lambda}_T+a_1+\mu_1+\hat{\lambda}_H)\right\}},\\
\hat{f}_3(\hat{S}_1,\hat{E}_1,\hat{I}_1,\hat{S}_2,\hat{E}_2,\hat{I}_2) &= \frac{(1-\psi_3(\ell)b_1)\hat{I}_1+\psi_3(\ell)\left\{(p_1\hat{S}_1+q_1\hat{E}_1)\hat{\lambda}_T+a_1\hat{E}_1)\right\}}{1+\psi_3(\ell)\left\{m_1+\hat{\lambda}_H\right\}},\\
\hat{f}_4(\hat{S}_1,\hat{E}_1,\hat{I}_1,\hat{S}_2,\hat{E}_2,\hat{I}_2) &= \frac{\hat{S}_2+\psi_4(\ell)\hat{S}_1\hat{\lambda}_H}{1+\psi_4(\ell)\left\{\hat{\lambda}_T+\mu_2\right\}},\\
\hat{f}_5(\hat{S}_1,\hat{E}_1,\hat{I}_1,\hat{S}_2,\hat{E}_2,\hat{I}_2) &= \frac{\hat{E}_2+\psi_5(\ell)\left\{(1-p_2)\hat{S}_2\hat{\lambda}_T+b_2\hat{I}_2+\hat{E}_1\hat{\lambda}_H)\right\}}{1+\psi_5(\ell)\left\{q_2\hat{\lambda}_T+a_2+\mu_2\right\}},\\
\hat{f}_6(\hat{S}_1,\hat{E}_1,\hat{I}_1,\hat{S}_2,\hat{E}_2,\hat{I}_2) &= \frac{(1-\psi_6(\ell)b_2)\hat{I}_2+\psi_6(\ell)\left\{(p_2\hat{S}_2+q_2\hat{E}_2)\hat{\lambda}_T+a_2\hat{E}_2+\hat{I}_1\hat{\lambda}_H)\right\}}{1+m_2\psi_6(\ell)},
\end{aligned} \tag{6.3.1.2}$$

where

$$\hat{\lambda}_T = \frac{k_1\hat{I}_1+k_2\hat{I}_2}{\hat{S}_1+\hat{E}_1+\hat{I}_1+\hat{S}_2+\hat{E}_2+\hat{I}_2} \tag{6.3.1.3}$$

and

$$\hat{\lambda}_H = f(\hat{H})\hat{H}. \tag{6.3.1.4}$$

Solving (6.3.1.1), we obtain the following system

$$\begin{aligned}
\hat{F}(\hat{\lambda}_T,\hat{\lambda}_H) &= 0,\\
\hat{G}(\hat{\lambda}_T,\hat{\lambda}_H) &= 0,
\end{aligned} \tag{6.3.1.5}$$

where

$$\begin{aligned}\hat{F}(\hat{\lambda}_T,\hat{\lambda}_H) &= \hat{\lambda}_T\hat{P}(\hat{\lambda}_T,\hat{\lambda}_H) - \left\{k_1\hat{I}_1(\hat{\lambda}_T,\hat{\lambda}_H) + k_2\hat{I}_2(\hat{\lambda}_T,\hat{\lambda}_H)\right\},\\ \hat{G}(\hat{\lambda}_T,\hat{\lambda}_H) &= \hat{\lambda}_H\left\{1+\lambda_0(\hat{H}(\hat{\lambda}_T,\hat{\lambda}_H))^k\right\} - d\hat{H}(\hat{\lambda}_T,\hat{\lambda}_H).\end{aligned} \tag{6.3.1.6}$$

In the above system, the solution $\hat{\lambda}_T = 0$ and $\hat{\lambda}_H = 0$ corresponds to the disease free equilibrium

$$\hat{E}_0 = \left(\frac{B}{\mu_2}, 0, 0, 0, 0, 0\right), \tag{6.3.1.7}$$

whereas the system may have more than one endemic equilibrium which can be written in the following implicit form:

$$\begin{aligned}\hat{S}_1 &= \frac{B}{\hat{\lambda}_T+\mu_1+\hat{\lambda}_H},\\ \hat{E}_1 &= \frac{\hat{S}_1\hat{\lambda}_T(b_1+(1-p_1)(m_1+\hat{\lambda}_H))}{(\mu_1+\hat{\lambda}_H)(b_1+m_1+\hat{\lambda}_H)+(\hat{\lambda}_T q_1+a_1)(m_1+\hat{\lambda}_H)},\\ \hat{I}_1 &= \frac{\hat{S}_1\hat{\lambda}_T p_1+(\hat{\lambda}_T q_1+a_1)\hat{E}_1}{b_1+m_1+\hat{\lambda}_H},\\ \hat{S}_2 &= \frac{\hat{\lambda}_H\hat{S}_1}{\hat{\lambda}_T+\mu_2},\\ \hat{E}_2 &= \frac{\hat{S}_2\hat{\lambda}_T(b_2+m_2(1-p_2))+b_2\hat{\lambda}_H\hat{I}_1+\hat{\lambda}_H\hat{E}_1(b_2+m_2)}{\mu_2(b_2+m_2)+m_2(q_2\hat{\lambda}_T+a_2)},\\ \hat{I}_2 &= \frac{\hat{S}_2\hat{\lambda}_T p_2+\hat{\lambda}_T q_2\hat{E}_2+a_2\hat{E}_2+\hat{\lambda}_H\hat{I}_1}{b_2+m_2}.\end{aligned}$$

The solution $\hat{\lambda}_T = 0$ with $\hat{\lambda}_H > 0$ corresponds to the endemic equilibrium of the NSFDM given by (5.2.0.6) for the HIV sub-model and the solution $\hat{\lambda}_H = 0$ with $\hat{\lambda}_T > 0$ corresponds to the endemic equilibrium of the NSFDM (6.2.0.1) for TB sub-model. If

$\hat{\lambda}_T > 0$ and $\hat{\lambda}_H > 0$, then this solution correspond to the endemic equilibrium of both diseases of the NSFDM for the full model (6.3.0.1).

The equations of system (6.3.1.1) are highly nonlinear in $\hat{\lambda}_T$ and $\hat{\lambda}_H$ and hence explicit solutions are not obtainable. In Section 6.3.2.1, we solve this system numerically to obtain endemic fixed points of system (6.3.0.1). Their numerical stability properties also provided in that section.

The form of the characteristic equations (6.3.1.5) of the discrete system (6.3.0.1) is similar to that of the continuous system (3.2.0.1) given by (3.4.4.7). Therefore, both systems (3.2.0.1) and (6.3.0.1) have the same characteristic equation and expressions of equilibria. Hence, we have the following result.

Remark 6.3.1.1. The continuous system (3.2.0.1) and the discrete system (6.3.0.1) have the same equilibria.

Next,we determine the stability properties of the equilibria of system (6.3.0.1). The Jacobian matrix of the system (6.3.0.1) evaluated at the disease free equilibrium, $J(\hat{E}_0)$, is given by the following matrix

$$\begin{pmatrix}
\frac{1}{1+\psi_1(\ell)\mu_1} & 0 & -\frac{k_1\psi_1(\ell)}{1+\psi_1(\ell)\mu_1} & -\frac{d\psi_1(\ell)}{1+\psi_1(\ell)\mu_1} & -\frac{d\psi_1(\ell)}{1+\psi_1(\ell)\mu_1} & -\frac{(k_2+d)\psi_1(\ell)}{1+\psi_1(\ell)\mu_1} \\
0 & \frac{1}{1+\psi_2(\ell)(a_1+\mu_1)} & \frac{\psi_2(\ell)((1-p_1)k_1+b_1)}{1+\psi_2(\ell)(a_1+\mu_1)} & 0 & 0 & \frac{(1-p_1)k_2\psi_2(\ell)}{1+\psi_2(\ell)(a_1+\mu_1)} \\
0 & \frac{a_1\psi_3(\ell)}{1+m_1\psi_3(\ell)} & \frac{1-\psi_3(\ell)(b_1-p_1k_1)}{1+m_1\psi_3(\ell)} & 0 & 0 & \frac{p_1k_2\psi_3(\ell)}{1+m_1\psi_3(\ell)} \\
0 & 0 & 0 & \frac{1+\psi_4(\ell)d}{1+\psi_4(\ell)\mu_2} & \frac{\psi_4(\ell)d}{1+\psi_4(\ell)\mu_2} & \frac{\psi_4(\ell)d}{1+\psi_4(\ell)\mu_2} \\
0 & 0 & 0 & 0 & \frac{1}{1+\psi_5(\ell)(a_2+\mu_2)} & \frac{\psi_5(\ell)b_2}{1+\psi_5(\ell)(a_2+\mu_2)} \\
0 & 0 & 0 & 0 & \frac{a_2\psi_6(\ell)}{1+m_2\psi_6(\ell)} & \frac{1-\psi_6(\ell)b_2}{1+m_2\psi_6(\ell)}
\end{pmatrix}.$$

It should be noted that the nature of the eigenvalues of this matrix is difficult to be determined for general set of parameters due to the complexity of their analytic expressions. However, we will determine the stability of the fixed points of system (6.3.0.1) numerically in Section 6.3.2.2.

6.3.2 Numerical results and simulations

We present some numerical simulations using the proposed NSFDM in this section. The method is also tested for convergence. We numerically show that the NSFDM is elementary stable. A number of different numerical simulations are carried out and comparisons are made with other well-known numerical methods for various time step-sizes ℓ. Some of these parameters are varied to test the robustness of the methods. Parameters used for the simulations are taken from Table 3.2.0.1.

6.3.2.1 Numerical stability analysis of the endemic equilibria

In order to investigate numerically the dynamic consistency between the continuous model and the NSFDM, in this section, we develop a linear stability analysis of system (3.2.0.1) for a particular set of values of the parameters. We tabulate the equilibria and corresponding eigenvalues associated with the Jacobian matrices for the continuous system (3.2.0.1) for different values of Hill coefficient k. It should be noted that when solving system (3.2.0.1) for its equilibria when $k \geq 1$, it always has the disease free equilibrium $E_0^* = (10000, 0, 0, 0, 0, 0)$ and other endemic equilibria (for the set of parameter values presented in Table 3.2.0.1 which give $(R_0 > 1)$), but only one endemic equilibrium is relevant for each value of k.

Table 6.3.2.1: Endemic equilibria and corresponding eigenvalues for system (3.2.0.1) when $k \geq 1$.

	$k=1$	$k=2$	$k=5$	$k=10$
S_1^*	837	666	485	376
E_1^*	1051	548	215	106
I_1^*	20	13	7	4
S_2^*	291	390	546	657
E_2^*	877	902	866	821
I_2^*	25	27	27	26
$\Re(\lambda_1)$	-3.896926	-3.815514	-3.701581	-3.617004
$\Re(\lambda_2)$	-0.388269	-0.420033	-0.533822	-0.606353
$\Re(\lambda_3)$	-0.388269	-0.420033	-0.373532	-0.343104
$\Re(\lambda_4)$	-0.108870	-0.114237	-0.120655	-0.126139
$\Re(\lambda_5)$	-0.108870	-0.114237	-0.120655	-0.126139
$\Re(\lambda_6)$	-0.151081	-0.171254	-0.173915	-0.164184

It is clear from the above tabular results that the real parts of the eigenvalues for each value of k are negative. We therefore have the following result.

Remark 6.3.2.1. For $k = 1, 2, 5, 10$, the system (3.2.0.1) has a disease free equilibrium when $R_0 < 1$ and it possesses a number of endemic equilibria as presented above in Table 6.3.2.1 when $R_0 > 1$. Each of these endemic equilibria is locally asymptotically stable if $R_0 > 1$.

6.3.2.2 Numerical stability analysis of the fixed points

In this section, we tabulate the spectral radii of the Jacobian matrices corresponding to the fixed points of the NSFDM for different values of the time step-size ℓ as shown in tables 6.3.2.2 and 6.3.2.3. A general stability analysis has not been performed since general parameters gives unmanageable analytic expressions. However, we used several sets of values of the parameters to check numerically the stability properties of the method. We recall from Remark 6.3.1.1 that the equilibria of both systems (3.2.0.1) and (6.3.0.1) remain the same.

Table 6.3.2.2: The spectral radii of the Jacobian matrices corresponding to the disease free equilibrium of the NSFDM for $R_0 < 1$.

	The spectral radii when		
ℓ	$k_1 = 1$, $d = 0.03$	$k_1 = 5$, $d = 0.07$	$k_1 = 8$, $d = 0.09$
0.01	0.999769	0.999725	0.999700
0.1	0.997701	0.997281	0.997037
0.5	0.988765	0.987150	0.985975
1	0.978158	0.976010	0.973712
7	0.890525	0.917218	0.897338
10	0.866664	0.911749	0.881171
20	0.836983	0.921225	0.857404
50	0.879566	0.968137	0.848466

Table 6.3.2.3: The spectral radii of the Jacobian matrices corresponding to the endemic equilibriums of the NSFDM for $R_0 > 1$.

	The spectral radii when			
ℓ	$k = 1$	$k = 2$	$k = 5$	$k = 10$
0.01	0.999014	0.998784	0.998502	0.998633
0.5	0.954546	0.946629	0.934450	0.941954
1	0.915574	0.905803	0.885037	0.901094
7	0.755628	0.746206	0.707981	0.773471
10	0.732748	0.724808	0.687103	0.762712
20	0.700287	0.697408	0.662911	0.750716
50	0.679891	0.683600	0.654925	0.748200

It can be seen from the two tables above, that all the spectral radii are less than one in magnitude irrespective of the time step-size used in the simulations. Hence, by Theorem 1.3.3.1, we have the following result.

Remark 6.3.2.2. The disease free equilibrium for system (6.3.0.1) is locally asymptotically stable when $R_0 < 1$ and unstable if $R_0 > 1$, whereas for $k = 1, 2, 5, 10$, each endemic equilibrium of system (6.3.0.1) is locally asymptotically stable if $R_0 > 1$. Moreover, the system is unconditionally elementary stable.

6.3.2.3 Numerical simulations for the disease free equilibrium

The disease free equilibrium (DFE) is calculated using the proposed NSFDM along with other numerical methods conventionally used. A thorough comparison of these methods is presented for many different scenarios.

As in the previous section, here the MTB infection rate, k_1, and the maximum contact rate of HIV, d, are varied in a certain range while keeping $R_0 < 1$ (as needed for DFE).

In Section 3.4, we have shown that system (3.2.0.1) has asymptotically stable disease free equilibrium if $R_0 = \max\left\{R_0^{TB}, R_0^{HIV}\right\} < 1$, e.g., $k_1 < k^* = 8.7$ and $d < d^* = 0.7$. The numerical value of this DFE is given by $E_0^* = (10000, 0, 0)$.

In order to check whether these numerical methods converge to the theoretical value of the DFE, we require a tolerance value. We consider 200 and 100 individuals

as the tolerances values for S_1 and E_1 populations respectively and 10 individuals as the tolerance for I_1, S_2, E_2 and I_2 populations.

The convergence of different numerical methods to the correct disease free equilibrium $E_0^* = (10000, 0, 0)$ for different values of k_1 and d while keeping $R_0 < 1$ is shown in Table 6.3.2.4 and Table 6.3.2.5. All numerical methods converge well for small step-size ℓ. The NSFDM is shown to converge for larger ℓ while other methods diverge or fail. The convergence of the different numerical methods for step-size $\ell = 0.1$ can be seen in Figure 6.3.2.1. Further, we have shown in Figure 6.3.2.2 that for $\ell = 1$, the fourth order Runge-Kutta method neither converges nor preserves the positivity of the model state variables.

Table 6.3.2.4: Results obtained by different numerical methods for $k_1 = 1$ and $d = 0.03$ ($R_0 < 1$) and initial conditions as $(S_1(0), E_1(0), I_1(0), S_2(0), E_2(0), I_2(0)) = (9940, 20, 15, 13, 7, 5)$ with different step-sizes.

ℓ	*ode45*	RK4	NSFDM
0.01	Convergent	Convergent	Convergent
0.1	Convergent	Convergent	Convergent
0.5	Failed	Convergent	Convergent
1	Failed	Divergent	Convergent
7	Failed	Divergent	Convergent
10	Failed	Divergent	Convergent

The disease free equilibrium is: $(S_1^*, E_1^*, I_1^*, S_2^*, E_2^*, I_2^*) = (10000, 0, 0, 0, 0, 0)$.

Table 6.3.2.5: Results obtained by different numerical methods for $k_1 = 4$ and $d = 0.05$ ($R_0 < 1$) and initial conditions as $(S_1(0), E_1(0), I_1(0), S_2(0), E_2(0), I_2(0)) = (9940, 20, 15, 13, 7, 5)$ with different step-sizes.

ℓ	*ode45*	RK4	NSFDM
0.01	Convergent	Convergent	Convergent
0.1	Convergent	Convergent	Convergent
0.5	Failed	Convergent	Convergent
1	Failed	Divergent	Convergent
2	Failed	Divergent	Convergent

The disease free equilibrium is: $(S_1^*, E_1^*, I_1^*, S_2^*, E_2^*, I_2^*) = (10000, 0, 0, 0, 0, 0)$.

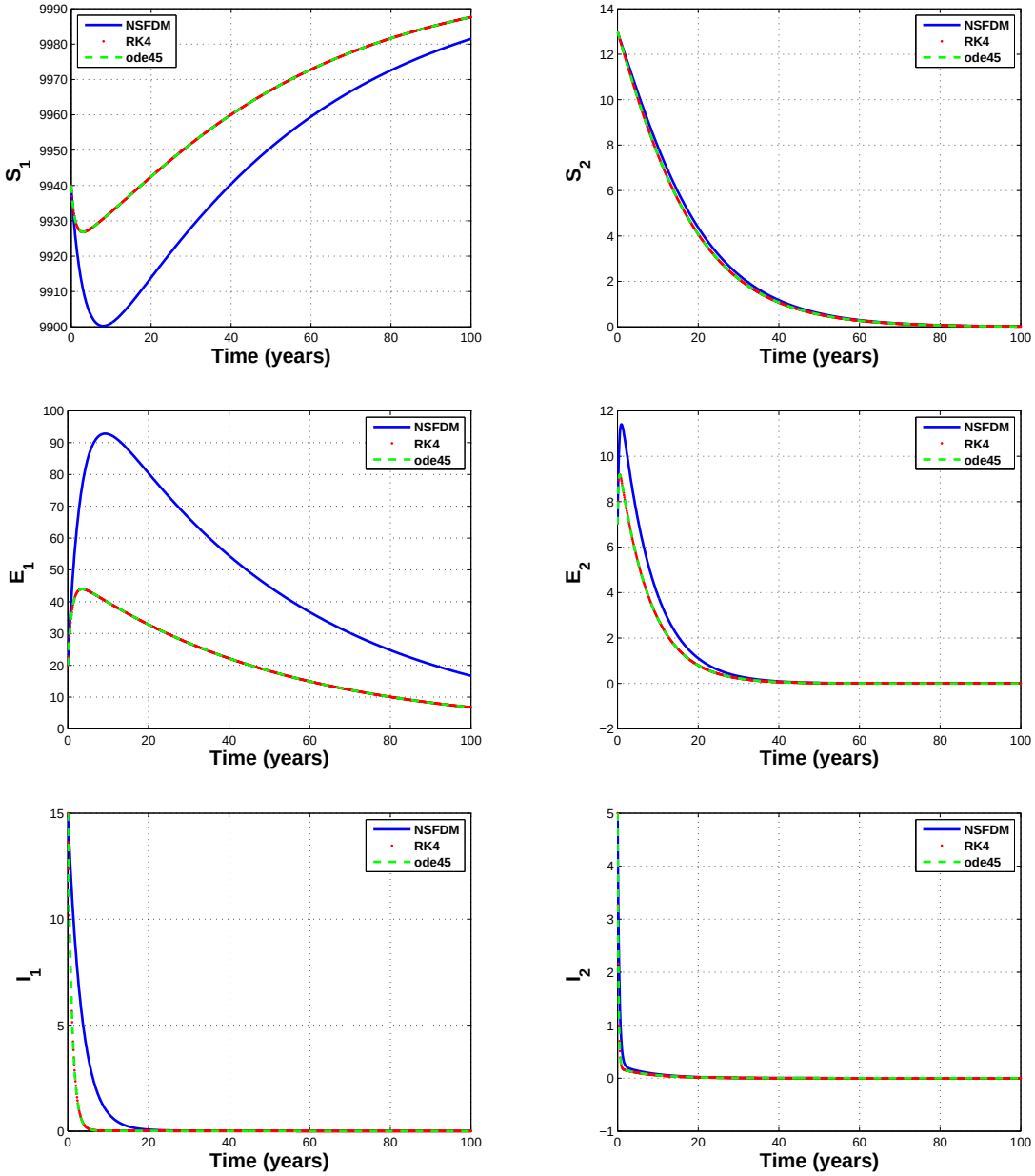

Figure 6.3.2.1: The DFE of system (3.2.0.1) when $k_1 = 1$ and $d = 0.03$ ($R_0 < 1$) obtained by using different numerical methods with $\ell = 0.1$ and initial conditions as $(S_1(0), E_1(0), I_1(0), S_2(0), E_2(0), I_2(0)) = (9940, 20, 15, 13, 7, 5)$.

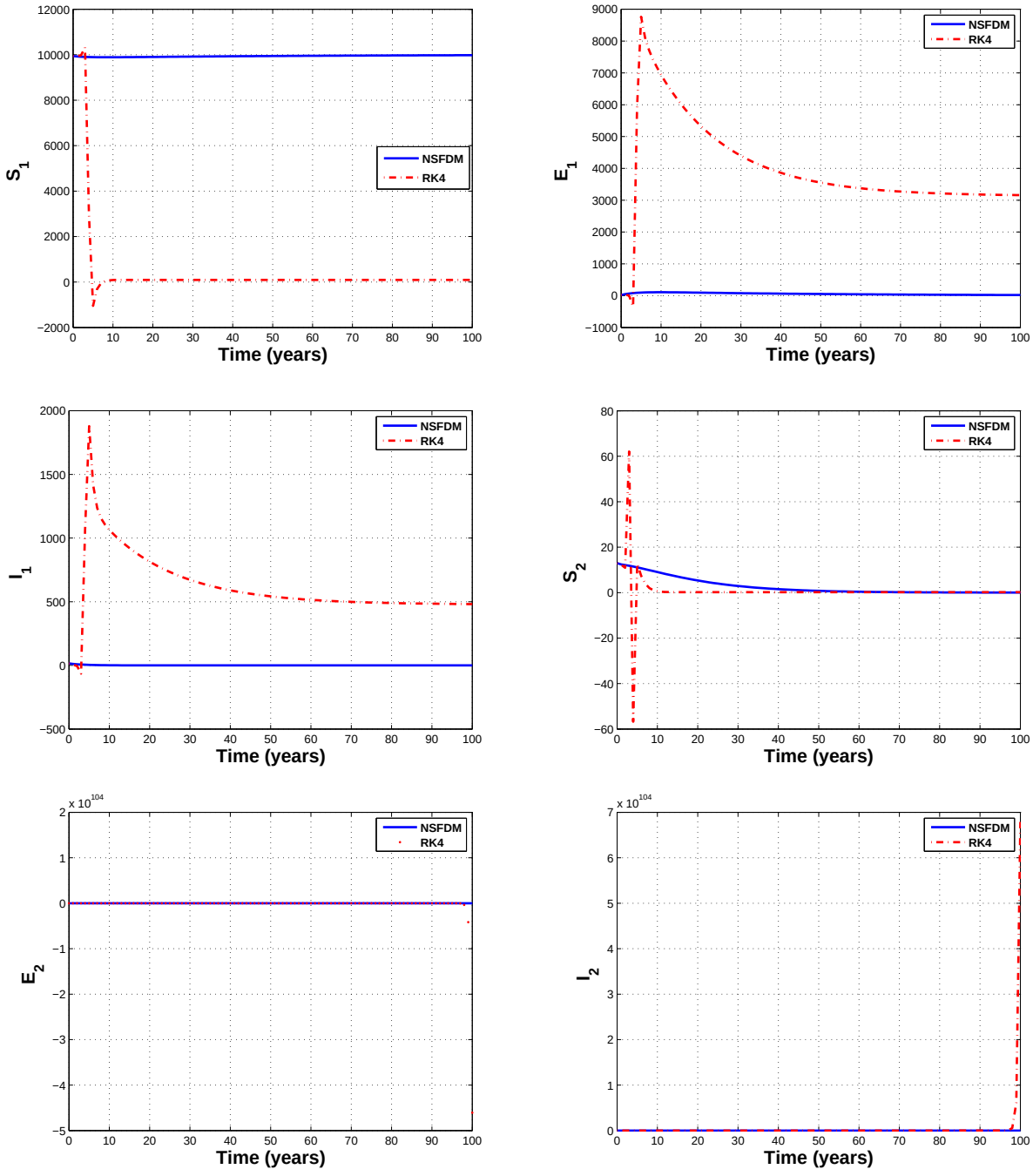

Figure 6.3.2.2: The DFE of system (3.2.0.1) when $k_1 = 1$ and $d = 0.03$ ($R_0 < 1$) obtained by using the NSFDM and RK4 with $\ell = 1$ and initial conditions as $(S_1(0), E_1(0), I_1(0), S_2(0), E_2(0), I_2(0)) = (9940, 20, 15, 13, 7, 5)$.

6.3.2.4 Numerical simulations for the endemic equilibria

In this section, we study the convergence behavior of the numerical methods to the endemic equilibria of system (3.2.0.1). We provide the results for various values of the Hill coefficient k. Parameters values used in this section are taken from Table 3.2.0.1 which gives $R_0 = \max\left\{R_0^{TB}, R_0^{HIV}\right\} > 1$.

As presented in Table 6.3.2.1, the endemic equilibrium of system (3.2.0.1), E^*, for each $k = 1, 2, 5, 10$ (for example), is locally asymptotically stable if ($R_0 > 1$). We have shown in Remark 6.3.1.1 that the equilibria of both system (3.2.0.1) and system (6.3.0.1) remain the same for any values of k.

The tolerance values for this set of simulations are 10% for S_1^*, E_1^*, I_1^*, S_2^*, E_2^* and I_2^* respectively. The endemic equilibrium with TB only, i.e,
$(S_1(0), E_1(0), I_1(0), S_2(0), E_2(0), I_2(0)) = (3904, 5764, 26, 1, 0, 0)$, will be used as the initial condition in the simulations for the complete model with both HIV and TB in this part of the simulations.

In Table 6.3.2.6, we can see that only the NSFDM converges to the correct endemic equilibrium E^* when $k = 1$ for small or large step-size ℓ. The other methods diverge or fail when larger step-sizes are used. When k is increased, we obtain similar convergence results. Convergence results for $k = 1$ and $k = 2$ are shown in Figure 6.3.2.3 and Figure 6.3.2.4.

As in the previous section, the Runge-Kutta method neither preserved the positivity of the state variables in the model nor converged for some values of ℓ. This is shown in Figure 6.3.2.5.

Table 6.3.2.6: Results obtained by different numerical methods when $R_0 > 1$ and $k = 1$ with different step-sizes.

ℓ	*ode45*	RK4	NSFDM
0.01	Convergent	Convergent	Convergent
0.1	Convergent	Convergent	Convergent
0.5	Convergent	Convergent	Convergent
1	Failed	Divergent	Convergent
2	Failed	Divergent	Convergent
6	Failed	Divergent	Convergent

The endemic equilibrium is: $(S_1^*, E_1^*, I_1^*, S_2^*, E_2^*, I_2^*) = (837, 1051, 20, 291, 877, 25)$.

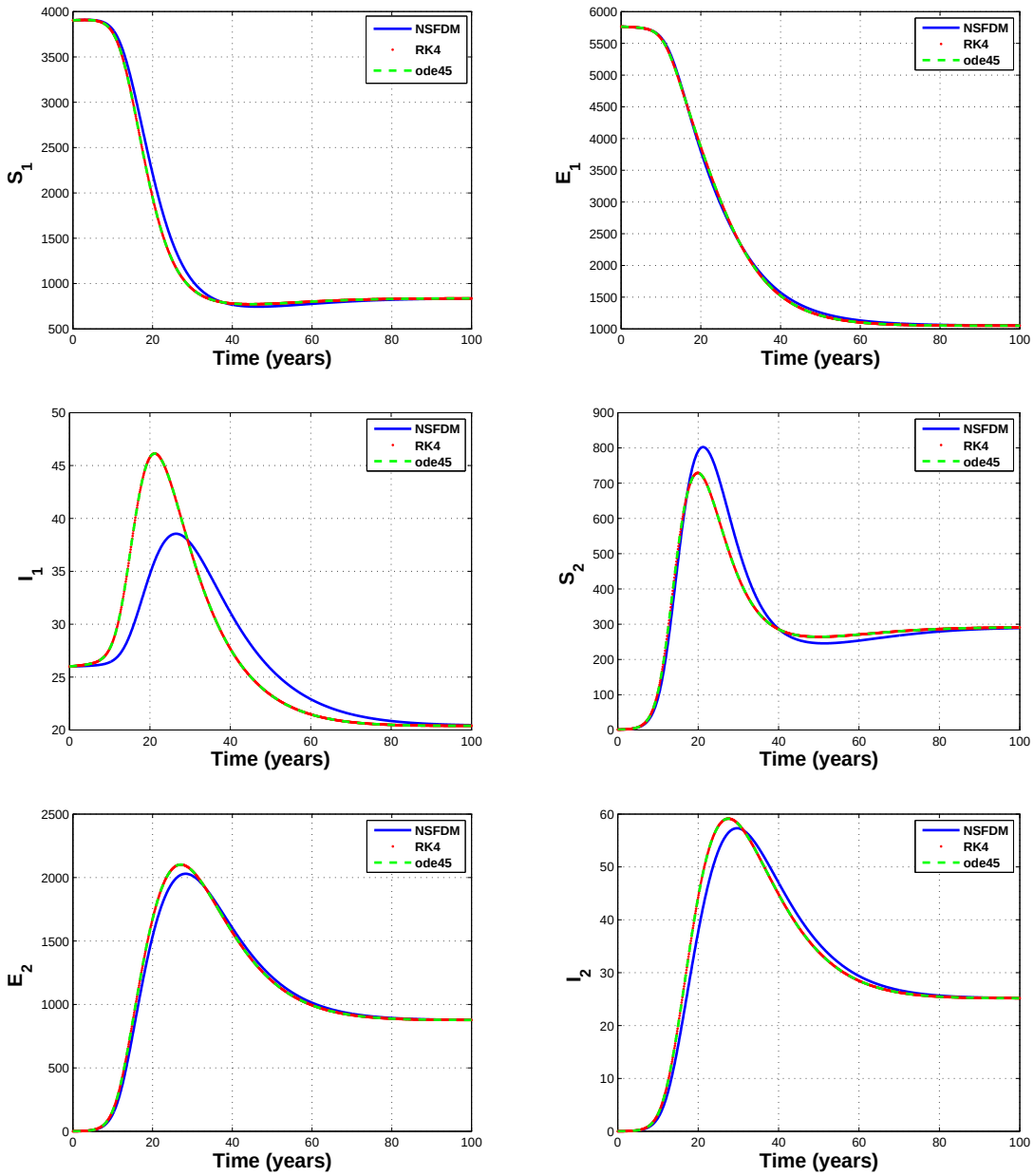

Figure 6.3.2.3: The EE of system (3.2.0.1) when $R_0 > 1$ and $k = 1$ obtained by using different numerical methods with $\ell = 0.1$.

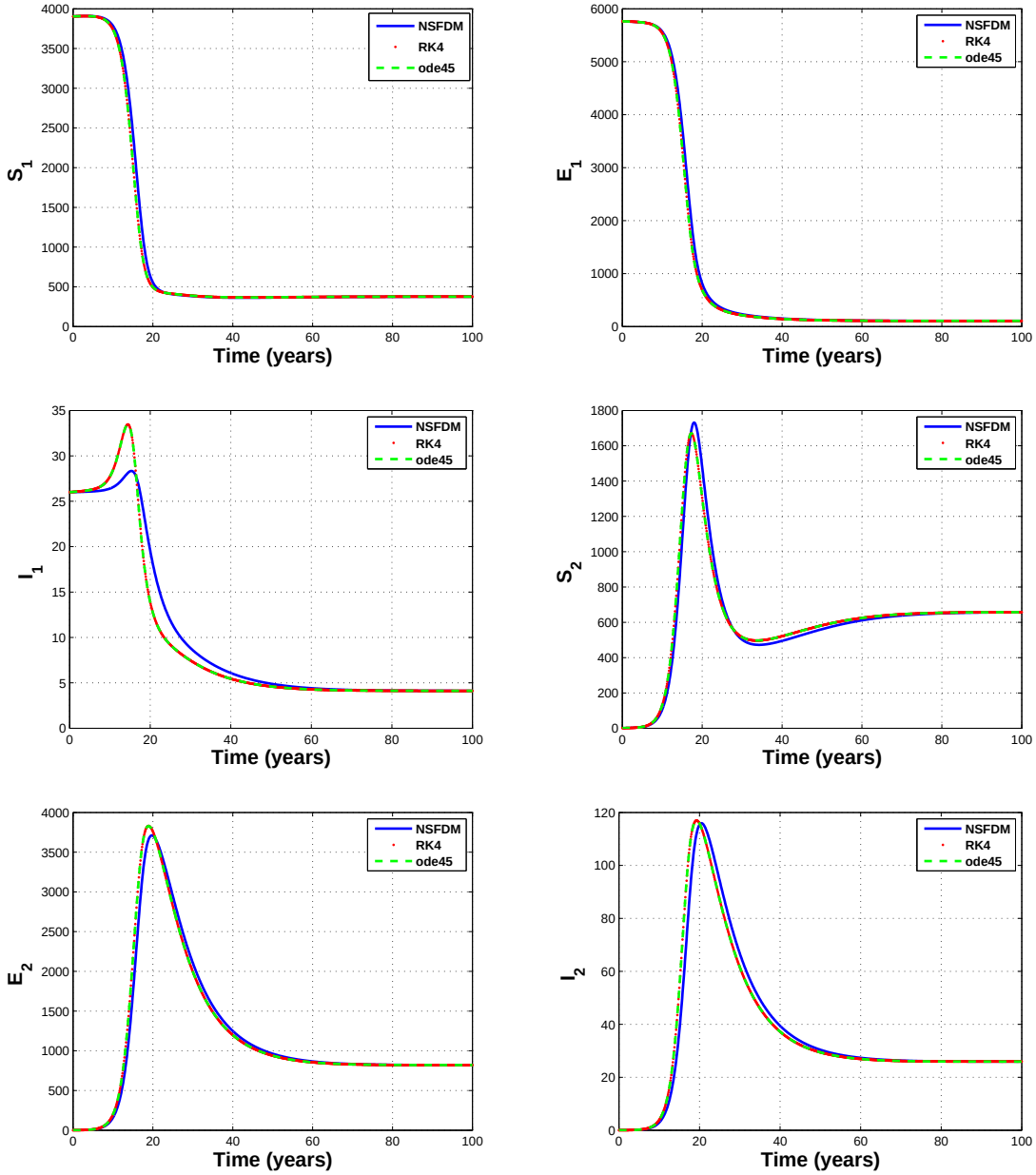

Figure 6.3.2.4: The EE of system (3.2.0.1) when $R_0 > 1$ and $k = 10$ obtained by using different numerical methods with $\ell = 0.1$.

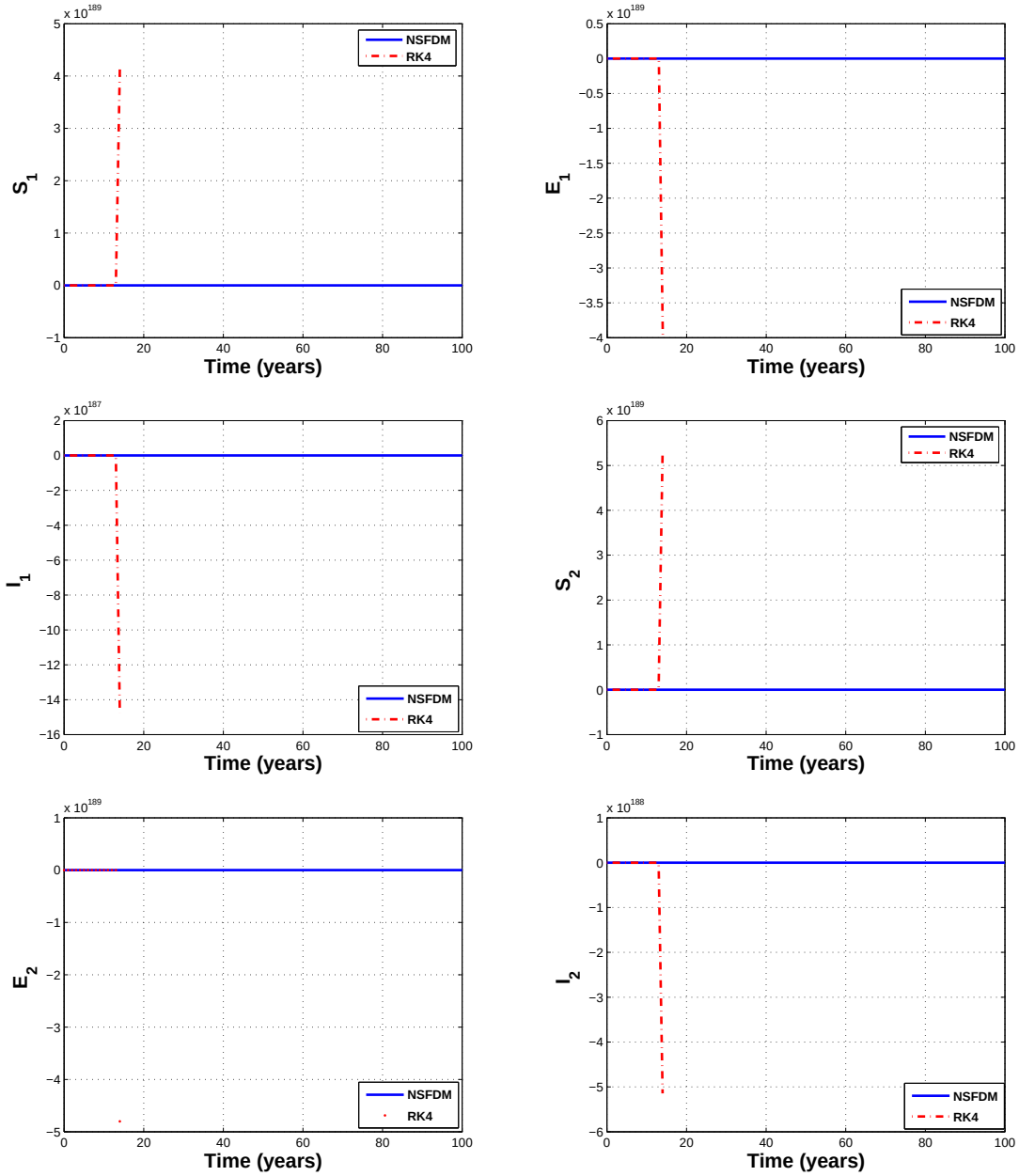

Figure 6.3.2.5: The EE of system (3.2.0.1) when $R_0 > 1$ with $k = 1$ obtained by using the NSFDM and RK4 with $\ell = 1$.

6.4 Summary and discussion

In this chapter, competitive unconditionally stable nonstandard finite difference methods are proposed for solving TB-only sub-model and full HIV-TB co-infection model represented by a nonlinear system of ordinary differential equations. The proposed methods are qualitatively stable, that is, they produce results which are dynamically consistent with those of the continuous systems.

Numerical results presented in Section 6.2.2 and Section 6.3.2 confirm the applicability of the proposed NSFDMs for the biological systems. These methods preserve the positivity of solutions and the stability properties of the equilibria for arbitrary step-sizes, whereas the solutions obtained by other numerical methods experience difficulties in either preserving the positivity of the solutions or in converging to the correct equilibria.

In the next chapter, we give some concluding remarks and also discuss the scope for future research.

Chapter 7

Concluding remarks and scope for future research

This thesis deals with the construction and analysis of robust numerical methods for solving HIV-TB co-infection models. We have systematically proceed in this direction by studying first the sub-models and then the full model. More specific details are provided below.

In Chapter 2, we developed and analyzed a mathematical model describing the transmission dynamics of HIV. The model accounts for behavior change, where a response function is considered. This function allowed us to study various responses of the individuals to the HIV prevalence. The system was analyzed mathematically with regard to well-posedness, positivity, invariant region, boundedness of solutions. We also analyzed the system's equilibria and their stability. We found that the basic reproduction number completely determines the dynamics of the system around the models' equilibria. If $R_0^{HIV} < 1$, only the disease-free equilibrium exists and it is globally asymptotically stable. If $R_0^{HIV} > 1$, then only one stable endemic equilibrium exists.

Although the parameters of the response function k and λ_0 were found not affecting the stability of the system equilibria, they affected the HIV prevalence. It was shown

that, the HIV prevalence is increasing with k and decreasing with λ_0. The message we receive from this, even with the presence of the behavior change, the dynamics of the HIV prevalence is affected by the way individuals respond to educational campaigns. We have shown that, even with the presence of behavior change, the prevalence increases if individuals do not reduce their risky behaviors unless the prevalence reaches a high value.

The model developed in Chapter 2 is combined with a tuberculosis model (TB-only sub-model) to formulate a deterministic model of an HIV and TB co-infection in Chapter 3. The resulting model is investigated for existence and uniqueness of solutions and positivity-invariant region. Further, we studied the impact of the response function on the dynamics of the model. The full HIV-TB model is shown to have a local asymptotical stable disease free equilibrium when its basic reproduction number R_0 (described by the maximum of the basic reproduction numbers of the two sub-models HIV and TB) is less than unity, and unstable if R_0 is greater than unity.

We have also shown in Chapter 3 that the full model undergoes the phenomenon of backward bifurcation when the associated basic reproduction number R_0 is greater than and close to 1 and some of the model parameters meet some criteria. Numerical simulations of the full model were carried out to show that the two diseases co-exist whenever R_0 exceeds unity. If any one of the basic reproduction numbers associated with one of the sub-models is greater than unity and the other is less than unity, the epidemics of the model is driven by the disease which has the largest value of the basic reproduction numbers.

Further numerical simulations of the full model were carried out to assess the impact of the response function in its parameters: Hill coefficient k and behavior change λ_0 on the HIV and TB prevalences. Both prevalences were found increasing with k (decreasing with λ_0). This suggests that the way individuals respond to the HIV prevalence not only affecting it but also affecting the TB prevalence. Thus, by incorporating behavior change and by taking into consideration the various responses of individuals to the HIV prevalence, the number of the HIV-TB co-infected individuals can be

controlled.

By considering a distributed delay in the prevalence, the HIV-only sub-model is studied in Chapter 4 for the impact of the time needed for the individuals to reduce their risky behaviors on the stability of the model equilibria. The disease free equilibrium is found globally asymptotically stable when $R_0^{HIV} < 1$ and unstable when $R_0^{HIV} > 1$ independently of the parameters of gamma function: the mean delay $\bar{\tau}$ and the shape parameter n. We showed that the introduction of the distributed delay in the model leads to a Hopf bifurcations around the endemic equilibria of the model. These bifurcations correspond to the existence of periodic solutions that oscillate around the equilibria at given thresholds.

In addition, we showed how the incorporation of the delay affected the HIV prevalence. In situations where individuals do not respond until the HIV prevalence reaches a high value (modeled by a large value of Hill coefficient k, i.e., $k = 10$), this resulted in more HIV infections causing more increase in the HIV prevalence. On the other hand, in situations where individuals respond very quickly to the HIV prevalence (modeled by a small value of Hill coefficient k, i.e., $k = 1$), the delay was found to have a little impact on the prevalence as in this case when individuals delay their response will not result in more infections. Theses effects can be seen in Figure 4.4.2.4.

In Chapter 5, competitive unconditionally stable nonstandard finite difference methods are proposed for solving the HIV mathematical model represented in Chapter 2. The proposed methods are found to be qualitatively stable, that is, they produced results which are dynamically consistent with those of the continuous system. Numerical results presented in the chapter confirmed the applicability of the proposed NSFDMs for the biological systems. These methods preserve the positivity of solutions and the stability properties of the equilibria for arbitrary step-sizes, while the solutions obtained by other numerical methods experience difficulties in either preserving the positivity of the solutions or in converging to the correct equilibria. Furthermore, since large step-sizes can be used, these methods save the computations time and memory.

It should be noted that when numerical simulations using a particular method are

performed for a set of parameters that usually fit the model well then the method normally tends to converge. However, a slight change in the values of these parameters can make some methods unreliable. In reality, one might expect (with a very little probability) some situations, for example, disease outbreaks in a community, when at a particular time there may be more infectious individuals than susceptibles. To test whether the numerical methods capture this dynamics, we have provided some more numerical simulations, see, tables 5.3.2.2, 5.3.3.1 and figures 5.3.2.4, 5.3.3.5. It is clear from these results that NSFDMs could mimic the relevant dynamics whereas the other numerical methods failed to do so.

In Chapter 6, we extended the NSFDMs developed in Chapter 5 to solve the HIV-TB co-infection model presented in Chapter 3. We first investigated the applicability of the method for solving the TB-only sub-model before constructing an NSFDM for solving the full model of the HIV-TB co-infections. The equations of the discrete model in each case developed in this chapter were highly nonlinear. This gave us unmanageable expressions for the eigenvalues when we do linear stability on any equilibria of each model. To this end, we studied the stability of these equilibria numerically. The proposed methods were qualitatively stable, that is, they produced results which were dynamically consistent with those of the continuous system. As in Chapter 5, numerical results presented in the chapter again confirmed the applicability of the proposed NSFDM for the biological systems. These methods preserved the positivity of solutions and the stability properties of the equilibria for arbitrary step-sizes, while the solutions obtained by other numerical methods experience difficulties in either preserving the positivity of the solutions or in converging to the correct equilibria.

As far as the scope of our future research is concerned, we list down the following:

- Currently we are investigating a number of techniques to control the co-infections of HIV and TB. We considered the model presented in this thesis as a case study.

- We then intend to extend our numerical methods developed to solve the models for HIV-TB co-infection for the systems that we will obtain by considering the

optimal control formulations of the associated problems.

- We are also extending the techniques developed for the HIV model in Chapter 4 for the full model of HIV-TB co-infection.

- It should be noted that the numerical methods developed in this thesis are mostly first order accurate and developed only for biological systems described by ordinary differential equations. The fact that despite of being low order accurate, they are very competitive as compared to other conventional higher order methods, e.g., RK-4, we are currently busy investigating the applicability of such methods for partial differential equation models in biology. We further intend to improve the order of convergence of these NSFDMs (both for ODE and PDE models).

Bibliography

[1] S. Abelman and K.C. Patidar, Comparison of some recent numerical methods for initial-value problems for stiff ordinary differential equations, *Computers and Mathematics with Applications* **55** (2008) 733–744.

[2] M.E. Alexander, A.R Summers and S.M Moghadas, Neimark-Sacker bifurcations in a non-standard numerical scheme for a class of positivity-preserving ODEs, *Proceedings of the Royal Society A* **462** (2006) 3167–3184.

[3] L.J.S. Allen, *An Introduction to Mathematical Biology*, Prentice Hall, NJ, 2007.

[4] R.M. Anderson and R.M. May, *Infectious Diseases of Humans*, Oxford University Press, London, 1992.

[5] R. Anguelov, J.M.-S. Lubuma and M. Shillor, Dynamically consistent nonstandard finite difference schemes for continuous dynamical systems, *Discrete and Continuous Dynamical Systems: Supplement 2009* **61** (2009) 34–43.

[6] J.P. Aparicio, A.F. Capurro and C. Castillo-Chavez, Markers of disease evolution: The case of Tuberculosis, *Theoretical Biology* **215** (2002) 227–237.

[7] AVERT: http://www.avert.org/tuberc.htm, AIDS, HIV and Tuberculosis, 2006.

[8] A.J. Arenas, J.A. Moraño and J.C. Cortés, Nonstandard numerical method for a mathematical model of RSV epidemiological transmission, *Computers and Mathematics with Applications* **56** (2008) 670–678.

[9] L.-G. Bekker and R. Wood, The Changing Natural History of Tuberculosis and HIV Coinfection in an Urban Area of Hyperendemicity, *Clinical Infectious Diseases* **50(S3)** (2010) S208–S214.

[10] N. Bacaër, R. Ouifki, C. Pretorius, R. Wood and B. Williams, Modeling the joint epidemics of TB and HIV in a South African township, *Journal of Mathematical Biology* **57** (2008) 557–593.

[11] F. Baryarama, J.Y.T. Mugisha and L.S. Luboobi, A mathematical model for the dynamics of HIV/AIDS with gradual behaviour change, *Computational and Mathematical Methods in Medicine* **7(1)** (2006) 15–26.

[12] I. Bates, C. Fenton, J. Gruber, D. Lalloo, A.M. Lara, S. Squire, S. Theobald, R. Thomson and R. Tolhurst, Vulnerability to malaria, tuberculosis, and HIV/AIDS infection and disease. Part 1: determinants operating at individual and household level, *The Lancet Infectious Diseases* **4(5)** (2004) 267–277.

[13] E. Beretta and Y. Kuang, Geometric stability switch criteria in delay differential systems with delay dependent parameters, *SIAM Journal on Mathematical Analysis* **33(5)** (1991) 1144–1165.

[14] A. Berkman, J. Garcia, M. Muñoz-Laboy, V. Paiva and R. Parker, A critical analysis of the Brazilian response to HIV/AIDS: Lessons learned for controlling and mitigating the epidemic in developing countries, *American Journal of Public Health* **97(7)** (2005) 1162.

[15] R. Bessinger, C. Katendeb and N. Guptac, Multi-media campaign exposure effects on knowledge and use of condoms for STI and HIV/AIDS prevention in Uganda, *Evaluation and Program Planning* **27** (2004) 397–407.

[16] C.P. Bhunu, S. Mushayabasa, W. Garira, E. Ngarakana-Gwasira and J.M. Tchuenche, Is the world doing enough for the poor? A case of HIV/AIDS testing and counselling, *World Journal of Modelling and Simulation* **6(3)** (2010) 163–176.

[17] C.P. Bhunu, W. Garira and Z. Mukandavire, Modeling HIV/AIDS and Tuberculosis Coinfection, *Bulletin of Mathematical Biology* **71** (2009) 1745–1780.

[18] C.P. Bhunu, W. Garira, Z. Mukandavire and M. Zimbab, Tuberculosis Transmission Model with Chemoprophylaxis and Treatment, *Bulletin of Mathematical Biology* **70** (2008) 1163–1191.

[19] G. Birkhoff and G.-C Rota, *Ordinary Differential Equations*, John Wiley & Sons Inc, New York, 1989.

[20] D.M. Bortz and P.W. Nelson, Sensitivity analysis of a nonlinear lumped parameter model of HIV infection dynamics, *Bulletin of Mathematical Biology* **66(5)** (2004) 1009–1026.

[21] F. Brauer and C. Castillo-Chavez, *Mathematical Models in Population Biology and Epidemiology*, Springer-Verlag, New York, 2001.

[22] R. Brookmeyer, Accounting for Follow-up Bias in Estimation of Human Immunodeficiency Virus Incidence Rates, *Journal of the Royal Statistical Society. Series A* **160(1)** (1997) 127–140.

[23] A.B. Bryt and D.E. Rogers, Human immunodeficiency virus infection and tuberculosis: An analysis and a course of action, *Bulletin of the New York Academy of Medicine: Journal of Urban Health* **71(1)** (1994) 18–36.

[24] C. Castillo-Chavez and Z. Feng, Global stability of an age-structure model for TB and its applications to optimal vaccination strategies, *Mathematical Biosciences* **51** (1998) 135–154.

[25] C. Castillo-Chavez and B. Song, Dynamical models of tuberculosis and their applications, *Mathematical Biosciences and Engineering*, **1(2)** (2004) 361–404.

[26] F.H. Chen, On the transmission of HIV with self-protective behavior and preferred mixing, *Mathematical Biosciences* **199** (2006) 141–159.

[27] T. Cohen, B. Sommers and M. Murray, The effect of drug resistance on the fitness of Mycobacterium tuberculosis, *The Lancet Infectious Diseases* **3(1)** (2003) 13–21.

[28] T. Cohen, M. Lipsitch, R.P. Walensky and M. Murray, Beneficial and perverse effects of isoniazid preventive therapy for latent tuberculosis infection in HIV-tuberculosis coinfected populations, *Proceedings of the National Academy of Sciences of the United States of America* **103** (2006) 7042–7047.

[29] S. Colgate, E. Stanley, J.M. Hyman, S.P. Layne and C. Qualis, Risk behavior-based model of the cubic growth of acquired immunodeficiency syndrome in the United States, *Proceedings of the National Academy of Sciences of the United States of America* **86** (1989) 4793–4797.

[30] E.L. Corbett, T. Bandason, Y.B. Cheung, S. Munyati, P. Godfrey-Faussett, R. Hayes, G. Churchyard, A. Butterworth, P. Mason, Epidemiology of tuberculosis in a high HIV prevalence population provided with enhanced diagnosis of symptomatic disease, *PLoS Medicine* **4(1)** (2007) e22.

[31] L.E. Cosler, T.R. Fanning and B.J. Turner, Understanding behavioral and social illnesses: the impact on the health care system. Tuberculosis and HIV co-infections in the NYS Medicaid Program: epidemiology and utilisation patterns. Health services research: implications for policy, management and clinical practice, *AHSR Annual Meeting Abstracts*, Washington, DC: Washington Hilton and Towers, 1993.

[32] F.A.B. Coutinho, L.F. Lopez, M.N. Burattini and E. Massad, Modelling the natural history of HIV infection in individuals and its epidemiological implications, *Bulletin of Mathematical Biology* **63(6)** (2001) 1041–1062.

[33] C.S.M. Currie, K. Floyd, B.G. Williams and C. Dye, Cost, affordability and cost-effectiveness of strategies to control tuberculosis in countries with high HIV prevalence, *BMC Public Health* **5(130)** (2005).

[34] K. M. De Cock and R. E. Chaisson, Will DOTS do it? A reappraisal of tuberculosis control in countries with high rates oh HIV infection, *The International Journal of Tuberculosis and Lung Disease* **3** (1999) 457–65.

[35] K. DeRiemer, L.M. Kawamura, P.C. Hopewell and C.L. Daley, Quantitative impact of human immunodeficiency virus infection on tuberculosis dynamics, *American Journal of Respiratory and Critical Care Medicine*, **176** (2007) 936–944.

[36] D.T. Dimitrov and H.V. Kojouharov, Nonstandard finite-difference schemes for general two-dimensional autonomous dynamical systems, *Applied Mathematics Letters* **18** (2005) 769–774.

[37] D.T. Dimitrov and H.V. Kojouharov, Positive and elementary stable nonstandard numerical methods with applications to predator-prey models, *Journal of Computational and Applied Mathematics* **189** (2006) 98–108.

[38] D.T. Dimitrov and H.V. Kojouharov, Stability-preserving finite-difference methods for general multi-dimensional autonomous dynamical systems, *International Journal of Numerical Analysis Modeling* **4(2)** (2007) 280–290.

[39] P.J. Dolin, M.C. Raviglione and A. Kochi, Global tuberculosis incidence and mortality during, *Bulletin of the World Health Organization* **72** (1994) 213–220.

[40] Yves Dumont and Jean M.-S Lubuma, Non-standard finite-difference methods for vibro-impact problems, *Proceedings of the Royal Society A* **461** (2005) 1927–1950.

[41] A.R. Escombe, D.A.J. Moore, R.H. Gilman, W. Pan, M. Navincopa, E. Ticona, C.Marinez, L. Caviedes, P. Sheen, A. Gonzalez, C.J. Noakes, J.S. Friedland and C.A. Evans, The infectiousness of tuberculosis patients co-infected with HIV, *PLoS Medicine* **5(9)** (2008) e188.

[42] A.M. Eliott, N. Luc, G. Tembo, B. Halwiindi, G. Steenbergen, L. Machiels, J. Pobee, P. Nunn, R. J. Hayes and K.P. McAdam, Impact of HIV on tuberculosis in Zambia: a cross-sectional study, *British Medical Journal* **301** (1990) 412–415.

[43] A.M. Elliot, K. Namaabo, B.W. Allen, N. Luo, R.J. Hayes, J.O. Pobee and K.P. McAdam, Negative sputum smear results in HIV-positive patient with pulmonary tuberculosis in Lusaka, Zambia, *Tuberculosis and Lung Disease* **74(3)** (1993) 191–194.

[44] A.I. El-Sony, The cost to health services of human immunodeficiency virus (HIV) co-infection among tuberculosis patients in Sudan, *Health Policy* **75(3)** (2006) 272–279.

[45] A.I. El-Sony, A.H. Khamis, D.A. Enarson, O. Baraka, S.A. Mustafa and G. Bjune, Treatment results of DOTS in 1797 Sudanese tuberculosis patients with or without HIV co-infection, *International Journal of Tuberculosis and Lung Disease* **6(12)** (2002) 1–9.

[46] J.M. FitzGerald and S. Houston, Tuberculosis: 8. The disease in association with HIV infection, *Canadian Medical Association* **161(1)** (1999) 47–51.

[47] H.I. Freedman and Y. Kuang, Stability switches in linear scalar neutral delay equations, *Funkcialaj Ekvacioj* **34** (1991) 187–209.

[48] A. Friedman, J. Turner and B. Szomolay, A model on the influence of age on immunity to infection with Mycobacterium tuberculosis, *Experimental Gerontology* **43(4)** (2008) 275–285.

[49] D. Gammack, C.R. Doering and D.E. Kirschner, Macrophage response to Mycobacterium tuberculosis infection, *Journal of Mathematical Biology* **48** (2004) 218–242.

[50] A. Gumel and B. Song, Existence of multiple-stable equilibria for a multi-drug resistant model of mycobacterium tuberculosis, *Mathematical Biosciences and Engineering* **5(3)** (2008) 437–455.

[51] J. van Gorkom and D. Kibuga, Cost-effectiveness and total costs of three alternative strategies for the prevention and management of severe skin reactions attributable to Thiacetazone in the treatment of human immunodeficiency virus positive patients with tuberculosis in Kenya, *International Journal of Tuberculosis and Lung Disease* **77** (1996) 30–36.

[52] S. Gregson, G.P. Garnett, C.A. Nyamukapa, T.B. Hallet, J.J.C. Lewis, P.R. Mason, S.K. Chandiwana and R.M. Anderson, HIV decline associated with behavior change in Eastern Zimbabwe, *Science* **311** (2006) 664.

[53] H. Grosskurth, F. Mosha, J. Todd, E. Mwijarubi, A. Klokke, K. Senkoro, P. Mayaud, J. Changalucha, A. Nicoll, G. Ka-Gina, J. Newell, K. Mugeye, D. Mabey and R. Hayes, Ipmact of improved treatment of sexually transmitted diseases on HIV infection in rural Tanzania: randomized controlled trial, *Lancet* **346** (1995) 530–536.

[54] A.B. Gumel, K.C. Patidar and R.J. Spiteri, Asymptotically consistent nonstandard finite difference methods for solving mathematical models arising in population biology. In R.E. Mickens (ed.): *Applications of Nonstandard Finite Difference Schemes*, World Scientific, Singapore, 2005, pp. 385–421.

[55] J.K. Hale and J. Kato, Phase space for retarded equation with infinite delay, *Funkcialaj Ekvacioj* **21** (1978) 11–41.

[56] A.D. Harries, R. Zachariah, E.L. Corbett, S.D. Lawn, E.T. Santos-Filho, R. Chimzizi, M. Harrington, D. Maher, B.G. Williams and K.M. De Cock, The HIV-associated tuberculosis epidemic-when will we act? *Lancet* **375** (2010) 1906–19.

[57] H.P. Hausler, E. Sinanovic, L. Kumaranayake, P. Naidoo, H. Schoeman and B. Karpakis, Costs of measures to control tuberculosis/HIV in public primary care facilities in Cape Town, South Africa, Bulletin of the World Health Organization 84 (2006) 528–536.

[58] M. Hawken, P. Nunn, S. Gathua, R. Brindle, P. Godfrey-Faussett, W. Githui, J. Odhiambo, B. Batchelor, C. Gilks and J. Morris, Increased recurrence of tuberculosis in HIV-1-infected patients in Kenya, *Lancet* **342** (1993) 332–337.

[59] D.L Heymann, *Control of Communicable Diseases Manuel*, American Public Health association, Washington, DC, 2008.

[60] Y.-H Hsieh and Y.-S Wang, Basic Reproduction Number for HIV Model Incorporating Commercial Sex and Behavior Change, *Bulletin of Mathematical Biology* **68** (2006) 551–575.

[61] E.A. Ibijola, R.B. Ogunrinde and O.A Ade-Ibijola, On the theory and applications of new nonstandard finite difference methods for the solution of initial value problems in

ordinary differential equations, *Advances in Natural and Applied Sciences* **2(3)** (2008) 214–224.

[62] V. Idemyor, HIV and Tuberculosis Coinfection: Inextricably Linked Liaison, *Journal of the National Medical Association* **99(12)** (2007) 1414.

[63] S. Iwami, S. Nakaoka and Y.Takeuchi, Mathematical analysis of a HIV model with frequency and viral diversity *Mathematical Biosiences and engineering* **5(3)** (2008) 457–476.

[64] N. Jha, B. Khanal, K.P. Prahalad, S. Rijal, B.K. Deo, D.K. Khadka and P. Malla, TB/HIV co-infection status among the newly diagnosed TB patients: A Study from Eastern Nepal, *SAARC Journal of Tuberclosis, Lung Diseases and HIV/AIDS* **5(2)** (2008) 22–25.

[65] L. Jódar, R.J. Villanueva, A.J. Arenas and G.C. González, Nonstandard numerical methods for a mathematical model for influenza disease, *Mathematics and Computers in Simulation* **79** (2008) 622–633.

[66] M.K. Kadalbajoo, K.C. Patidar and K.K. Sharma, ε-uniformly convergent fitted methods for the numerical solution of the problems arising from singularly perturbed general DDEs, *Applied Mathematics and Computation* **182** (2006) 119–139.

[67] A. Kamali, M. Quigley, J. Nakiyingi, J. Kinsman, J. Kengeya-Kayondo, R. Gopal, A. Ojwiya, P.Hughes, L. M. Carpenter and J. Whitworth, Syndromic management of sexually-transmitted infections and behaviour change interventions on transmission of HIV-1 in rural Uganda: a community randomized trial, *Lancet* **361** (2003) 645–52.

[68] J. Karrakchou, M. Rachik and S. Gourari, Optimal control and infectiology:Application to an HIV/AIDS model, *Applied Mathematics and Computation* **177** (2006) 807–818.

[69] J. Keating, D. Meekers and A. Adewuyi, Assessing effects of a media campaign on HIV/AIDS awareness and prevention in Nigeria: results from the VISION Project, *BMC Public Health* **6** (2006) 123.

[70] E. Keeler, M.D. Perkins, P. Small, C. Hanson, S. Reed, J. Cunningham, J.E. Aledort, L. Hillborne, M.E. Rafael, F. Girosi1 and C. Dye, Reducing the global burden of tuberculosis: the contribution of improved diagnostics, *Nature Publishing Group*, (2006).

[71] A. Kiers, A.P. Drost, D. van Soolingen and J. Veen, Use of DNA fingerprinting in international source case finding during a large outbreak of tuberculosis in The Netherlands, *International Journal of Tuberculosis and Lung Disease* **1(3)** (1997) 239–245.

[72] D. Kirschner, Dynamics of Co-infection with M. tuberculosis and HIV-1, *Theoretical Population Biology* **55(1)** (1999) 94–109.

[73] D. Kirschner and S. Marino, Mycobacterium tuberculosis as viewed through a computer, *Trends in Microbiology* **13(5)** (2005) 206–211.

[74] Y.A. Kuznetssov, *Elements of Applied Bifurcation Theory*, Springer-Verlag, New York, 1995.

[75] Y. Kuang, *Delay Differential Equations with Applications in Population Dynamics*, Academic Press, San Diego, 1993.

[76] S.D. Lawn, L.-G. Bekker, K. Middelkoop, L. Myer and R. Wood, Impact of HIV infection on the epidemiology of tuberculosis in a peri-urban community in South Africa: The need for age-specific interventions, *Clinical Infectious Diseases* **42** (2006) 1040–1047.

[77] S. Lenhart and J.T. Workman, S. Lenhart and J.T. Workman, *Optimal Control Applied to Biological Models*, CRC Press, 2007.

[78] C. Letellier, S. Elaydi, L.A. Aguirre and A. Alaoui, Difference equations versus differential equations, a possible equivalence for the Rössler system *Physica D* **195** (2004) 29–49.

[79] E.F. Long, N.K. Vaidya and M.L. Brandeau, Controlling Co-Epidemics: Analysis of HIV and tuberculosis infection dynamics, *Operations Research* **56(6)** (2008) 1366–1381.

[80] J.M.-S. Lubuma and K.C. Patidar, Uniformly convergent non-standard finite difference methods for self-adjoint singular perturbation problems, *Journal of Computational and Applied Mathematics* **191** (2006) 229–238.

[81] J.M.-S. Lubuma and K.C. Patidar, Solving singularly perturbed advection reaction equation via non-standard finite difference methods, *Mathematical Methods in the Applied Sciences* **30(14)** (2007) 1627–1637.

[82] J.M.-S. Lubuma and K.C. Patidar, ε-uniform non-standard finite difference methods for singularly perturbed nonlinear boundary value problems, *Advances in Mathematical Sciences and Applications* **17(2)** (2007) 651–665.

[83] J.M.-S. Lubuma and K.C. Patidar, Non-standard methods for singularly perturbed problems possessing oscillatory/layer solutions, *Applied Mathematics and Computation* **187** (2007) 1147–1160.

[84] C.M. Lyles, L.S. Kay, N. Crepaz, J.H. Herbst, W.F. Passin, A.S. Kim, S.M. Rama, S. Thadiparthi, J.B. DeLuca and M.M. Mullins for the HIV/AIDS Prevention Research Synthesis Team, Best-evidence interventions: Findings from a systematic review of HIV behavioral Interventions for US populations at high risk, 2000–2004, *American Journal of Public Health* **9(1)** (2007).

[85] N. MacDonald, *Biological Delay Systems*, *Cambridge University Press*, Cambridge, 1989.

[86] S. Marino and D.E. Kirschner, The human immune response to Mycobacterium tuberculosis in lung and lymph node, *Journal of Theoretical Biology* **227(4)** (2004) 463–486.

[87] L. Marison, The global epidemiology of HIV/AIDS, *British Medical Bulletin* **58** (2001) 7–18.

[88] E. Massad, M.N. Burattini, F.A.B. Coutinho, H.M. YANG and S.M. Raimundo, Modeling the interaction between AIDS and tuberculosis, *Mathematical and Computer Modelling* **17(9)** (1993) 7–21.

[89] C.C. McCluskey and P. van den Driessche1, Global Analysis of Two Tuberculosis Models, *Journal of Dynamics and Differential Equations* **16(1)** (2004) 139–166

[90] D.L. McLeish, *Monte Carlo Simulation and Finance*, John Wiley and Sons, New York, 2005.

[91] R.E. Mickens and A. Smith, Finite difference models of ordinary differential equations: Influence of denominator functions, *Journal of the Franklin Institute* **327** (1990) 143–145.

[92] R.E. Mickens and I. Ramadhani, Finite-difference schemes having the correct linear stability properties for all finite step-sizes III, *Computer in Mathematics with Applications* **27** (1994) 77–84.

[93] R.E. Mickens, Calculation of denominator functions for nonstandard finite difference schemes for differential equations satisfying a positivity condition, *Numerical Methods for Partial Differential Equations* **23(3)** (2007) 672–691.

[94] G.B. Migliori, A. Borghesi, C. Adriko, V. Manfrin, S.Okware, W. Naamara, A. Bartoloni, M. Neri and G. Acocella, Tuberculosis and HIV infection association in a rural district of Northern Uganda: epidemiological and clinical considerations, *International Journal of Tuberculosis and Lung Disease* **73** (1992) 285–290.

[95] S.M. Moghadas, M.E. Alexander and B.D. Corbett, A non-standard numerical scheme for a generalized Gause-type predator-prey model, *Physica D* **188** (2004) 134–151.

[96] Z. Mukandavire, W. Garira and J.M. Tchuenche, Modelling effects of public health educational campaigns on HIV/AIDS transmission dynamics, *Applied Mathematical Modelling* (2008) doi:10.1016/j.apm.2008.05.017.

[97] J.B. Munyakazi and K.C. Patidar, Higher order numerical methods for singularly perturbed elliptic problems, *Neural, Parallel & Scientific Computations* **18 (1)** (2010) 75–88.

[98] C.J.L. Murray and J.A. Salomon, Modeling the impact of global tuberculosis control strategies, *Proceedings of the National Academy of Sciences of the United States of America* **95** (1998) 13881–13886. .

[99] S.L. Myhre and J.A. Flora, HIV/AIDS Communication Campaigns: Progress and Prospects, *Journal of Health Communication* **5** (2000) 29–45.

[100] J.D. Murray, *Mathematical Biology I: An Introduction*, Springer-Verlag Berlin Heidelberg, New York, 1993.

[101] B. M. Murphy, B. H. Singer, S. Anderson and D. Kirschner, Comparing epidemic tuberculosis in demographically distinct heterogeneous populations, *Mathematical Biosciences* **180** (2002) 161–185.

[102] J.F. Murray and Cursed duel: HIV infection and tuberculosis, *Respiration* **57** (1990) 210–220.

[103] C.J.L. Murray, E. Dejonghe, H.J. Chum, D.S. Nyangulu, A. Salomao and K. Styblo, Cost effectiveness of chemotherapy for pulmonary tuberculosis in three sub-Saharan African countries, *Lancet* **338(8778)** (1991) 1305–1308.

[104] B.M. Murphy, B.H. Singer and D. Kirschner, On treatment of tuberculosis in heterogeneous populations, *Journal of Theoretical Biology* **223(4)** (2003) 391–404.

[105] J.P. Narain, M.C. Raviglione and A. Kochi, HIV-associated tuberculosis in developing countries: epidemiology and strategies for prevention, *International Journal of Tubercle and Lung Disease* **73(6)** (1992) 311–321.

[106] R. Naresh, D. Sharma and A. Tripathi, Modelling the effect of risky sexual behaviour on the spread of HIV/AIDS, *International Journal of Applied Mathematics and Computation* **1(3)** (2009) 132–147.

[107] P.W. Nelson and A.S. Perelson, Mathematical analysis of delay differential equating models of HIV-1 infection, *Mathematical Biosciences* **179** (2002) 73–94.

[108] P. Nunn, D. Kibuga, A. Elliott and S. Gathua, Impact of human immunodeficiency virus on transmission and severity of tuberculosis, *Transactions of the Royal Society of Tropical Medicine and Hygiene* **84** (1990) 9–13.

[109] P. Nunn, S. Gathua, D. Kibuga, R. Brindle, R. Binge, J. Odhiambo and K. McAdam, The impact of HIV on resources utilisation by patients with tuberculosis in tertiary referral hospital, Nairobi, Kenya, *International Journal of Tuberculosis and Lung Disease* **74** (1993) 273–279.

[110] V.U. Oboh and R.M. Sani, The role of radio in the campaign against the spread of HIV/AIDS among farmers in Makurdi local government area of Benue State, Nigeria, *Journal of Social Sciences* **19(3)** (2009) 179–184.

[111] P.C. Onyebujoh, I. Ribeiro and C.C. Whalen, Treatment options for HIV-associated tuberculosis, *The Journal of Infectious Diseases*, **196** (2007) S35–45.

[112] K.C. Patidar, On the use of nonstandard finite difference methods, *Journal of Difference Equations and Applications* **11(8)** (2005) 735–758.

[113] K.C. Patidar and K. K. Sharma, Uniformly convergent nonstandard finite difference methods for singularly perturbed differential difference equations with delay and advance, *International Journal for Numerical Methods in Engineering* **66** (2006) 272–296.

[114] K.C. Patidar and K.K. Sharma, ε-uniformly convergent non-standard finite difference methods for singularly perturbed differential difference equations with small delay, *Applied Mathematics and Computation* **175** (2006) 864–890.

[115] K.C. Patidar, A robust fitted operator finite difference method for a two-parameter singular perturbation problem, *Journal of Difference Equations and Applications* **14 (12)** (2008) 1197–1214.

[116] L. Perko, *Differential Equations and Dynamical Systems*, Springer-Verlag, New York, 1991.

[117] K.D. Phillips, A Look at Tuberculosis and Its Relationship to HIV/AIDS, *Journal of the Association of Nurses in AIDS Care* **18(1)** (2007) 75–78.

[118] J.H. Perriens, Y. Mukadi and P. Nunn, Tuberculosis and HIV infection: implication for Africa, AIDS **43** (suppl) (1991) S127–S133.

[119] W. Piyawong, E.H. Twizell, A.B. Gumel, An unconditionally convergent finite-difference scheme for the SIR model, *Applied Mathematics and Computation*, **146** (2003) 611–625.

[120] T.C. Quinn, Global burden of the HIV pandemic, *Lancet* **348** (1996) 99–106.

[121] L-I.W. Roeger, Z. Feng and C. Castillo-Chavez, Modeling TB and HIV Co-infections, *Mathematical Biosciences and Engineering* **6(4)** (2009) 815–837.

[122] L.S. Rosenblum, K.G. Castro, S. Dooley and M. Morgan, Effect of HIV infection and tuberculosis on hospitalization and cost of care for young adult in the united states, 1985 to 1990, *Annals of Internal Medicine* **121(10)** (1994) 786–792.

[123] J.D.C. Ross and G.R. Scott, The association between HIV media campaigns and number of patients coming forward for HIV antibody testing, *Genitourinary Medicine* **69** (1993) 193–195.

[124] S.M. Ross, *Introduction to Probability and Statistics for Engineers and Scientists*, Elsevier Academic Press, Burlington, 2004.

[125] M.S. Sánchez, J.O. Lloyd-Smith, B.G. Williams, T.C. Porco, S.J. Ryan, M.W. Borgdorff, J. Mansoer, C. Dye and W.M. Getz, Incongruent HIV and tuberculosis co-dynamics in Kenya: Interacting epidemics monitor each other, *Epidemics* **1** (2009) 14–20.

[126] A. Sani and D.P. Kroese, Controlling the number of HIV infectives in a mobile population, *Mathematical Biosciences*, in press.

[127] B.D. Saunders and R.G. Trapp, *Basic and Clinical Biostatistics*, Appleton & Lange, East Norwalk, 1994.

[128] B.E. Scott, H.A. Weiss and J.I. Viljoen, The acceptability of male circumcision as an HIV intervention among a rural Zulu population, KwaZulu-Natal, South Africa, *AIDS Care* **17(3)** (2005) 304–313.

[129] O. Sharomi, C.N. Podder, A.B. Gumel and B. Song, Mathematical analysis of the transmission dynamics of HIV-TB coinfection in the presence of treatment, *Mathematical Biosciences and engineering* **5(1)** (2008) 145–174.

[130] T. Smart, Think TB in people with HIV: the 3 I's for TB control in people with HIV, NAM, London, 2008, 48 pages.

[131] B. Song, C. Castillo-Chavez and J. P. Aparicio, Tuberculosis models with fast and slow dynamics: the role of close and casual contacts, *Mathematical Biosciences* **180(1-2)** (2002) 187–205.

[132] B.H. Singer and D.E. Kirschner, Influnce of backward bifurcation on interpretation of R_0 in a model of epidemic tuberculosis with reinfection, *Mathematical Biosciences and Engineering* **1(1)** (2004) 81–93.

[133] G. Sunderham, R.J. McDonald, T. Maniatis, J. Oleske, R. Kapila and L.B. Reichman, Tuberculosis as a manifestation of the acquired immunodeficiency syndrome, *Journal of the American Medical Association* **256** (1986) 362–366.

[134] C.P. Theurer, P.C. Hopewell, D. Elias, G.F. Schecter, G.W. Rutherford and R.E. Chaisson, Human immunodeficiency infection in tuberculosis patients, *Journal of Infectious Diseases* **162** (1990) 8–12.

[135] A. Tripathi, R. Naresh and D. Sharma, Modelling the effect of screening of unaware infectives on the spread of HIV infection, *Applied Mathematics and Computation* **184** (2007) 1053–1068.

[136] UNAIDS Terminology Guidelines (January 2011): http://data.unaids.org/pub/Manual/2008/jc1336_unaids_terminology_guide_en.pdf

[137] P. Van den Driessche, J. Watmough, Reproduction numbers and sub-threshold endemic equilibria for compartmental models of disease transmission *Mathematical Biosciences* **180** (2002) 29–48.

[138] J. Vidanapathirana, M.J. Abramson, A. Forbes and C. Fairley, Mass media interventions for promoting HIV testing: Cochrane systematic review, *International Journal of Epidemiology* **35** (2005) 233–236.

[139] R.J. Villanueva, A.J. Arenas and G. Gonzalez-Parra, A nonstandard dynamically consistent numerical scheme applied to obesity dynamics, *Journal of Applied Mathematics* **2008**, doi:10.1155/2008/640154.

[140] M. J. Wawer, N. K. Sewankambo, D. Serwadda, T. C Quinn, L. A Paxton, N. Kiwanuka, F. Wabwire-Mangen, C. Li, T. Lutalo, F. Nalugoda, C. AGaydos, L. H. Moulton, M. O. Meehan and S. Ahmed, The Rakai Project Study Group and R. H. Gray, Control of sexually transmitted diseases for AIDS prevention in Uganda: randomized community trial, *Lancet* **353** (1999) 525–35.

[141] R.W. West and J.R. Thompson, Modeling the Impact of HIV on the Spread of Tuberculosis in the United States, *Mathematical Biosciences* **143** (1997) 35–60.

[142] B.G. Williams, R. Granich, L.S. Chauhan, N.S. Dharmshaktu and C. Dye, The impact of HIV/AIDS on the control of tuberculosis in India, *Proceedings of the National Academy of Sciences*, **102(27)** (2005) 9619–9624.

[143] R. Wood, K. Middelkoop, L. Myer, A.D. Grant, A. Whitelaw, S.D. Lawn, G. Kaplan, R. Huebner, J. McIntyre and L.-G. Bekker, Undiagnosed tuberculosis in a community with high HIV-prevalence: implications for TB control, *American Journal of Respiratory and Critical Care Medicine* **175** (2007) 87–93.

[144] World Health Organisation, Global Tuberculosis Programme. A deadly partnership. Tuberculosis in the era of HIV. Geneva: World Health Organization; 1996, WHO/TB/96.204.

[145] World Health Organisation, Preventing HIV/AIDS in young people: a systematic review of the evidence from developing countries, WHO Technical Report Series No. 938, 2006.

[146] H. Ying-Hen, A two-sex model for treatment of HIV/AIDS and behaviour change in a population of varying size, *IMA Journal of Mathematics Applied in Medicine and Biology* **13** (1996) 151–173.

[147] D. Young, J. Stark and D. Kirschner, Systems biology of persistent infection: tuberculosis as a case study, *Nature Reviews Microbiology* **6** (2008) 520–528.

[148] A. Zwi and D. Bachmayer, HIV and AIDS in South Africa: what is an appropriate public health response? *Health Policy and Planning* **5(4)** (1990) 316–326.